Chair for Computer Aided Medical
Procedures and Augmented Reality
Prof. Dr. Nassir Navab

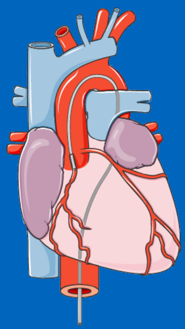

Dissertation

Multimodal Catheter Tracking Concepts and Methodologies for Endovascular Procedures

Ardit Ramadani

TUM School of Computation,
Information and Technology
Technical University of Munich

Technische Universität München
TUM School of Computation, Information and Technology

Multimodal Catheter Tracking Concepts and Methodologies for Endovascular Procedures

Ardit Ramadani

Vollständiger Abdruck der von der TUM School of Computation, Information and Technology der Technischen Universität München zur Erlangung eines

Doktors der Naturwissenschaften (Dr. rer. nat.)

genehmigten Dissertation.

Vorsitz: **Prof. Dr.-Ing. Alin Albu-Schäffer**

Prüfende der Dissertation:

1. Prof. Dr. Nassir Navab

2. Prof. Dr. Gabor Fichtinger

Die Dissertation wurde am 21.06.2024 bei der Technischen Universität München eingereicht und durch die TUM School of Computation, Information and Technology am 11.12.2024 angenommen.

Ardit Ramadani
Multimodal Catheter Tracking Concepts and Methodologies for Endovascular Procedures
Dissertation, Version 1.0
February 25th, 2025

Technical University of Munich
TUM School of Computation, Information and Technology
Chair for Computer Aided Medical Procedures and Augmented Reality
Boltzmannstr. 3, 85748 Garching near Munich

TUM University Hospital German Heart Center
TUM School of Medicine and Health
Department of Congenital Heart Defects and Pediatric Cardiology
Lazarettstr. 36, 80636 Munich

Abstract

Navigating the complexities of minimally invasive endovascular procedures demands precise and efficient catheter-tracking technologies. As these procedures evolve, the integration of sophisticated tracking methodologies becomes essential in enhancing procedural accuracy and patient outcomes. The field of catheter-based tracking solutions, therefore, stands at the forefront of significant medical advancements, combining technical innovation with clinical application to improve the standards of endovascular procedures.

The heart of this dissertation lies in a comprehensive literature review and a series of catheterization laboratory observations across different hospitals, highlighting the current state and challenges of catheter tracking technologies. Through an extensive analysis, it categorizes existing methodologies, identifies research gaps, and emphasizes the need for technologies that translate seamlessly into clinical practices. This dissertation underlines the technical limitations and the barriers that hinder the translation of these innovations from the lab to the bedside, advocating for stronger collaborations between researchers and clinical partners.

Further, the dissertation introduces novel catheter-tracking solutions, including a hybrid approach combining bioelectric and electromagnetic tracking for improved registration accuracy and dynamic time warping algorithms in catheter localization. These innovations represent steps toward minimizing the variability of surgical outcomes, leveraging preoperative and intraoperative imaging data to guide a new generation of intelligent surgical solutions and personalized medicine.

Envisioning a future where automated tracking and the use of robotics and machine learning in catheter-based endovascular procedures become standard, this dissertation emphasizes the importance of developing technologies tailored to the clinical environment. It calls for the next generation of physicians to be adept at these advanced techniques, ensuring that the evolution of catheter-tracking technologies continues to accelerate, thereby enriching the landscape of minimally invasive endovascular procedures and enhancing patient care.

Zusammenfassung

Navigieren in den Komplexitäten minimal-invasiver endovaskulärer Verfahren erfordert präzise und effiziente Katheterverfolgungstechnologien. Mit der Weiterentwicklung dieser Verfahren wird die Integration fortschrittlicher Verfolgungsmethoden essenziell, um die Genauigkeit der Eingriffe und die Patientenergebnisse zu verbessern. Das Feld der katheterbasierten Verfolgungslösungen steht daher an der Spitze bedeutender medizinischer Fortschritte, indem es technische Innovationen mit klinischen Anwendungen kombiniert, um die Standards endovaskulärer Verfahren zu erhöhen.

Der Kern dieser Dissertation liegt in einer umfassenden Literaturübersicht und einer Reihe von Beobachtungen in Katheterisierungslaboren in verschiedenen Krankenhäusern, die den aktuellen Stand und die Herausforderungen der Katheterverfolgungstechnologien hervorheben. Durch eine umfangreiche Analyse kategorisiert sie bestehende Methoden, identifiziert Forschungslücken und betont die Notwendigkeit von Technologien, die nahtlos in die klinische Praxis übergehen. Diese Dissertation unterstreicht die technischen Einschränkungen und die Barrieren, die die Umsetzung dieser Innovationen vom Labor ans Krankenbett behindern, und plädiert für stärkere Kooperationen zwischen Forschern und klinischen Partnern.

Darüber hinaus stellt die Dissertation neuartige Verfolgungslösungen vor, einschließlich eines hybriden Katheterverfolgungsansatzes, der bioelektrische und elektromagnetische Verfolgung zur Verbesserung der Registrierungsgenauigkeit und dynamische Zeitverzerrungsalgorithmen in der Katheterlokalisierung kombiniert. Diese Innovationen sind Schritte zur Minimierung der Variabilität der chirurgischen Ergebnisse, indem präoperative und intraoperative Bildgebungsdaten genutzt werden, um eine neue Generation intelligenter chirurgischer Lösungen und personalisierter Medizin zu leiten.

Mit der Vision einer Zukunft, in der automatisierte Verfolgung und der Einsatz von Robotik und maschinellem Lernen in katheterbasierten endovaskulären Verfahren zum Standard werden, betont diese Dissertation die Bedeutung der Entwicklung von Technologien, die auf die klinische Umgebung zugeschnitten sind. Sie fordert die nächste Generation von Ärzten auf, diese fortschrittlichen Techniken zu beherrschen, um sicherzustellen, dass die Entwicklung der Katheterverfolgungstechnologien weiter beschleunigt wird, wodurch das Spektrum minimal-invasiver endovaskulärer Verfahren bereichert und die Patientenversorgung verbessert wird.

To my family, whose love and support have made this doctoral journey possible!

Për familjen time, dashuria dhe mbështetja e të cilëve bënë të mundur këtë udhëtim doktorate!

Acknowledgments

First, I would like to express my deepest appreciation towards my supervisor, Prof. Nassir Navab, for his engagement and unparalleled support throughout my doctoral journey. Our weekly meetings, characterized by his reachable nature and constructive, meaningful feedback, have been crucial to my development. His keen ability to understand, propose innovative ideas, and steer my research in the right direction, coupled with his efforts to connect me with numerous people, has been crucial in achieving my goals.

I also wish to express my sincere appreciation to Prof. Thomas Wendler for his foundational support during the early stages of my doctorate. His collaboration was crucial in setting the initial steps of my research path. Thomas's kindness and support have significantly enriched my doctoral experience.

I want to thank Prof. med. Heribert Schunkert, Prof. med. Peter Ewert, and PD Dr. Dr. med. Christian Meierhofer for their professional and medical expertise, which greatly impacted my doctoral journey. Their willingness to offer help and guidance was invaluable in aligning my technical solutions more closely with clinical needs.

My colleagues at the IFL and DHM deserve special credit for their collaborative spirit and the fun we shared, from CAMPings to our conference experiences in Singapore, United States, and Canada. Their encouragement and assistance in pushing me to excel professionally and personally have been invaluable.

My brother, Joni, has been a pillar of support throughout this doctoral journey, showing immense pride in my work and always ready to help in any way he could. Whether through reading my papers, providing constructive feedback, or simply offering words of encouragement, his involvement has been a true blessing.

While my beloved parents might not understand the entirety of this dissertation, mainly due to the language in which it is written, I am confident in their pride in my accomplishment. Therefore, I have included their acknowledgment in our native Albanian language to express my gratitude.

To my beloved parents, whose support has been unwavering. To my father, Xhavit, an academic and mentor, whose curiosity about my work and eagerness to exchange ideas on teaching and writing has been a source of inspiration. To my mother, Valbona, whose interest in my

well-being and progress in my career has provided me with love, comfort, and motivation. Your tremendous help and love has been the backbone of my doctoral journey. I am eternally grateful for everything you have done!

Për prindërit e mi të dashur, të cilët më kanë mbështetur pa rezerva. Për babain tim, Xhavitin, një akademik dhe mentor, i cili ka treguar kuriozitet për punën time dhe ka pasur dëshirë të ndajë gjithmonë ide rreth mësimdhënies dhe shkrimit, ka qenë burim frymëzimi për mua. Për nënën time, Valbonën, e cila ka treguar interes për mirëqenien dhe përparimin tim në karrierë, më ka ofruar dashuri, qetësi dhe motivim. Ndihma dhe dashuria e juaj e madhe ka qenë shtylla kryesore e udhëtimit tim akademik. Jam përgjithmonë mirënjohës për gjithçka që keni bërë!

Last but not least, to my beloved wife, Krenare, for your love, endless support, selflessness, and care, which have been beyond measure not only throughout this doctoral journey but always. Your constant presence and belief in me have been a cornerstone of my success, and I am incredibly thankful for your role in my life and career. I am very proud of your accomplishments, for the person you are, and for your glow of love and kindness. Love you!

Thank you all for your part in this doctoral journey. Your support means more to me than words can express. I hope to have you all in good health, and cheers to future challenges!

"A person engages in science throughout their entire life. In childhood, they learn; in youth, they apply this knowledge; and as they get older, they teach and share it with others."

"Njeriu merret me dituri dhe me shkencë gjatë gjithë jetës së tij. Në fëmijëri i mëson ato, në rini i vë në zbatim e në pleqëri ua mëson të tjerëve."

– Sami Frashëri

Acronyms

A

AAA Abdominal Aortic Aneurysm.

ASD Atrial Septal Defects.

C

CAD Coronary Artery Disease.

CPD Coherent Point Drift.

CT Computed Tomography.

CTA Computed Tomography Angiography.

D

DoF Degrees of Freedom.

DSA Digital Substraction Angiography.

DTW Dynamic Time Warping.

E

ECG Electrocardiogram.

EM Electromagnetic.

EP Electrophysiology.

EVAR Endovascular Aneurysm Repair.

F

FBG Fiber Bragg Grating.

FFT Fast Fourier Transform.

fMRI Functional Magnetic Resonance Imaging.

FOSS Fiber Optic Shape Sensing.

G

GPS Global Positioning System.

GT Ground-truth.

I

ICP Iterative Closest Point.

IV Intravenous Line.

IVUS Intravascular Ultrasound.

L

LAD Left Anterior Descending.

LCA Left Coronary Artery.

LCx Left Coronary Circumflex.

M

MIS Minimally Invasive Surgery.

MME Mean Minimum Error.

MRA Magnetic Resonance Angiography.

MRI Magnetic Resonance Imaging.

MSS Magnetic Stereotaxis System.

P

PAD Peripheral Arterial Disease.

PCI Percutaneous Coronary Interventions.

PDA Posterior Descending Artery.

PET Positron Emission Tomography.

PLV Posterior Left Ventricular.

R

RCA Right Coronary Artery.

RF Radio Frequency.

RI Ramus Intermedius.

RMSE Root Mean Square Error.

S

SIRT Selective Internal Radiation Therapy.

SPECT Single-Photon Emission Computed Tomography.

SVD Singular Value Decomposition.

T

TACE Transarterial Chemoembolization.

TAVI Transcatheter Aortic Valve Implantation.

TEE Transesophageal Echocardiography.

U

US Ultrasound.

V

VCP Ventricular Catheter Placement.

Contents

Part I

Introduction

Introduction 1

The growing focus in minimally invasive surgeries is driven mainly by its significant benefits for patients and surgeons. This transition towards less invasive surgical procedures has led to the development of new surgical approaches and the reassessment of traditional procedures. Notably, minimally invasive surgery has played a crucial role in the introduction of endovascular procedures – procedures that involve accessing targeted anatomies via the vascular system to perform diagnostics or treatment, such as in the heart, liver, or brain [4].

The transition from traditional to minimally invasive procedures is not without its challenges. Physicians must learn new techniques and face technical challenges related to the medical instruments used in such procedures. These challenges include issues with the reusability of instruments, their manipulation, need for precise hand-eye coordination, and the complexities of tracking and navigating medical instruments within the body [54, 154].

Minimally invasive endovascular procedures are typically guided through fluoroscopy, and utilize a contrast agent to enhance the visibility of the vascular system. However, the guidance through fluoroscopy presents concerns due to the exposure to ionizing radiation, which is known to be a risk factor for developing cancer. This affects not only patients but also the physicians who are exposed to radiation regularly during these procedures [89, 176].

Despite advancements that have reduced radiation exposure in minimally invasive endovascular procedures, the risk associated with it remains significant. There is a clear need to improve imaging modalities used in these procedures for better visualization of medical instruments and anatomical region of interest. The goal is to reduce or even eliminate radiation exposure, thus enhancing the safety of these procedures without compromising their effectiveness.

The increasing reliance on minimally invasive endovascular procedures underscores their importance as the new standard in many medical applications. As such, the ability to accurately visualize, track, and guide medical instruments with minimal radiation exposure is becoming increasingly crucial. This need drives the ongoing research and development to find safer and more effective ways to conduct these procedures.

Robotic, automatized, intelligent, and multimodal catheter tracking technologies represent the future of minimally invasive endovascular procedures. These advancements promise to enhance precision and efficiency while ensuring patient safety and reducing radiation exposure [154]. As tracking technologies evolve, there is a critical need for improved accuracy and integration with advanced imaging modalities. These innovations must maintain the principles of minimally invasiveness and low radiation exposure. The tracking aspect of medical instruments in these procedures is vital, and the future undoubtedly lies in intelligent, robotic, automated, and patient-centirc solutions.

1.1 Problem Statement

The introduction of minimally invasive surgery, particularly catheter-guided endovascular procedures, have introduced a few challenges. Typically, these procedures involve the use of flexible instruments such as catheters and guidewires, which can be challenging to properly visualize, track, and navigate. These instruments vary in stiffness, shape, and form and are designed for specific applications and targeted anatomies [3].

Some of the main challenges in catheter-guided endovascular procedures are the visualization, tracking, and navigation aspects of the instruments, particularly the ability to visualize and accurately identify its location, which involves the imaging aspect of the procedure. Commonly, these procedures rely on fluoroscopy for guidance, exposing both the patient and the surgeon to radiation [89, 176]. Furthermore, such intraoperative imaging modalities are not ideal, primarily because they lack 3D representation. They also struggle to effectively visualize complex 3D vascular systems in 2D intraoperative images and, most critically, require physicians to mentally map these 2D intraoperative images into the 3D anatomical structures they are navigating, adding significant cognitive load and potential for error [195].

Another important area of research in this field concerns the accurate localization and tracking of the catheter tip within these images. Whether it involves image-based tracking or integrating other tracking technologies into the procedure, numerous technical challenges must be addressed for these procedures to succeed. One such challenge is the registration process, which ensures all components are accurately aligned within the same coordinate system [99, 154, 198]. Typically, these processes can be cumbersome and may change the standard workflow of the procedure, making it difficult for some physicians to adapt. As a result, translating technical advancements into clinical practice can sometimes be challenging.

1.2 Motivation

As highlighted in the previous section, catheter-guided endovascular procedures currently face numerous challenges. These include a steep learning curve associated with instrument manipulation, the visualization and mental mapping of 2D intraoperative images to 3D anatomical structures, and the integration of tracking technologies and registration procedures. Despite significant time and research invested in developing various methods and approaches to address these issues, insights collected from numerous catheterization laboratory (cath lab) visits and discussions with physicians indicate that considerable work still needs to be done.

On the one hand, from a technical perspective, there have been significant advancements in catheter tracking technologies, which could offer very intuitive guidance within the cath lab. However, these technologies have yet to be fully adopted and utilized in most clinical practices. According to the literature, several factors may restrict this translation into routine clinical use. These factors include the novelty of the method, ease of integration into existing systems, user-friendliness, cost, and the necessity for close collaboration with physicians to ensure the technology meets practical needs effectively [54, 74, 154].

Therefore, the primary motivation for this doctoral journey was to closely analyze the state-of-the-art in catheter-guided endovascular procedures and to observe numerous clinical practices to gain a more in-depth understanding of the current technologies. Additionally, driven by this research question, the motivation was to identify potential problems and develop ideas to facilitate the transition of these technologies into clinical practice. This could be achieved by bridging the gap between researchers and physicians, better understanding clinical needs, improving the technologies themselves, or developing strategies for easier integration.

1.3 Aim and Objectives

Throughout this research into the challenges of catheter-guided endovascular procedures, numerous gaps were identified within the current state-of-the-art methods. A few important challenges with integrating these tracking technologies involved their efficiency, accuracy, and translation into clinical practice. Consequently, the aim of this dissertation is manifold: (1) Gain a comprehensive understanding of the latest trends in catheter-guided endovascular procedures, including examining existing tracking technologies, ongoing research, and their clinical application; (2) Conceptualize a comprehensive overarching pipeline that would simplify the development and integration of such technologies into the clinical practice. Last, through this collective knowledge and following closely the pipeline mentioned above, (3) develop innovative methods to facilitate the process of catheter tracking in endovascular procedures and its translation into clinical practice.

In order to fulfill the aim of this project, considerable effort was put across various fronts, including research, clinical visits, and extensive discussions with physicians and industry representatives. These investigations helped refine the project's aim into distinct objectives, allowing for precisely measuring the success of each point. While the depth of research on each topic could potentially stand as a separate doctoral project, this dissertation analyzes each aspect as thoroughly and comprehensively as possible, providing a wide-ranging and in-depth analysis of the challenges and solutions in catheter-guided endovascular procedures. For the scope of this dissertation, the following objectives are set and elaborated in detail:

- **Conduct a comprehensive survey**: Perform an exhaustive review of state-of-the-art catheter tracking concepts and methodologies for endovascular procedures, providing a thorough understanding of the current research and future trends.

- **Diversify the research focus**: Focus on various aspects of catheter tracking, including tracking methods, technologies, available products, integration with imaging modalities, ease of use, targeted anatomy, and their clinical applications.

- **Define a catheter-tracking pipeline**: Create a generalized framework or pipeline that could be adapted or accommodate modern catheter-guided endovascular procedures.

- **Examine pipeline components**: Analyze each component of the introduced pipeline by evaluating state-of-the-art methods available to fulfill each component's objective.

- **Identify research gaps**: Identify unanswered research questions from the state-of-the-art survey and clinical discussions, highlighting areas needing further research.

- **Focus on clinical translation**: Validate the clinical necessity for these research questions and implement solutions within the pipeline, emphasizing the importance of translating these solutions into clinical practice.

1.4 Contributions

The main contributions towards fulfilling the objectives and achieving the aim of this dissertation are outlined as follows. Several research areas have been studied throughout this doctoral journey leading to this dissertation. Firstly, an exhaustive state-of-the-art review of all catheter-tracking concepts and methodologies was conducted, which involved grouping and categorizing the various catheter-tracking technologies, fulfilling objectives one and two of this dissertation. This foundational work set the stage for subsequent contributions inspired by the current challenges and open research questions identified from the review.

Building on the foundational knowledge from the initial contribution and through extensive discussions with physicians about clinical needs, an overarching catheter-tracking pipeline has been introduced. This pipeline is designed to accommodate most catheter-guided endovascular procedures. Each component of this multi-faceted pipeline was then thoroughly analyzed by evaluating state-of-the-art methods for their completeness, accuracy, and ease of use. This analysis specifically addresses and fulfills objectives three and four of the dissertation.

Finally, two subsequent published contributions followed that primarily focused on developing new registration techniques for catheter-guided endovascular procedures. These new methods provide more accurate and intuitive solutions that could easily integrate into existing interventional workflows without disruptions, fulfilling the final objectives five and six of this dissertation.

Each scientific published contribution, including their titles, full list of authors, and abstracts, is presented in detail in the following section. This structured presentation demonstrates how, collectively, each work advances the field of catheter-guided endovascular procedures.

Medical Image Analysis (MedIA)

Ardit Ramadani[†,*], M. Bui[*], T. Wendler, H. Schunkert, P. Ewert, and N. Navab, "A Survey of Catheter Tracking Concepts and Methodologies," *Medical Image Analysis*, vol. 82, p. 102584, Nov. 2022, doi: 10.1016/j.media.2022.102584.

Abstract [© 2022 Elsevier. Reprinted with permission under CC BY 4.0.]
Catheter tracking has become an integral part of interventional radiology. Over the last decades, researchers have significantly contributed to theoretical and technical catheter tracking solutions. However, most of the published work thus far focuses on a single application or a single tracking technology. This paper provides an exhaustive review of the state-of-the-art for catheter tracking in general by analyzing significant contributions in this field. We first present a historical overview that led to catheter tracking and continue with a survey of leading tracking technologies. These include image-based tracking, active and passive tracking, electromagnetic tracking, fiber optic shape sensing, bioelectric navigation, robotic tracking solutions and hybrid tracking. As for imaging modalities, the focus is on x-ray based modalities, ultrasound, and magnetic resonance imaging. Finally, we review each tracking technology with respect to the imaging modality and establish the relation between the two and the underlying anatomy of interest.

IEEE Robotics and Automation Letters (RA-L), and IEEE/RSJ International Conference on Intelligent Robots and Systems (IROS 2023)

Ardit Ramadani[†,*], H. Maier[*], F. Bourier, C. Meierhofer, P. Ewert, H. Schunkert, and N. Navab, "Feature-Based Electromagnetic Tracking Registration Using Bioelectric Sensing," *IEEE Robotics and Automation Letters*, vol. 8, no. 6, pp. 3286–3293, Jun. 2023, doi: 10.1109/LRA.2023.3262988.

Abstract [© 2023 IEEE. Reprinted with permission.]
Catheter tracking is essential during minimally invasive endovascular procedures, and Electromagnetic (EM) tracking is a widely used technology for this purpose. When preoperative patient images are available, they can be used to guide EM-tracked interventions. However, a registration step between preoperative images and intraoperative EM tracking space is usually required. Most existing solutions for this registration process require manual interactions, which can add additional steps to the workflow. In this paper, a novel automatic feature-based registration method is proposed, based on electric sensing of vascular geometry by the catheter, also known as Bioelectric sensing. The technique employs the Bioelectric sensing capabilities of the catheter to identify vascular features, such as bifurcations, aneurysms, or stenosis. The known EM position of these features is then utilized to register the EM tracking space and the preoperative images. The registration is refined using iterative closest point (ICP) registration algorithms. Unlike existing solutions, the proposed method does not require external markers, interventional imaging, or additional surgeon actions, and hence does not impact the interventional workflow.

† – Corresponding Author
∗ – Equal Contribution

International Conference on Medical Image Computing and Computer Assisted Intervention (MICCAI 2023)

Ardit Ramadani†, P. Ewert, H. Schunkert, and N. Navab, "WarpEM: Dynamic Time Warping for Accurate Catheter Registration in EM-guided Procedures," in *Medical Image Computing and Computer Assisted Intervention – MICCAI 2023*, vol. 14226, pp. 802–811, Oct. 2023, doi: 10.1007/978-3-031-43990-2_75.

Abstract [© 2023 Springer Nature. Reprinted with permission. License number 5811030633568.]
Catheter tracking is essential during minimally invasive endovascular procedures, and Electromagnetic (EM) tracking is a widely used technology for this purpose. When preoperative patient images are available, they can be used to guide EM-tracked interventions. However, a registration step between preoperative images and intraoperative EM tracking space is usually required. Most existing solutions for this registration process require manual interactions, which can add additional steps to the workflow. In this paper, a novel automatic feature-based registration method is proposed, based on electric sensing of vascular geometry by the catheter, also known as Bioelectric sensing. The technique employs the Bioelectric sensing capabilities of the catheter to identify vascular features, such as bifurcations, aneurysms, or stenosis. The known EM position of these features is then utilized to register the EM tracking space and the preoperative images. The registration is refined using iterative closest point (ICP) registration algorithms. Unlike existing solutions, the proposed method does not require external markers, interventional imaging, or additional surgeon actions, and hence does not impact the interventional workflow.

1.5 Dissertation Structure

This dissertation is organized into four main parts, starting with (1) Introduction and Fundamental Concepts, followed by (2) Background Theory, (3) Methodology and Discussion, and (4) Conclusions and Future Work. The chapters of this dissertation are outlined as follow:

Chapter 2 delves into fundamental catheter tracking concepts and methodologies, providing readers with a comprehensive understanding of key terminologies within the domain. It explores catheter movement kinematics and manipulation techniques and then discusses the significance of registration procedures. Finally, it integrates these concepts with an overview of tracking systems and imaging modalities, offering a holistic perspective on their interconnections and importance in catheter-guided endovascular procedures.

Chapter 3 delves into the anatomy of the human body, focusing mainly on the systems and structures relevant to catheter-guided endovascular procedures. It provides detailed insights into the cardiovascular system, the heart, and various vascular and heart diseases. Additionally, the chapter explores related catheter-guided endovascular procedures, highlighting their significance in addressing these conditions.

† – Corresponding Author

Chapter 4 provides a detailed overview of a patient's journey during a clinical visit, specifically when dealing with cardiovascular issues requiring catheter-guided endovascular procedures. It begins with the patient's admission to the hospital and the necessary consultations. The chapter then outlines the subsequent cardiac examinations, including physical assessments and imaging techniques. It details the catheterization procedure, offering a comprehensive view of this journey.

Chapter 5 offers an exhaustive literature review on catheter-tracking concepts and methodologies. It begins by introducing the history of catheter-tracking technologies and then explains their classification. Each class is discussed in detail, focusing on tracking technology, state-of-the-art solutions, clinical applications, and integration with imaging modalities. This structured approach provides a deep understanding of the various aspects and advancements in catheter tracking.

Chapter 6 aims to familiarize the reader with the essential domain knowledge and principles of catheter tracking solutions. It begins by elaborating on tracking concepts and focuses on a catheter-tracking pipeline, highlighting the key characteristics an effective catheter-tracking technology should possess. Finally, one catheter tracking solution is proposed, based on the principles and characteristics discussed earlier, providing a practical framework for implementation.

Chapter 7 introduces one of the significant European projects undertaken during this doctoral journey, focusing on image-based catheter tracking solutions. First, the overall project is outlined with its procedural pipeline and key components, followed by an elaboration of the clinical trials. Most importantly, this chapter delves into the implementation details of the ultrasound image-based catheter tracking algorithm.

Chapter 8 discusses another important project, focusing on feature-based electromagnetic catheter tracking registration using bioelectric navigation. It begins by elaborating on the two tracking technologies individually and the proposed idea of leveraging their advantages through integration for easier registration. The integration methodology is thoroughly discussed, followed by a discussion of the evaluation criteria and presentation of the results.

Chapter 9 presents another significant contribution to the field of catheter-guided endovascular procedures, introducing a novel registration technique using electromagnetic tracking. It begins by reviewing related works on electromagnetic tracking and registration. Following this, the dynamic time warping algorithm, the main technique employed for registration, is presented. The chapter then delves into the methodology, followed by a discussion and the presentation of results.

Chapter 10 focuses on a conclusive discussion of multimodal catheter tracking concepts and methodologies for endovascular procedures. It provides an overall summary of the dissertation, highlighting the main contributions. Furthermore, it offers a perspective on the clinical translation and future outlook of catheter-guided endovascular procedures, emphasizing the technology's relevance and potential advancements.

Fundamentals 2

Explaining a few fundamental concepts and key terminologies within the domain is important to better understand catheter tracking concepts and methodologies. This dissertation primarily focuses on tracking technologies and concepts related to catheters, even though the techniques presented could also be relevant to other medical instruments for which similar tracking technology might be applicable. Additionally, this chapter discusses important topics such as a detailed exploration of navigation techniques specific to catheters, movement kinematics of catheters, endovascular procedure instruments, the process of registration, tracking systems, affine transformations, and the role of imaging in endovascular procedures.

2.1 Domain-specific Terminology

At the beginning of this fundamentals chapter, it is necessary to focus on some basic concepts and domain-specific terminology related to catheter concepts and methodologies. To fully understand the various procedures and movements catheters undergo in endovascular procedures, it is crucial to become familiar with a few keywords that are used interchangeably. The following fundamental concepts, such as visualization, detection, tracking, and navigation, must be clearly defined and described. These catheter-related terminologies are especially significant, as they originate from our paper contribution, "A Survey of Catheter Tracking Concepts and Methodologies" [154]. For the first time, these concepts have been clearly defined and articulated in the domain of catheter-tracking concepts and methodologies, offering a clear understanding of their representation.

2.1.1 Visualization

The first domain-specific terminology to elaborate in this dissertation is visualization. Visualization represents the ability to clearly see medical instruments in medical images, which is crucial for the success of endovascular procedures. Before digitizing medical images, physicians and engineers dedicated considerable time to selecting appropriate materials and shapes for medical instruments based on the specific imaging modality. Unique materials with distinct properties were essential for achieving optimal contrast and visualizing instruments like catheters, guidewires, and needles [154].

Traditionally, catheters and guidewires were made from flexible, soft metallic materials easily identifiable in x-ray and ultrasound. With technological advancements, modern catheters, and guidewires are constructed from polymers and coated with contrast-enhancing materials to improve their visibility [3]. Visualization refers explicitly to the clear perception of the medical instrument within the image, facilitating visual tracking but not providing information about the instrument's position or orientation. This concept dates back to the discovery of x-rays, enabling physicians to directly observe medical instruments within the human anatomy.

2.1.2 Detection

The following domain-specific terminology to explore is detection. Detection involves identifying the position and orientation of a medical instrument within a single frame of a medical image sequence. This step is vital in catheter tracking as it establishes the initial reference point for subsequent tracking calculations. Detection algorithms utilize various techniques to identify distinctive medical instrument features in images, ensuring accurate localization [154].

While detection primarily focuses on identifying the medical instrument in a single frame, it is closely linked to tracking. Tracking algorithms utilize the detection results from previous frames to estimate the instrument's position in subsequent frames. This continuous process enables real-time visualization and manipulation of the instrument within the anatomy [154].

In essence, detection lays the foundation for tracking, providing the initial position and orientation of the medical instrument, which tracking algorithms then refine and update over time. Together, these two processes enable precise navigation and manipulation of medical instruments during endovascular procedures [154]. A visual representation that highlights the differences between visualization and detection is presented in Fig. 2.1.

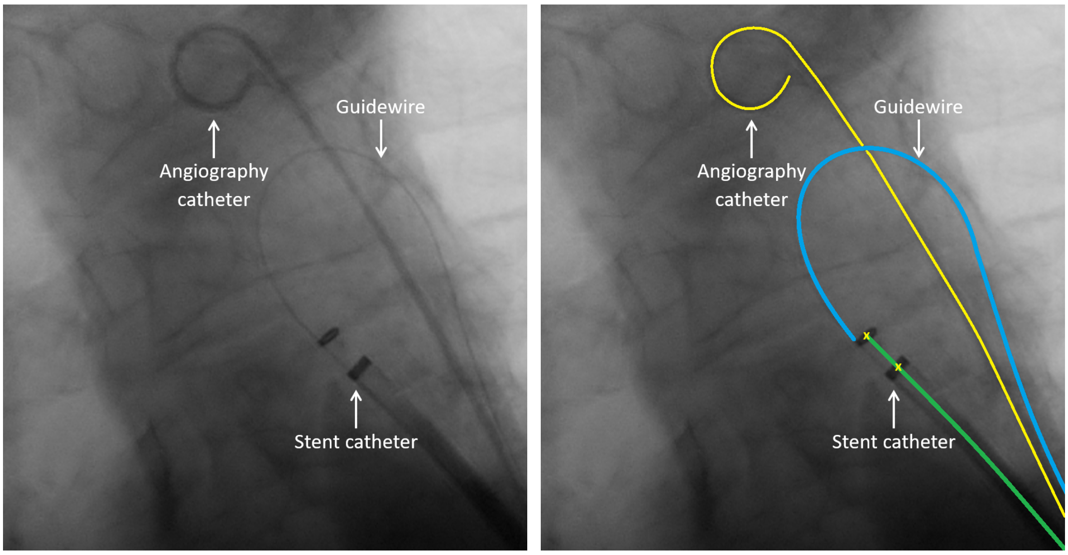

(a) (b)

Fig. 2.1. Fluoroscopic image during a minimally invasive endovascular procedure, showcasing multiple instruments. (a) Visualization of medical instruments, and (b) Image-based detection of instruments, color-coded to highlight the guidewire, angiography catheter, and stent catheter.

2.1.3 Tracking

The third domain-specific terminology to elaborate on is tracking. Tracking refers to identifying and continuously monitoring the position and orientation of a medical instrument within a medical image sequence. It builds upon the initial detection phase, quantitatively measuring the instrument's location and orientation over time. Tracking algorithms typically use various techniques to follow the instrument's trajectory, ensuring accurate and consistent localization throughout the procedure. This ongoing process is crucial for real-time navigation and guidance during endovascular procedures.

Tracking is significantly more complex than visualization, as it requires continuous monitoring and updating of the instrument's position. This computational intensity necessitates digitizing medical images, enabling the precise manipulation and analysis of image data. In essence, tracking combines visualization and detection, quantitatively measuring the instrument's location and movement over time. It is a crucial component of catheter navigation within endovascular procedures, enabling physicians to precisely guide the instrument to the desired region of interest [112, 154].

2.1.4 Navigation

The final domain-specific terminology to elaborate on is navigation. Navigation represents the ability to monitor, control, and guide the 3D movement of a medical instrument to a targeted region within the patient's anatomy. It involves sophisticated visualization, detection, and tracking integration, allowing physicians to precisely maneuver the instrument through the vascular system and reach specific anatomical structures [154]. This interplay ensures the instrument can be accurately directed to the desired region of interest, facilitating effective and efficient endovascular procedure.

Medical instrument navigation is critical to various minimally invasive endovascular procedures, enabling physicians to reach target areas with precision and safety. The evolution of navigation techniques, from manual to robotic control, has significantly improved patient outcomes and reduced the risk of complications.

2.2 Catheter Navigation Techniques

Catheter navigation techniques play a pivotal role in minimally invasive endovascular procedures. The introduction of fluoroscopy-enabled catheter navigation techniques allowed physicians to visualize instrument movements in real-time, facilitating precise control. Traditional manual catheter navigation techniques have become standard practice in endovascular procedures for decades. However, technological advancements have paved the way for robotic navigation systems that offer enhanced precision, dexterity, and control, significantly improving the effectiveness and safety of catheter-based endovascular procedures [152].

Push, Pull, Rotate, Pivot (Tip Bend): These are the four basic catheter navigation techniques used to guide catheters through the vascular system during endovascular procedures. Each technique has a specific purpose and is used in combination with the others to achieve precise catheter navigation. An illustration of the four basic catheter navigation techniques is presented in Fig. 2.2.

- **Push**: Pushing a catheter forward is the most common navigation technique. It is used to advance the catheter further into the vessel or to navigate through obstacles.
- **Pull**: Pulling a catheter backward is used to retract or manipulate it around tight curves.
- **Rotate**: Rotating a catheter allows for changing the direction of the catheter tip. This technique is often used to align the catheter tip with the desired target or to maneuver through obstacles.
- **Pivot (Tip Bend)**: Pivoting refers to the ability to bend the tip of a catheter in a specific direction. This technique is used to navigate catheters through vasculature branching or to access specific anatomical structures.

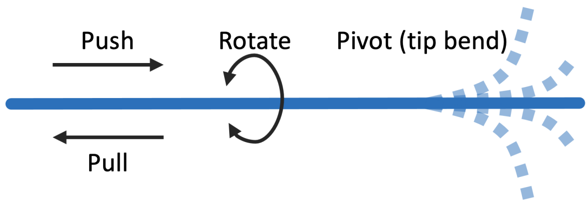

Fig. 2.2. Illustration of the four basic catheter navigation techniques: push, pull, rotate, and pivot (tip bend), essential for maneuvering catheters through vascular structures during endovascular procedures.

In most cases, catheter navigation involves a combination of these basic techniques. For example, physicians may push the catheter forward while rotating it simultaneously to guide it through a stenosis. The specific combination of techniques used will depend on the individual patient's anatomy and the specific goals of the procedure. In summary, the push, pull, rotate, and pivot (tip bend) techniques are the cornerstone of catheter navigation during endovascular procedures. By understanding and mastering these techniques, physicians can guide catheters precisely and accurately, ensuring successful procedure outcomes.

2.2.1 Catheter Movement Kinematics

Understanding catheter movement kinematics, particularly forward and backward movement, is essential for accurate navigation during endovascular procedures. Catheters and other minimally invasive endovascular instruments assume different shapes based on the direction of movement, a concept essential in modern catheterization laboratories (cath labs). For instance, when a catheter is pushed forward, it typically adheres to the vasculature wall, forming a more rigid and defined shape. Conversely, when pulled backward, it tends to straighten and become less constrained by the vasculature walls, sometimes even inducing deformations on the vasculature. In technical terms, these two states are called compression and tension, respectively illustrated in Fig. 2.3a and Fig. 2.3b [87].

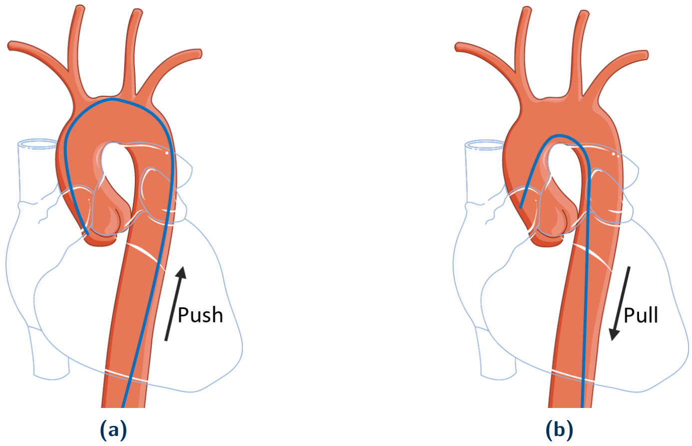

Fig. 2.3. Illustration of forward and backward catheter movement kinematics in the aortic arch. (a) Visualization of the catheter shape under compression when pushed in the aortic arch, and (b) Visualization of the catheter shape under tension when pulled in the aortic arch.

This distinction in shape is essential for physicians to interpret the catheter's position and orientation within the patient's anatomy. By analyzing the catheter's trajectory and the resulting shape changes, physicians can gain valuable insights into the catheter's interactions with the surrounding vasculature without needing a contrast agent for visualization. This information is crucial for navigationg the catheter accurately to the desired region of interest.

In addition to shape changes, the catheter's forward and backward movements influence its maneuverability within the vascular system. Pushing forward allows for further advancement into the vasculature, while pulling backward can help manipulate the catheter around bends. Understanding these kinematics enables physicians to adapt their navigation strategies accordingly, ensuring successful catheter navigation and procedure outcomes.

On the other hand, most recent applications focusing on registering the catheter shape attempt to predict the trajectory by relying on the vasculature's centerline. This approach results in higher registration errors and fails to depict the actual shape precisely. Consequently, understanding the forward and backward movements of catheter kinematics becomes crucial. This understanding helps accurately comprehend catheter trajectories and estimate their position within the vasculature more precisely.

2.3 Endovascular Instruments

Up to this point, this dissertation has discussed fundamental catheter-related terminology specific to the domain. Another essential aspect of catheter tracking concepts and methodologies involves the medical instruments used in endovascular procedures. These sophisticated procedures require navigating various instruments through the patient's vascular system using previously mentioned techniques. Therefore, beyond the techniques themselves, it is crucial to know the medical instruments employed in such procedures. This knowledge is vital for understanding the complexity and technical requirements of endovascular procedures.

The variety of medical instruments suitable for endovascular procedures is extensive, correlating with the numerous applications within the field. Each procedure typically employs a wide range of instruments, varying significantly depending on the targeted anatomy. The careful selection and use of these instruments allow physicians to perform tasks such as angioplasty, stenting, plaque compression, and clot extraction with enhanced safety and efficacy [84]. Illustrations of relevant endovascular instrument categories, including specific shape examples, are presented in Fig. 2.4. Below is an elaboration on the categories of instruments used in standard endovascular procedures.

- **Puncture needles**: are the initial instruments used in endovascular procedures to make a percutaneous incision. They enable the insertion of other instruments by creating an entry point into the vascular system. These needles are designed to be sharp and precise, ensuring minimal tissue trauma.

- **Sheaths**: are hollow tubes inserted into the vascular system following an initial incision. They serve dual functionality: allowing fluid injection while preventing blood from escaping and providing a conduit to easily exchange other medical instruments during the endovascular procedure.

- **Guidewires**: are flexible wires made of metal or polymer, essential for navigating complex vasculature pathways during endovascular procedures. Their primary function is to facilitate a navigation path for other endovascular instruments to follow.

- **Catheters**: are versatile instruments used for diagnostic and treatment purposes in endovascular procedures. They come in various designs and sizes, with some featuring steerable tips to navigate the vasculature more effectively. Catheters are used for procedures such as stenting, dilation, ablation, and grafting.

- **Contrast Injectors**: are specific catheters designed to inject contrast agent into the bloodstream, enhancing the visibility of the vasculature system during imaging.

- **Intravascular Ultrasound (IVUS)**: are specialized catheters equipped with a high-frequency ultrasound transducers that provide detailed, real-time images of the vasculature wall. These instruments are crucial for diagnosing and evaluating plaque build-up and vasculature wall degeneration.

As discussed above, this list includes some key categories of medical instruments used in endovascular procedures. The categories are listed based on the sequence of their use during a procedure. Initially, puncture needles are employed to make a percutaneous incision, facilitating the insertion of other instruments. Following this, a sheath is introduced. The sheath, a standard hollow tube of varying diameter, serves dual purposes: it acts as a one-way valve for fluid insertion and provides a channel for other instruments to access the targeted region of interest directly [84].

Once the sheath is in place, physicians utilize guidewires of various forms and shapes to navigate toward the region of interest. Guidewires, typically thin metallic or polymer wires, are designed to traverse complex vascular systems effortlessly. It is important to note that guidewires do not have a steerable tip; instead, the shape of the tip varies depending on the application [84]. Guidewires are usually navigated through pushing, pulling, and rotating techniques. Some standard guidewire shapes are illustrated in Fig. 2.4a.

Once the physician has reached the region of interest by alternating different guidewires and advancing the sheath surrounding the guidewire toward the target area, various catheters can be easily interchanged. Catheters are more advanced endovascular instruments with diagnostic and therapeutic capabilities, available in diverse tip shapes, diameters, and specific applications. Unlike guidewires, catheters can have steerable tips, allowing physicians to pivot the catheter in different directions during the procedure. There are numerous catheter types in cardiovascular applications, including stenting, dilating, ablating, and puncturing catheters [84]. Different catheter types and shapes are illustrated in Fig. 2.4b and Fig. 2.4c.

The next category of medical instruments used in endovascular procedures is contrast injectors. Due to their resemblance to catheters, these instruments are sometimes considered a subcategory of catheters. However, given their specific function, they are categorized separately in this dissertation. Contrast injectors are specialized instruments used to inject contrast agents into the vasculature, enhancing the visibility of vascular structures and blood flow dynamics for physicians. For instance, angiography catheters, a type of contrast injector, are often visually distinguished by their circular tip (pigtail). This distinctive shape helps physicians quickly identify and differentiate them from other endovascular instruments during procedures [84]. An example of an angiography catheter is shown in yellow in Fig. 2.1b.

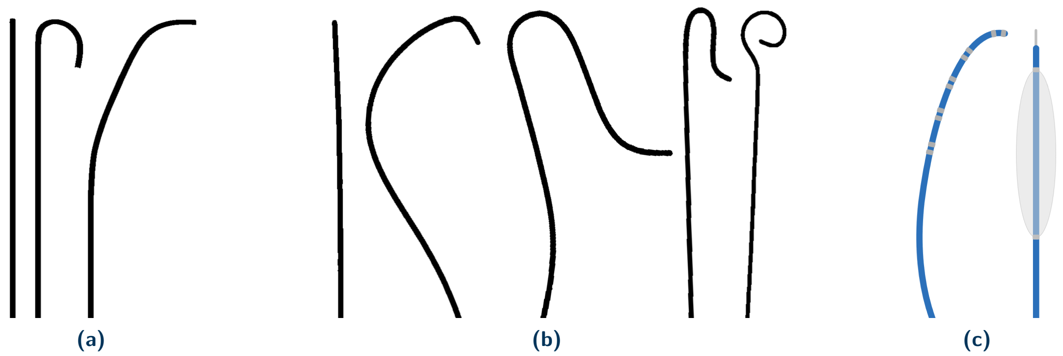

Fig. 2.4. Illustration of standard endovascular instrument shapes used in modern catheterization laboratories. (a) Standard guidewire shapes, ranging from straight to slight tip bends, (b) Application-specific catheter shapes, ranging from straight to typical bends for easy access in specific vascular branches, and (c) Electrophysiology catheter with multiple electrodes inscribed towards the tip, along with an angioplasty catheter for enlarging narrow vascular openings.

The final category of minimally invasive endovascular instruments is Intravascular Ultrasound (IVUS). These highly specialized instruments are crucial for imaging, diagnostics, and treatment from within the vasculature. IVUS catheters are equipped with an array of piezoelectric elements at their tips, which generate high-frequency, high-resolution, 360-degree images of the vasculature lumen. These versatile instruments are invaluable in modern cath labs for identifying various vascular conditions, including vascular lumen degeneration, plaque buildup, and calcification, thereby providing detailed insights into vascular health [75, 84].

Guidewires and catheters are the primary focus of most current research applications for tracking medical instruments in endovascular procedures. This dissertation similarly emphasizes the tracking of catheters and guidewires. However, it is important to note that some tracking techniques can be applied to other categories of endovascular instruments. For example, ultrasound image-based tracking is commonly used to guide puncture needles. Due to the complexity of procedures involving guidewires, especially catheters, these categories are prioritized in research and development efforts.

2.4 Registration

Registration is a fundamental process in medical imaging that involves aligning or superimposing two or more medical images to align corresponding anatomical structures. This alignment is crucial for a variety of applications, including:

- **Image Fusion**: Combining images from different modalities, such as Computed Tomography (CT) and Positron Emission Tomography (PET), to gain a comprehensive overview of the patient's anatomical and physiological state.
- **Catheter Navigation**: Aligning preoperative and real-time intraoperative images to guide instruments during endovascular procedures. Also, registering different tracking technologies for more accurate catheterization.

Registration techniques can be broadly classified into two categories: rigid registration and deformable registration. Rigid registration assumes that the two images have undergone a simple affine transformation. Deformable registration, conversely, can handle more complex deformations, such as those caused by organ movement or breathing [71, 139, 167].

2.4.1 Catheter Registration

In catheter navigation techniques, registration is often used to align the catheter's trajectory with the patient's anatomy and, in some cases, with the preoperative/intraoperative images. This alignment ensures the catheter is visualized in the same reference frame and facilitates accurate navigation to the region of interest. Registration is a critical tool in medical imaging, enabling physicians to combine images from different modalities, plan interventions, and navigate catheters with precision and accuracy.

Regarding catheter registration, multiple approaches exist to register the catheter with the patient and their preoperative/intraoperative images. Each approach introduces advantages and disadvantages, and the one employed depends significantly on the specific clinical application. One specific approach for registration is using external markers on the skin, which can be advantageous for its simplicity but may lack precision for endovascular procedures [115, 119, 124]. Another approach involves using external anatomical landmarks on the patient, offering more reliable accuracy but still limited.

Since the focus in this field is mainly on vasculatures inside the patient's anatomy, without direct internal access, some of the more advanced techniques for registration include utilizing the curvature and shape of the vasculature for registration [104, 135]. This approach leverages the unique anatomical features within the vascular system, allowing for precise catheter alignment within the internal structures.

Some of the algorithms implemented for such a registration approach mainly record the catheter's path or shape, and using an Iterative Closest Point (ICP) algorithm, for example, try to minimize the catheter's shape to the centerline of the vasculature. Other implementations may consider internal vascular features or the vessel wall for registration [91, 156]. Nevertheless, the end goal in all implementations is to achieve accurate registration between all the components. This ensures that the catheter's position is precisely mapped to the patient's anatomy, enhancing the safety and efficacy of the endovascular procedure.

2.5 Tracking Systems

In the field of minimally invasive endovascular procedures, tracking systems play a crucial role in determining the location and orientation of medical instruments in space. They are essential for various applications, including navigation, robotics, and medical imaging device positioning. A tracking system typically consists of three components: a sensor that measures the object's position and/or orientation, a reference frame that provides a fixed reference point, and a computational algorithm that processes the sensor's data and determines the object's pose [54, 154]. Nevertheless, other tracking systems exist that can be integrated only through image-based solutions, which are not necessarily composed of these components. Since we have a complete chapter on tracking technologies for catheter-based endovascular procedures (Chapter 5: Literature Review), we will dive deeper into other important aspects within this chapter.

2.5.1 Degrees of Freedom

The term Degrees of Freedom (DoF) refers to the number of independent fundamental movements a rigid object can perform within 3D space. There are six DoF for a rigid object in 3D space. These six DoF can be categorized into two types: translational and rotational [191].

- **Translational movement**: refers to linear and non-rotational movement. The three DoF associated with translation corresponds to movement along a coordinate system's x, y, and z axes. These can be visualized as moving forward/backward, left/right, and up/down [191].

- **Rotational movement**: is the opposite of translational movement, where the object rotates about an axis without linear displacement. The three DoF associated with rotation correspond to rotations around the x, y, and z axes, commonly referred to as pitch, yaw, and roll [191].

It is important to note that not all objects can be manipulated in six DoF. A typical catheter, for instance, has limited DoF. This typically includes the ability to move forward/backward, bend the tip, and rotate along the direction of movement. Catheter tracking technologies can often track the tip in five or six DoF. This means they can track translational movements along any axis and rotational movements around the x, y, and z axes. However, some tracking technologies may not be able to detect rotation along the direction of catheter movement.

2.5.2 Affine Transformations

Understanding the various types of affine transformations is fundamental in many fields, including computer graphics and medical imaging. These transformations include identity, mirror, translation, scale, rotation, and shear. Through the use of homogeneous coordinates, it is possible to express each transformation type within a matrix format. In 3D space, transformations of an object convert point $P = (x, y, z)$ to $P' = (x', y', z')$ using transformation matrix $T_{4\times4}$. All affine transformations adhere to the formula $P' = T \times P$. If there is a need to apply more than one transformation to the object, this can be achieved using the same formula multiple times. However, the sequence in which transformations are applied matters, as they do not follow commutative properties [191].

Affine transformations play a critical role in catheter tracking solutions because preoperative/intraoperative images, the patient, or the tracking system must be registered through different transformations. Thus, it is crucial to understand and be able to transform any of these components through affine transformations to register them in the same coordinate space. A visual representation of each transformation is presented in Fig. 2.5.

Identity

The identity transformation represents the most fundamental matrix, resulting in no changes to the object in 3D space. The identity transformation is represented by the following homogeneous matrix [191].

$$I = \begin{bmatrix} 1 & 0 & 0 & 0 \\ 0 & 1 & 0 & 0 \\ 0 & 0 & 1 & 0 \\ 0 & 0 & 0 & 1 \end{bmatrix} \tag{Identity}$$

Mirror

The mirror transformation involves reflecting an object in 3D space across any axis plane. This means a point can be mirrored around the xy, yz, and zx axis planes [191].

$$M_{xy} = \begin{bmatrix} 1 & 0 & 0 & 0 \\ 0 & 1 & 0 & 0 \\ 0 & 0 & -1 & 0 \\ 0 & 0 & 0 & 1 \end{bmatrix} M_{yz} = \begin{bmatrix} -1 & 0 & 0 & 0 \\ 0 & 1 & 0 & 0 \\ 0 & 0 & 1 & 0 \\ 0 & 0 & 0 & 1 \end{bmatrix}$$

$$M_{zx} = \begin{bmatrix} 1 & 0 & 0 & 0 \\ 0 & -1 & 0 & 0 \\ 0 & 0 & 1 & 0 \\ 0 & 0 & 0 & 1 \end{bmatrix} \tag{Mirror}$$

Translation

Translation is the process of translating (shifting) an object in 3D space from $P = (x, y, z)$ to $P' = (x', y', z')$. The translation vector $\vec{t} = (t_x, t_y, t_z)$ denotes the amount of movement along each axis [191].

$$T_{(t_x,t_y,t_z)} = \begin{bmatrix} 1 & 0 & 0 & t_x \\ 0 & 1 & 0 & t_y \\ 0 & 0 & 1 & t_z \\ 0 & 0 & 0 & 1 \end{bmatrix} \tag{Translation}$$

Scale

Scaling refers to modifying an object's size, allowing for either expansion or compression in 3D space. The scaling vector $\vec{s} = (s_x, s_y, s_z)$ indicates the scaling factor along each axis. For uniform scaling, the condition $s_x = s_y = s_z$ must be met. An object is expanded when $s_x, s_y, s_z > 1$ and compressed when $0 < s_x, s_y, s_z < 1$ [191].

$$S_{(s_x,s_y,s_z)} = \begin{bmatrix} s_x & 0 & 0 & 0 \\ 0 & s_y & 0 & 0 \\ 0 & 0 & s_z & 0 \\ 0 & 0 & 0 & 1 \end{bmatrix} \tag{Scaling}$$

Rotation

Rotation involves altering the position of an object in 3D space, with rotation matrices turning the object around a specific axis by an angle θ. Negative values represent clockwise rotations, while anti-clockwise rotations take positive values. The points undergo rotation around the x, y, and z axis, respectively [191].

$$R_x(\theta) = \begin{bmatrix} 1 & 0 & 0 & 0 \\ 0 & \cos\theta & -\sin\theta & 0 \\ 0 & \sin\theta & \cos\theta & 0 \\ 0 & 0 & 0 & 1 \end{bmatrix} R_y(\theta) = \begin{bmatrix} \cos\theta & 0 & \sin\theta & 0 \\ 0 & 1 & 0 & 0 \\ -\sin\theta & 0 & \cos\theta & 0 \\ 0 & 0 & 0 & 1 \end{bmatrix}$$

$$R_z(\theta) = \begin{bmatrix} \cos\theta & -\sin\theta & 0 & 0 \\ \sin\theta & \cos\theta & 0 & 0 \\ 0 & 0 & 1 & 0 \\ 0 & 0 & 0 & 1 \end{bmatrix} \qquad \text{(Rotation)}$$

Shear

The shear transformation modifies the shape of an object by skewing it along one axis in 3D space, often referred to as a deformable transformation. Shear can act in three directions within 3D space, leading to object distortion when applied. Nevertheless, the parallelism of lines is maintained. The parameters (c, e) denote the shear units along the x axis, (a, f) along the y axis, and (b, d) along the z axis [191].

$$S_{(a,b,c,d,e,f)} = \begin{bmatrix} 1 & a & b & 0 \\ c & 1 & d & 0 \\ e & f & 1 & 0 \\ 0 & 0 & 0 & 1 \end{bmatrix} \qquad \text{(Shear)}$$

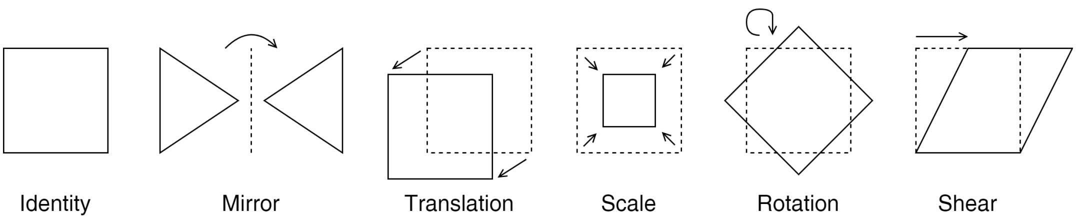

Fig. 2.5. Illustration of the basic affine transformations. The transformations shown include: identity, mirror, translation, scale, rotation, and shear. This illustration demonstrates how each transformation manipulates the 2D shapes within the context of affine geometry.

2.6 Imaging

In the context of medical imaging, this dissertation addresses two key distinctions. Initially, the focus is on the differences between cross-sectional and projection imaging. Cross-sectional imaging is particularly interesting for preoperative diagnostics (ultrasound being an exception), while projection imaging is more relevant for intraoperative procedures. Furthermore, an emphasis is placed on highlighting some of the most common imaging modalities and their classifications, applicable to both preoperative and intraoperative procedures.

2.6.1 Cross-sectional and Projection Imaging

Cross-sectional imaging and projection imaging are two fundamental approaches to medical imaging, each providing unique insights into the human body. Cross-sectional imaging, also known as tomographic imaging, generates images of the body in thin slices, allowing for detailed analysis of internal structures. This technique is used in various imaging modalities, such as Computed Tomography (CT) and Magnetic Resonance Imaging (MRI) [12, 67, 151].

Projection imaging, on the other hand, generates images of the body in a single plane, typically perpendicular to the patient's body. Examples of projection imaging modalities include x-ray radiography and fluoroscopy. These modalities provide valuable information about the overall structure and relationship of anatomical structures within a specific plane [12, 151].

In minimally invasive catheter-guided endovascular procedures, projection imaging devices are more commonly utilized because they provide a comprehensive overview of the relationship between the catheter and anatomical structures. In some endovascular procedures, two projection imaging devices might be employed to obtain two distinct viewpoints, enhancing the anatomical comprehension [12, 151].

On the other hand, cross-sectional imaging is primarily used for planning and diagnostic purposes, as well as for gaining a better understanding of the 3D anatomical structure around the region of interest [12, 67]. An exception is noted for ultrasound, which, despite its ability to produce cross-sectional imaging, is increasingly being used as a less invasive option (in terms of radiation exposure) for catheter-guided endovascular procedures.

2.6.2 Classification of Imaging Modalities

In the field of medical imaging, categorizing imaging modalities based on their underlying principles and the type of information they provide is essential for understanding their applications and capabilities. These imaging modalities are commonly divided into two main categories: structural and functional imaging [151].

Structural imaging techniques, such as x-ray radiography, CT, and MRI, generate detailed images of the body's anatomy, revealing the shape, size, and position of organs and tissues. These modalities are crucial for diagnosing various medical conditions and guiding endovascular procedures. Functional imaging techniques, such as Positron Emission Tomography (PET), Single-Photon Emission Computed Tomography (SPECT), and Functional Magnetic Resonance Imaging (fMRI), measure the body's physiological processes and metabolic activity. They provide information about how organs and tissues function, aiding in assessing disease progression and treatment response [12, 151].

Medical imaging modalities can also be classified based on their invasiveness, particularly in terms of radiation exposure. More invasive imaging modalities include those that utilize x-rays and radioactive agents, such as CT scans and nuclear medicine. In contrast, non-invasive imaging modalities, such as ultrasound and MRI, do not expose patients to ionizing radiation, making them safer alternatives for repeated use [12, 151].

Another way to classify imaging modalities is based on their use in preoperative versus intraoperative settings. However, the distinction between these two categories is becoming increasingly blurred. Nowadays, nearly all imaging modalities can be used intraoperatively, with the primary consideration being the time required for image acquisition. Recent trends and advancements in imaging modalities have steadily reduced acquisition times, making it feasible to use a wide range of imaging modalities intraoperatively [12, 151].

For catheter-guided minimally invasive endovascular procedures, various imaging modalities can be utilized. However, there are several key requirements to consider when choosing a specific imaging modality, including but not limited to acquisition time, radiation exposure, ease of use, and compatibility with clinical application. Some of the most frequently utilized imaging modalities in catheter-guided endovascular procedures, selected based on specific clinical requirements, balancing factors like imaging speed, patient safety, and the detailed visualization needed for effective intervention.

Ultrasound

Ultrasound is a non-invasive imaging modality utilized intraoperatively. It emits high-frequency sound waves to capture real-time images of internal organs or soft tissues, including vasculature. Ultrasound is particularly advantageous for catheter tracking due to its broad availability in clinical practices, user-friendliness, and the distinct contrast it provides of vascular structures. An ultrasound system along with some exemplary images are presented in Fig. 2.6. A notable limitation of ultrasound is its significant dependence on both the operator and the device, which can affect the consistency and quality of the imaging results [151].

Physicians may employ ultrasound for procedures where precision and real-time guidance are crucial. Ultrasound is frequently used to guide the placement of puncturing needles or catheters during endovascular procedures. Typically, physicians opt for handheld external ultrasound devices for tracking catheters or Transesophageal Echocardiography (TEE) to obtain visualizations of catheters and other medical instruments within the heart. Ultrasound-guided catheter procedures can also integrate with robotic systems, enabling automatic tracking of the catheter tip [92, 151]. Advances in technology now allow for compounding 2D ultrasound images and rendering real-time 3D volumetric images. These 3D volumetric images provide significantly detailed information, enhancing the effectiveness of intraoperative procedures.

Another approach to ultrasound imaging used in interventional procedures is IVUS. As explained earlier, this imaging modality typically incorporates a very thin, short, high-frequency ultrasound array at the tip of a catheter. The IVUS catheter is inserted into the patient's vascular system similarly to a standard catheter. Once inserted, it is pushed or pulled to provide a 360-degree visualization of the vascular wall structure. IVUS is frequently utilized to assess the severity of plaque buildup inside arteries [75]. A similar approach is being developed by LUMA Vision[1] (Munich, Bavaria, Germany), which involves automatically rotating the catheter tip at high speeds to reconstruct 3D volumetric ultrasound images of the heart. This advanced technique aims to enhance the accuracy and efficiency of cardiac imaging.

[1] www.lumavision.com

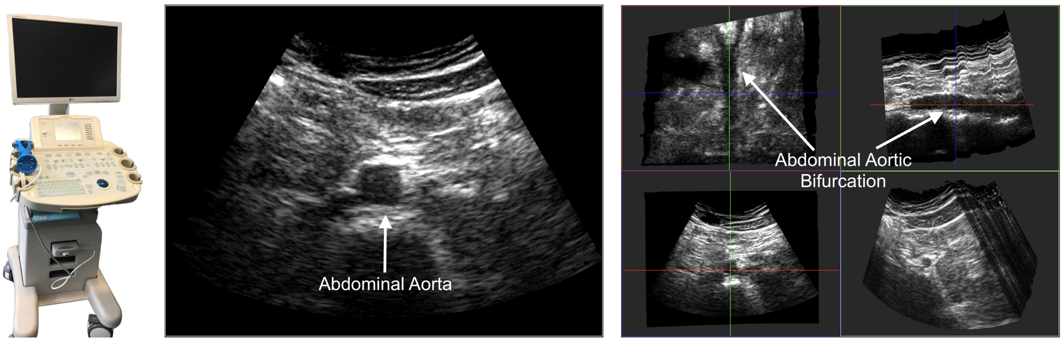

(a) (b) (c)

Fig. 2.6. The Ultrasound imaging modality with exemplary images. (a) An ultrasound device used for preoperative/intraoperative imaging, (b) A 2D cross-sectional ultrasound image of the abdominal aorta, and (c) Robotically tracked 2D ultrasound images compounded into a 3D volume, displaying three anatomical planes and the abdominal aortic bifurcation.

Fluoroscopy

Fluoroscopy is an interventional imaging modality that enables the continuous transmission and visualization of x-ray images on a monitor, typically positioned in front of the physician. In a fluoroscopic-guided procedure, x-rays are generated from a source and pass through the patient's body to be captured by a detector. The resulting images are then displayed on a monitor, allowing for real-time visualization of catheters, guidewires, and other minimally invasive medical instruments as they move within the body [12, 151]. Fluoroscopes, often integral to cath labs, usually feature a C-arm design. An image of a robotic C-arm fluoroscope is presented in Fig. 2.7a. In specific setups, they may be mounted on the ceiling of the cath lab and can include dual C-arm systems. These dual systems provide images from two distinct viewpoints, offering physicians the ability to observe and navigate medical instruments from different angles, enhancing the precision and safety of the procedure.

Recent trends in fluoroscopic imaging emphasize the mobility of C-arm devices, which now vary in shape and size to accommodate different clinical application needs. In a fully integrated system, fluoroscopic imaging systems should facilitate the automatic tracking of catheter movement, and adjusting the viewing angle to optimize visualization. Advancements in this imaging modality are pursued by numerous companies in the medical field. Notably, the system developed by Brainlab AG[2] (Munich, Bavaria, Germany) exemplifies such innovation. Their Loop-X device not only generates fluoroscopic images for interventional use but also incorporates movement and tracking capabilities of the device, showing a notable advancement in the field. A visual representation of the system is shown in Fig. 2.7b.

Angiography

Angiography is a specialized medical imaging technique to visualize the inside volume of vascular structures, focusing mainly on arteries, veins, and heart chambers. Like fluoroscopy, angiography employs a C-arm imaging modality for imaging. However, a key difference is introducing a radio-opaque contrast agent into the bloodstream prior to imaging. This contrast agent enhances the visibility of the vasculature, providing a clearer distinction in the images.

[2] www.brainlab.com

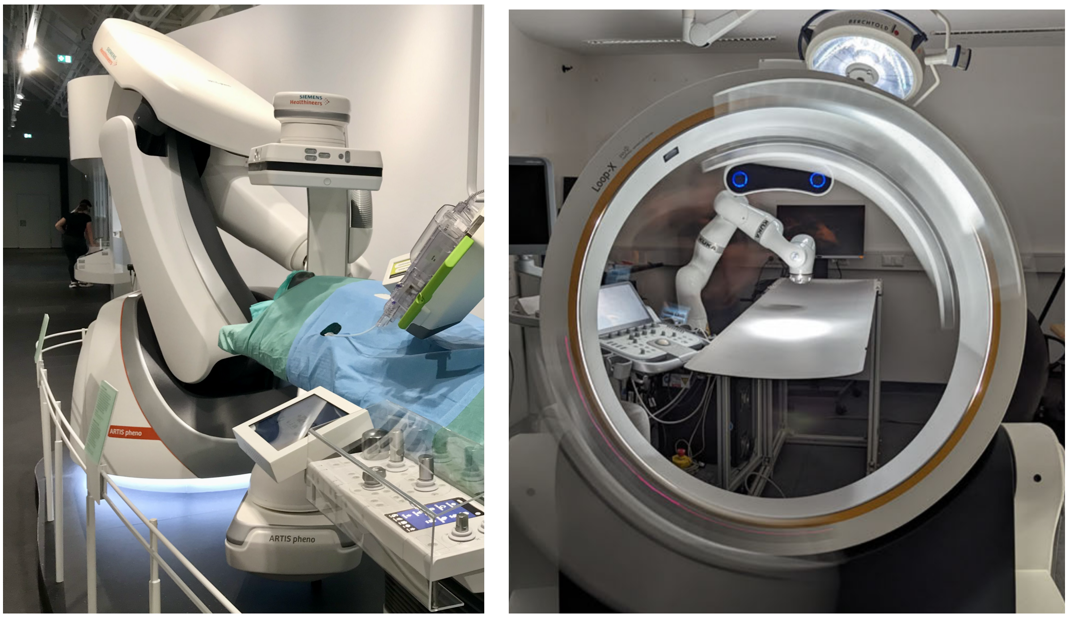

(a) (b)

Fig. 2.7. Fluoroscopic imaging modalities used in modern catheterization laboratories. (a) Robotically controlled C-arm fluoroscope from Siemens, and (b) Loop-X, a circular-shaped fluoroscope from Brainlab AG, capable of capturing cone-beam CTs.

Unlike fluoroscopy, angiography requires a higher dose of x-rays and yields higher-resolution images. This allows for more precise visualization of the vascular structures and identifying potential stenosis, offering critical insights for diagnostic and therapeutic planning [12, 151]. Captured differences between a standard fluoroscopic image and angiograph with visualized vasculature structures are presented in Fig. 2.8.

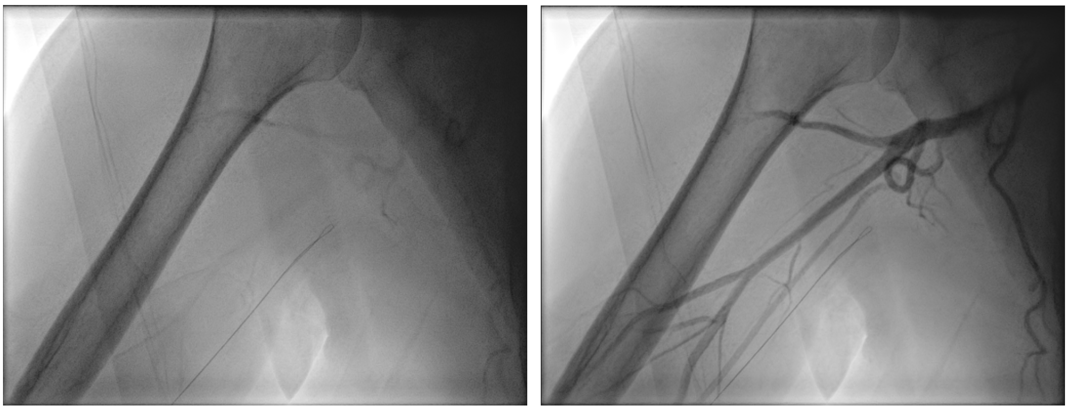

(a) (b)

Fig. 2.8. Fluoroscopic image and Angiograph captured during a minimally invasive endovascular procedure near the right upper-arm. (a) Standard fluoroscopic image showing bones and rough anatomical structures, and (b) Angiograph with enhanced resolution, highlighting the vasculature structures in the region of interest using a contrast agent.

Computed Tomography Angiography

Computed Tomography Angiography (CTA) is a specialized form of CT utilized specifically for angiography, which is the imaging of arteries and veins throughout the body. This technique involves the injection of a contrast agent into the bloodstream, which enhances the visibility of the vasculature in the tomographic images. These images are then used to search for vascular abnormalities such as calcification, stenosis, and aneurysms. The process typically involves the patient receiving an intravenous injection of contrast agent before the heart and surrounding vascular structures are scanned using a high-speed CT scanner. The primary distinction between a standard CT scan and CTA is the visibility of the vascular system. Usually, vascular systems are not easily distinguishable in a regular CT scan; the injection of contrast agents makes them visible in CTA. This visibility is crucial for diagnosis and procedural planning, making CTA an invaluable tool in assessing vascular health [12, 151]. An illustration of a CTA scanner can be seen in Fig. 2.9a, whereas Fig. 2.9b shows a CTA image of the thoracic and abdominal aorta from different anatomical planes.

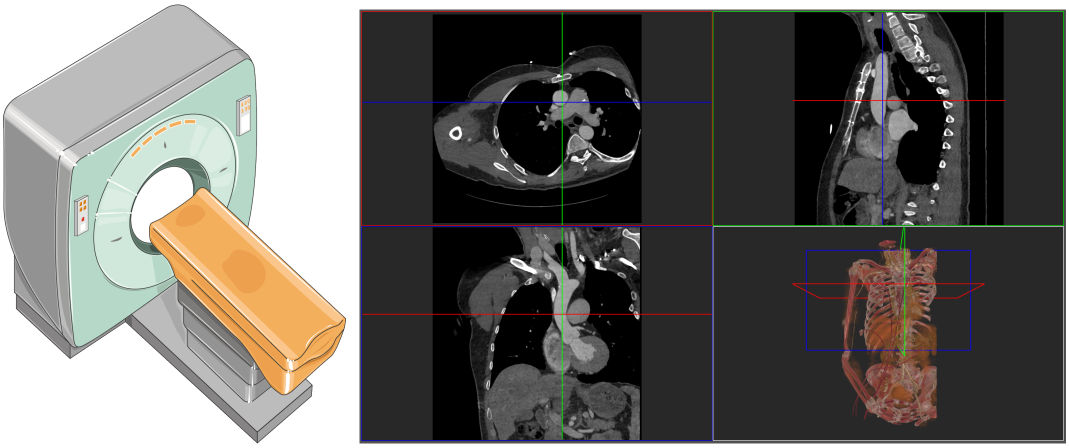

(a) (b)

Fig. 2.9. Computed Tomography Angiography (CTA) imaging. (a) Illustration of a CT scanner capable of capturing CTA images, and (b) CTA volume displaying the three anatomical planes and the 3D reconstructed volume, with the thoracic and abdominal aorta highlighted using contrast agent during imaging.
Note: Figure (a) reused without changes © 2024 Servier Medical Art. Used with permission under CC BY 4.0.

Magnetic Resonance Angiography

Similar to CTA, Magnetic Resonance Angiography (MRA) is a specialized type of MRI focusing on imaging the body's vascular system. Unlike CTA, which uses radiation during image acquisition, MRA offers a less invasive alternative. MRA generates images of arteries and occasionally veins to assess conditions such as stenosis, occlusions, aneurysms, or other abnormalities.

It is frequently used to evaluate the arteries of the neck and brain, the thoracic and abdominal aorta, the renal arteries, and the legs [12, 151]. Especially when radiation exposure is a significant concern, for example to children with congenital heart defects, MRA is prioritized over CTA. A visual representation of an MRA image of brain vasculatures is presented in Fig. 2.10.

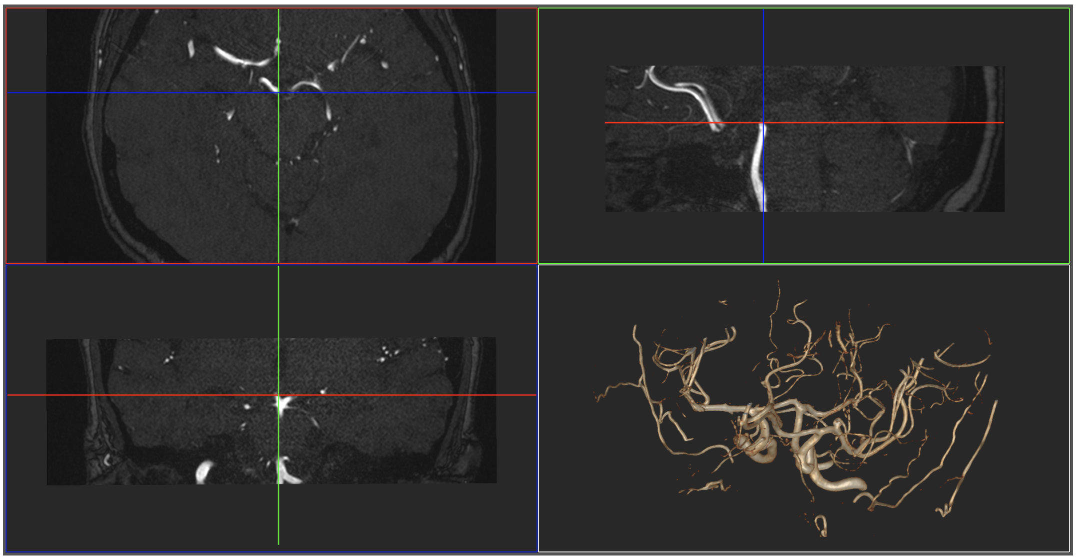

Fig. 2.10. Magnetic Resonance Angiography (MRA) imaging. An MRA volume with the three anatomical planes and the 3D reconstructed brain vasculature, highlighted using contrast agent during imaging.
Note: Figure generated from Dataset ds005096 © 2024 OpenNeuro [136]. Used with permission under CC0.

2.6.3 Anatomical Planes

Human body anatomical planes are a reference framework to understand the spatial relationship between anatomical structures. These planes are used to identify and communicate the position of organs and medical instruments during endovascular procedures [116, 149]. A visual representation of the three principal anatomical planes is shown in Fig. 2.11.

- **Sagittal plane**: Divides the body into left and right halves, and the medical terms used to indicate the sides are medial and lateral.
- **Coronal/Frontal plane**: Divides the body into front and back halves, and the medical terminology representing these halves are anterior and posterior.
- **Axial/Transverse plane**: Divides the body into upper and lower halves, with the medical use of terms superior and inferior, or proximal and distal.

2.7 Summary

This chapter was integral to this dissertation to familiarize the reader with some of the main terminology and concepts that will be used throughout. Initially, it was essential to introduce domain-specific terminology, such as visualization, detection, tracking, and navigation. These foundational terms set the stage for understanding the complex processes around catheter-based endovascular procedures. Furthermore, the chapter delved into catheter navigation techniques and their movement kinematics, providing a detailed overview of how catheters are maneuvered through vascular structures during endovascular procedures.

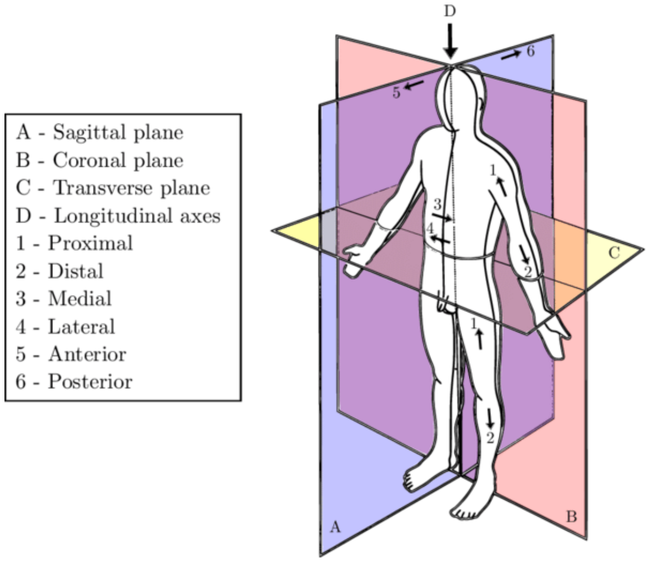

Fig. 2.11. Three principal planes of the human body: sagittal, coronal/frontal, and axial/transverse planes provide a reference framework for understanding the spatial relationships between anatomical structures.
Note: Figure reused without changes © 2019 Roothaer [166]. Used with permission under CC BY-NC-ND 4.0.

Understanding the different endovascular instruments, their basic shapes, and applications is essential for appreciating the nuances of these procedures. The chapter continued by discussing the importance of registration and various catheter registration techniques, highlighting how precise alignment of preoperative and intraoperative images enhances procedural accuracy. Finally, the chapter covered tracking systems and basic affine transformations, along with imaging classifications and their interrelations, which are pivotal for developing effective navigation and tracking strategies in minimally invasive endovascular procedures.

Part II

Background Theory

The Anatomy of the Human Body

3

In order to understand the complexities of the human body, it is essential to explore its various parts and how they integrate to form a cohesive system. The human body consists of various cell types forming tissues and organs, which assemble into organ systems. The human anatomy, the field that examines the body's structure, shows that the body is characterized by bilateral symmetry and includes a head, neck, and torso – divided into the thorax and abdomen. Additionally, the body has two upper limbs, each leading to hands, and two lower limbs, each concluding with feet [116, 149].

The human skeleton, made of bone and cartilage, forms the framework of the body and is surrounded by soft tissues like muscle and fat. The spine surrounds the spinal cord, connecting the brain to the rest of the body via an extensive network of nerves. The heart drives the circulatory system, circulating blood through arteries and veins. In the lungs, blood is oxygenated and then distributed to the tissues of the body through the aorta, with nutrient and gas exchange occurring in the capillaries. Deoxygenated blood is then returned to the heart via the veins, enabling the cycle to continue [20, 116, 121, 149]. Fig. 3.1 presents a cross-sectional coronal view of human anatomy, highlighting some major thoracic and abdominal organs and the circulatory system.

3.1 Cardiovascular System

The circulatory system, also known as the cardiovascular or vascular system, constitutes an organ network responsible for blood circulation throughout the human body. This system includes the heart, blood vessels, and the blood itself, drawing its name from the Greek word "kardia," meaning heart, and the Latin "vascula," meaning vessels [20, 116].

The blood vessel network encompasses the great vessels of the heart, which include the large elastic arteries and veins, alongside other arteries, smaller arterioles, and capillaries that connect to venules (the smaller veins), leading into larger veins. It is essential to recognize that the cardiovascular system operates as a closed loop, meaning the blood is continuously contained within the network of vessels [116, 149].

Blood, a fluid composed of plasma, red and white blood cells, and platelets, flows constantly throughout the body. This continuous flow is essential for delivering oxygen and nutrients to tissues and gathering and removing waste products [20].

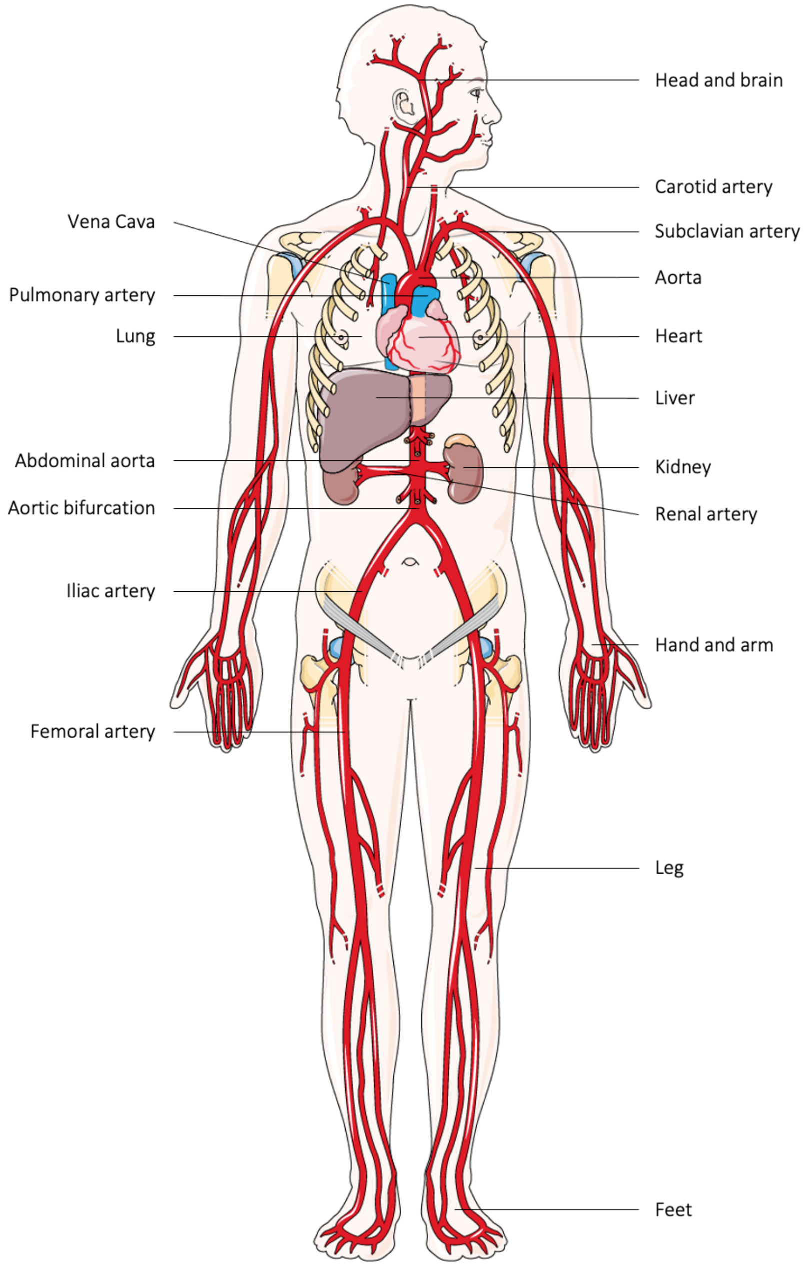

Fig. 3.1. The anatomy of the human body, illustrating vital organs and the cardiovascular system. The illustration of the human body highlights the head, neck, torso (thorax and abdomen), upper and lower limbs, as well as the heart, aorta, liver, and kidneys, emphasizing the pathways of the major blood vessels.

The cardiovascular system is divided into two principal circulations: pulmonary and systemic circulation. The pulmonary circulation carries deoxygenated blood from the heart's right side to the lungs for oxygenation before returning it to the heart's left side. A visual representation of this process is illustrated in Fig. 3.2a. The systemic circulation then distributes oxygen-rich blood from the left side of the heart to all parts of the body, subsequently returning oxygen-poor blood to the heart's right side via the venae cavae [116, 149]. For a visual representation of the systemic circulation, refer to Fig. 3.2b.

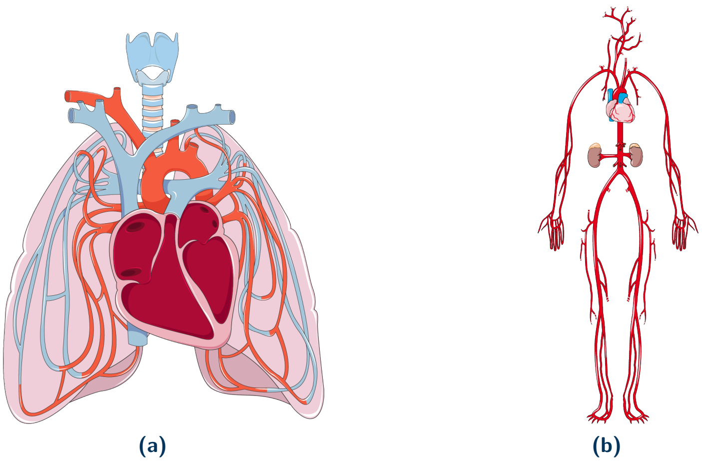

Fig. 3.2. The two principal blood circulation systems. (a) Pulmonary circulation, showing the circulation of blood between the heart and lungs through the pulmonary artery and vein, and (b) Systemic circulation, illustrating the circulation of the blood from the heart through the aorta to the rest of the body.
Note: Figures reused without changes © 2024 Servier Medical Art. Used with permission under CC BY 4.0.

Once the blood is oxygenated in the lungs, it enters the systemic circulation via the left ventricle, beginning with the aorta, a major artery characterized by its thick and elastic wall structure. Initially, the aorta arches upwards (ascending aorta), branching towards the brain via the two carotid arteries, one on either side of the neck, and the two subclavian arteries, supplying blood to the neck, head, and arms. Then, the aorta arches downwards (descending aorta), passing through the diaphragm to enter the abdominal cavity. From the descending aorta, additional branches emerge, supplying blood to the major organs in the torso, including the kidneys through the renal arteries and the liver via the hepatic artery. As it continues to descend, the aorta further branches out to the abdomen, pelvis, and lower limbs [116, 149].

The aorta ends by bifurcating into the right and left common iliac arteries, which supply blood to the lower body and branch further into the femoral arteries. A visual representation of the aorta and its main branches is presented in Fig. 3.3. This area of the arterial system holds significant clinical importance, as it often serves as the entry point for catheter-guided endovascular procedures, utilizing either the femoral veins or arteries for access. Additional entry points for such procedures may involve the jugular veins or arteries in the neck and the subclavian veins or arteries in the shoulder area [149].

3.2 Heart

The heart is a vital muscular organ within the circulatory system, located in the thoracic cavity between the lungs and slightly left of center. Encased by the pericardium, a protective sac, it sits within the mediastinum area. The pericardium shields the heart from physical injuries and infections and aids its movement by secreting pericardial fluid. The primary function of the heart is to circulate blood throughout the body, ensuring the continuous transport of oxygen, nutrients, waste materials, hormones, and white blood cells [20, 116, 149].

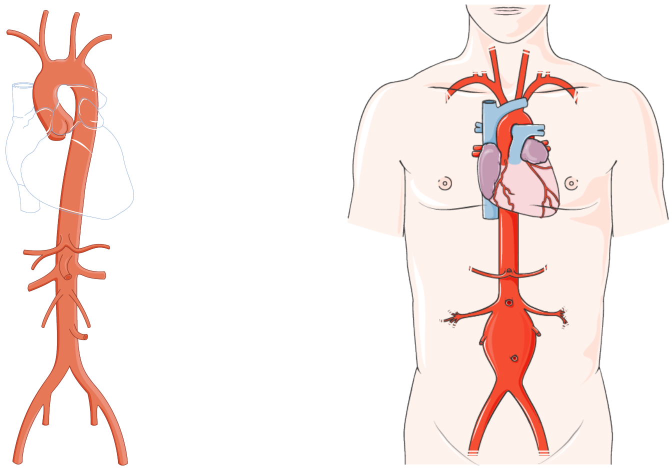

(a) (b)

Fig. 3.3. The anatomy of the aorta and abdominal aortic aneurysm. (a) Anatomy of the aorta showing its major branches, including the carotid and subclavian arteries (top), the renal and hepatic arteries (middle), and the aortic bifurcation into the iliac and femoral arteries (bottom), and (b) Representation of an abdominal aortic aneurysm, dilation between the renal arteries and the aortic bifurcation.
Note: Figures reused without changes © 2024 Servier Medical Art. Used with permission under CC BY 4.0.

Structurally, the heart consists of four chambers: the upper chambers, known as atria, and the lower chambers, called ventricles. The atria are essential for receiving blood returning to the heart from the body and lungs and facilitating its advancement into the ventricles. The ventricles are primarily responsible for pumping blood: the right ventricle sends deoxygenated blood to the lungs for oxygenation. In contrast, the left ventricle distributes oxygen-rich (oxygenated) blood to the rest of the body via the aorta [20, 116, 121, 149]. The structure of the heart is depicted through illustrations in Fig. 3.4, with Fig. 3.4a providing a comprehensive view of the heart, including the arteries and veins that enter and exit it. Meanwhile, Fig. 3.4b offers a detailed look at the anatomical features of the chambers.

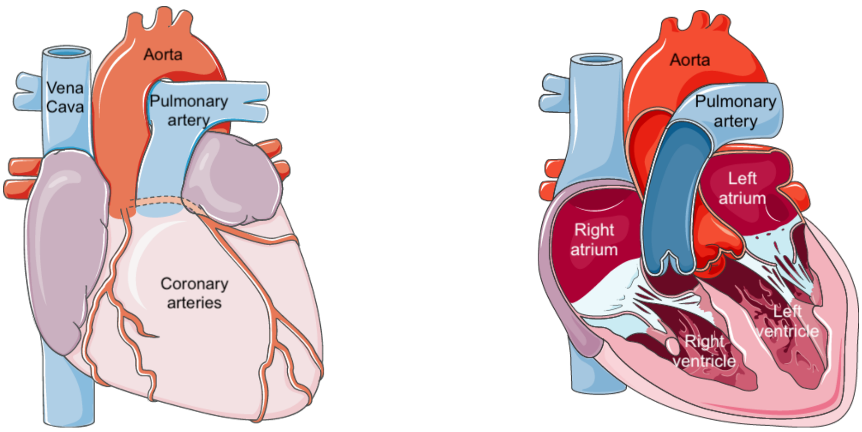

(a) (b)

Fig. 3.4. The anatomy of the heart. (a) Overview of the heart showing the major blood vessels including the aorta, vena cava, pulmonary artery, and the coronary arteries, and (b) Cross-sectional view displaying the heart's chambers – two atria and two ventricles – and their internal structures, highlighting the connections with the aorta and pulmonary artery.
Note: Figure reused without changes © 2024 Servier Medical Art. Used with permission under CC BY 4.0.

As the heart works to circulate blood across the body, it also requires a dedicated supply of oxygen and nutrients to sustain its own function. This is achieved by the coronary circulation system, a specialized part of the systemic circulation that delivers blood to the heart muscle or myocardium. The coronary circulation originates near the aorta's base; the coronary circulation comprises two primary arteries: the Right Coronary Artery (RCA) and the Left Coronary Artery (LCA). The RCA bifurcates into several branches, including the conus artery, sinoatrial nodal artery, acute marginal branches, the Posterior Descending Artery (PDA), and the Posterior Left Ventricular (PLV) branch. Similarly, the LCA bifurcates into the Left Anterior Descending (LAD) artery, Left Coronary Circumflex (LCx) artery, and Ramus Intermedius (RI) artery, each playing a vital role in nourishing the heart muscle [116, 149].

Coronary Artery Disease (CAD) stands as one of the leading cause of mortality globally. It develops due to plaque accumulation within the coronary arteries that supply blood to the heart muscle or myocardium. The medical term for this narrowing of arteries is called stenosis, which happens in the vessel's lumen due to the buildup of inflammatory substances and cholesterol deposits. This plaque buildup can significantly reduce the arteries' diameter, potentially obstructing sufficient blood flow to the myocardium and leading to a myocardial infarction [116, 121, 149]. Fig. 3.5a offers a simplified representation of this process. Such an event may further result in heart failure, cardiac arrest, and possibly death, with Fig. 3.5b providing a visual representation of the potential outcome. Various risk factors contribute to the development of CAD, including obesity, smoking, elevated cholesterol levels, high blood pressure, sedentary lifestyle, and diabetes.

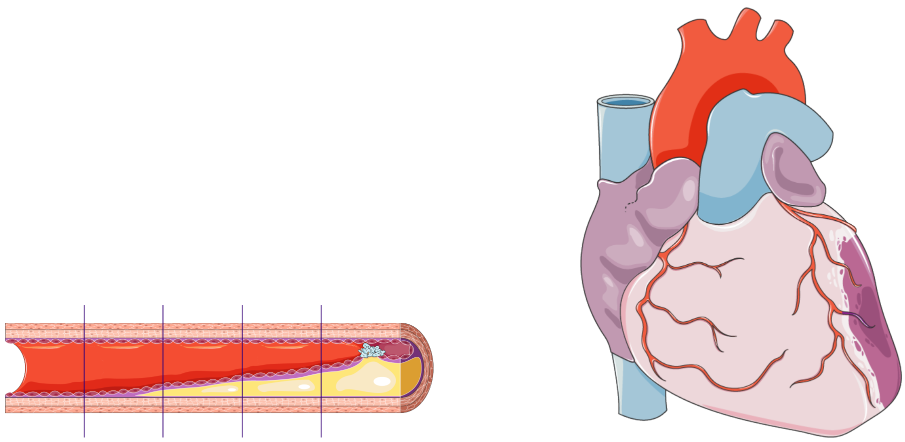

(a) (b)

Fig. 3.5. Vessel narrowing and plaque build-up leading to myocardial infarction. (a) Different stages of atherosclerosis, illustrating the progressive narrowing of the vessel lumen and the formation of a thrombus (embolus) blocking blood flow, and (b) The effect of atherosclerosis in the coronary arteries, leading to myocardial infarction, the death of heart tissue due to a lack of oxygen-rich blood and nutrients.

Heart valves function as biological one-way mechanisms within the heart, guaranteeing that blood moves through its chambers in a specific direction. The heart typically contains four valves, which collectively regulate the direction of blood flow. The activity of these valves, encompassing their opening and closing actions, is controlled by the variations in blood pressure across each side of the valve [149]. Fig. 3.6 illustrates all the heart valves in a cross-sectional axial view. The four valves in the heart include:

- **Two Atrioventricular Valves**: The valves dividing the upper atria from the lower ventricles include the mitral valve, located on the left side of the heart, and the tricuspid valve, positioned on the right side.

- **Two Semilunar Valves**: Located at the outflow tracts of the heart, these valves protect the entrances to the arteries. They consist of the aortic valve at the base of the aorta and the pulmonary valve at the base of the pulmonary artery.

Heart valves are predominantly categorized into two types: bicuspid, featuring two flaps, and tricuspid, with three flaps. Among all the heart valves, only the mitral valve is bicuspid. Additionally, it is worth noting that the heart contains other minor valves, such as the coronary sinus valve and the inferior vena cava valve. However, the primary focus remains on the previously described four valves, crucial in directing blood flow within the heart [121, 149].

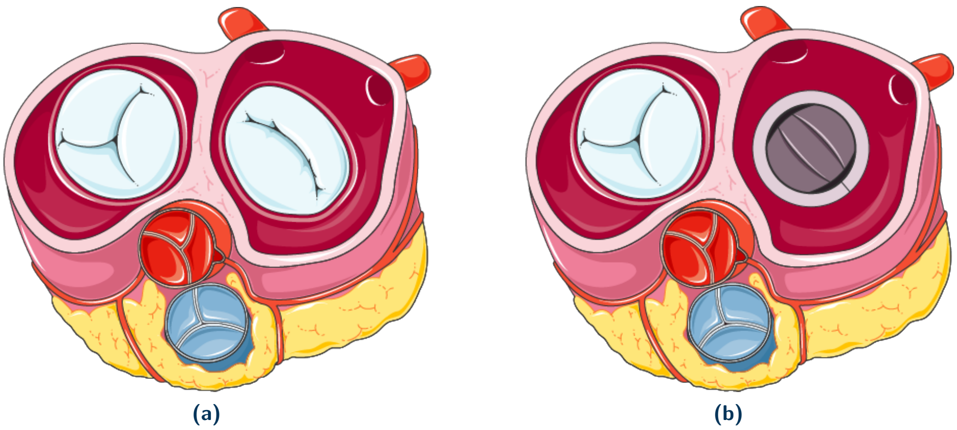

Fig. 3.6. Anatomy of the heart valves and valve flaps. (a) Healthy heart showing the two atrioventricular valves (tricuspid valve on the right and mitral valve on the left) located between the atria and ventricles, and the two semilunar valves (aortic valve in red and pulmonary valve in blue), and (b) Outcome of mitral valve replacement surgery with a mechanical valve, illustrating the placement of the prosthetic valve.

3.3 Vascular and Heart Valve Disease

Vascular diseases encompass a range of conditions affecting the blood vessels, essential conduits for transporting oxygen, nutrients, and waste throughout the body. Typically, these conditions originate from the accumulation of plaque – comprising fat and cholesterol – in the vessel's lumen (wall), leading to obstructions or diminished blood flow [149]. Fig. 3.7 graphically depicts the progression of plaque buildup in four distinct stages. While lifestyle changes can prove beneficial, some cases may require pharmacological treatment or endovascular interventions for effective treatment.

Vascular diseases vary in manifestation, affecting either arteries that transport oxygenated blood away from the heart or veins that bring deoxygenated blood back to the heart. Moreover, these conditions may be localized, affecting particular areas of the body.

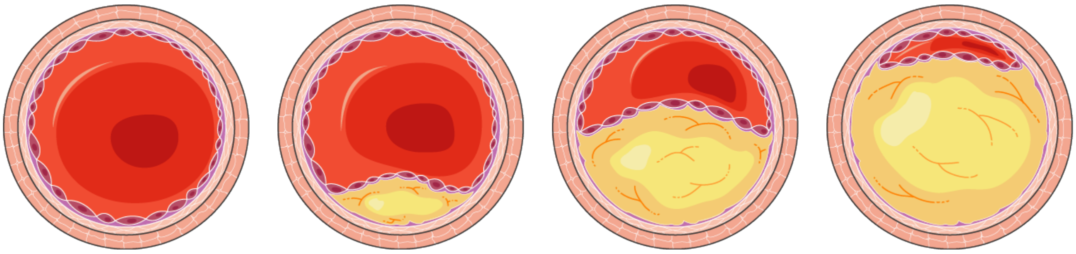

Fig. 3.7. Stages of atherosclerosis illustrated through cross-sectional views of the vessel. The images depict the degenerative process of plaque buildup (calcification) within the vessel wall (lumen). (a) No vessel narrowing, (b) 10% vessel narrowing, (c) 50% vessel narrowing, and (d) 90-100% vessel narrowing.

Peripheral Arterial Disease (PAD) explicitly targets the peripheral arteries – those located outside the heart – and bears resemblance to CAD, which impacts the coronary arteries that supply the heart. Both PAD and CAD are characterized by atherosclerosis, where plaque buildup narrows the vessels, restricts blood flow, and potentially causes ischemia, which is the lack of oxygen in tissues [149]. Some well-known vascular diseases include:

- **Coronary Artery Disease (CAD)**: Reduced blood flow to the heart muscle.
- **Carotid artery stenosis**: Narrowing of the arteries supplying the brain.
- **Renal artery stenosis**: Narrowing of the arteries supplying the kidneys.

Aneurysms, characterized by unusual or atypical swellings (bulges) in the blood vessel wall, can develop in various vascular regions. These dilations are commonly found in the aorta, the main artery leading from the heart [116, 121]. An illustration of an aneurysm is depicted in Fig. 3.3b. The two categories of aortic aneurysms include:

- **Thoracic Aortic Aneurysm**: Located in the chest (thoracic) region.
- **Abdominal Aortic Aneurysm (AAA)**: Located in the abdomen (abdominal) region.

Physicians may use pharmacological therapies or catheter-based endovascular procedures to manage vascular diseases. Cardiac catheterization involves inserting a catheter through the femoral, jugular, or subclavian arteries. This catheter is then carefully navigated through the vascular system to the aorta and navigated toward the heart. Once correctly positioned, the catheter can facilitate a range of diagnostic tests. These may involve placing the catheter's tip in specific regions of interest within the heart to measure chamber pressures or extracting blood samples to assess oxygen levels [20, 116].

The catheter can also be navigated into the coronary arteries for the purpose of coronary angiography, which entails the injection of a contrast agent to visualize blood flow within these arteries on imaging modalities. During cardiac catheterization, various procedures, such as angioplasty, can be executed. This procedure involves inflating a small balloon located at the catheter's tip to compress the plaque against the artery wall, thus enhancing blood flow, as depicted in Fig. 3.8a. Stent placement entails the deployment and expansion of a small metal mesh coil or tube at the catheter's end within an artery to maintain its openness [116, 149]. Fig. 3.8b and Fig. 3.8c illustrate the procedure of balloon expansion of a stent and its successful deployment in the vasculature, respectively.

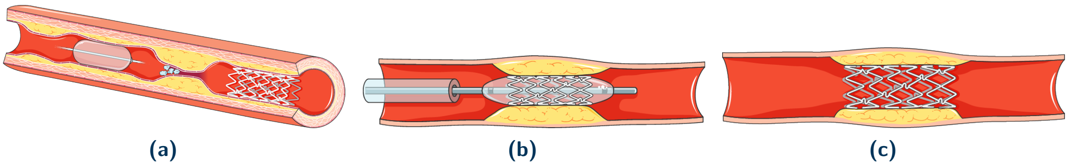

Fig. 3.8. Treatment strategies for vascular disease through catheter-based endovascular procedures. (a) Angioplasty process showing the dilation of the vessel by inflating a catheter balloon to compact the plaque, with a visible thrombus (embolus) blocking the blood flow and a stent in place, (b) Stenting process where a balloon is used to expand the stent around the calcified area to hold the vessel open, and (c) Stenting results, illustrating the stent remaining open in place for unrestricted blood flow.

In addition to vascular diseases, heart valves may suffer from disorders such as regurgitation – where blood flows backward due to valve inefficiency – or stenosis, often caused by plaque buildup or congenital abnormalities. Common valve issues include a bicuspid aortic valve, a condition where the aortic valve has only two flaps instead of the usual three, and mitral valve prolapse, where the mitral valve flaps extend back into the left atrium, hindering a complete closure. These valve dysfunctions can be addressed through catheter-guided approaches, providing a less invasive option compared to traditional open surgery, replaced by synthetic or mechanical valves [149]. An example of a mechanical valve is illustrated in Fig. 3.6b.

3.4 Summary

This chapter provided an in-depth exploration of the human anatomy, focusing on the cardiovascular system, the heart, and related vascular and heart valve diseases. The cardiovascular system is described in detail, emphasizing its role in circulating blood throughout the body and its composition, including the heart, blood vessels, and blood. The structure and function of the heart are examined, highlighting its chambers, major blood vessels, and the importance of its rhythmic contractions in maintaining blood flow.

The discussion extended to vascular diseases, which affect the blood vessels and are often characterized by plaque buildup, leading to conditions such as atherosclerosis, aneurysms, and peripheral artery disease. Heart valve diseases include conditions like regurgitation, where blood leaks backward through a valve, and stenosis, where valve openings become narrowed, impeding blood flow.

Overall, this chapter provided a comprehensive overview of human anatomy, focusing on the cardiovascular system, heart structure, and associated diseases. Understanding these aspects is crucial for appreciating the complexity of the human body and the intricate systems that sustain life. By delving into the structural and functional details, this chapter sets a foundation for further exploration of medical procedures discussed in subsequent chapters.

4 Clinical Routine

This chapter of the dissertation outlines the clinical routine for a patient undergoing a catheterization procedure on the heart, drawing upon research and, mostly, observations made at the Deutsches Herzzentrum München[1] (DHM), and Klinikum rechts der Isar der Technischen Universität München[2]. The aim is to describe the sequential phases of such a procedure, from the patient's admission to the hospital to their following release after a catheter-guided cardiac endovascular procedure. While the clinical routine for catheter-guided endovascular procedures in other anatomies, beside the heart, would be considerably similar, the primary distinction lies in the specific diagnostic and interventional steps involved.

4.1 Cardiovascular Examination

Upon arrival at the hospital, a general (assistant) cardiologist collects the patient's medical history and that of their family. The discussion includes general health questions and more specific questions to the patient's reason for visit. It is a standard practice to ask about any cardiac-related health issues, medications, symptoms, and other relevant details.

Following the health history collection, the cardiologist may suggest blood tests and a physical examination, depending on the initial assessment results. The physical examination could involve visual inspection, palpation, and listening to the heart using a stethoscope, a technique known as auscultation. Additionally, the cardiologist may assess the arterial pulse, record blood pressure, and conduct an Electrocardiogram (ECG) to monitor the heart's rhythm and identify any irregularities or abnormal heart rates [149].

Blood tests are often conducted next and serve as a crucial source of information regarding the cardiac state, offering valuable insights into cardiovascular health. These blood tests enable cardiologists to identify potential risk factors, such as elevated cholesterol levels, which could suggest the potential presence of heart disease or other cardiovascular conditions [149].

A stress test might be conducted if the initial examinations indicate the necessity. This test evaluates how the heart functions under physical stress. During the test, the patient is asked to walk or run on a treadmill (or bicycle) while their heart rate, blood pressure, and ECG readings are closely monitored. As the exercise's intensity increases, the test reveals how effectively the heart copes, helping identify potential cardiovascular issues.

[1] German Heart Center Munich
[2] University Clinic of the Technical University of Munich

If the cardiologist identifies a potential issue that requires closer examination, an ultrasound test may be recommended. Ultrasound can be employed in various ways, including as a handheld scanning device applied externally or through Transesophageal Echocardiography (TEE). In TEE, a thin tube is passed through the patient's mouth, throat, and esophagus. Because the esophagus lies in close proximity to the heart's upper chambers, TEE can produce exceptionally clear images of the heart's structures and valves. Through ultrasound examinations, cardiologists aim to assess the heart's size and the thickness of its walls, evaluate the heart's pumping efficiency, measure blood flow using the Doppler effect, investigate the function of the heart valves and their blood flow to detect any regurgitation and measure the diameter of the valves.

Lastly, the cardiologist may find it necessary to obtain a more detailed view of the heart using a Computed Tomography Angiography (CTA) or Magnetic Resonance Angiography (MRA). This step is often one of the final tests required to comprehensively understand the symptoms and conclude the examination process. CTA scans usually focus on the coronary arteries in a noninvasive manner.

Typically, the patient is injected with an iodine-based contrast agent to enhance the visibility of the heart's vessels during the scan. During this process, the scans are timed precisely to capture the high-speed CTA when the contrast agent is present in the coronary arteries. Through this test, radiologists can determine whether there are any blockages in the heart's arteries and refer the patient to the cardiologists for further procedures. The resulting images, which provide 3D heart volumes, can reveal plaque buildup within the coronary arteries and assist in planning any necessary procedures.

4.2 Cardiac Catheterization

Cardiologists may recommend a cardiac catheterization procedure if the initial examinations indicate the need for a more detailed examination. This is a more invasive method conducted via a catheter to assess the pressure and blood flow in the heart and surrounding areas. It can also serve therapeutic purposes for certain heart conditions. During the procedure, the interventional cardiologist might measure the pressure within the heart's chambers, collect blood samples to evaluate oxygen levels, and inject a contrast agent to observe the blood flow through the heart's arteries.

As previously mentioned, catheterization procedures can also be conducted in other anatomical sites, such as the carotid arteries, aorta, kidneys, and liver. The individuals who typically perform these procedures are surgeons, but interventional radiologists or interventional cardiologists can also carry them out. The key difference lies in their focus areas: cardiologists primarily focus on the heart and aorta, while radiologists might undertake procedures targeting different anatomical sites, including the kidney and liver. Furthermore, interventional radiologists can administer radioactive substances directly to tumor sites. For instance, procedures where chemotherapy is directly injected into a liver tumor are known as Transarterial Chemoembolization (TACE), and Selective Internal Radiation Therapy (SIRT) involves delivering radioactive substances into the vicinity of a tumor's vascular supply.

At the beginning of the cardiac catheterization procedure, the patient is given a gown to change into and prepared for entry into the catheterization laboratory (cath lab). A healthcare professional prepares the catheter entry point, often the femoral arteries. An Intravenous Line (IV) is then set up in the patient's hand or arm to administer IV fluids and medications as necessary. The patient is positioned lying on their back on the cath lab table. The patient's ECG, heart rate, blood pressure, respiratory rate, and oxygen saturation are monitored continuously throughout the procedure. In order to ensure comfort, the patient is sedated before the procedure starts, helping them relax; however, they typically may remain awake as well.

After the local anesthetic at the insertion site has taken effect, the interventional cardiologist inserts a sheath into the femoral artery manually or with ultrasound guidance. This sheath serves as an entry point through which the catheter is introduced into the blood vessel and then navigated towards the heart. A combination of guidewires and catheters are initially placed and pushed through the aorta to reach the coronary arteries, guided through fluoroscopy. A 3D volume of the preoperative CTA is also displayed on one of the screens so that interventional cardiologists can mentally map the intraoperative 2D fluoroscopic images to the preoperative 3D volumetric images. When the catheter reaches the region of interest, a contrast agent is injected to enable the visualization of the heart and its coronary arteries. Subsequently, a series of x-ray images, known as angiography, are captured. These high-resolution x-ray images of the coronary arteries allow the interventional cardiologist to determine the presence of any stenosis due to plaque buildup that could restrict blood flow in specific areas.

The flexibility to switch to different catheters and guidewires allows the interventional cardiologist to perform various interventional procedures alongside the cardiac catheterization. These procedures aim to enhance blood flow to the heart by addressing narrowed coronary arteries. One common endovascular procedure is angioplasty, where a balloon is inserted and inflated within the vessel to compress plaque against the vessel wall, thereby widening the vessel's diameter. Other interventional procedures include:

- **Balloon Angioplasty**: Catheter-based procedure that involves inflating a balloon inside the vessel to compact the plaque and widen the vessel.
- **Stent Placement**: A stent – a small metal mesh tube – is deployed to mechanically expand the vessel's diameter, ensuring it remains open.
- **Heart Valve Replacement**: Catheter-based procedure that replaces a damaged heart valve with a synthetic (mechanic) one, improving heart function.
- **Repair of Congenital Heart Defects**: Involves procedures such as closing Atrial Septal Defects (ASD) (hole between the two atria).
- **Aortic Procedures**: Catheter-based procedures for stent placement in the aorta to treat conditions like Abdominal Aortic Aneurysm (AAA) by reinforcing the aortic wall.
- **Ablation**: Procedures that are performed to correct heart rhythm issues. Ablation involves either heating or cooling the tip of the catheter to modify heart muscle tissue that is causing rhythm problems.

As previously discussed, a combination of a guidewires and catheters are navigated through the patient's vascular system toward the region of interest. Typically, the guidewire is advanced first due to its thinner and more flexible construction, allowing for easier manipulation through various branches toward the heart. Upon reaching the region of interest with the guidewire, a sheath is inserted over it to establish a direct access channel to the area of interest. With the sheath securely in place, the guidewire is removed, enabling the insertion of various catheter-based instruments through the sheath to directly access the region of interest.

An essential aspect of these procedures is the ability of interventional cardiologists to monitor and track the catheter's location during the intervention. It is essential to mention that x-ray-based imaging modalities, such as fluoroscopes, do not visualize soft-tissue anatomical structures, including vessels. Interventional cardiologists inject a contrast agent to visualize the vascular tree, briefly highlighting the vasculature until the bloodstream flushes it.

Typically, these procedures rely on visual tracking, with the fluoroscope positioned to keep the catheter's tip centrally within the view. In some cath labs, advanced image-based tracking software is utilized to identify and highlight the catheter within fluoroscopic images. However, even with such technology, interventional cardiologists may be able to see, at best, two 2D fluoroscopic views in cases when a dual C-arm fluoroscope is available. The task of translating these 2D images into a comprehensive 3D visualization of the catheter within the actual anatomical context is performed mentally by the interventional cardiologist. This mental mapping from the observed fluoroscopic images to a 3D understanding of the patient's anatomy is a sophisticated skill that interventional cardiologists develop through experience.

More innovative approaches are being explored for tracking in the Electrophysiology (EP) department, where interventional cardiologists conduct catheter-based endovascular procedures to ablate atrial tissue. These procedures aim to regulate the electrical signals traversing the heart, thereby regulating heart rate. During such procedures, more sophisticated tracking systems are employed, primarily to map accurately the electrical activity within the atria.

An Electromagnetic (EM) tracking system could be used in certain instances, which must first be registered with the patient's anatomy. Following this registration process, the interventional cardiologist introduces a mapping catheter into the atria. The instrument's tip is carefully tracked, and its position is used to map electrical signal inputs, thereby generating a 3D model of the atria. However, it is essential to note that this 3D structure is not typically integrated with any preoperative imaging, presenting a distinct method of visualization that relies solely on the output structure from the real-time tracking of the catheter's tip to understand atrial structures and functions.

4.3 Postoperative Recovery

Following the endovascular procedure, the interventional cardiologist will secure the vessel access site by applying direct pressure or, in some cases, using a suture device or a vascular closure plug. These methods aim to promote the body's natural healing process, encouraging clot formation at the artery site to minimize bleeding risks. Afterward, the patient is moved to an intensive care unit or a recovery room based on the extent of the interventional procedure.

In order to prevent bleeding, patients are required to remain lying flat with their legs straight for a duration ranging from two to six hours. A sterile dressing is applied to the access area to prevent infection, and this is monitored and changed as necessary to ensure proper healing and cleanliness.

4.4 Summary

This chapter outlined a standard clinical routine for patients undergoing cardiac catheterization based on observations from two major clinics in Munich. The chapter begins by elaborating on the cardiovascular examinations. The process involves collecting medical history, conducting physical and blood work examinations, and utilizing various monitoring and imaging techniques such as ECG, stress tests, ultrasound, and advanced imaging like CTA and MRA. These steps ensure a comprehensive understanding of the patient's condition before proceeding with the catheterization.

The cardiac catheterization procedure itself is detailed, covering preparation steps, the insertion of the catheter, and the role of real-time imaging in guiding the intervention. The use of contrast agents and fluoroscopy allows for precise visualization of the coronary arteries, aiding in diagnosing and treating conditions such as plaque buildup and valve disorders. Various interventional procedures, including angioplasty, stent placement, and ablation, are also discussed, highlighting their similar approach.

Finally, the chapter emphasizes the skills required by interventional cardiologists to translate intraoperative 2D fluoroscopic images into a 3D understanding of the patient's anatomy, ensuring precise and effective interventions. This comprehensive overview underscores the complexity and precision involved in cardiac catheterization procedures.

Literature Review 5

The following chapter elaborates on a exhaustive literature review of the current advancements in catheter tracking concepts and methodologies. This chapter is not limited to discussing various studies, their categorization, and a critical evaluation of their findings. It also makes a significant contribution to the current state of the art by introducing novel definitions for commonly used but previously interchangeable terminology. Additionally, it includes an exhaustive survey on various tracking technologies with a specific emphasis on catheter tracking, addressing the fact that existing literature focuses on a single tracking technology. It is crucial to acknowledge that this chapter is inspired by and serves as a novel contribution based on our paper “A Survey of Catheter Tracking Concepts and Methodologies”, published in the Medical Image Analysis Journal, enriching the discourse on catheter tracking by broadening the understanding and application of these technologies in medical procedures [154].

5.1 Introduction

Minimally Invasive Surgery (MIS) has revolutionized the medical field, enabling physicians to perform interventions with smaller incisions, reduced pain, and faster recovery times compared to traditional open surgery [70]. This minimally invasive approach dates back to the early 1920s, and catheterization, a specific form of MIS, has become an integral part of interventional radiology and cardiology.

In its early days, catheterization relied on a combination of catheters, guidewires, and medical x-ray imaging to navigate through the patient’s anatomy. Today, catheter-based interventions are standard procedures, and their seamless integration into the medical workflow is essential for successful outcomes. To achieve this, it is crucial for physicians to accurately guide catheters to the desired anatomical region of interest and precisely localize their tips. To address this need, advanced technologies known as catheter tracking have emerged, providing physicians with real-time information about the catheter’s position and orientation.

Catheters have emerged as indispensable instruments in interventional medicine, enabling minimally invasive procedures for a wide range of diagnostic and therapeutic applications. These flexible instruments are typically inserted into blood vessels to access specific anatomical regions from within the body. Various catheter tracking technologies have been developed to ensure precise navigation and manipulation of catheters, each tailored to specific imaging modalities and anatomical contexts.

5.2 History of Catheter Tracking

Catheter tracking has played an important role in the evolution of interventional medicine, enabling physicians to perform minimally invasive endovascular procedures with high precision. The discovery of x-rays in 1895 by Wilhelm Röntgen revolutionized medical imaging, allowing physicians to visualize anatomical internal structures and pave the way for catheter-based diagnostic and treatment approaches [23, 67].

Fluoroscopy, an imaging modality that generates sequential x-ray images, laid the foundation for visual tracking. This modality constitute the foundation of modern catheter tracking, initially relied solely on visual tracking [23]. These advancements have changed catheter tracking, enabling physicians to perform increasingly more complex and precise interventions with minimal patient discomfort [67, 153].

In 1927, Portuguese physician and neurologist Egas Moniz revolutionized medical imaging by pioneering the technique of angiography, which involves injecting radio-opaque substances like bromine into the bloodstream to visualize blood vessels in the brain [44]. This breakthrough enabled physicians to gain insights into the structure of cerebral vessels, paving the way for more precise and effective catheter navigation [23, 44].

Taking advantage of the opportunity presented by advancements in fluoroscopy, Werner Forssmann, a pioneering urologist, made history in 1929 by inserting a catheter into his own heart (right atrium) and tracking its position using fluoroscopy [206]. This groundbreaking intervention, performed without anesthesia, marked the beginning of cardiac catheterization. One of the images taken during this procedure is presented in Fig. 5.1. Forssmann explained this journey in his book, "Experiments on Myself: Memoirs of a Surgeon in Germany" [53, 206]. His innovative approach inspired generations of surgeons to pursue cardiac catheterization, significantly influencing subsequent pulmonary catheter insertions [206]. While numerous catheter insertions followed Forssmann's groundbreaking procedure, catheter tracking remained solely visual for several decades, lacking any quantitative position measure.

During the 1920s and 1950s, x-ray technology underwent significant advancements, leading to the development of cross-sectional imaging, commonly referred to as x-ray tomography. This technique laid the foundation for modern Computed Tomography (CT), which emerged as a revolutionary modality for medical imaging [67].

In 1917, mathematician Johann Radon established the fundamental principles of CT by introducing the concept of reconstructing an object from its projections [67]. Godfrey Hounsfield, an engineer, independently delved into this field and made significant contributions that transformed CT from an abstract concept into a clinical reality. Working in the late 1960s, Hounsfield, unaware of Radon's work, tackled the mathematical challenges of projection imaging and successfully developed a prototype CT scanner in 1968 [67]. By the early 1970s, early adopters began utilizing CT scanners, which offered far superior and more precise anatomical visualization compared to traditional x-ray projection imaging. This breakthrough enabled the quantitative measurement of positions within the body, paving the way for advancements in minimally invasive endovascular procedures.

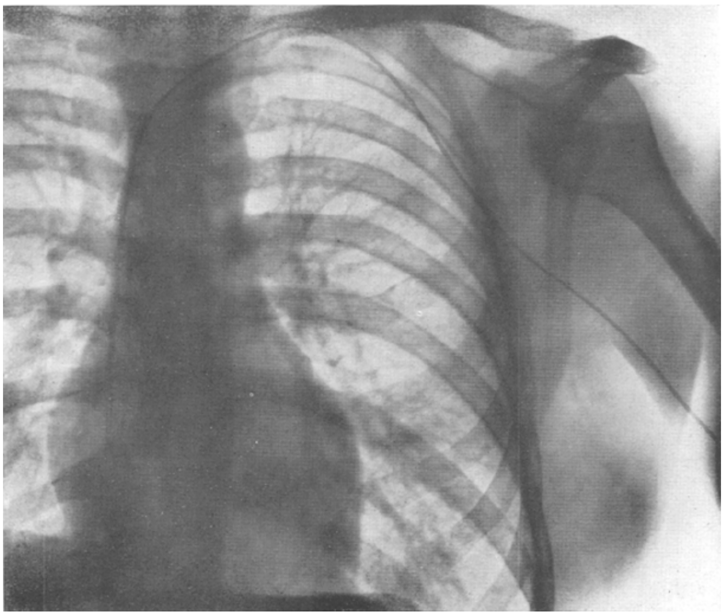

Fig. 5.1. Dr. Werner Forssmann's pioneering catheter insertion into the right atrium. This historical x-ray image captures the first human cardiac catheterization performed by Dr. Forssmann on himself, demonstrating the catheter's path from his left arm into the heart.

In the 1950s, another groundbreaking invention emerged in the field of medical imaging, namely ultrasound. Unlike x-rays, which employ ionizing radiation, ultrasound utilizes high-frequency sound waves to generate cross-sectional images [67]. This innovation offered physicians an alternative imaging modality for visual catheter tracking without the associated risks of radiation exposure. While ultrasound has primarily been employed for diagnostic purposes in clinical practice, research has explored its potential for tracking catheters during percutaneous procedures. This exploration aims to establish ultrasound as a viable alternative to x-rays, particularly in settings where radiation exposure is a concern.

Despite the remarkable advancements in medical imaging throughout the first half of the 20th century, catheter tracking remained solely qualitative until the digitization of the medical imaging field. Only after x-ray fluoroscopes, ultrasound, and CT were digitized did the ability to quantify the position and orientation of the catheter's tip become a reality. As a result, the vast majority of catheter tracking and navigation solutions emerged after the 1970s. Charles Mistretta, a pioneer in Digital Substraction Angiography (DSA), deserves a special mention. Mistretta led one of the first efforts toward digital vessel segmentation, paving the way for more precise and accurate catheter tracking [41, 196].

To the best of our knowledge, the first attempt to establish quantitative catheter tracking using ultrasound was made by Breyer and Cikeš [25]. Their work introduced a novel approach for tracking and visualizing catheters in ultrasound images, utilizing a piezoelectric element embedded within the catheter tip. The ultrasound transducer detected these pulses, generating a visual representation of the catheter within the ultrasound image. This innovation, along with the advancements in x-ray and ultrasound-based vascular image enhancement and catheter detection and visualization, laid the foundation for quantified catheter tracking, building upon the pioneering work of Forssmann and those who followed in his footsteps.

5.3 Clinical Applications

This dissertation focuses on the clinical applications of catheter-based procedures in interventional cardiology, radiology, and endovascular procedures. These procedures involve inserting catheters and guidewires into the patient's vascular system to reach specific target areas, such as the heart, aorta, brain, or liver. As discussed in the previous chapters, with their smaller diameter and easier manipulation, guidewires serve as the initial pathfinding instruments, while catheters follow them. Catheters perform various tasks, including injecting contrast agent to enhance vessel visualization in interventional x-ray images, positioning instruments for stenting or ballooning, or delivering localized therapy.

While numerous catheter types are used in medical settings, this dissertation primarily addresses catheters employed in endovascular procedures, specifically those used in the cardiac domain for stent placement, ballooning, aneurysm repairs, or electrophysiology interventions. However, due to the methodological similarities in tracking, this dissertation also incorporates tracking techniques for other tubular medical instruments, such as guidewires, bronchoscopes, brachytherapy needles, and flexible needle navigation solutions.

All of the tracking technologies reviewed in this dissertation have the potential to be integrated into catheter tracking applications in the future. Common concepts are highlighted to provide a technical overview for the reader, and exemplary methods and concepts are presented when appropriate. The overarching aim is to offer a comprehensive overview of catheter-tracking concepts and a broad understanding of catheter-based tracking technologies.

5.4 Classification of Catheter Tracking Technologies

Drawing upon our previous work, Ramadani et al. [154], we identify and propose categorizing catheter tracking technologies based on a comprehensive analysis of the current technological landscape. A detailed discussion of these categories, including technical considerations and comparative analyses, follows.

- **Image-based tracking**: This approach utilizes real-time intraoperative imaging modalities like fluoroscopes or ultrasound to track the catheter's position and orientation.
- **Active/passive tracking**: Active tracking involves embedding emitters within the catheter so that external sensors can detect and track them. Passive tracking relies on markers or reflectors attached to the catheter that external sensors track.
- **Electromagnetic (EM) tracking**: This method utilizes electromagnetic fields and sensors attached at the tip of the catheter to determine the catheter's pose.

- **Fiber Optic Shape Sensing (FOSS)**: This technology employs embedded fiber optic sensors within the catheter to monitor its deflections and infer (reconstruct) its shape, position, and orientation.

- **Bioelectric navigation**: This technique utilizes the electrical properties of catheters, such as impedance, to track the catheter's position within the vascular tree.

- **Robotic tracking solutions**: These advanced systems employ robotic manipulators guided by real-time tracking data for precise catheter navigation.

- **Hybrid tracking**: This approach combines two or more tracking technologies to achieve comprehensive and robust tracking capabilities.

5.4.1 Image-based Catheter Tracking

Through state-of-the-art research, x-ray, ultrasound, and Magnetic Resonance Imaging (MRI) are determined to be the most used image modalities for catheter navigation during endovascular procedures that rely solely on acquired image information. One significant advantage of image-based methods is that they do not require specialized catheters or the modification of medical instruments for tracking purposes. Instead, they depend exclusively on the information from acquired interventional images, facilitating seamless integration into clinical workflows, often achieved through software-based solutions.

Image-based Catheter Tracking – x-ray

Fluoroscopy and 2D x-ray projections, in general, have long been the standard imaging modalities used to guide catheter-based endovascular procedures, such as Percutaneous Coronary Interventions (PCI), Cardiac Electrophysiology (EP), or Transarterial Chemoembolization (TACE). These minimally invasive procedures are employed to treat a range of conditions, including arterial diseases, atrial fibrillation, and liver cancer. However, the precision required for catheter navigation necessitates more advanced imaging techniques.

During catheter-based endovascular procedures, physicians rely mostly on real-time visual feedback from 2D x-ray projections to guide the catheter through the patient's vasculature to the desired anatomical region of interest. However, this approach is inherently limited by the projective nature of x-ray imaging, which can lead to foreshortening and occlusions, making precise catheter navigation challenging and highly dependent on the physician's expertise. Additionally, radiation exposure during these procedures poses a risk to the patient and the medical staff, necessitating the development of techniques to minimize radiation exposure.

Various techniques have been developed to enhance x-ray-based navigation, including 3D road mapping. Visualizing the catheter in relation to the patient's vascular anatomy can generate a visual roadmap for navigation in 2D or 3D. This roadmap allows physicians to perceptually localize the catheter by visually comparing the current fluoroscopic image with the roadmap, potentially reducing the contrast agent required during a procedure. Research indicates that a visual overlay of the patient's anatomy can also lower radiation exposure and the overall duration of the procedure [184].

Three principal methodologies are utilized for image-based catheter tracking:

- **3D reconstruction of the vessel anatomy**: This process involves digitally generating a 3D model of the patient's vascular system from multiple 2D images acquired during the procedure.

- **Detection and tracking of catheter and guidewires**: Accurate tracking of the catheter and guidewire throughout the procedure is crucial for successful navigation. This involves identifying the catheter and guidewire in each 2D image and determining their position and orientation relative to the patient's anatomy.

- **Registration of the patient's 3D model to the 2D images**: Synchronizing the patient's 3D vascular model with real-time 2D imaging data is essential for seamless navigation. Registration involves aligning the 3D model with the current 2D image to superimpose the corresponding anatomical structures.

Combining these three methodologies enables physicians to navigate catheters and guidewires precisely and accurately, even in complex vascular anatomies. 3D reconstruction provides a comprehensive overview of the target vessels, while catheter and guidewire tracking ensures precise positioning. Registration ensures that the 3D model remains synchronized with the real-time 2D imaging data, providing continuous guidance throughout the procedure.

Deformations of anatomical structures due to respiration and cardiac motion can significantly impact the accuracy of catheter tracking. Therefore, advanced tracking algorithms must account for these dynamic changes and maintain accurate catheter localization during the procedure. Additionally, real-time performance is paramount for image-based catheter tracking systems to provide physicians with immediate feedback and facilitate seamless navigation. This real-time processing requirement necessitates the development of efficient and robust tracking algorithms that can handle the high-speed acquisition of imaging data and rapidly update the catheter's position and orientation.

Catheter Detection and Tracking – x-ray

A wide variety of catheters are used during endovascular procedures tailored to the specific clinical application being performed. For example, specially designed catheters are utilized in EP procedures, each equipped with various attached electrodes based on their specific application. These catheters are used for heart treatments, measuring electrical signals, and applying radio-frequency ablation. Due to their technical design, the electrodes along the catheter are particularly visible in x-ray images, facilitating precise navigation and treatment.

An effective EP catheter detection and tracking method in fluoroscopic images involves several steps. Initially, the electrodes are detected, distinguishing between the catheter tip and the remaining electrodes. Next, catheter hypotheses are generated based on this information and ranked to identify the most probable catheter position. Over time, this framework has been refined and optimized using model-based, machine-learning, and deep-learning approaches, enhancing accuracy and efficiency in catheter tracking.

Model-based approaches involve constructing geometric and appearance models of the catheters to facilitate their detection and tracking. These models serve as a foundation for identifying catheter patterns in fluoroscopic images. Machine learning methods enhance these models by training algorithms to recognize and predict catheter patterns based on annotated images. Deep learning approaches take this further by utilizing neural networks, which can learn complex features from extensive dataset, thereby improving the accuracy and robustness of catheter detection and tracking.

Catheter-specific methods utilize prior knowledge of the catheter's form, such as its visual appearance and the number of electrodes, to develop an initial model for tracking in subsequent frames. Initial catheter hypotheses can be generated manually by labeling the catheter tip and electrodes [208] or automatically detecting these components as blob-like structures. Automatic detection techniques include Laplacian-of-Gaussian, Difference-of-Gaussian filters, and SURF features [107, 109, 122, 123], as well as Kalman Filter-Based Growing [209].

Catheter hypotheses can be generated through techniques like dictionary learning [28, 122] or fully convolutional neural networks [16]. With multiple views, the 3D position of the catheter can be calculated using epipolar constraints between pairs of views [17, 200], which supports 3D road mapping and navigation during endovascular procedures. These methods provide fully automatic and computationally efficient frameworks but are generally confined to specific catheters used in EP procedures.

Alternative methods do not need specific prior knowledge of the catheter's structure for tracking but require an initial position to be identified or computed. These approaches often model the catheter as a B-spline curve, defined by a set of control points and basis functions. Typically, the B-spline model is initialized using a manual label of the catheter in the first frame and then tracked across subsequent frames.

During tracking, the goal is to adjust the curve's parameters and control points to align with the catheter's current position and shape in the image [32, 66, 144]. The curve's displacement between frames is typically achieved by optimizing image data and applying regularization terms to maintain curve length or smoothness. This method allows for the potential tracking of various catheters as they adapt to different shapes and positions through these adjustments.

Tracking other medical instruments, like guidewires in x-ray images, often employs similar principles to catheter tracking and encounters comparable challenges. Therefore, many techniques focus on generalized frameworks applicable to catheter and guidewire tracking, particularly for tubular-shaped instruments. Below are some exemplary methods used for guidewire tracking in endovascular procedures.

For instance, Wang et al. [202] utilize a combination of intensity-based and learning-based models to find a hypothesis for the catheter tip, guidewire tip, and guidewire segment in fluoroscopic images. The posterior probability of the guidewire presence is maximized by training a guidewire feature classification using Haar features and additional visual information, optimizing for respiratory and non-rigid cardiac motion.

In contrast, Vandini et al. [197] propose dividing the guidewire into several segments, detecting each segment in each frame based on image data, and forming guidewire hypotheses. The most likely hypothesis is then chosen according to the tracking result from the previous frame, addressing some drawbacks of the B-spline representation.

Similar concepts are applied for image-based tracking in neurosurgery applications. One example is described by Lessard et al. [95], requiring an initial segmentation of the guidewire in the first frame, while Zweng et al. [223] rely on the movement of the guidewire for tracking. These methods, whether segment-based or motion-based, are designed to improve the accuracy and reliability of guidewire tracking by leveraging different aspects of image information and motion dynamics.

Recent advancements in medical image segmentation using deep learning, particularly with the introduction of U-Net, have led to numerous methods focusing on catheter and guidewire detection and tracking based on instance segmentation [10, 133, 188, 222]. Extracting an ordered set of points on the catheter centerline allows for fully automatic catheter tracking frameworks [10]. Another method involves two stages: detecting the region of interest and target segmentation [97]. Machine learning methods, though effective, require large annotated dataset, which are time-consuming to acquire.

Unsupervised methods utilizing optical flow offer a promising direction to mitigate this issue, but they have yet to be evaluated for 3D catheter reconstruction and tracking [199]. Tab. 5.1 summarizes state-of-the-art x-ray-based catheter tracking methods reviewed in this dissertation, highlighting their computational time, average error, and automation. Direct comparisons can be challenging due to differences in evaluation criteria and clinical applications.

2D/3D Registration – x-ray

Once detected in a 2D image, the catheter's position can be visualized in 3D if its depth can be determined. Depth perception can be achieved through multiple views or constraints provided by preoperatively acquired 3D scans, assuming 2D/3D mapping can be computed. For this, 2D/3D registration methods align intraoperative 2D images, such as fluoroscopy, with preoperative 3D images.

We will explore some fundamental approaches and applications in 2D/3D registration techniques. This topic has been extensively researched, with various methods addressing different surgical procedures. An overview of 2D/3D registration methods for CT or MRI and x-ray projections up to 2012 is provided by Markelj et al. [117], while Liao et al. [99] focuses on methods for minimally invasive procedures from 2006 to 2013.

One critical step in 2D/3D registration is extracting relevant features present in both preoperative and intraoperative images. These features are typically computed for vascular intraoperative navigation by segmenting the vasculature in the preoperative image [34, 94]. This segmentation can then be processed to obtain a 3D model for visualization during the intervention. Other methods, such as the one of Wu et al. [209], utilize preoperative data and intraoperative ultrasound volumes to register with fluoroscopic images for further guidance.

Maintaining accurate registration over time is challenging for structures significantly deformed by respiratory and cardiac motion or instrument-tissue interactions. Such motion complicates the accurate display of the anatomy or roadmap, making frame-to-frame registration necessary. Many methods have focused on motion estimation in subsequent frames to address this challenge. A common approach involves acquiring an initial catheter position and then using it to track and update the registration in subsequent frames. This method continuously estimates and compensates for motion to ensure accurate, real-time catheter alignment with anatomy.

For example, Ambrosini et al. [9] propose an algorithm for rigid 3D to 2D registration for TACE procedures. The method matches the 2D catheter centerline to the most similar part of the 3D vessel model, determining corresponding points sparsely. This results in a continuous, computationally efficient representation for automatic registration.

Additionally, Ambrosini et al. [11] suggest using a Hidden Markov Model (HMM) to track the catheter tip over time after initial registration in x-ray with a 3D vessel model. Points on the 3D vessel centerline are defined as HMM states, and the model estimates the catheter tip's probability at each point. The HMM updates based on the 3D vessel tree's registration with the current 2D image frame, reporting an error of less than 1.9 mm.

Brost et al. [26] utilize a lasso catheter's ellipsoid shape to reconstruct the catheter in 3D using bi-plane fluoroscopy images and manual initialization. After initial reconstruction, filter-based segmentation is applied, and distance map images relative to the catheter are estimated in subsequent frames. A deformable 2D/3D registration aligns the re-projected 3D model with the current frame, compensating for breathing motion. A learning-based classification approach improves segmentation [27], achieving a mean 3D tracking error of 0.7 mm, outperforming vesselness-based filters like the Frangi filter.

The coronary sinus catheter, which maintains a nearly static position relative to the anatomy during the procedure, is a reliable reference for motion estimation [109]. Tracking this catheter enhances 2D/3D registration accuracy, with a mean 2D registration error of 1.6 mm.

For PCI, Ma et al. [105] developed a neural network predicting a heatmap for the catheter tip used for contrast agent injection, using this prediction for respiratory motion correction. Alternatively, Electrocardiogram (ECG)-gating optimizes roadmap selection based on the cardiac phase, providing a framework for cardiac motion with real-time computational capability.

3D Reconstruction – x-ray

Preoperative 3D images commonly provide essential visual information during interventions. However, accurately displaying the catheter's location within the anatomy requires estimating its 3D position. As a result, extensive research has focused on 3D/4D catheter reconstruction methods based on 2D images acquired during interventions. Fluoroscopic image sequences from multiple views facilitate catheter reconstruction through triangulation.

Bender et al. [18] introduced a method for reconstructing pulmonary artery catheters, assuming and initial 3D position and tangent to the catheter shape is known. An iterative algorithm is applied to reconstruct the 3D shape of the catheter as a series of 3D points constrained by the edge information in 2D x-ray images.

For EP catheter reconstruction, Baur et al. [17] and Hoffmann et al. [73] use epipolar constraints from bi-planar angiographic imaging systems. By detecting the catheter in one view, they leverage these constraints for 3D reconstruction. While bi-plane x-ray systems can provide synchronous image sequences, monoplane systems require gating for synchronization, making single-view reconstruction methods desirable.

Petković et al. [146] use preoperative 3D scans to extract a volume containing the vessel tree. They compute 3D catheter hypotheses based on x-ray system geometry and 2D catheter detection, assuming the catheter is within the vascular tree. This method's resolution, accuracy, and computational time are linked to the preoperative 3D scan's voxel size and volume.

In contrast, Eulig et al. [50] propose reconstructing medical instruments using four cone-beam CT projections and a learning-based approach. This method segments instruments in a sparse volume reconstruction without requiring view correspondences or patient-specific prior knowledge and registration, though it has only been tested on simulated data.

Current methods often rely on preoperative CT or MRI scans to visualize catheters within the 3D patient anatomy. However, such scans might not always be available, and catheterized procedures are frequently used for initial diagnostics, such as diagnosing vessel stenosis without prior CT scans. Methods less reliant on patient-specific knowledge are appealing. Çimen et al. [38] review 3D/4D reconstruction of coronary vessels from x-ray angiography, discussing how corresponding points on vessel centerlines in multiple views can be matched and ECG-gating used to enhance reconstruction accuracy.

Deformable models offer an alternative for estimating the 3D anatomy or medical instrument during endovascular procedures. These models adjust an initial 3D model based on current image data, making them helpful in tracking instrument deformation over time [201]. Despite promising results, 3D model reconstruction is challenging due to the complexity of real-time dynamic modeling. Pursuing this research could significantly improve the precision and reliability of endovascular procedures.

Image-based Catheter Tracking – Ultrasound

Ultrasound imaging offers several advantages over x-ray imaging for catheter navigation. The high soft-tissue contrast provided by ultrasound enables clear visualization of vascular structures, including the catheter itself, without the need for contrast agents. Additionally, ultrasound imaging is relatively inexpensive and does not generate ionizing radiation.

However, ultrasound imaging also faces several limitations that can hinder catheter navigation. The resolution of ultrasound images is typically lower than that of x-rays, making it more challenging to detect small anatomical details. Moreover, ultrasound probes have a smaller field of view compared to x-ray devices, limiting the area that can be visualized at once.

Tab. 5.1. Summary of x-ray image-based catheter tracking methods categorized by their clinical focus, computational time, level of automation, and average error. (Tip – evaluating only the catheter tip; E – evaluating individual electrodes of EP catheters).

Note: Table reused without changes © 2022 Elsevier [154]. Used with permission under CC BY 4.0.

Authors	Clinical focus	Time (FPS)	Level of automation	Average error (target)
Ambrosini et al. [10]	TACE	8 GPU	Automatic	Median 0.2/0.9 mm (Tip)
Baur et al. [16]	EP/Ablation	∼5	Automatic	–
Chang et al. [32]	TAVI	20	Semi-aut. init.	–
Heibel et al. [66]	Cardiac/TACE	16.7	Semi-aut. init.	0.8–3.9 px
Ma et al. [105]	PCI	∼18 GPU	Manual init.	1.3 mm (Tip)
Ma et al. [109]	EP/Ablation	21	Automatic	0.4 mm (E)
Ma et al. [107]	EP/Ablation	15	Automatic	0.96 mm det., 0.67 mm track. (E)
Milletari et al. [123]	EP/Ablation	∼3	Automatic	0.5 mm (E)
Milletari et al. [122]	EP/Ablation	∼12	Automatic	0.71 mm (E)
Pauly et al. [144]	TACE	1.5	Manual init.	–
Vandini et al. [197]	Angioplasty	∼.5–1	Manual init.	2.4/25.6 px (Tip)
Wang et al. [202]	Cardiac	2	Manual init.	2 px/0.4 mm
Wu et al. [208]	EP	∼5	Manual init.	0.76 mm (E)
Wu et al. [209]	EP/Ablation	30	Automatic	<1 mm
		Registration/Reconstruction		
Ambrosini et al. [9]	TACE	∼5	Semi-aut.	Median 4.7–5.4 mm
Ambrosini et al. [11]	TACE	∼17	Semi-aut.	Median <1.9 mm
Baur et al. [17]	EP/Ablation	–	Automatic	0.67 mm (E)
Brost et al. [27]	EP/Ablation	1	Semi-aut.	2D 0.8 mm/3D 0.7 mm
Ma et al. [109]	EP/Ablation	21	Automatic	1.6 mm (E)
Hoffmann et al. [73]	EP/Ablation	∼.13	Semi-aut.	0.4 mm

Additionally, ultrasound images are susceptible to artifacts caused by respiratory and cardiac motion and tissue deformation induced by the sonographer's hand pressure to the probe. These artifacts can obscure the catheter, making it difficult to track its position accurately.

Chen et al. [35] and Chen et al. [36] present a particle filter approach for tracking catheters and estimating their 3D shape from 2D ultrasound images. This method achieves a shape estimation error of about 3 mm in in-vivo experiments. Similarly, Langsch et al. [92] use robot-guided ultrasound and template matching to track catheters in 2D ultrasound images, achieving an average catheter tip detection error <2 mm, enhancing both accuracy and real-time performance. A screenshot of the catheter tracking system is shown in Fig. 5.2.

Some studies merge multiple imaging modalities, like preoperative CT/MRI scans and live x-ray sequences, to improve catheter tracking in ultrasound images. For example, Wu et al. [209] use live x-ray sequences to guide catheter segmentation in 3D Transesophageal Echocardiography (TEE) for EP procedures. The catheter is initially detected and tracked in real-time fluoroscopy images, constraining the search space within the ultrasound volume by constructing a feature-based graph.

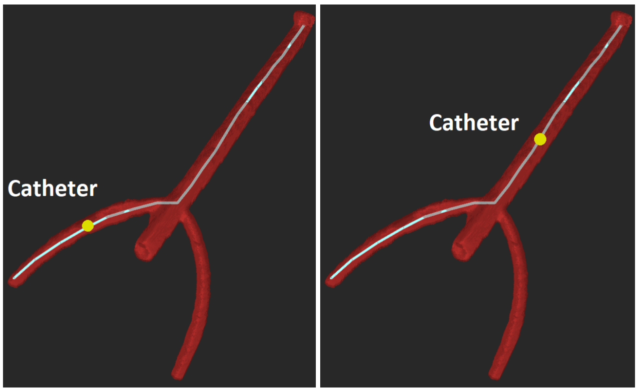

Fig. 5.2. Automatic robotic catheter tracking using ultrasound, introduced by Langsch et al. [92]. The figure shows the insertion of a catheter into the aorta, with the solution maintaining the catheter tip within the ultrasound image and visualizing its position in a segmented preoperative image of the aorta.
Note: Figure reused without changes © 2022 Elsevier [154]. Used with permission under CC BY 4.0.

Recently, deep learning-based methods have shown promise in 3D ultrasound catheter segmentation [212, 213, 214, 215]. These methods typically classify each voxel of the ultrasound volume as belonging to the catheter or not, facing challenges like high computational processing time, large annotated dataset, and class imbalance. Yang et al. [213] address these issues with adaptive thresholding and patch-based classification, achieving an average error of 2 mm but with a computational time of 10 s per volume, limiting its real-time applicability.

Subsequent works improve computational efficiency by using reinforcement learning to estimate an initial 3D position and a semi-supervised learning approach with two neural networks. This two-stage method achieves an average run-time of 1.2 s per volume [214]. Further efficiency is achieved by replacing a 3D-3D encoder-decoder network with a 3D encoder and two 2D decoders, reducing computational time to 0.12 s per volume [212].

Combining ultrasound images with other modalities, such as intraoperative fluoroscopy or preoperative CT volumes, can enhance visualization. For example, Chen et al. [35] use fiducial markers for registering preoperative CT scans with the ultrasound device. In contrast, Langsch et al. [92] present a framework for robotic ultrasound guidance and 3D roadmapping for aortic aneurysm treatment without additional markers.

While not directly tracking catheters, approaches like merging TEE with interventional x-ray sequences to locate the TEE probe and infer its pose have been successful. For instance, Gao et al. [56] match a 3D model of the ultrasound probe to its x-ray projection, achieving an error below 2mm with a computational time of 1.3 s per frame. Ma et al. [108] propose a framework operating at 20 fps with a 2.6 mm error, using a cascade classifier for probe detection and a template database for pose estimation. A summary of image-based ultrasound catheter tracking methods can be found in Tab. 5.2.

Within this context, such methods have led to the successful development of commercial products such as the Philips EchoNavigator[1] (Andover, Massachusetts, USA) or the Siemens Syngo TrueFusion[2] (Malvern, Pennsylvania, USA).

[1] `www.usa.philips.com/healthcare`
[2] `www.siemens-healthineers.com/`

Image-based Catheter Tracking – MRI

The introduction of real-time MRI has opened up new possibilities for intraoperative navigation, offering a radiation-free alternative to conventional x-ray and ultrasound-based techniques. MRI provides enhanced soft-tissue contrast, a wider field of view, and superior image quality compared to ultrasound. However, the use of MRI for interventional procedures faces a significant challenge: the visualization of medical instruments like catheters. The presence of metallic components in commonly used EP catheters poses a significant obstacle due to the magnetic field of the MRI scanner, which can interfere with their operation and lead to artifacts and signal distortions. Despite these limitations, recent advancements have demonstrated the feasibility of interventional MRI and catheter tracking in cardiac EP procedures [30, 125]. To address these challenges, specifically designed catheters have emerged, incorporating features that enhance their visibility in MRI modalities.

Image-based detection and tracking techniques can streamline catheter tracking by matching a template signal and using the k-space signal matched via cross-correlation [49, 138, 157, 158]. For 3D catheter positioning, these methods are applied on three orthogonal slices of the MRI reconstructed volume, detecting the catheter in each slice through a 2D Gaussian template fitting approach [193]. This approach allows precise tracking of the catheter's position within the 3D space of the MRI volume.

Like most image-based methods, MRI image-based methods generally utilize a reconstructed image to detect the catheter. This means the tracking system must first reconstruct the image from the MRI data, which can introduce artifacts and noise. Additionally, the catheter's visibility in the image plane is crucial for accurate detection. If the catheter is not visible, the tracking system may not identify it correctly. Finally, the differentiation between the catheter and background tissue is also important. If the catheter is not well-defined or blends in with the surrounding tissue, the tracking system may have difficulty tracking its movement. A summary of MRI image-based tracking methods can be found in Tab. 5.2.

Tab. 5.2. Summary of Ultrasound and MRI image-based catheter tracking and segmentation methods, categorized by clinical focus, data type, imaging modality, computational time, and average error.
Note: Table reused without changes © 2022 Elsevier [154]. Used with permission under CC BY 4.0.

Authors	Clinical focus	Data	Modality	Time	Average error
Chen et al. [35]	IVUS	Phantom	US/Optical tracking/CT	–	2.23 mm
Chen et al. [36]	Cardiac	in-vitro/in-vivo	US/Optical tracking	∼14 fps	2.13/3.37 mm
Langsch et al. [92]	EVAR	Phantom/Volunteers	2D/3D US/MRI	–	1.78 mm
Wu et al. [210]	Cardiac	Phantom	US/x-ray	1.5 fps	$<$2 mm
Wu et al. [209]	EP/Ablation	Porcine/Patient	US/x-ray	1.3 s	2 mm
Yang et al. [212]	EP/Ablation	Porcine/Chicken	3D US	0.12 s GPU	2–3 voxel
Eldirdiri et al. [49]	Catheterization	Phantom	MRI	100 ms	$<$1 mm
Oliveira et al. [138]	Biopsy needle	Phantom	MRI	1 fps	1.5 mm
Rea et al. [157]	Catheterization	Phantom	MRI	0.3 ms	max 0.22 mm
Reichert et al. [158]	Needle placement	Phantom	MRI	62 s	∼1.1 mm
Thörmer et al. [193]	Needle placement	Phantom	MRI	∼350 ms	∼1 mm

5.4.2 Active/Passive Catheter Tracking

Despite its advantages, image-based catheter tracking can prove challenging in the dynamic environment of endovascular procedures. To overcome these difficulties, active and passive catheter tracking methods employing additional hardware components offer promising solutions. We first introduce the concepts of active and passive tracking, then explore state-of-the-art techniques based on used imaging modalities, namely ultrasound and MRI.

Passive catheter tracking involves using a passive element, such as a marker or reflector, attached to the catheter tip to receive signals transmitted by an imaging modality. The direction and time of arrival of the received signal are used to determine the position of the passive element relative to the transmitter. This method is relatively simple and efficient but is also scanner-dependent, meaning it may only work with some imaging modalities.

Active catheter tracking utilizes an active element, often a miniature radiofrequency transmitter, embedded in the catheter tip to emit signals into the body. The imaging modality then detects these signals, and their location is determined using signal processing techniques. This method is more versatile than passive tracking as it is not limited by the imaging modality. However, it is also more complex and expensive to implement.

Many research projects and publications have been dedicated to overcoming the challenges of using ultrasound for catheter tracking. These studies explore various methods for visualizing and detecting catheters using active and passive elements in ultrasound images. Among these efforts, Breyer and Cikeš [25] introduced the concept of active/passive ultrasound catheter tracking, utilizing a piezoelectric element attached to the catheter tip and an ultrasound transducer to capture the emitted pulses. This simple system significantly enhances catheter visualization in ultrasound images.

Active/Passive Catheter Tracking – Ultrasound

The numerous projects and papers published highlight the ongoing efforts to address the limitations of using ultrasound for catheter tracking. These studies evaluate various methodologies for visualizing and detecting catheters in ultrasound images using active and passive elements. Literature on ultrasound catheter tracking dates back to the 1980s, with Breyer and Cikeš [25] introducing the fundamentals of active/passive ultrasound catheter tracking. They presented a novel approach involving a piezoelectric element attached to the catheter tip and an ultrasound transducer capturing pulses from the element alongside regular ultrasound images. A schematic of the proposed system is presented in Fig. 5.3.

Inspired by Breyer and Cikeš [25], Guo et al. [62] developed the active ultrasound pattern injection system (AUSPIS). This system operates on similar principles but employs an active echo approach, triggering the piezoelectric element only when a signal is received from the ultrasound transducer, ensuring the catheter tip is within the field of view. This system enhances localization accuracy with performance configurations, achieving mid-plane accuracy of 0.3 mm up to a depth of 8.5 cm.

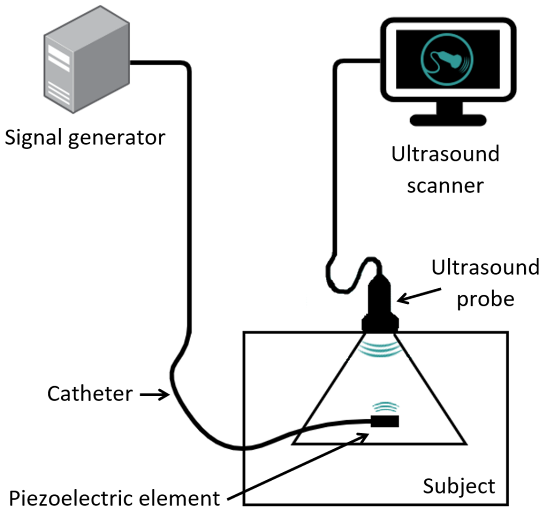

Fig. 5.3. Schematic of an active ultrasound catheter tracking approach, proposed by Breyer and Cikeš [25]. The schematic shows an ultrasound scanner and probe capturing signals generated by a piezoelectric element attached to the tip of the catheter from within the human body, powered by an external signal generator. *Note: Figure reused without changes © 2022 Elsevier [154]. Used with permission under CC BY 4.0.*

Building on AUSPIS, Ma et al. [106] introduced the robotic ultrasound system for tracking a catheter with an active piezoelectric element (RUSTCAPE). This system uses catheter tip localization for autonomous tracking with a robotic arm equipped with an ultrasound probe. AUSPIS and RUSTCAPE rely on mid-plane detection, assuming proper catheter alignment with the transducer's center. Alignment is evaluated based on the signal strength received but lacks capabilities for detecting the catheter's position within the ultrasound image.

Mung et al. [127] presented another approach, using a piezoelectric element at the catheter tip and a custom-made array of seven transducers to receive pulses and determine its position. Each transducer comprises a piezoelectric element, focusing solely on catheter localization without imaging capabilities. The configuration of the system components is presented in Fig. 5.4. Despite this limitation, the system achieves mean errors of 1.05 mm, 2.42 mm, and 3.23 mm along the x, y, z axes, respectively. While similar to Electromagnetic (EM) tracking, this method necessitates skin contact, setting it apart from conventional EM systems.

Cheng et al. [37] and Meyer and Wolf [120] also use active elements for catheter tracking, leveraging sonomicrometry to measure distances between piezoelectric elements for accurate localization. Additionally, Mung et al. [128] propose a method using ultrasound energy emitted from the catheter tip, detected by an external sensor array on the body surface. This system measures the time of flight to pinpoint the catheter tip's position, which is then registered with the patient's CT scan for better visualization.

Xia et al. [211] introduce the fiber optic hydrophone, a thin, flexible fiber placed within the needle. This method, emitting visible pulses in ultrasound, is accurate for various depths and angles, with errors of 0.71 mm and 1.02 mm in the x and y axes, respectively. The system configuration and fiber optic hydrophone sensors are presented in Fig. 5.5. While this technology accommodates different needle and catheter diameters, it is significantly more costly than piezoelectric elements.

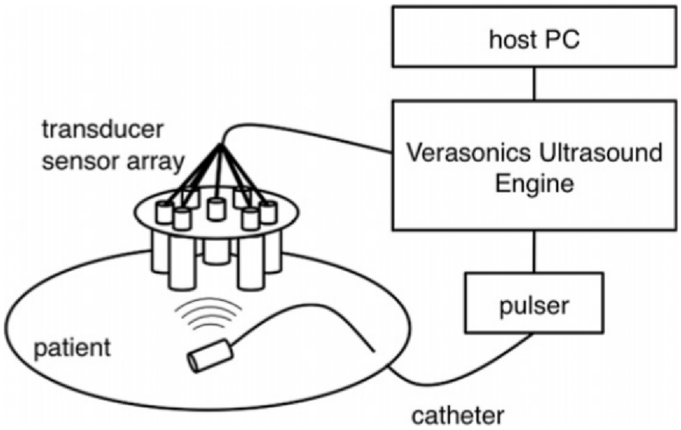

Fig. 5.4. Schematic of an active ultrasound catheter tracking approach with a custom-made seven-transducer layout, introduced by Mung et al. [127]. The system uses an ultrasound engine to operate the transducer sensor array, while a piezoelectric element at the catheter tip generates pulses. The seven transducers receive pulses from the catheter, and triangulation methods are used to calculate the catheter's position.
Note: Figure reused without changes © 2011 Elsevier [127]. Used with permission. License Number 5811031263901.

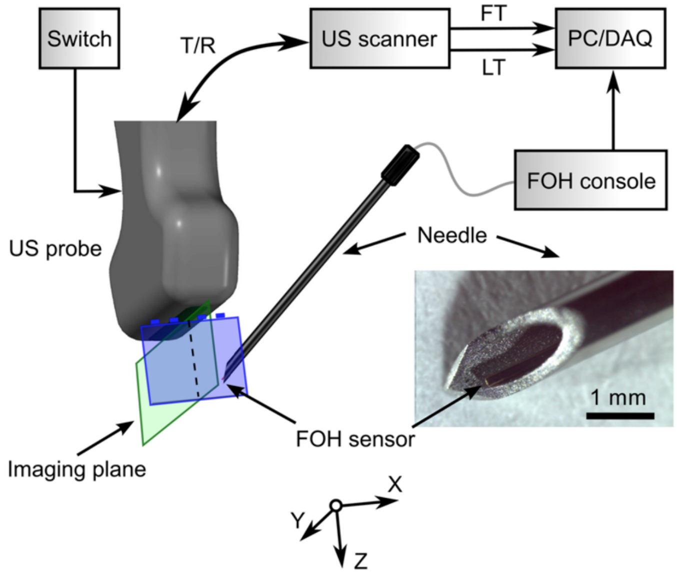

Fig. 5.5. Schematic of an active ultrasound catheter tracking approach using a fiber optic hydrophone, introduced by Xia et al. [211]. This method uses a fiber optic hydrophone to generate pulses, instead of a piezoelectric element. A standard 2D ultrasound probe detects the location of the needle tip.
Note: Figure reused without changes © 2017 Springer Nature [211]. Used with permission under CC BY 4.0.

In passive ultrasound-based instrument tracking, significant contributions have been introduced through the collaborative efforts of J. Stoll and P. Dupont. Their publications have focused on passive ultrasound marker-based tracking, integrating image-based tracking with passive markers to ensure precise detection of medical instruments [185, 186, 187].

Their systems have been evaluated in various experimental setups, reporting accuracy between 0.22 mm and 1.7 mm. These systems notably use ring-shaped echogenic markers attached to the distal end of instruments in various configurations, enhancing visibility and tracking accuracy within ultrasound images. A summary of the ultrasound-based active/passive catheter tracking methods can be found in Tab. 5.3.

Active/Passive Catheter Tracking – MRI

Both active and passive tracking technologies in MRI enhance the catheter's visibility. Active methods embed micro-coils in the catheter, connecting them to the MRI's receiver channel. These coils produce signals that show the catheter's 3D position within the magnetic field when gradients are applied along the MRI's spatial axes [170]. For better accuracy, Hillenbrand et al. [72] attached two independent coils to a catheter, though concerns about tissue heating remain [90]. To address this, Nassar et al. [132] proposed using inductive coupling instead.

Passive tracking methods use markers made of ferromagnetic [219] or paramagnetic materials [205] that distort the MRI magnetic field, creating artifacts in the images for localization. Early methods involved impregnated catheters or contrast agents causing local magnetic field changes [204]. Catheters filled with contrast agents allow complete visualization [110].

Recent semi-active methods employ resonant coils tuned to the proton frequency and inductively coupled to the MRI's receiver coil. This enhances the local B1 field near the catheter tip, improving contrast in the image and facilitating tracking with standard methods [29].

Tab. 5.3 summarizes MRI-based active and passive catheter tracking methods, their average errors, and the experimental settings. MRI-based methods are mainly tested in phantom or animal studies. While passive or semi-active methods avoid some safety issues of active tracking, they still require fully reconstructed images and depend on the catheter's visibility against surrounding tissue.

Tab. 5.3. Summary of Ultrasound and MRI active/passive catheter tracking methods, categorized by clinical focus, data type, imaging modality, method, and average error.
Note: Table reused without changes © 2022 Elsevier [154]. Used with permission under CC BY 4.0.

Authors	Clinical focus	Data	Modality	Method	Average error
Breyer and Cikeš [25]	Catheterization	Water tank/in-vivo	US	Active/Passive	–
Cheng et al. [37]	Catheterization	Phantom/Simulation/in-vivo	US	Active	0.5 mm at best
Guo et al. [62]	Catheterization	ex-vitro/in-vivo	US	Active	mid-plane detection of 0.3 mm
Ma et al. [106]	Cardiac catheterization	Water tank/Phantom	US	Active	Det. range from 10 mm–1 cm
Meyer and Wolf [120]	Cardiac catheterization	Simulation/in-vivo	US	Active	1.06±0.27 mm and 0.52±0.66 mm
Mung et al. [127]	EVAR	Water tank/in-vitro	US	Active	1.94±0.06 mm and 2.54±0.31 mm
Mung et al. [128]		in-vivo stent placement			6.43 mm
Stoll and Dupont [187]	MIS	Water tank	US	Passive	0.22 mm
Stoll et al. [185]		Water tank			0.81 mm
Stoll et al. [186]		Water tank and ex-vivo			0.7 mm and 1.7 mm
Xia et al. [211]	MIS	Water tank/in-vivo	US	Active	0.38 mm in water tank
Busse et al. [29]	Needle placement	Phantom	MRI	Semi-active	1.7 mm
Hillenbrand et al. [72]	Endovascular	Phantom/Porcine aorta	MRI	Active	$<$ 2 mm
Magnusson et al. [110]	Endovascular	Porcine aorta	MRI	Passive	–
Weide et al. [205]	Endovascular	Phantom/Porcine carotid	MRI	Passive	<3 mm/–
Zhang et al. [219]	Endovascular	Aorta phantom/Porcine	MRI	Passive	1 mm/4 mm

5.4.3 Electromagnetic Catheter Tracking

Electromagnetic (EM) tracking is a widely used technology in the medical field, with numerous applications and publications supporting its effectiveness. Unlike optical tracking, which requires a direct line of sight, EM tracking continuously tracks small sensors within the EM field, even if the sensors are inside the human anatomy. This allows physicians to track flexible instruments in real-time, enhancing the precision and safety of minimally invasive endovascular procedures [54].

Through our research, we identified a need for more standardization in the naming conventions used for the components of EM tracking technology. To ensure clarity, we propose classifying these components into three core elements: Field Generator, EM Sensor – with Sensor Interface Units, and the Integrated Tracking Module [54, 154, 216]. An image of the introduced standardised EM tracking system components is presented in Fig. 5.6.

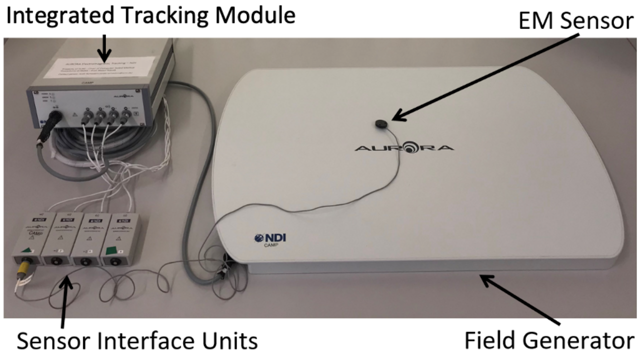

Fig. 5.6. Electromagnetic tracking system and its components, introduced by Ramadani et al. [154]. The system consists of the integrated tracking module, sensors with the sensor interface units, and field generator. *Note: Figure reused without changes © 2022 Elsevier [154]. Used with permission under CC BY 4.0.*

The field generator is responsible for creating an EM field of known geometry. It typically consists of one or multiple EM coils. When an EM sensor is moved within this field, its position and orientation can be determined by the integrated tracking module.

The integrated tracking module is the central hub for EM tracking, overseeing data acquisition, sensor pose calculation, and providing position and orientation information to computer-assisted intervention systems. EM tracking has been a well-established technology in the medical field since its introduction in the 1970s, with numerous commercial products available. Field generators and EM sensors come in various shapes and sizes, including cubic or flat-bed configurations, and are compatible with various medical instruments. They can also be integrated directly into medical instruments and catheters for seamless tracking during procedures [40, 137, 154].

Despite its widespread use, EM tracking has some limitations that hinder its adoption. EM signals can be distorted in the presence of large imaging modalities or ferromagnetic objects, potentially compromising accuracy. Additionally, positioning the EM field generator can be challenging, and specialized catheters with integrated EM sensors are expensive. For in-depth insights into the challenges of manufacturing small-size catheters with integrated sensors, we recommend reading Abdelaziz et al. [3], Condino et al. [40], and Piazza et al. [147].

Throughout the literature, two main error types have been identified in regards to EM tracking systems and their applications:

- **Internal errors** arise from the EM tracking system itself, such as sensor misalignment or signal noise. They can be characterized as systematic errors, as they are inherent to the system and can be mitigated through calibration and optimization.

- **External errors**: arise from factors external to the EM tracking system, such as patient motion, registration to anatomical images, and calibration of tracked medical instruments. They are often unpredictable and can degrade tracking accuracy.

A comprehensive study on EM tracking sensor interference with metallic objects was conducted by Nafis et al. [130]. The paper primarily examined the errors introduced in the EM trackers' relative coordinate system due to the presence of metallic objects. The study employed various EM tracking vendors and consistently positioned metallic objects around the sensors to assess the impact of different scenarios. However, the setups in the study did not closely mimic real-world medical procedures and instrument usage.

A similar study conducted by Maier-Hein et al. [111], evaluated the interference error introduced in interventional radiology environments by three different EM tracking field generators. The study found that while the interference errors were relatively small, EM tracking devices should be evaluated and calibrated precisely for their intended application and the environment in which they will be used. This assessment was previously conducted by Yaniv et al. [216], who compared two different EM tracking systems in four clinical environments.

Attivissimo et al. [13] describes efforts to enhance EM tracking accuracy by redesigning the field generator. The proposed generator consists of five electromagnetic coils utilizing frequency division multiplexing to improve system sensitivity and provide modularity and scalability for various applications. Similarly, Jaeger and Cantillon-Murphy [81] examines the accuracy of modular tilted field generators, suggesting that using multiple planar printed circuit board field generators at specific angles reduces EM sensor localization error.

Motion compensation is another significant challenge that requires real-time tracking. Gergel et al. [57] propose an EM tracking system for dual respiratory motion compensation, using two filters: one compensating for bronchoscope motion and the other estimating the relative movement of an integrated needle, with a mean error of 10.8±3.0 mm in 18 procedures.

Jaeger et al. [80] presents an automated catheter navigation system similar to Gergel et al. [57], targeting lung anatomy with experiments conducted both ex-vivo and in-vivo. The study reports the time taken to reach targeted lung points, averaging 29 s ex-vivo and 9.71 s in-vivo, but does not evaluate EM system accuracy.

Hautmann et al. [65] evaluated an EM system for lung lesion localization. A portable field generator was positioned on the subjects' chests, and a catheter with an integrated EM sensor was inserted into the lungs. The study reported mean errors of 4.2 mm and 5.1 mm from the EM sensor's position compared to two endobronchial points in CT images.

Several studies have evaluated EM tracking systems for targeting regions of interest, focusing on positioning accuracy or task completion time, as summarized in Tab. 5.4 [59, 96, 102, 114, 131, 194, 221].

Lund et al. [103] applied EM tracking to aortic endovascular procedures, comparing its accuracy to conventional x-ray fluoroscopy in a phantom study. While no significant difference in cannulation time was observed, using EM tracking alone could enhance procedural safety by avoiding ionizing radiation and contrast agents.

Lambert et al. [91] investigated EM-tracked catheters in Endovascular Aneurysm Repair (EVAR) procedures, tested in two phantoms. EM-tracked signal paths registered the EM system with preoperative images, showing an average mean registration error of 1.3 mm. However, the authors did not thoroughly explain the initialization or component alignment in the same space. A visual schematic of the introduced method is presented in Fig. 5.7.

A more recent study by Nypan et al. [135] suggests that registering to the vessel centerline provides a more accurate representation of motion and blood flow conditions. However, the accuracy was slightly lower at 3.75 mm.

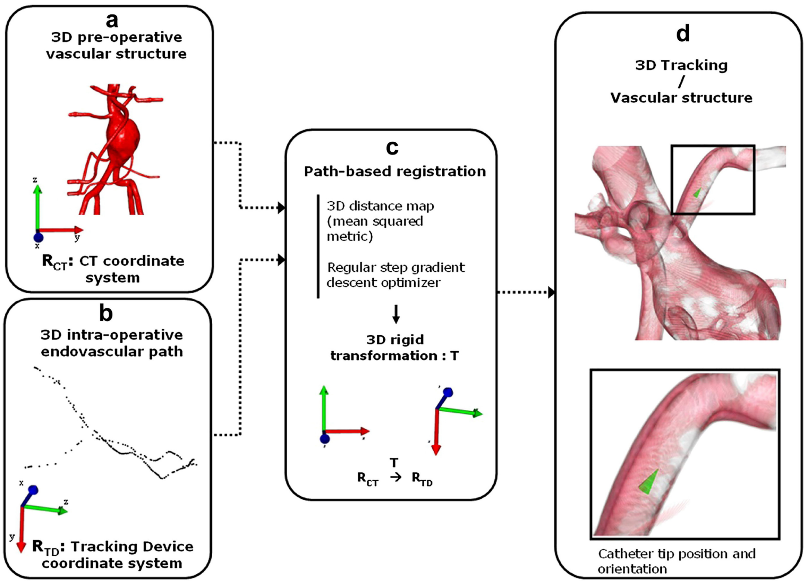

Fig. 5.7. Schematic of an EM-tracked catheter registration procedure, introduced by Lambert et al. [91]. (a) Preoperative image data acquisition of the anatomical region of interest, (b) Collection of intraoperative EM tracking data for the catheter's path, (c) Registration process aligning preoperative images with intraoperative EM-tracked path, and (d) Visualization of the EM-tracked catheter within the preoperative anatomical image, highlighting the catheter tip position and orientation.
Note: Figure reused without changes © 2012 Elsevier [91]. Used with permission. License Number 5811031417943.

Penzkofer et al. [145] describe an EM catheter navigation system designed for aortic stent placement and in-situ fenestration. This system offers an alternative method for restoring perfusion to the renal arteries post-stent placement, successfully tested in seven animal experiments with a 93% success rate in fenestrations. However, most re-perfusions exceeded the 30 minute ischemia limit, and the average fenestration and re-perfusion times were 10.5±9.2 minutes and 32.7±17.5 minutes, respectively, indicating the approach requires further refinement for clinical use.

Shi et al. [181] present an approach using EM sensors attached to an Intravascular Ultrasound (IVUS) device for real-time intravascular reconstruction and navigation. This method aims to improve placement accuracy during stent grafting by fusing IVUS data with EM tracking, achieving a reconstruction accuracy of 0.64 mm in a phantom setup. However, further clinical evaluations are needed to confirm these findings.

In neurosurgical applications, Gilard et al. [58] and Hermann et al. [69] evaluate the success of EM-guided ventricular catheter placement against free-hand techniques. Both studies highlight the benefits of EM navigation despite limitations such as patient number, follow-up duration, and group randomization. Hermann et al. [69] focus on pediatric cases, while Gilard et al. [58] assess adults, showing EM tracking's effectiveness in neurosurgical procedures.

Several companies offer commercial EM tracking solutions for medical applications. One of the leading providers is Northern Digital Inc – NDI[3] (Waterloo, Ontario, Canada), offering the Aurora and 3D Guidance systems. NDI's EM sensors come in various sizes, ranging from 0.3 mm to 10 mm in diameter, depending on the specific application. Other significant players in the EM tracking market include Philips[4] (Andover, Massachusetts, USA), Siemens Healthineers[5] (Malvern, Pennsylvania, USA), Brainlab AG[6] (Munich, Bavaria, Germany), GE Healthcare[7] (Chicago, Illinois, USA), and many others.

Successful implementation of such systems for catheter-based applications are presented by Carto® 3 System[8] (Irvine, California, USA) and Rhythmia HDx™[9] (Natick, Massachusetts, USA) in current clinical environments. The catheters of these systems integrate many technologies at their tip, including cardiac mapping, pressure sensing, radiofrequency ablation, and ThermoCool SmartTouch tip for tissue cooling.

Magnetic-based Catheter Navigation

Another subcategory of EM tracking is permanent magnetic-based catheter manipulation and navigation. This approach utilizes magnets to guide catheters remotely, without direct contact. This method employs a three-component system: (1) sizeable external magnet that generates a magnetic field around the target area, (2) catheter equipped with magnets at its distal end to interact with the magnetic field, and (3) magnet interface that allows for precise control of the magnetic field to manipulate the catheter's position [46].

While the primary focus of this approach is catheter movement, some implementations utilize permanent magnets or instrument magnetization for localization purposes. These methods require additional components and have yet to be as widely adopted. However, integrating permanent magnets at the catheter tip for localization alone remains an unexplored area of research. One major drawback of permanent magnetic-based catheter manipulation is the potential for magnetic interference and the cumbersome size of the magnets, which can make their use challenging in clinical settings.

[3] www.ndigital.com
[4] www.usa.philips.com/healthcare/
[5] www.siemens-healthineers.com
[6] www.brainlab.com
[7] www.gehealthcare.com
[8] www.jnjmedtech.com/en-US
[9] www.bostonscientific.com

A recent study by Pancaldi et al. [141] proposes using magnets to navigate catheters within the brain's vasculature, harnessing the power of blood flow. Their approach, dubbed "flow-driven robotic navigation," involves designing endovascular catheters that harness the hydrokinetic energy of blood flow to enhance their reach into the periphery of the brain's vascular network. A magnetic actuator, located outside of the vasculature, guides the catheter through targeted branches. However, the study does not provide data on the accuracy of this system. A visual representation of the workings of this method is presented in Fig. 5.8.

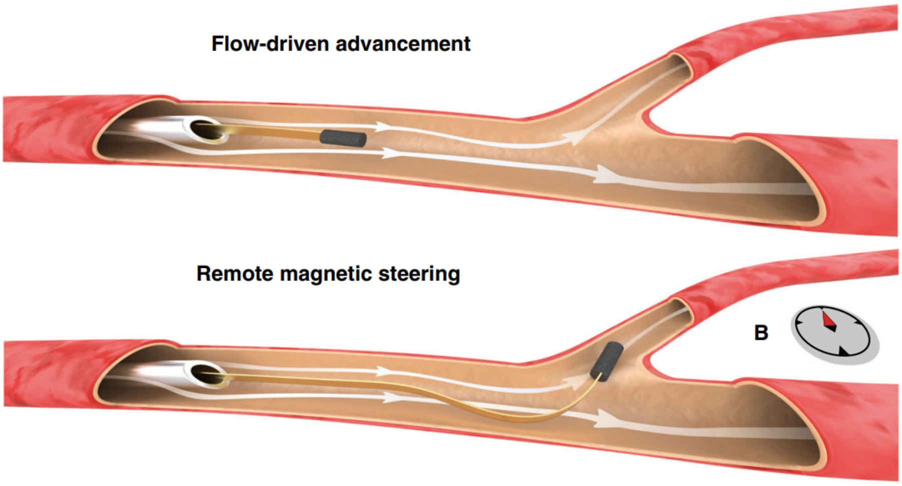

Fig. 5.8. Magnetic-based catheter navigation method, introduced by Pancaldi et al. [141]. A flexible catheter advances through the vascular system utilizing the hydrokinetic energy of blood flow. An external magnet steers the catheter tip into targeted branches, allowing precise navigation.
Note: Figure reused without changes © 2020 Springer Nature [141]. Used with permission under CC BY 4.0.

One commercially available magnetic navigation system is the Niobe® robotic system from Stereotaxis[10] (St. Louis, Missouri, USA). The Niobe® system is certified for magnetic navigation of magnetically enabled instruments, particularly for catheter ablation procedures for atrial fibrillation. In a study by Carpi and Pappone [31], the authors discuss the advantages and disadvantages of the Niobe® system for catheter ablation procedures for atrial fibrillation and maneuvering ingestible video capsules for endoscopy.

5.4.4 Fiber Optic Shape Sensing

Fiber Optic Shape Sensing (FOSS), also known as Fiber Bragg Grating (FBG)-based sensing, is a relatively new technique gaining traction in medical applications. It utilizes FBG sensors embedded within optical fibers to reconstruct the 3D shape of an instrument. These shape-sensing systems employ FBGs as strain sensors, reflecting a specific wavelength inscribed on single or multi-core fibers. The fibers are typically arranged in a triangular pattern around the instrument to be tracked. However, alternative configurations exist, including multi-core fibers and helical twists. The number of FBG sensors can vary depending on the application, and they can be classified into three types: single-point, quasi-distributed, or distributed sensors [8]. One particular FOSS system and its components is presented in Fig. 5.9.

[10] `www.stereotaxis.com`

Tab. 5.4. Summary of Electromagnetic tracking and Magnetic-based catheter navigation methods, categorized by clinical focus, data type, imaging modality, and average error.

Authors	Clinical focus	Data	Modality	Average error
		Electromagnetic catheter tracking		
Condino et al. [40]	Endovascular procedures	Abdominal phantom	x-ray	1.2±0.3 mm
Lambert et al. [91]	EVAR	Aortic phantoms	–	1.3 mm
Gergel et al. [57]	Transbronchial interventions	Thoracic phantom	x-ray	10.8±3.0 mm
Gilard et al. [58]	VCP	Patients	x-ray	0.17±8.74 mm
Gildea et al. [59]	Bronchoscopy	Patients	x-ray	6.6±2.1 mm
Hautmann et al. [65]	Bronchoscopy	Patients	x-ray	4.2/5.1 mm
Hermann et al. [69]	VCP	Pediatric patients	x-ray	<2 mm
Jaeger et al. [80]	Bronchoscopy	Thorax phantom/Swine	x-ray	–
Jaeger et al. [82]		Swine		<10 mm
Li et al. [96]	MIS	Aneurysm phantom	x-ray	1.4 mm
Lugez et al. [102]	Brachytherapy (prostate)	Phantom	US	1.7–1.9 mm
Lund et al. [103]	EVAR	Aortic phantom	x-ray	–
Manstad-Hulaas et al. [114]	EVAR	Patients	x-ray	–
Nagel et al. [131]	MIS	Wax phantoms	x-ray	<2.0 mm
Nypan et al. [135]	EVAR	Abdominal phantoms	x-ray	3.75/3.21 mm
Penzkofer et al. [145]	EVAR fenestration	Swine	x-ray	–
Piazza et al. [147]	EVAR fenestration	Phantom	–	–
Shi et al. [181]	EVAR	Abdominal phantom	x-ray	0.64 mm
Tinguely et al. [194]	TACE	Swine	x-ray	2.9±1.6 mm
Zhou et al. [221]	Brachytherapy (prostate)	Phantom	–	0.9±0.2 mm
		Magnetic-based catheter navigation		
Chautems et al. [33]	Cardiac RF ablation	Phantom	–	–
Carpi and Pappone [31]	Cardiac RF ablation	Patients	MSS	–
	Capsule endoscopy	Phantom		–
Edelmann et al. [46]	Atrial fibrillation	Phantom	MSS	<2.7 mm
Grady et al. [61]	Catheter navigation in brain	Swine	MSS	1.5 mm
Pancaldi et al. [141]	Catheter navigation in brain	ex-vivo/Rabbit ears	x-ray	–
Shao and Guo [178]	Capsule endoscopy	Phantom	–	0.0364 mm
Watson and Morimoto [203]	Growing robots	Phantom	–	4.3±2.3 mm

The placement of FBG sensors in the optical fiber categorizes of shape-sensing systems. Single-point sensors can only reconstruct the position and orientation of a single sensor. The quasi-distributed configuration uses data from multiple FBG sensors to reconstruct the optical fiber's shape in real time. Distributed sensors, however, rely on scattering-based FOSS, enabling continuous measurements along the fiber [8, 88]. The three configurations are visually presented in Fig. 5.10. An alternative to FBG is optical frequency domain reflectometry (OFDR), based on Rayleigh scattering. Amanzadeh et al. [8] provide a comprehensive evaluation of OFDR technology. Parent et al. [142, 143] demonstrate the implementation of OFDR in medical applications. For a detailed description of different FBG-based shape sensing methods, one can read Al-Ahmad et al. [6] and Shi et al. [180].

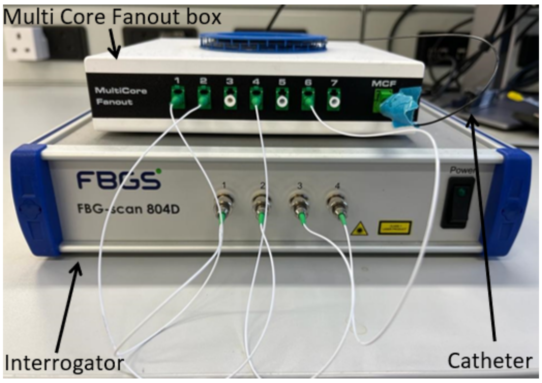

Fig. 5.9. Fiber optic shape sensing technology and its components, introduced by Ramadani et al. [154].
Note: Figure reused without changes © 2022 Elsevier [154]. Used with permission under CC BY 4.0.

FOSS is rapidly gaining traction in medical applications due to its unique advantages over traditional tracking technologies. FOSS offers exceptional shape sensing accuracy, immunity to EM interference, high flexibility, small size, and compatibility with medical devices and imaging modalities [6, 8]. Nevertheless, despite its benefits, FOSS has some limitations, such as increased complexity, the need for registration and calibration, and a steeper learning curve than other tracking methods. For a comprehensive overview of shape reconstruction methods in interventional applications and future directions, we encourage to read Sahu et al. [169].

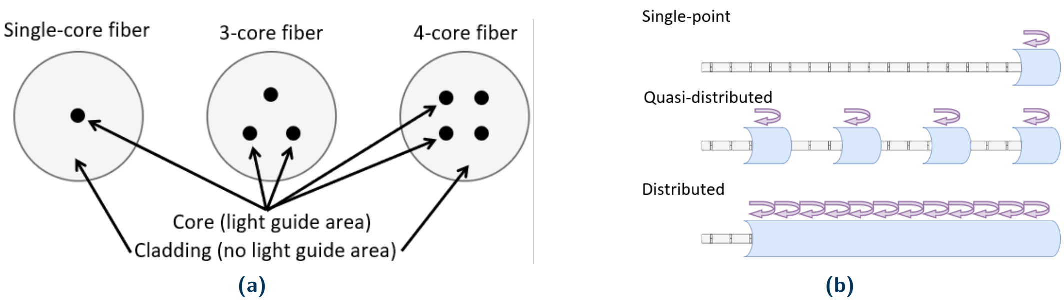

Fig. 5.10. Different configurations of shape sensing fibers, presented by Ramadani et al. [154]. (a) Core configurations of shape sensing fibers, showing single-core, three-core, and four-core fibers, and (b) Fiber core FBG configurations, illustrating single-point, quasi-distributed, and distributed configurations.
Note: Figures reused without changes © 2022 Elsevier [154]. Used with permission under CC BY 4.0.

It is crucial to recognize that FOSS and EM alone cannot accurately represent the shape of the targeted anatomy. These technologies require registration to an image of the anatomy, either preoperative or intraoperative, to provide a reliable representation of the anatomical structure. While the tracked shape of the instrument can provide a rough estimate of the anatomical shape, it is essential to register this information with an anatomical image to account for motion-induced artifacts and ensure accurate anatomical representation.

Numerous researchers have utilized FOSS configured with various FBG setups, distinguished by the number of FBGs per optical fiber and shape determination methods. The average error of these methods ranges from 0.24 mm to 4.2 mm. A typical configuration involves three equidistant outer optical fibers arranged in a triangular formation [1, 21, 48, 68, 113, 163, 164, 165, 168, 175]. Tab. 5.5 summarizes all studies discussed in this dissertation.

For instance, Yi et al. [217] used four single-core optical fibers in a square configuration around the colonoscope, each with five FBG sensors along its length, reporting a minimum reconstruction error of 4.1 mm.

Jäckle et al. [77] analyzed shape sensing errors and their impact on shape estimation, developing mitigation strategies. They used a configuration with one multi-core fiber containing a central core and six outer fibers, each with 38 FBGs. Their methods were validated against CT images of 3D printed vessels, resulting in an average reconstruction error of 1.13 mm. A visual representation of the introduced system can be seen in Fig. 5.11.

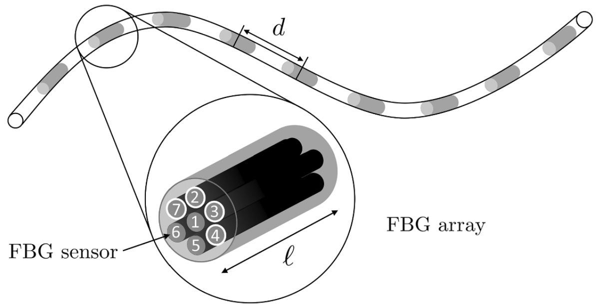

Fig. 5.11. Multi-core fiber optic shape sensing system, presented by Jäckle et al. [77]. The FOSS system consists of a fiber with multiple cores, featuring multiple FBG sensors with length l and distance d between them. The FBG array is illustrated with numbered sensors in the image.
Note: Figure reused without changes © 2019 Springer Nature [77]. Used with permission under CC BY 4.0.

Khan et al. [88] employed a four-fiber configuration similar to Yi et al. [217], utilizing multi-core fibers and FBG sensors to determine the shape of flexible medical instruments. The shape determination process involves (1) calculating strain from FBG sensors, (2) computing curvature and torsion from these strains, (3) determining central curvature and torsion using the four outer fibers in a square configuration, and (4) estimating the instrument's shape using Frenet-Serret equations. This multi-core fiber approach enhances the reliability of shape sensing, especially for long instruments like the 118 mm catheter used in their experiments, with a maximum reconstruction error of 1.05 mm across eight configurations.

FOSS has emerged as a promising technology for catheter tracking, and several companies have developed commercial solutions. Fraunhofer HHI[11] (Berlin, Germany), Philips[12] (Andover, Massachusetts, USA), FBGS[13] (Jena, Thuringia, Germany), and TSSC[14] (Austin, Texas, USA) are among the leading providers of FOSS catheter tracking solutions. Fraunhofer HHI and TSSC primarily focus on endoscopic applications and real-time 3D tracking and navigation of catheters within vessels. FBGS offers a broader range of FOSS solutions for various medical applications, including shape, strain, force, and pressure sensing. Philips' Fiber Optic RealShape solution utilizes a multi-core fiber configuration with helical twists and claims an accuracy of 2.2 mm for tip-to-tip distance measurements. These FOSS catheter tracking solutions enable real-time position tracking, navigation, and deformation detection.

[11] `www.hhi.fraunhofer.de`
[12] `www.usa.philips.com/healthcare/`
[13] `www.fbgs.com`
[14] `www.shapesensing.com`

Tab. 5.5. Summary of Fiber optic shape sensing catheter tracking methods, categorized by their clinical focus, data type, imaging modality, FBG configuration, number of sensors, and average error.
Note: Table reused without changes © 2022 Elsevier [154]. Used with permission under CC BY 4.0.

Authors	Clinical focus	Data	Modality	FBG configuration	Sensors per fiber	Average error
Abayazid et al. [1]	Brachytherapy	Phantom	Camera images	3 outer fibers	4 FBGs	1.8 mm
Al-Ahmad et al. [6]	MIS	Phantom	3D printed GT	4 multicore fibers	18 FBGs	2.84 mm
Borot de Battisti et al. [21]	Brachytherapy	Phantom	MRI	3 outer fibers	9 FBGs	0.27 mm
Elayaperumal et al. [48]	Needle tracking	Phantom	MRI	3 outer fibers	2 FBGs	4.2 mm
Finnesgard et al. [52]	EVAR	Phantom/Porcine	x-ray	4 helical fibers	–	<2.2 mm
Henken et al. [68]	Needle tracking	Phantom	Known GT	3 outer fibers	2 FBGs	0.89 mm
Jäckle et al. [77]	EVAR	Vessel phantom	x-ray	6 outer and 1 center fibers	38 FBGs	0.35–1.15 mm
Khan et al. [88]	MIS	–	3D printed GT	4x4 helical outer fibers	6 sets of 4 FBGs	0.44 mm
Mandal et al. [113]	Needle tracking	Phantom	3D printed GT	3 outer fibers	2 FBGs	$\sim$1 mm
Parent et al. [143]	Needle tracking	Phantom	3D printed GT	3 outer fibers	Dist. Sens.	0.6 mm
Parent et al. [142]	TACE	Phantom/Porcine	MRI and US			2.8$\pm$0.9 mm
Roesthuis et al. [163]						0.76 mm
Roesthuis et al. [164]	Needle tracking	Phantom	Camera images	3 outer fibers	4 FBGs	0.74 mm
Roesthuis and Misra [165]						0.24 mm
Ryu and Dupont [168]	Robotics (MIS)	Phantom	3D printed GT	3 outer fibers	–	0.84$\pm$0.62 mm
Sefati et al. [175]	Orthopedics	–	Camera images	3 outer fibers	3 FBGs	1.52 mm
Yi et al. [217]	Colonoscopy	Phantom	Known GT	4 outer fibers	5 FBGs	4.1 mm

5.4.5 Bioelectric Navigation – Tracking

Bioelectric navigation offers a novel approach to non-fluoroscopic catheter tracking that draws inspiration from the bio-localization mechanisms employed by weakly electric fish to reconstruct their surroundings [15, 189]. Bioelectric navigation utilizes a weak electrical field generated by electrodes embedded in the catheter. The catheter's location is determined by analyzing the changes in the electrical field sensed by the electrodes as it traverses the vascular system. These changes are influenced by vessel morphology, including bifurcations and stenosis. A simulated impedance signal map is created from a segmented vascular tree derived from preoperative CT or MRI volumes. This simulated map is synchronized with the online signals received from the catheter, and the similarities between these signals are used to determine the catheter's relative position within the vascular tree. A visual representation of the bioelectric signals extracted from the preoperative images can be seen in Fig. 5.12.

A proof-of-concept study utilizing a modified EP catheter demonstrated the feasibility of this approach. The animal tirals showed that matching the simulated electric signals from the segmented vascular tree in CTA with the real-time acquired signals could accurately track the catheter's position. While this method does not provide exact 3D position, it provides valuable information about the branch of the vessel tree where the catheter is located [55, 189]. This level of accuracy was satisfactory for navigation by the physicians involved in the study.

Svendsen et al. [190] leveraged the concept of local impedance changes correlated to vessel cross-sections to accurately place peripheral inserted central catheters (PICC). Typically guided by fluoroscopy, PICC placement has an accuracy of around 70%. The proposed system uses a conductance guidewire with electrodes to introduce and measure electrical current, allowing non-ionizing identification of vascular structures. Validated both in-vitro and in-vivo, this method achieved a root mean square error of 6.6% and 5.1%.

In a broader application, Sutton et al. [189] developed a navigation system for real-time vessel tree mapping by matching conductance signals with preoperative CTA scans, improving navigation accuracy. Their approach also considers the impact of diseased vessels on conductance signals, an aspect not explored by Svendsen et al. [190].

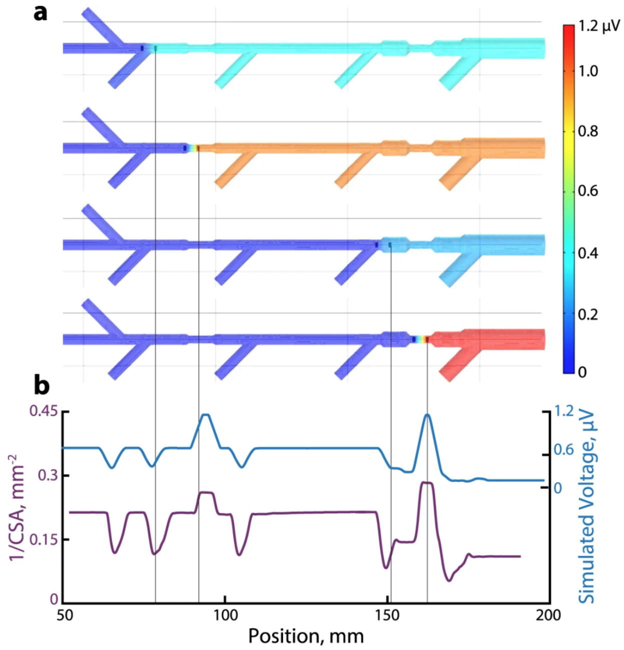

Fig. 5.12. Bioelectric navigation concept, presented by Sutton et al. [189]. Local electrical impedance variations at vessel bifurcations, stenosis, and enlargements are utilized for guidance. The identification of the current vessel branch is facilitated by matching the measured signal with a simulated signal based on the inverse vessel cross-section.

5.4.6 Robotic Tracking Solutions

Robotic catheter navigation/tracking solutions emerged in the medical field in the mid-2000s. These systems typically consist of the manipulator (master) and an actuator (slave), also known as master-slave systems. These components work in sync and can be positioned independently during the procedure. The manipulator is typically integrated into a joystick or custom-built device, while the actuator provides various gears and components that enable catheter manipulation. The actuator allows forward/backward movement, rotation, and tip movement through different gear grips that hold and guide the catheter. These movements can be tailored to specific needs and may vary between vendors and research groups. Examples of such robotic catheterization systems can be found in Abdelaziz et al. [2], Bao et al. [14], Matheson and Rodriguez y Baena [118], and Rafii-Tari et al. [152].

Over time, several steerable catheters have been developed, including magnetically steered catheters and those powered by tendons or soft materials [74]. These advancements have enabled precise catheter manipulation and provided essential feedback for physicians. Fiber optic sensors have been integrated into some catheters to measure forces at the tip [152]. This has led to a reduction in vessel wall injuries during robotic catheterization. Additionally, remote manipulation of the catheter minimizes radiation exposure to physicians.

In addition to visual guidance, researchers are exploring ways to incorporate direct physical feedback into catheter navigation systems. Typically absent in current systems, this feedback provides valuable information about catheter-tissue interactions and helps prevent vessel wall damage. Researchers are investigating the use of additional sensors to provide this feedback, such as force sensors and haptic feedback systems [24].

Robotic catheterization offers another advantage: the possibility of automatic navigation based on integration of image-based path planning and real-time tracking. Favaro et al. [51] present a 3D path planning approach for minimally invasive neurosurgery using MRI volumes. Their approach constructs potential path proposals considering catheter kinematics and path uncertainties arising from inaccuracies. The paths are then ranked according to a cost function that incorporates the distances between the start and endpoint and surrounding structures along the path, allowing the selection of an optimized path to a user-defined target.

Preoperatively defined paths can guide physicians in planning the best treatment approach. However, these paths need to be adapted to the dynamic nature of interventions. Pinzi et al. [148], propose a method to optimize these paths in real-time to account for tissue deformations. Their approach allows for calculating local path deformations while maintaining consistency with the planned trajectory. EM tracking is used to constrain a steerable needle's pose, enabling subsequent path information and smooth path updates during neurosurgical procedures.

Matheson and Rodriguez y Baena [118] utilize similar techniques to enhance minimally invasive percutaneous interventions, claiming improved accuracy and reduced tissue damage when targeting brain regions. The catheter is joystick-controlled, integrated with the physician's telemanipulation system, and consists of four sliding segments for independent movement. This design allows expert users to achieve an accuracy of 0.70±0.69 mm, while non-expert users reach 0.97±0.72 mm. However, this system cannot steer within vasculature due to the lack of soft tissue resistance necessary for its operation. A schematic of the operational aspect of the system is presented in Fig. 5.13.

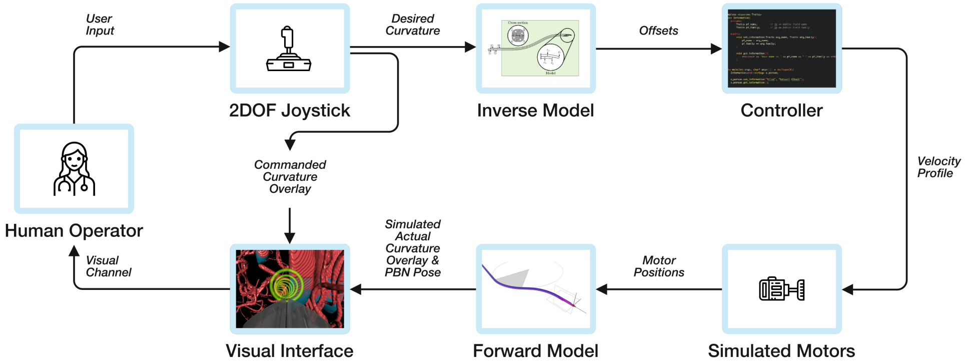

Fig. 5.13. Biologically inspired needle steering. Programmable bevel-tip needle system architecture for percutaneous interventions, introduced by Matheson and Rodriguez y Baena [118].
Note: Figure reused without changes © 2020 Matheson and Rodriguez y Baena [118]. Used with permission under CC BY 4.0.

In their respective studies, Abdelaziz et al. [2] and Dagnino et al. [42] introduce an innovative master-slave robotic platform for endovascular catheterization. This system allows physicians to steer the catheter using a master manipulator, incorporating vision-based haptic feedback and dynamic motion tracking. This setup helps avoid vessel wall injuries by providing dynamic movement constraints. Recent evaluations highlight the platform's superior effectiveness, precision, and safety in endovascular procedures compared to existing methods, particularly under MRI guidance. A summary of all robotic catheter navigation/tracking solutions discussed in this dissertation are presented in Tab. 5.6.

Several commercial robotic catheterization systems are available in addition to ongoing research. Legeza et al. [93] evaluated a master-slave system from Corindus[15] (Waltham, Massachusetts, USA) that enabled a physician to perform a vascular intervention remotely in an ex-vivo model. All the components of the Coridnus system are presented in Fig. 5.14. The physician was located 45 miles from the intervention site. The system provided remote physicians real-time catheter navigation, visualization, and tracking. However, Lo et al. [101] emphasize the importance of a reliable internet connection between the two sites and the need to evaluate the cost-effectiveness of such systems.

Several major robotic catheterization solutions are currently available in the market, including the Magellan Robotic System and the Sensei Robotic System from Auris Health[16] (Redwood City, California, USA), Vdrive from Stereotaxis[17] (St. Louis, Missouri, USA), Ion Endoluminal System from Intuitive Surgical[18] (Sunnyvale, California, USA), and Amigo™ from Catheter Precision[19] (Ledgewood, New Jersey, USA).

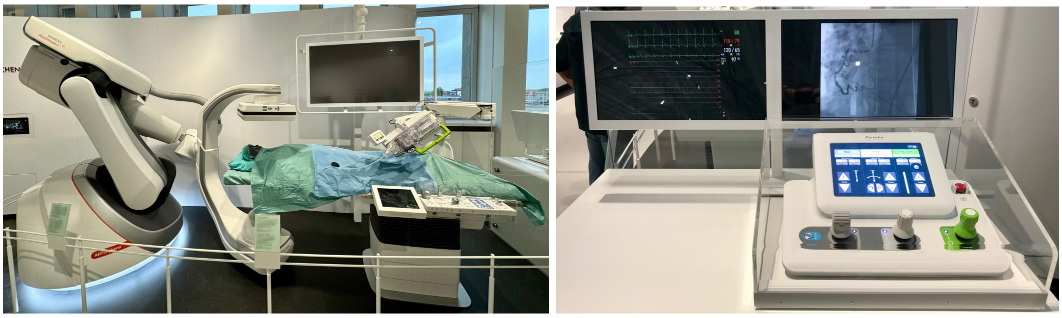

(a) (b)

Fig. 5.14. Corindus system displayed at the Deutsches Museum in Munich. (a) Robotic C-arm fluoroscope and robotically navigated catheter manipulator, and (b) Master system from which the physician manipulates the remote catheter, featuring two screens displaying vitals and live fluoroscopic images, as well as controls for catheter manipulation.

The Amigo™ system from Catheter Precision was evaluated in a "Concept to Bedside" study by Shaikh et al. [177]. The authors concluded that the Amigo™ system had better performance and a lower cost than the Sensei Robotic System. Clements et al. [39] reviewed the Magellan Robotic System from Auris Health. They tested the system in a clinical setting with six patients undergoing TACE. The study found that the system reduced fluoroscopic radiation exposure and was successful in all cases.

[15] `www.corindus.com`
[16] `www.aurishealth.com/hansen-medical/`
[17] `www.stereotaxis.com`
[18] `www.intuitive.com`
[19] `www.catheterprecision.com`

Tab. 5.6. Summary of Robotic catheter tracking methods categorized by their clinical focus, data type, imaging modality, and average error.

Authors	Clinical focus	Data	Modality	Average error
Abdelaziz et al. [2]	MIS	Vascular phantom	x-ray	–
Bao et al. [14]	MIS	Phantom	Lin. motion	0.33 mm
Brett et al. [24]	Endovascular procedures	Phantom	x-ray	–
Clements et al. [39]	TACE	Patients	x-ray	–
Dagnino et al. [42]	Endovascular procedures	Aortic phantom	Camera images	8.98±3.31 mm
Favaro et al. [51]	MIS neurosurgery	Simulation	–	–
Legeza et al. [93]	Endovascular procedures	Simulation	–	1.7±5.25%
Matheson and Rodriguez y Baena [118]	Percutaneous MIS	Simulation	–	0.70±0.69 mm
Pinzi et al. [148]	MIS neurosurgery	Phantom	EM and MRI	1.81±0.51 mm
Shaikh et al. [177]	Cardiac EP and RF ablation	Patients	x-ray	–

5.4.7 Hybrid Catheter Tracking

Thus far, all the tracking technologies discussed have been presented as standalone systems or in the context of specific imaging modalities. However, in the context of this dissertation, we have identified several cases where multiple tracking technologies are combined. Typical combinations of tracking technologies reported in the literature include image-based tracking and EM, image-based tracking and FOSS, EM tracking and FOSS, EM tracking and robotics solutions, and FOSS and robotic solutions. These hybrid tracking solutions represent an exciting advancement in catheter tracking technology, offering enhanced accuracy, robustness, and flexibility compared to standalone systems.

Denasi et al. [43] present a sensor fusion algorithm that integrates data from a FOSS catheter and an image-based ultrasound system using Luenberger and Kalman observers. The FOSS catheter includes one multi-core fiber with 32 FBGs. The ultrasound system tracks the catheter tip transversely. Alongside template tracking, they propose using convolutional neural networks for catheter tip tracking, achieving an average error of 1.41 mm. The Luenberger observer and Kalman filter report mean errors of 0.2 mm and 0.18 mm, respectively.

Shi et al. [179] propose a method for Transcatheter Aortic Valve Implantation (TAVI) that integrates IVUS, EM tracking, and FOSS. This system reconstructs the catheter shape using data from the FOSS system and poses information from the EM tracker, with an Aurora sensor providing six DoF at the catheter tip. The catheter features three optical fibers arranged in a triangular configuration, each with 8 FBGs. The system focuses on catheter localization, vessel reconstruction, and shape-sensing but does not report tracking or reconstruction errors.

Ha et al. [63] present a solution integrating FOSS with EM tracking and x-ray imaging. Two EM sensors are attached along the shaft of a FOSS catheter, consisting of four cores and 68 FBGs, to address twisting uncertainties. The authors report a RMSE of 0.54 mm.

To address the variability in EM tracking accuracy, Reichl et al. [159] introduce EM servoing. This method uses a robotic arm to dynamically move the EM field generator, ensuring it consistently follows the sensor and maintains high localization accuracy. The robotic arm-mounted field generator mitigates the non-linear magnetic field's impact, significantly improving overall error from 6.64±7.86 mm to 3.83±6.43 mm.

Jäckle et al. [78, 79] develop a shape reconstruction and tracking system combining FOSS and EM tracking for EVAR. Using a single multi-core FOSS fiber with 38 FBG sensors and two EM sensors, preoperative CT images are rigidly registered with the EM sensor's positions. Shape reconstruction errors average 0.9 mm, and EM tracking errors average 1.0 mm. A more comprehensive phantom evaluation compares two versus three EM sensors, finding slight accuracy improvements with three sensors, achieving a mean error of 1.35 mm to 2.43 mm. An illustration of the integration of the two tracking techniques is presented in Fig. 5.15.

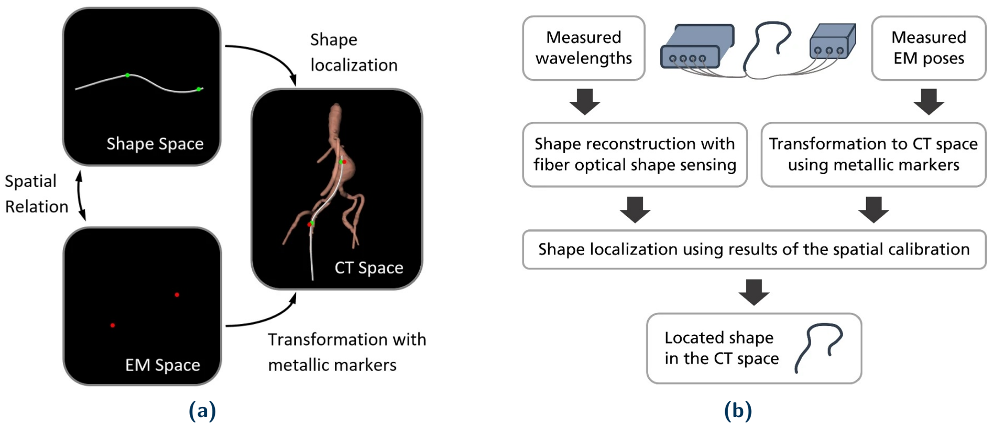

Fig. 5.15. Hybrid tracking system combining electromagnetic tracking and fiber optic shape sensing, presented by Jäckle et al. [78]. (a) Illustration of the three different spaces and their integration: EM, FOSS, and CT space, and (b) Processing pipeline for guidance based on output data from FOSS and EM sensors.
Note: Figures reused without changes © 2020 Jäckle et al. [78]. Used with permission under CC BY 4.0.

Schwein et al. [172] examine the integration of EM tracking with robotic tracking solutions using the Magellan Robotic System. Their phantom study compares traditional fluoroscopy-based navigation to 3D EM-based navigation. The findings suggest that using EM tracking can potentially reduce reliance on fluoroscopy. However, the study only tested one C-arm angulation and predicted possible EM interference issues with different angulations. In a subsequent study, Schwein et al. [173] confirm the system's limitations. They report an average registration accuracy of 4.18 mm in-vitro, which could pose challenges for navigating smaller vascular structures.

Similarly, Ji et al. [83] evaluate a robotic system combined with EM tracking. This solution involves robotically navigating to a desired branch using EM tracker data for the catheter tip localization. Unlike Schwein et al. [172], they do not address potential EM interference issues, though investigating such effects would be beneficial.

Combining FOSS with robotic solutions can mitigate EM interference issues. Agrawal et al. [5] compare the Monarch platform by Auris Health and the Ion Endoluminal System by Intuitive Surgical. The Ion System uses real-time shape sensing for flexible catheters in a robotic system, whereas the Monarch platform relies on EM guidance for bronchoscope control.

Reisenauer et al. [160] review the Ion Endoluminal System's use in pulmonary biopsies involving around 240 patients. They highlight its integration of FOSS with robotic navigation and note a trend toward decreased operation times. However, the study primarily relies on qualitative assessments and lacks quantitative evaluations of the system's accuracy. A summary of all hybrid tracking solutions discussed in this dissertation is presented in Tab. 5.7.

Tab. 5.7. Summary of Hybrid catheter tracking methods categorized by their clinical focus, data type, imaging modality, tracking technologies, and average error.
Note: Table reused without changes © 2022 Elsevier [154]. Used with permission under CC BY 4.0.

Authors	Clinical focus	Data	Modality	Tracking technologies	Average error
Denasi et al. [43]	MIS	Phantom	US	US + FOSS	0.2±0.11 mm, 0.18±0.13mm
Ha et al. [63]	Endovascular procedures	Phantom	x-ray	EM + FOSS	–
Jäckle et al. [78]	EVAR	Vascular phantom	x-ray	EM + FOSS	2.79–6.27 mm, 1.35–2.43 mm
Jäckle et al. [79]		Phantom			0.99–2.29 mm
Ji et al. [83]	Cardiology interventions	Phantom	–	EM + Robotic	<2 mm
Reichl et al. [159]	Bronchoscopy	Broncoscopy phantom	x-ray	EM + Robotic	3.83±6.43 mm
Reisenauer et al. [160]	Broncoscopy	Patients	x-ray	FOSS + Robotic	–
Schwein et al. [172]	Endovascular procedures	Aortic phantom	x-ray	EM + Robotic	–
Schwein et al. [173]					
Shi et al. [179]	Aortic valve replacement	Phantom	US	EM + FOSS + IVUS	–

5.5 Summary

This chapter has presented a review of over 150 papers on catheter-tracking technologies by delving into the cutting-edge of important catheter tracking technologies. We begin by tracing the historical milestones in interventional imaging, which paved the way for endovascular procedures and the subsequent development of catheter-tracking technologies. The reviewed tracking technologies are evaluated based on their accuracy, ease of use, and reproducibility.

This chapter reviewed state-of-the-art catheter tracking technologies, discussing seven approaches and their applications. We discuss each technology's advantages and limitations and compatibility with various imaging modalities and anatomical applications. Catheter-based interventions are minimally invasive procedures that enable precise targeting of anatomical structures with reduced patient trauma. Integrating robotic catheterization and machine learning could lead to semi-automatic and automatic manipulation, allowing computer-assisted systems to capture more semantic information. Automated tracking solutions will play a crucial role in this development. We anticipate further advancements in catheter tracking technologies, combining existing approaches and adaptability to specific anatomical structures and clinical procedures.

Most automatic and semi-automatic image-based approaches are data-driven, which presents its own set of development challenges. With the beginning of artificial intelligence and deep learning, various fields, including medical image analysis, have experienced rapid advancements. However, due to security and privacy regulations, machine learning methods demand large dataset that are often hard to access. Consequently, image-based algorithms are typically evaluated using clinical data from partner sites, which is not publicly available. This lack of access complicates the direct comparison and reproducibility of different methodologies.

Despite these challenges, recent progress in building large-scale medical databases and developing federated learning approaches offers promising paths for advancement [98]. Successes in related areas, such as medical image segmentation, also indicate potential improvements in catheter tracking techniques that rely on image data [34, 192]. As these technological and methodological landscapes evolve, the enhancement of image-based catheter tracking methods will likely happen in the near future.

Electromagnetic tracking is a widely used technology that requires additional hardware for tracking purposes. As a well-established technology in the research and commercial field, it is often discussed in many publications. EM tracking relies on generated EM fields, requiring the exclusive use of compatible non-ferromagnetic instruments in close proximity. This requirement is a significant reason why many research groups continue to prioritize x-ray and ultrasound imaging modalities for catheter tracking. Another limitation of EM tracking technology is the size of the sensors and the need for specialized catheters. The integration of EM sensors often results in catheters with an increased diameter, posing a notable challenge for clinical adoption, particularly in pediatric procedures where smaller device sizes are critical. Despite these challenges, there have been instances of successful implementation of this technology. For example, specialized EM-based solutions for EP procedures, such as the Carto® 3 System, have significantly impacted their application areas, demonstrating the potential benefits of EM tracking in their field of application.

There is a growing interest in fiber optic shape sensing, driven by its user-friendliness and the extensive possibilities for integration with other tracking technologies and imaging modalities. FOSS offers relatively precise 3D reconstruction of catheter shapes, with the flexibility to customize fiber configurations and sensors for specific applications. Additionally, the decreasing costs of these technologies are laying a solid foundation for further research and commercial expansion. Despite these advantages, FOSS still requires considerable clinical validation before it can be widely implemented. Recent studies reviewed here indicate that the accuracy of catheter tip reconstruction using FOSS is around 2 mm, which aligns with the performance of other tracking technologies. This suggests that while promising, FOSS must undergo further testing and refinement to confirm its efficacy and reliability in clinical settings.

Bioelectric catheter navigation, currently discussed in the literature as a proof-of-concept, emerges as a promising alternative. This method positions the catheter within branches of the vascular tree identified from preoperative CTA, allowing physicians to navigate these paths without relying on additional imaging modalities during the intervention. This opens up new potential opportunities for surgical procedures. The technology is reported for its ease of use and reproducibility. However, comprehensive evaluations and further animal and patient studies are essential to facilitate the transition of this technology into clinical practice.

Robotic tracking solutions are also gaining traction in the field of catheter tracking. Robotic catheterization is becoming increasingly appealing, with several products from Auris Health, Siemens Healthineers, and Intuitive Surgical already on the market. These robotic solutions claim to offer more straightforward navigation and reduce the risk of vessel wall injuries, as highlighted in current literature [152]. Additionally, they offer significant benefits to physicians, notably reducing their radiation exposure, thereby enhancing the safety and ergonomics of surgical procedures.

Hybrid tracking solutions capitalize on the strengths of combining diverse tracking techniques while inheriting their respective challenges and drawbacks, including the complexities of integrating multiple tracking systems. However, the majority of the literature discussed in this dissertation suggests that the benefits of hybrid tracking technologies generally outweigh the drawbacks, particularly when the integration of different technologies becomes straightforward and user-friendly. For instance, hybrid tracking by Denasi et al. [43] achieved an average reconstruction accuracy of less than 0.2 mm. Similarly, the combination of EM tracking and FOSS, as explored by Jäckle et al. [78], yielded an accuracy of about 1 mm. These examples underscore the potential for hybrid tracking solutions to enhance precision in applications where high accuracy is crucial.

Part III

Methodology and Discussion

6 Catheter Tracking Concepts and Methodologies

The integration of catheter tracking technologies into modern catheterization laboratories (cath labs) presents ongoing challenges, as explored in the previous chapters. The effectiveness of catheter tracking varies with the choice of technology, the clinical application, and the anatomical target of the endovascular procedure. This chapter outlines the core principles behind catheter tracking concepts, provides a theoretical understanding of tracking methodologies, and proposes an overarching catheter tracking pipeline. The catheter tracking pipeline is designed to be adaptable, and it can be applied to a wide range of catheter tracking applications, ensuring adherence to essential procedural steps in endovascular procedures.

6.1 Introduction

In order to tackle any challenge effectively, it is helpful to employ associative thinking – identifying similar problems and examining their solutions. This approach aligns with the principles of Biomimicry, a field where inspiration is drawn from natural processes and the behaviors of organisms. By observing how biological entities accomplish tasks, researchers can mimic these methods to achieve goals more naturally and intuitively [19].

In the context of catheter tracking during endovascular procedures, the primary objective is to localize the tip of the catheter within the human body, show its relative position to the anatomy, and maintain visual tracking throughout the procedure. Various catheter tracking technologies relevant to this challenge have been identified and categorized in Chapter 5: Literature Review. As we set aside the selection of a specific tracking technology for now, we aim to explain the underlying principles of catheter tracking as a general concept in this chapter.

By addressing these foundational principles, the aim is to clearly understand catheter-tracking concepts and methodologies suitable for endovascular procedures. This understanding will guide the development of solutions that enhance accuracy, safety, and efficiency.

6.2 Tracking Principles

Considering tracking as an abstract and general concept, it is evident that this issue has been effectively addressed in everyday life. To draw parallels, one might consider the example of navigating in nature and its relation to the current topic of catheter tracking. Historically, in the absence of maps, individuals navigated long distances by following linear paths guided by cosmic bodies like the sun, stars, or planets. This approach gradually evolved with the introduction of cartography, where landmarks were marked on maps to aid travelers in recognizing and orienting themselves during their journeys [64].

The challenge in those early days was the uncertainty of one's current location in nature. Determining the current location required estimations based on recognizable landmarks and their placement on a map [64]. The navigation process experienced a revolutionary transformation with the development of Global Positioning System (GPS) technology. GPS systems provide users with their precise location, within a certain margin of error, along with a detailed map of their surroundings. These systems are now seamlessly integrated into our smartphones, and we rely on them daily to travel from point A to point B. The process has become so intuitive and natural that the complex technology in the background is taken for granted, its workings remaining largely unnoticed as we navigate our environment.

Therefore, modern catheter tracking applications aim to create a system that operates effortlessly within clinical environments, an abstracted tool that operates with the ease of modern GPS technology. We believe all the necessary components to overcome existing challenges are available; however, the limitation remains in achieving seamless integration [154]. Employing the principle of association, the following correlations to our challenges can be drawn: maps are associated with patient images; landmarks correlate with anatomical and vascular features; and, similar to a GPS system giving the current location, the catheter position in the human anatomy is determined by the underlying tracking system.

However, translating these navigational components from natural settings to the context of catheter tracking in the cath lab is complex and has many challenges. Several challenges must be addressed to achieve a comprehensive solution applicable to most if not all, catheter-tracking applications. Among these challenges, two are particularly significant: motion compensation and registration [154]. Addressing these issues is crucial for advancing the effectiveness and reliability of catheter-tracking technologies within clinical environments.

Firstly, unlike static natural environments, the human body presents a highly dynamic setting, with intraoperative images – or maps – undergoing fast changes. In addition to potential patient movement on the cath lab table, numerous other types of motion must be considered, especially in endovascular procedures. These include cardiac and respiratory movements, diaphragm shifts, vascular deformation, and body position alterations from preoperative imaging to the intraoperative procedure [154]. Secondly, the data provided by tracking systems offer no inherent anatomical context, only returning a point in three-dimensional space. Advancements towards more intelligent systems are required to map this spatial data with anatomical structures. Achieving this necessitates a careful and accurate registration process aligning the tracking system with the patient and their images [151].

6.3 Catheter Tracking Pipeline

Upon establishing an understanding of tracking as a fundamental concept, the following section introduces a step-by-step pipeline to include a few current catheter-tracking solutions. We believe that any system following this abstracted pipeline carefully and addressing each stage to the best of its capabilities would result in a highly integrated solution for catheter-based endovascular procedures.

The introduced pipeline includes a preoperative and intraoperative phase, where Fig. 6.1 provides a visual representation of this structured approach. Each phase holds critical significance for achieving a complete catheter-tracking solution. While numerous systems excel in addressing specific challenges within these individual components, a notable gap often exists in the seamless transition from the preoperative phase to the intraoperative phase [154]. As previously discussed, current intraoperative components frequently depend on the physician's experience and capability to mentally map 3D preoperative plans into real-time intraoperative surgical activities. Through the development of this pipeline, the objective is to establish a framework that could effectively narrow this divide, enhancing the coherence and efficiency of catheter-based endovascular procedures.

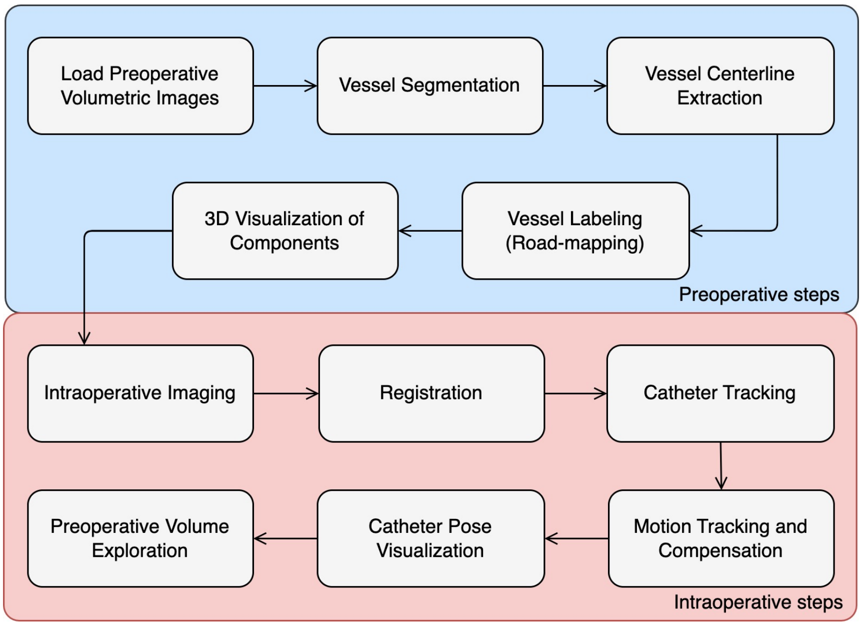

Fig. 6.1. Conceptual pipeline of a catheter tracking system framework, designed to address current challenges in the field. The framework consists of two phases: preoperative and intraoperative. Each phase includes a series of essential components representing steps of the procedure. These steps are crucial for effective catheter tracking, from initial imaging and segmentation to registration, real-time tracking, and motion compensation during endovascular procedures.

The preoperative phase of the introduced pipeline starts with a system designed to import preoperative volumetric images of the patient. Afterward, this system would autonomously segment the vasculature, enabling the physician to detect any stenosis, aneurysms, or other abnormalities present. In addition to segmenting the vasculature, the system performs a deeper analysis of the vascular structures by segmenting different plaque build-ups and the lumen of the vasculature. This allows physician to have a better understanding of the anatomy.

Following segmentation, the process continues to conduct further automatic analyses, mainly the extraction of the vessel's centerline. This step additionally includes measurements of the vessel's cross-sectional diameter, as it complements the segmentation by assisting physicians in making informed decisions about the intervention's approach and potential challenges.

Following the centerline extraction and segmentation of the vascular tree, as proposed in the pipeline, the system should autonomously perform vessel labeling. This process should involve identifying specific branches within the vasculature, assigning accurate labels, and, depending on the identified region of interest, outlining a path for a catheter-based endovascular procedure. The final stage of the preoperative phase involves the framework's capability to render all these components, tailored to the preferences of the physician. This should include the availability of 3D visualizations, offering a comprehensive understanding of the interventional site, facilitating a more informed approach to the procedure.

The second phase of the proposed pipeline involves the intraoperative steps, starting with the essential component of intraoperative imaging. This component can utilize various imaging modalities suited for intraoperative application, such as fluoroscopy or ultrasound. Nonetheless, the intraoperative imaging component, as it will be discussed later, can be considered optional if the integrated solution effectively combines preoperative images with tracking and motion compensation. Notably, the intraoperative imaging modality must be registered to the preoperative volumetric images through contemporary registration methods, ensuring alignment of intraoperative images and preoperative volumetric images [151, 167].

The immediate next step is the registration step, which is tasked with aligning the components from the preoperative planning phase within the intraoperative coordinate space, thereby bridging the preoperative and intraoperative phases of the intervention. This connection between the preoperative and intraoperative phases is often managed as supplementary information in the cath lab rather than as an integrated part of the procedural workflow. Achieving a seamless registration process is essential; foremost, it must maintain the existing interventional procedure workflow. Any deviation that complicates the process or requires considerable changes in how physicians operate could be an obstruction, potentially preventing the adoption of such solutions in the cath lab. Thus, the registration step aims to enhance the intervention without imposing additional responsibilities on the clinical partners.

Upon successful registration, the next step involves a real-time tracking system that monitors the catheter's tip pose (ideally, shape). This functionality will assist physicians throughout the procedure by providing precise navigation. Importantly, the tracking system should show more than just the tip or shape of the catheter without context. The integration must happen so that the tracking system is aware of the anatomy, ensuring that the localization provided is not only a point in space but within the anatomical context, as accurately reflecting the actual position in the human body as possible. In addition to tracking the catheter's pose, the proposed pipeline includes monitoring patient movements and vital signs. This approach aims to account for any motion that might affect the catheter's position, acknowledging the dynamic nature of the operating environment. By compensating for these movements, the system should ensure the accuracy of the catheter's placement, facilitating a smoother and more efficient procedural flow.

The final steps of the introduced pipeline involve accurately visualizing the catheter's tip position within preoperative high-resolution volumetric images. This essential phase requires innovative solutions capable of synthesizing all preceding steps into one framework. Such a system would empower physicians with tools to interact with 3D volumes – enabling rotation, zooming in and out – while visualizing the catheter's real-time movements within the anatomical environment. Implementing this technology not only aids physicians in navigating procedures more effectively but also supports more informed decision-making regarding interventions. By offering a more profound understanding of surgical sites and seamlessly integrating preoperative planning with the procedural workflow, these anatomy-aware intelligent tracking solutions should significantly enhance the precision and outcomes of catheter-based endovascular procedures.

6.3.1 Registration and Tracking

The previously outlined catheter tracking pipeline may remind readers of several existing technological solutions. While it is true that software offerings from leading companies closely align with the steps of this pipeline, it is essential to note that they often do not thoroughly address every component. Particularly, the market's current solutions frequently do not manage to integrate and intelligently utilize preoperative components during the intraoperative phase. Indeed, many solutions excel in specific intraoperative functions, achieving high standards in automatic vessel segmentation, centerline extraction, road mapping, labeling, and visualization. An example of such an end-goal solution is illustrated in Fig. 6.2, providing good visualization, segmentation, and centerline extraction. However, integrating these capabilities intelligently within intraoperative procedures remains underdeveloped, indicating a gap in achieving a seamless and integrated catheter-tracking system.

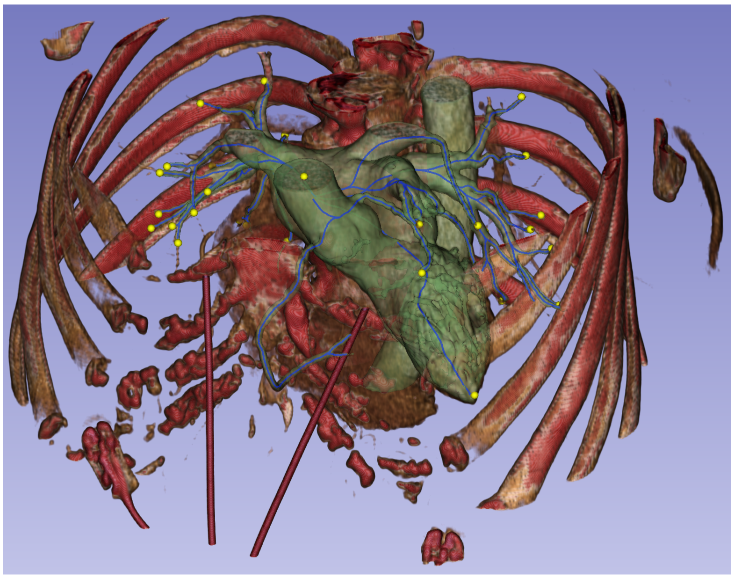

Fig. 6.2. Exemplary system demonstrating components of the preoperative phase of the catheter tracking pipeline. The image showcases automatic segmentation of the vasculature around the heart, including centerline extraction and rendered visualization. The ribcage and parts of the heart's tissue are shown in red, while the segmented vasculature, including the aorta, left atrium and ventricle, pulmonary veins, and coronary arteries, are depicted in green. Blue lines represent the centerlines of these anatomical structures, and yellow points indicate the termination points of the vasculatures.

As the registration step is one of the first steps of the intraoperative phase and the foremost challenge in current research, it is identified as a crucial component for future research trends [154]. While catheter tracking is fundamentally linked to the choice among available tracking technologies, this is also equally crucial in future research. Monitoring patient motion and implementing motion compensation strategies are essential, mainly when the introduced framework relies primarily on static preoperative volumetric images. Given the complexity and significance of each component of the intraoperative phase – where any component could constitute a doctoral project on its own – this dissertation has primarily focused on aspects of registration. These will be explored in greater depth in subsequent chapters. Additionally, within this dissertation's scope, we will address multiple contemporary catheter tracking solutions using technologies such as electromagnetic, bioelectric, and image-based tracking.

6.4 Catheter Tracking Technological Characteristics

In catheter-based endovascular procedures, various tracking technologies are available for selection. However, specific criteria must be met for a technology to be considered suitable for specific clinical applications. Given the non-rigid nature of catheters, it is essential that the tracking technology can at least track the catheter's tip. While solutions exist that track the base of rigid instruments, inferring the tip's position through geometric translation, these methods do not apply to catheters. The flexibility of catheters prevents the use of such strategies, necessitating technologies that can directly monitor the dynamic position of the catheter tip throughout the procedure.

Moreover, the essential requirement for catheter tracking technologies extends beyond simply tracking the catheter's tip location; they must also capture the tip's pose, tracking its exact position and orientation. This dual capability is crucial, as physicians need to precisely navigate the catheter, ensuring its alignment with the intended vascular pathways. Advanced tracking solutions are expected to provide comprehensive monitoring, not just of the catheter tip's but of the overall shape as well. This broader tracking scope offers physicians important insights, enabling more nuanced navigation and intervention strategies. Technologies capable of achieving this include those that incorporate shape sensing directly into the catheter or utilize image-based methods capable of tracking the catheter's shape within the anatomy.

An essential factor in catheter tracking is the necessity for real-time tracking frequency. This specification is important because physicians often navigate catheters very quickly, requiring a tracking system that can keep pace without missing any frames during these movements. A typical electromagnetic tracking system achieves a tracking rate of approximately 40-60 Hz. This range should serve as a baseline or general guideline for the tracking frequency of catheter tracking systems, ensuring that they provide the timely feedback necessary for the accurate and safe navigation of catheters during endovascular procedures.

Since catheters are flexible instruments inserted into the human body, the underlying tracking technologies must be capable of tracking catheters without requiring a direct line of sight. Tracking or compensating for patient motion is another crucial aspect these technologies must integrate. While existing tracking systems can track multiple sensors simultaneously, cardiac and respiratory motions may require specialized systems. These motions can then be intelligently integrated into the tracking system, enhancing the accuracy and reliability of catheter navigation by accounting for dynamic changes in the patient's position or physiological state during the procedure. This integrated approach to motion tracking and compensation is vital for the success of catheter-based endovascular procedures, ensuring that the movements of both the catheter and the patient are accurately tracked and controlled.

Tracking systems must be designed for straightforward deployment across various environments, enabled by an effortless registration process. This adaptability extends to utilizing similar systems within different phantoms for training and testing purposes. The registration process is crucial, requiring that tracking systems support an intuitive registration phase, which integrates naturally without alterations to the interventional workflow. Achieving this level of integration ensures that the tracking technology enhances procedural efficiency without imposing additional responsibilities on the physicians [154].

Going towards the future, developing these tracking systems with an emphasis on robotization is essential. As automation becomes increasingly prevalent in various fields, minimally invasive surgical applications are also on the verge of adopting these advancements. Therefore, it is crucial that tracking technologies are designed to be easily integrated and compatible with automated and robotic systems. Additionally, these technologies must be cost-effective and environmentally friendly to ensure they can be widely deployed, including in poorer regions where they are most needed. By focusing on these aspects, we can advance medical interventions, making them more precise, accessible, and sustainable, ultimately improving patient outcomes globally.

6.5 Catheter Tracking Proposed Solution

Drawing from the previously introduced catheter tracking pipeline and the delineated technological specifications of catheter trackers, a possible catheter tracking solution is proposed in this section. The proposed tracking solution is designed to track the pose of the catheter's tip, containing a few of the previously discussed characteristics such as real-time tracking, flexibility to operate without a direct line of sight, and the capability to accommodate patient motion. Additionally, it integrates high-resolution preoperative patient images, facilitating precise and accurate visualization of the catheter tip throughout the endovascular procedure. Nevertheless, the proposed solution does not come without disadvantages, as it is very challenging to include all discussed characteristics in a stand-alone tracking technology. The list of characteristics explained above is extensive and could go beyond the scope of this dissertation; therefore, we believe that to check most of the characteristics discussed earlier, the technology of choice must be a hybrid tracking technology incorporating intelligent robotic solutions.

Nonetheless, in our conducted experiments, the tracking technology of choice is an Electromagnetic (EM) tracking system equipped with a sensor affixed to the catheter's tip, enabling the tracking of its pose in six Degrees of Freedom (DoF) at a frequency of 50 Hz. This setup facilitated the development of several solutions that follow the previously introduced tracking pipeline as closely as possible, mainly to registration algorithms. These registration algorithms aim to effectively bridge the divide between the procedure's preoperative and intraoperative phases while ensuring their integration is as seamless and unobtrusive to the interventional workflow. Further details on the implementation of these registration solutions will be discussed in Chapter 8: Feature-based Electromagnetic Registration Using Bioelectric Sensing, and Chapter 9: Dynamic Time Warping: Catheter Registration for EM-guided Procedures.

A general illustration of our proposed solution is visualized in Fig. 6.3. This illustration intends to offer an overview of how the tracking system interacts with preoperative volumetric patient images to facilitate the interventional procedure.

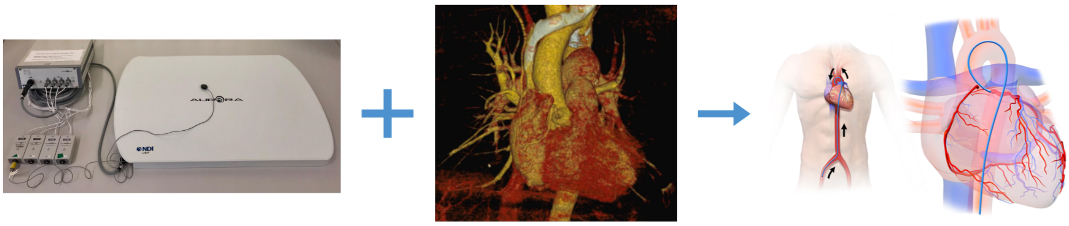

Fig. 6.3. Proposed solution for catheter tracking in endovascular procedures. The solution includes an electromagnetic tracking system interacting with preoperative volumetric images of the patient to guide physicians during catheter-based endovascular procedures. The approach also incorporates essential registration steps between the components and motion compensation.

6.5.1 Motion Compensation

Motion compensation is an essential component in our integrated proposed solution, particularly in tracking dynamic environments and correlating these movements with static preoperative patient images. Thus, a crucial element of our proposed solution involves the development of motion compensation algorithms designed to mitigate these challenges. This work primarily focuses on compensating for rigid patient movements. As highlighted earlier, this aspect was approached as a proof-of-concept study, acknowledging that a comprehensive exploration of motion compensation could constitute a doctoral project in its own right.

In the setup for our experiments, an Northern Digital Inc – NDI[1] (Waterloo, Ontario, Canada) EM tracking system was utilized to track the pose of the catheter tip, along with three reference sensors attached to the patient (a phantom was used for our experimental setup instead). A visual representation of this experimental configuration is provided in Fig. 6.4. An external force was applied to simulate motion on the phantom, with the solution's objective to compensate for this induced movement. For motion compensation, two algorithms were implemented: average motion compensation and weighted motion compensation.

The average motion compensation method is widely recognized in the field of motion compensation research [86]. This method involves subtracting the average motion detected by the reference sensors from the position of the catheter tip, resulting in the compensated motion of the catheter tip, as depicted in Eq. 6.1. However, this approach presents a limitation in requiring a minimum of three reference sensors to accurately account for motion within a 3D space. Furthermore, the placement of these sensors must be strategically considered to

[1] www.ndigital.com

ensure they effectively capture movement across all three planes, highlighting the need for thoughtful distribution of sensors to achieve comprehensive motion compensation.

$$\vec{c_c} = \vec{c} - \frac{1}{n}\sum_{i=1}^{n}\vec{m_i} \tag{6.1}$$

In Eq. 6.1, $\vec{c_c}$ represents the compensated position of the catheter tip. This position is calculated by taking the current position of the catheter, represented as $\vec{c}$, and subtracting the average sum of the displacements of n motion sensors, denoted as $\vec{m_i} = \vec{x_i} - \vec{x_{i0}}$. Here, $\vec{x_i}$ refers to the current position of a motion sensor, while $\vec{x_{i0}}$ indicates its initial position.

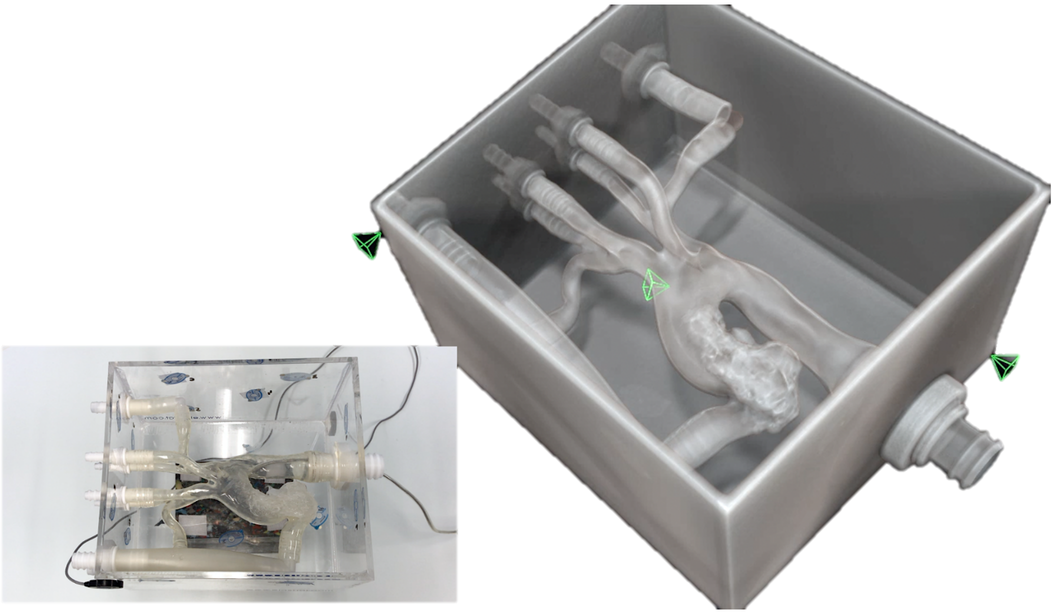

Fig. 6.4. Motion compensation system setup for the proof-of-concept study. The lower left image shows the physical phantom, while the right image visualizes the rendered preoperative CT of the phantom. Green pyramids at the corners of the phantom represent the reference sensors responsible for capturing motion, and the pyramid within the aortic arch indicates the catheter position.

The initial implementation of the average motion compensation algorithm treats each motion of sensors equally, which may not be true in practice. This is particularly noticeable in cases where motion applied to the phantom displays a rotational characteristic, causing parts of the phantom further from the point of rotation to move more than those closer.

In order to address this discrepancy and enhance the precision of motion compensation, an adaptation of the original algorithm was proposed, incorporating weights into the calculation. In this revised weighted motion compensation approach, sensors closer to the catheter's tip are assigned greater weight than those positioned further away. This adjustment allows for a more nuanced compensation that better reflects the actual distribution of motion across the phantom. The modified formula for weighted motion compensation is detailed in Eq. 6.2, providing a refined method for accurately compensating motion, especially in cases involving more complex movements.

$$\vec{c_c} = \vec{c} - \sum_{i=1}^{n} \vec{m_i}(1 - d_i) \tag{6.2}$$

In Eq. 6.2, the term $d_i = ||\vec{x_i} - \vec{c}||$ quantifies the distance between each motion sensor and the tip of the catheter, where $\vec{x_i}$ denotes the position of a motion sensor, and $\vec{c}$ represents the position of the catheter tip. Visual representations of the catheter's motion capture and the results of the motion compensation technique are illustrated in Fig. 6.5a and Fig. 6.5b, respectively.

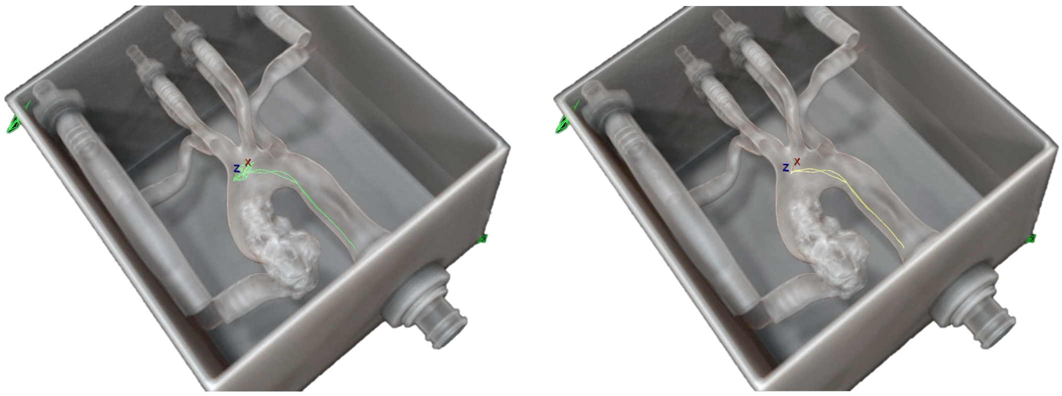

(a) (b)

Fig. 6.5. Motion capturing and motion compensation process from the proof-of-concept study. (a) Motion capturing capabilities of the algorithm. When external motion is applied to the phantom, reference sensors at the corners capture this motion, and the catheter path (green) within the aortic arch shows movement in different directions, especially clore to the tip, and (b) Motion-compensated catheter path (yellow) within the aortic arch, illustrating the accurate path the catheter took despite the applied motion, especially accurately represented at the tip.

Future research directions in motion compensation should focus on tracking non-rigid motions, particularly those related to cardiac or respiratory movement, and addressing deformable motions resulting from vascular deformation or the influence of catheter maneuvers and cardiac activity. A proposed method for managing such dynamics is gating, which aligns the catheter's position with specific phases of the cardiac and respiratory cycles. However, this approach may not be optimal due to its dependency on syncing the tracking system's frame rate with these physiological cycles, potentially slowing down the tracking frame rate.

Another promising research direction involves the use of dual-phase 4D preoperative imaging, capturing states of compression and decompression within the cardiac and respiratory cycle. This approach could enable interpolating between these two distinct image states, offering a dynamic representation that more accurately reflects the variations occurring throughout these cycles. Such a technique could significantly enhance the fidelity of motion compensation, allowing for a more nuanced understanding and adaptation to the movements within the patient's body during catheter-based endovascular procedures.

6.6 Summary

This chapter discussed a methodological overview of catheter-tracking technologies and the concept of tracking, setting the stage for a deeper exploration of these topics. It delved into the introduced catheter tracking pipeline, emphasizing three significant components of this framework: registration, catheter tracking, and motion compensation. Additionally, the chapter outlined the essential technological characteristics required for an effective catheter-tracking system. Building on this foundation, a comprehensive catheter tracking solution is proposed, leveraging preoperative imaging and electromagnetic tracking. The implementation of two motion compensation algorithms, integral to the proposed solution, is discussed in detail, showcasing their role in enhancing the accuracy and reliability of catheter tracking within dynamic clinical environments.

7 Image-based Catheter Tracking

In this chapter of the dissertation, we discuss and elaborate on one of the initial projects undertaken during this doctoral journey. This collaborative project involved several universities and focused on developing an advanced integrated technology platform for minimally invasive neurosurgery. The system integrated a robotic arm for precise instrument positioning, a remotely navigated shape-sensing catheter for drug delivery, and a real-time 3D ultrasound system. Besides developing and integrating a unique real-time bespoke 3D ultrasound system, the Technical University of Munich (TUM) team was also focused on developing an image-based 3D template catheter tracking module, as well as being involved in clinical trials, system-wide integration, and testing. This chapter of the dissertation presents the interdisciplinary collaboration and research direction followed through the beginning of this doctoral journey to develop the respective image-based template catheter tracking module.

7.1 Introduction

Current trends in surgery and neurosurgical procedures show an increasing gravitation towards minimally invasive techniques [118]. These approaches offer numerous benefits, such as reduced trauma and quicker patient recovery. However, to execute these complex surgeries effectively, surgeons require detailed planning, highly precise instruments, robust instrument-tracking algorithms, and adequate intraoperative imaging capabilities.

Ultrasound is a valuable intraoperative imaging device due to its excellent contrast between various soft anatomical tissues and its capability to monitor real-time anatomical changes [151]. While traditional ultrasound devices provide a 2D cross-sectional view, the development of 3D ultrasound technology is rapidly gaining interest. The primary advantage of real-time 3D volumetric ultrasound is its enhanced anatomical visualization and broader field of view.

Catheter tracking plays a crucial role in the success of minimally invasive neurosurgery. Considering the nature of these procedures and the non-linear paths catheters must navigate, precise and real-time catheter tracking is essential. As modern ultrasound systems are capable to provide real-time volumetric images, integrating image-based tracking algorithms in these solutions provide a natural complement to shape-sensing for catheter tracking. Thus, the overarching goal of this project was to develop a comprehensive ecosystem capable for successful minimally invasive neurosurgery. The following section will provide a detailed overview of all system components, emphasizing the areas covered in this doctoral journey, notably the image-based 3D template catheter tracking module and the clinical trials.

7.2 Enhanced Delivery Ecosystem for Neurosurgery in 2020

The Enhanced Delivery Ecosystem for Neurosurgery in 2020 (EDEN 2020) project is dedicated to setting the gold standard for the unified diagnosis and treatment of brain diseases by developing an integrated technology platform tailored for minimally invasive neurosurgery. Within this project, an interdisciplinary team has focused on integrating five key concepts into a prototype designed to meet the growing demand for more effective and less invasive neurosurgical methods [118]. These concepts include (1) preoperative and diffusion–MRI imaging, (2) intraoperative ultrasounds, (3) robotic–assisted catheter steering, (4) brain diffusion modeling, and (5) robotics–assisted neurosurgical device.

While most of the concepts mentioned previously were not the primary focus of this dissertation, this section will briefly discuss some of these aspects to provide a well-rounded understanding of the project. The primary emphasis will be on the image-based template catheter tracking module, clinical trials, and system-wide integration and testing. The EDEN 2020 project was a collaborative effort involving the Technical University of Munich (TUM), Imperial College London (ICL), Università degli Studi di Milano (UNIMI), Academisch Ziekenhuis Groningen (UMCG), and Politecnico di Milano (POLIMI).

The responsibilities of the EDEN 2020 project were distributed among the academic partners based on their specific areas of expertise, as outlined below. ICL managed the organizational aspects as the lead institution and designed the flexible catheter, robotic-assisted catheter steering, and catheter path planning. UNIMI and POLIMI focused on the robotic-assisted neurosurgical device and brain diffusion modeling. UMCG handled catheter shape sensing and integrating catheter tracking results. Our team at TUM primarily focused on the imaging components, including preoperative MRI and intraoperative ultrasounds. Our efforts were directed toward developing solutions for real-time brain tissue deformation compensation and accurate image-based localization of flexible catheters. These advancements are crucial for improving the precision and safety of neurosurgical procedures.

7.2.1 Procedural Pipeline

As introduced previously, the EDEN 2020 project aimed to establish a new standard for diagnosing and treating brain diseases. In order to achieve this, the project outlined a specific set of steps to be followed during the execution of such procedures. An exemplary illustration of the procedural steps is presented in Fig. 7.1.

To begin with, a preoperative MRI of the patient's head is obtained, serving both diagnostic purposes and precise procedural planning. The MRI is acquired while the patient's head is mounted on a platform to facilitate the registration process among all components during the procedure. An image of this head mount is presented in Fig. 7.7a. Once captured, the MRI volumes are uploaded into the Neuroinspire platform. The Neuroinspire platform is responsible for procedural planning, visualizing intraoperative images, guiding the robotic arm, and robotically controlling the catheter.

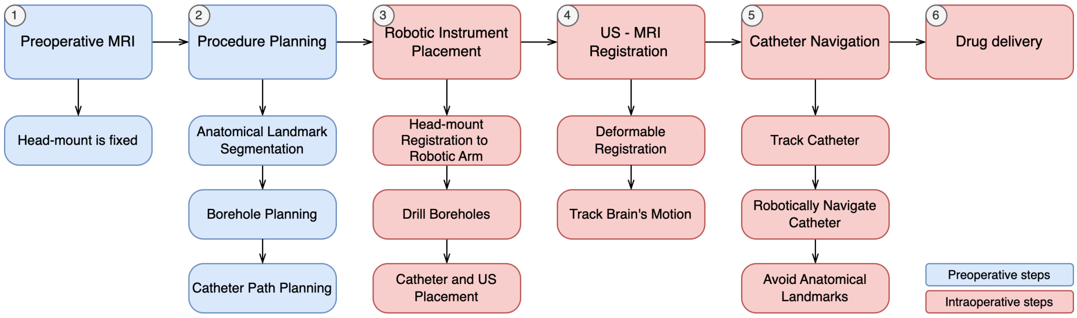

Fig. 7.1. EDEN 2020 procedural pipeline. The pipeline is divided into preoperative steps (blue) and intraoperative steps (red). Each of the six major components from the back-bone is numbered from one to six (indicating the order of completion), with specific sub-steps included within each major component.

A preoperative segmentation of vital anatomical landmarks such as ventricles and arteries is carried out. Following this segmentation, the software automatically plans the placement of two skull boreholes. These boreholes provide access to the brain, allowing for the insertion of the catheter and the real-time 3D ultrasound device necessary for the procedure. A preoperative MRI patient head volume and the superimposed 3D ultrasound image in the Neuroinspire platform are presented in Fig. 7.2.

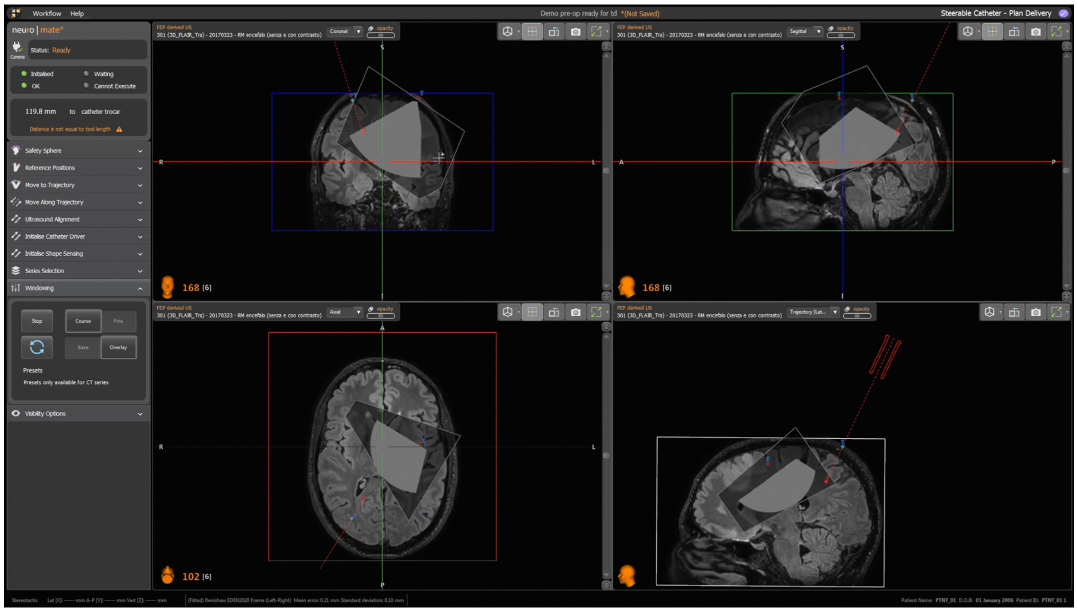

Fig. 7.2. Neuroinspire software from the EDEN 2020 project visualizing a procedural pipeline. The image displays a preoperative MRI of a human head with planning steps for catheter and ultrasound placement. The lower right image highlights the catheter trajectory in red and the registered ultrasound template.

Once the boreholes are planned, the patient is prepared for the intervention. The surgical site is set up such that the head mount is attached to the base of the robotic arm, ensuring that the registration between the preoperative planning and intraoperative navigation is maintained. With the head mount secured, the robotic arm is positioned to drill the two planned boreholes in the skull. The drilling process is carefully performed by the neurosurgeon, who carefully removes the bone structure of the skull to expose the dura matter and brain, setting the stage for the subsequent steps of the procedure.

Once the boreholes are drilled, a contraption is secured in one of the holes to hold the real-time 3D ultrasound probe. At the same time, the flexible, robotically controlled, shape-sensing catheter is inserted into the other hole. During the planning phase, the placement of these holes is carefully considered to ensure that the ultrasound can visualize both the catheter and its path toward the region of interest. This precise positioning is crucial for effective navigation and monitoring throughout the procedure.

The catheter, being an integral part of the project, requires a brief introduction regarding its design and capabilities. The catheter is composed of four interlocking segments with a diameter of 2.5 mm. These segments can slide independently, allowing the catheter to bend as it travels through soft tissues. This feature is crucial for the robotic (joystick controlled) manipulation of the catheter, enabling precise navigation toward the region of interest while avoiding critical anatomical structures. A more detailed explanation of the catheter construction and navigation is presented by Matheson and Rodriguez y Baena [118].

Each catheter segment includes a small channel that accommodates the integration of electromagnetic or fiber optic shape sensing capabilities. This design enhances the catheter's functionality and precision during procedures. A visual representation of the catheter is provided in Fig. 7.3 by Aktas et al. [7] and Secoli et al. [174], where the working channels of the catheter are visible.

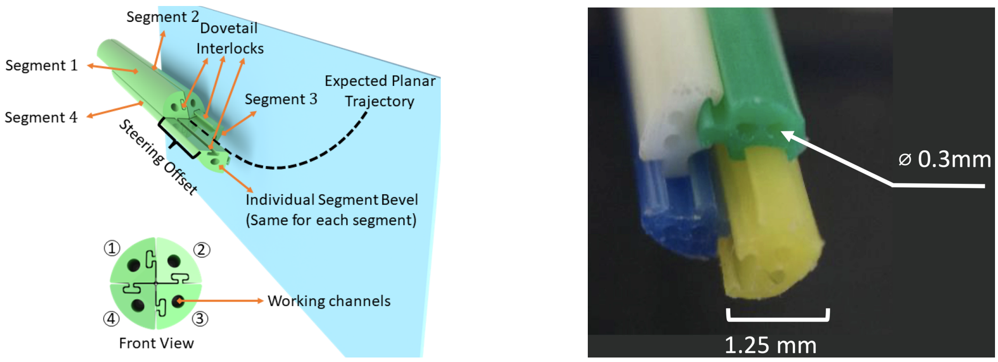

(a) (b)

Fig. 7.3. EDEN 2020 catheter and its components. (a) Illustration detailing the composition of the catheter, including the four interlocked segments and a cross-sectional view to visualize the working channels, and (b) Actual image of the catheter with color-coded interlocked segments and working channels.
Note: Figures reused without changes (a) © 2023 Aktas et al. [7], and (b) © 2022 Secoli et al. [174]. Used with permission under CC BY 4.0.

Following the secure placement of the ultrasound probe and catheter, the dura mater is punctured to insert the catheter into the brain's soft tissue. Puncturing the dura mater induces a phenomenon known as brain shift, which alters the brain's shape and position. Additionally, the interaction between the catheter and the brain causes further motion and deformations, which must be accurately captured.

These movements and anatomical changes are monitored using the 3D ultrasound, while the preoperative MRI is adjusted to match the ultrasound volume through deformable registration techniques [71, 151, 167]. This step ensures that the preoperative plan remains valid despite the anatomical changes, thereby maintaining the precision and safety of the procedure.

Finally, the catheter is robotically guided through the brain's soft tissue towards the region of interest. The catheter's position is tracked using shape sensing and real-time 3D ultrasound. Shape sensing provides data on the catheter's shape reconstruction, while ultrasound utilizes image-based template tracking to monitor the catheter tip. The information from these two modalities is then fused using a Kalman filter, which updates the tip position at every frame. This is also fed into the robotic catheter control unit, enabling real-time adjustments to the catheter's path and ensuring precise navigation toward the region of interest.

During the catheter insertion, the neurosurgeon ensures that all preoperatively segmented critical anatomical landmarks, such as ventricles and major arteries, are carefully avoided. Once the catheter reaches the region of interest, it is used to deliver the necessary drug or treatment. After the procedure, the catheter may be retracted or left in place for future treatments while the ultrasound probe is removed and the borehole is closed. This minimally invasive approach aims to result in minimal trauma, allowing for a quicker recovery.

7.2.2 Bespoke 3D Ultrasound

Even though the development of the bespoke 3D ultrasound device was beyond the scope of this dissertation, a brief discussion of its functionalities and capabilities is warranted for completeness. The image-based template catheter tracking, an integral component of the ultrasound system, necessitates a short introduction to this system and its advantages. By understanding the ultrasound system's role and benefits, the significance of the image-based tracking method within the broader context of the project becomes clearer.

The TUM team undertook the development of a real-time bespoke 3D ultrasound system and was introduced to the project as the preferred imaging modality for this neurosurgical application. This system is designed to provide real-time intraoperative imaging through a small borehole in the patient's skull. A concept visualization of such an implementation is presented in Fig. 7.5a. In order to maintain the minimally invasive nature of the procedure, the transducer needed to have a minimal footprint, leading to the system being custom-manufactured to meet these specific requirements.

The custom 3D ultrasound imaging system was manufactured-to-order by Cephasonics[1] (San Jose, California, USA). The 3D ultrasound probe features a matrix of piezoelectric elements arranged in a 32×32 grid (15×14 mm), providing full connectivity without prebeamforming, which ensures maximum flexibility. The probe operates at a center frequency of 7 MHz with a maximum imaging depth of 8.5 cm. The Cephasonics 3D ultrasound system is presented in Fig. 7.4a, while the probe is presented in Fig. 7.4b. The 3D ultrasound device is controlled through SUPRA (Software Defined Ultrasound Platform for Real-time Applications), an in-house developed software platform that performs the beamforming and image/volume reconstruction of the ultrasound data [60]. An exemplar 3D ultrasound image of a phantom from Cephasonics and SUPRA, including the three planes and the volume 3D reconstruction, is presented in Fig. 7.5b.

[1] www.cephasonics.com

(a) (b)

Fig. 7.4. 3D bespoke ultrasound system of the EDEN 2020 project. (a) The ultrasound system produced by Cephasonics, with all probe elements attached for 3D capabilities, and (b) Custom-produced 3D probe with a matrix array of piezoelectric elements, capable of capturing real-time volumetric images.

Integral to the ultrasound system is the image-based template tracking module, which was developed to utilize the bespoke 3D ultrasound system's real-time images to accurately track the catheter's tip. This software component is essential for ensuring precise navigation and positioning during neurosurgical procedures, leveraging the high-resolution imaging capabilities of the custom ultrasound device. A detailed description of the workings and development of this image-based template tracking module will follow in Section 7.5: Ultrasound Image-based Catheter Tracking.

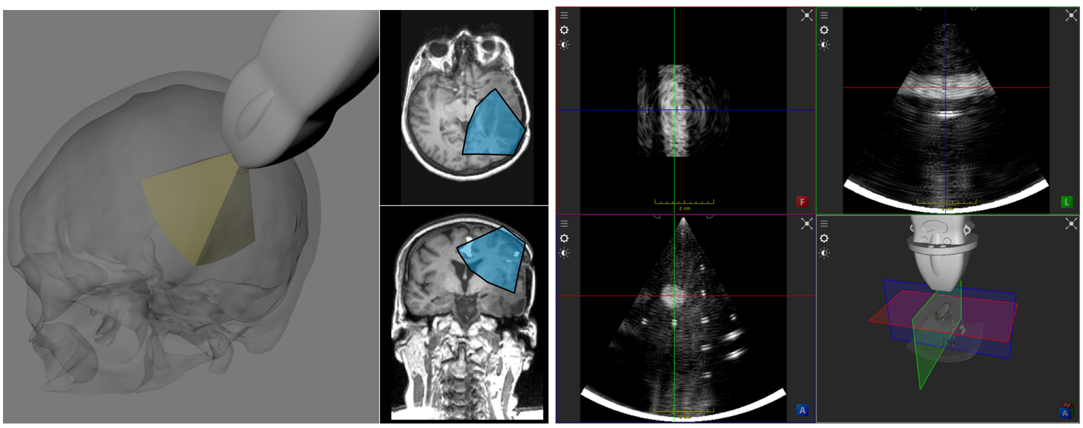

(a) (b)

Fig. 7.5. Conceptual system design and real-time ultrasound volumetric images. (a) Conceptual design of the system, illustrating the positioning of the ultrasound probe in a human skull and the corresponding MRI volume, and (b) Real-time volumetric phantom images captured by the ultrasound system.

7.3 Brain Anatomy

The brain is the central organ of the human nervous system, functioning alongside the spinal cord to form the central nervous system. It comprises three main parts: the cerebrum, the brainstem, and the cerebellum. The brain controls most of the body's activities by processing, integrating, and coordinating the information it receives from the sense organs and making decisions regarding the instructions sent to the rest of the body. Encased and protected by the dura mater and the skull bones, the brain is safeguarded from physical damage [116, 149].

The cerebrum, the largest part of the human brain, is divided into two cerebral hemispheres. Each hemisphere features an inner core of white matter and an outer layer of grey matter. The cerebrum houses four interconnected ventricles responsible for the production and circulation of cerebrospinal fluid. Situated posterior to the cerebrum, the cerebellum comprises multiple interconnected compartments. Lastly, the brainstem, located beneath the cerebrum, forms the upper portion of the spinal cord within the brain. It is a vital connection between the brain and the spinal cord, facilitating muscle movement and control [116, 121, 149]. A visual representation of these vital parts of the human brain are presented in Fig. 7.6a.

Several protective mechanisms have evolved to protect the brain from damage and ensure proper function. Anatomical protection consists of multiple layers, and the most well-known brain protectors include the scalp and skull bone, covered by skin and hair. Beneath the skull, three distinct membranes, known as the meninges, provide additional protection [20, 149].

- **Dura mater**: A tough membrane located directly beneath the skull, enveloping the entire brain and spinal cord.
- **Arachnoid membrane**: A layer of the meninges situated underneath the dura mater.
- **Pia mater**: A vascularized membrane that adheres to the brain's surface and spinal cord.

In order to prevent the brain from moving within the skull, the space between the arachnoid membrane and the pia mater is filled with cerebrospinal fluid. Additionally, the blood-brain barrier protects the brain from harmful molecules [149]. The brain's cerebrum and the cerebrospinal fluid are presented in Fig. 7.6c.

The brain also contains numerous critical arteries. The internal carotid arteries supply oxygenated blood to the front of the brain, while the vertebral arteries supply blood to the back of the brain. These two circulatory systems converge at the circle of Willis, a ring of interconnected arteries located between the midbrain and pons [116, 149]. The complex vascular system of the human brain, including the circle of Willis, is presented in Fig. 7.6b.

The brain is connected to the bloodstream to transport oxygen to its cells, ensuring proper brain function. In order to protect the brain from harmful substances, the blood-brain barrier permits only lipid-soluble molecules to pass through to the brain cells while ionic solutes are blocked. This mechanism helps control the brain's environment, thereby safeguarding its cells and maintaining optimal conditions for brain activity [20, 121, 149].

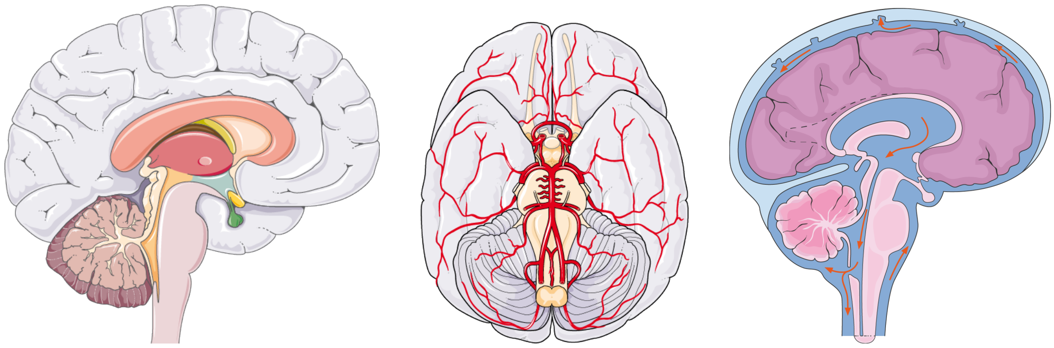

(a) (b) (c)

Fig. 7.6. Illustration of different anatomical views of the human brain. (a) Illustration of the main brain structures, highlighting the centrally located ventricles in light orange, (b) Vascularization of the brain with emphasis on the mid-brain and the circle of Willis, and (c) Brain membranes, focusing on the cerebrospinal fluid in blue, which encapsulates all brain tissues and the spinal cord, including the intraventricular space.
Note: Figures reused without changes © 2024 Servier Medical Art. Used with permission under CC BY 4.0.

Precise preoperative planning is crucial in neurosurgical procedures to avoid damaging vital structures and complex vascular systems. This careful approach is also essential for percutaneous minimally invasive neurosurgical procedures. These procedures involve making small incisions in the skull to access the brain using flexible instruments similar to the EDEN 2020 catheter introduced earlier. This technique minimizes damage to surrounding tissues while allowing effective navigation through the complex brain structures.

7.4 Clinical Trials

During the component testing and system-wide integration phases, all project partners gathered in Lodi, Italy, to conduct essential evaluations. For each of these gatherings, all project partners had to ship the necessary hardware from their respective institutions and actively participate in the system-wide integration process. For testing and evaluation purposes, each gathering included a small-scale ex-vivo clinical trial. A sheep head obtained from a butcher was used to closely simulate a human patient's head. The ultimate goal of these ex-vivo trials was to achieve a complete system-wide integration, culminating in a final in-vivo clinical trial at the end of the project.

During the clinical trials, the sheep head was first secured in the head mount, and a preoperative MRI was acquired. An image of the sheep head fixed in the head-mount, in the process of the MRI acquisition, is presented in Fig. 7.7a. Following the procedural pipeline, the preoperative MRI of the sheep head was uploaded into the Neuroinspire platform, where the procedure was planned.

During the planning phase, the ventricles and major blood vessels are segmented to ensure the catheter path planning avoids these critical anatomical structures. The sheep head and head mount are then secured to the base of the robotic arm. At this point, two access points for the ultrasound probe and the catheter are drilled into the skull. The skull drilling process with roboticall guidance is visualized in Fig. 7.7b.

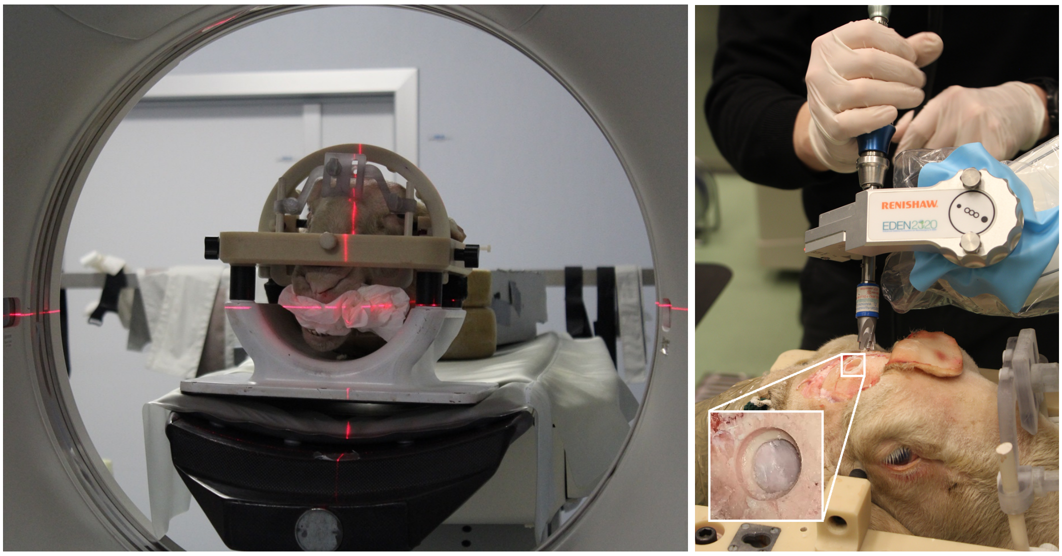

(a) (b)

Fig. 7.7. Two procedural steps of the EDEN 2020 neurosurgical procedure. (a) MRI acquisition of a sheep head mounted in a frame, and (b) Robotically-guided drilling process for ultrasound and catheter placement.

Once the 3D probe of the bespoke ultrasound is fixed in the sheep head, real-time 3D volumetric images of the sheep brain are acquired using the ultrasound platform and registered with the preoperative MRI. A visualization of the system configuration, with the correctly placed 3D ultrasound probe and the catheter, is presented in Fig. 7.8a. As soon as the catheter begins to move, the image-based template tracking is activated to track the tip of the catheter.

An intraoperative image showing the registered MRI and 3D ultrasound, with the catheter visible in the reconstructed 3D volume, is presented in Fig. 7.8b. The tracking results are then fused with the shape-sensing data to guide the robotically navigated catheter along the correct path toward the region of interest.

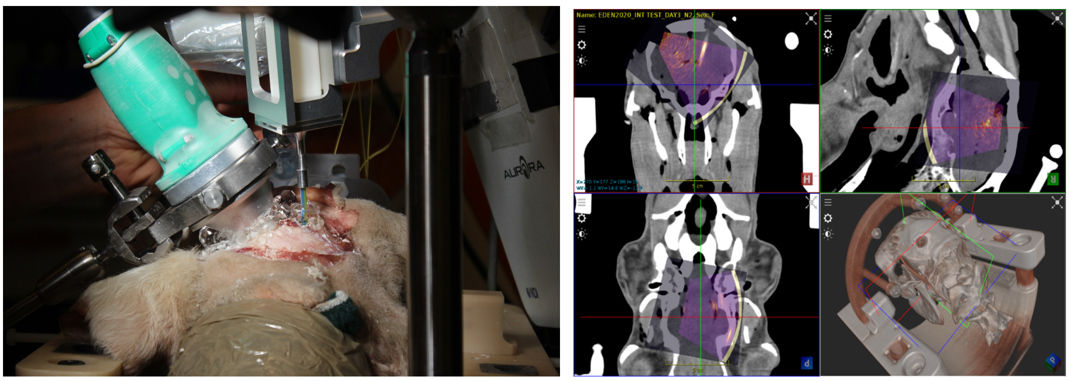

(a) (b)

Fig. 7.8. Complete EDEN 2020 project setup for neurosurgical procedures. (a) Image of a sheep head with the mounted ultrasound probe on the left and catheter on the right, and (b) Intraoperative real-time volumetric images of the ultrasound registered to the preoperative MRI. The top left image sector shows the catheter visualized in the ultrasound image as a bright yellow signal.

During these clinical trials and system-wide integration, extensive data were recorded from all components to further develop and enhance their functionalities. The data acquired during these trials proved crucial for improving the accuracy and reliability of the catheter tracking aspect and the image-based template tracking module. However, it is important to note that the quality limitations of the ultrasound system contributed to increased error rates in the tracking module, particularly when the catheter traveled deeper into the brain tissue. Additionally, tracking accuracy was adversely affected when the catheter was not centrally located within the ultrasound's field of view.

Although the image quality of the ultrasound system was not the primary focus of this dissertation, it nonetheless impacted the performance of the image-based template catheter tracking module, since it depended in the image quality. The quality observed during the clinical trials did not align with the results from tests conducted on phantoms or water baths within the lab environments. This discrepancy in image quality was mainly due to suboptimal conditions encountered during the acquisition of ultrasound images of the sheep's brain.

Three key factors influenced the quality of the ultrasound images. The most significant technical aspect was the beamforming algorithm used with the specific 3D probe. The matrix flat probe's sensor inherently possessed a narrow field of view. Attempts to adjust the beamforming to expand this view more broadly in all directions inadvertently resulted in a degradation of image quality. Additionally, two procedural aspects further degrade the quality of ultrasound imaging, which will be discussed to understand their roles and the potential for improvements in future implementations.

Regarding the procedural aspects, two key factors significantly hindered the ultrasound system's ability to capture high-quality volumetric images. Firstly, the testing medium, namely the sheep head, presented challenges. Since the sheep head was obtained from the butcher on the morning of each clinical trial day, the brain had likely lost all blood and cerebrospinal fluid, potentially introducing air into the system. When the ultrasound was positioned to acquire images, there was a high probability that air was present in its field of view. Air creates artifacts in ultrasound images, obstructing the ultrasound signals and preventing them from penetrating the tissue effectively.

Secondly, the design of the mounting contraption for the ultrasound probe to the sheep's head also contributed to image quality issues. The contraption ensured that the ultrasound probe did not touch the brain directly. To obtain accurate volumetric images, it was necessary to continuously fill the space between the ultrasound probe and the brain with saline solution. However, this process frequently introduced air bubbles, which interfered with the ultrasound signal and decreased image quality.

Overall, the clinical trials and system-wide integration were successful, yielding excellent results. The systems demonstrated compatibility during the integration phase and communicated seamlessly with other components. Each step of the procedural pipeline was executed effectively, achieving satisfactory accuracy and successfully completing the procedures.

7.5 Ultrasound Image-based Catheter Tracking

As discussed in previous sections, one of the key responsibilities for this project was the development of the image-based template tracking algorithm, which is also part of this dissertation. In conjunction with fiber optic shape sensing technology and fused via a Kalman filter, this algorithm was tasked with real-time tracking of the catheter shape/tip. It provided precise location data to the robotic catheter navigation system, ensuring accurate localization and adherence to the preoperative planned path. A visualization of the catheter tracking module is presented in Fig. 7.9.

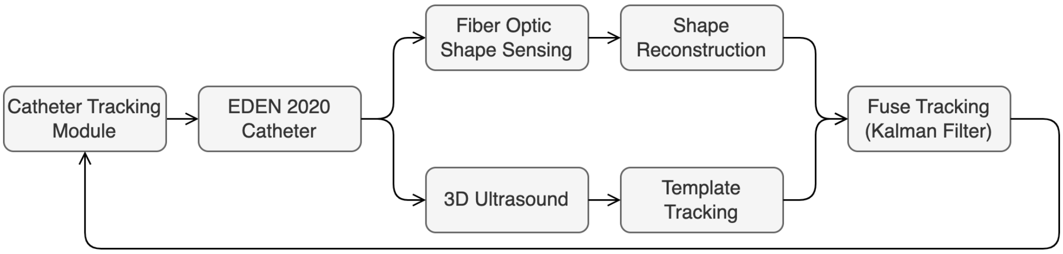

Fig. 7.9. Schematic of the EDEN 2020 catheter tracking module. This module consists of a fiber optic shape sensing system for catheter shape reconstruction and an ultrasound image-based tracking system with template tracking. Each system independently calculates the position of the catheter tip, and a Kalman filter fuses these measurements to determine the accurate location of the catheter. The position is then fed back into the catheter tracking module recursively to enable continuous navigation of the catheter.

The algorithm implements a 3D template tracking system designed for tracking the tip of a catheter in 3D ultrasound volumes. This tracking algorithm is crucial for medical procedures where precise catheter localization is needed in real-time. By leveraging the computational power of GPUs, the algorithm ensures that tracking is both fast and accurate, which is essential in dynamic medical environments where quick decision-making is critical.

Initially, the tracking algorithm node accepts the position of the catheter from the shape-sensing system as input and checks whether the reported location of the catheter is within the ultrasound's field of view. Afterward, the tracking algorithm starts by initializing the template, a predefined 3D volume representing the catheter within the first ultrasound image frame. As the catheter moves, subsequent ultrasound images are processed to update its position. The core of the tracking process involves cropping a region from the current image that contains the catheter and then comparing this region to the template.

This comparison is refined through an iterative process where the position and shape of the cropped region are adjusted to minimize the difference between the template and the current image. This is achieved by computing image gradients and using them to accurately adjust the catheter's position. The algorithm updates the position of the catheter by warping the template to match the current image, calculating the error, and iteratively refining the motion parameters until convergence. The algorithm can accurately track the catheter's position in real-time and publish the location results into the catheter tracking node. A pseudo-code representation of the algorithm can be seen in Algorithm 1.

Based on the data gathered from the clinical trials, the catheter tracking module was evaluated, resulting in a mean Euclidean error of 0.18±0.13 mm. The catheter tracking module comprised two tracking algorithms: shape-sensing and image-based template tracking using bespoke 3D ultrasound. During the evaluation, each module was assessed separately, with the shape-sensing algorithm achieving a mean Euclidean error of 0.24±0.096 mm and the template tracking algorithm achieving a mean Euclidean error of 0.27±0.15 mm.

Algorithm 1 Image-based Ultrasound Template Catheter Tracking Module

```
Input: UltrasoundImg, CatheterTemp, CatheterPos
Output: UpdatedCatheterPos

function InitializeTracking(UltrasoundImg, CatheterTemp, CatheterPos)
    if CatheterPos is not within the ultrasound field-of-view then
        return Error: move CatheterPos within the ultrasound field of view
    Initialize CurrentImg with UltrasoundImg
    Initialize CatheterTemp with the predefined 3D volume representing the catheter
    Initialize UpdatedCatheterPos with CatheterPos

function TrackTemplate(UltrasoundImg, CatheterTemp, CatheterPos)
    Crop a region from UltrasoundImg that potentially contains the catheter
    Compare the cropped region to the CatheterTemp
    Calculate the difference between the cropped region and the CatheterTemp
    Update CatheterPos to minimize the difference

procedure TrackMain(UltrasoundImg, CatheterTemp, CatheterPos)
    InitializeTracking(UltrasoundImg, CatheterTemp, CatheterPos)
    while tracking do
        Capture current ultrasound image as CurrentImg
        UpdatedCatheterPos = TrackTemplate(CurrentImg, CatheterTemp, CatheterPos)
        return UpdatedCatheterPos
```

7.6 Summary

In this chapter, we have discussed an integral project of this dissertation, specifically focusing on image-based catheter tracking. This project was part of the larger European initiative, EDEN 2020, which aims to provide an advanced platform for minimally invasive drug delivery in neurosurgical procedures. This project segment focused on component evaluations, system-wide integration, and developing an image-based template catheter tracking module.

The image-based template catheter tracking module was designed to focus on precise localization and real-time processing. The algorithm accurately matches catheter tip templates to 3D real-time volumetric ultrasound images to track the catheter tip across consecutive frames. The final evaluation and clinical trials demonstrated satisfying tracking accuracy, with excellent communication and integration between components.

8 Feature-based Electromagnetic Registration Using Bioelectric Sensing

The following chapter of the dissertation elaborates upon one of our work contributions to the IEEE Robotics and Automation Letters Journal (RA-L), which was later presented to the IEEE/RSJ International Conference on Intelligent Robots and Systems (IROS 2023), titled "Feature-based Electromagnetic Tracking Registration Using Bioelectric Sensing" [156]. This work serves as a direct contribution to the *Registration* component of the catheter tracking pipeline introduced in Chapter 6: Catheter Tracking Concepts and Methodologies.

Tracking of catheters is crucial in minimally invasive endovascular procedures, with Electromagnetic (EM) tracking being one of the technologies utilized for this aim. When available, preoperative patient images can assist physicians in navigation procedures tracked by EM. Nevertheless, a registration step is often needed to align preoperative images with the intraoperative EM tracking space. Many of the current methods for this registration require manual interactions, potentially introducing more steps into the procedural workflow.

This work introduces a new automatic feature-based registration method based on the catheter's electric sensing of vascular geometry, referred to as Bioelectric sensing. This approach uses the Bioelectric sensing capabilities of the catheter to detect vascular features, such as bifurcations, aneurysms, or stenosis. The recorded EM position of these features is then applied to register the EM tracking space with the preoperative images and the patient. This alignment is further refined through Iterative Closest Point (ICP) registration algorithms. In contrast to existing methods, the proposed approach eliminates the need for external markers, interventional imaging, or additional actions by the physician, thereby preserving the workflow of the interventional procedure.

8.1 Introduction

Physicians frequently utilize a minimally invasive endovascular approach in diagnosing and treating cardiovascular diseases. This method involves using tubular instruments, such as guidewires and catheters, which are navigated through the human vascular system to the targeted area for local treatment. Typically, physicians employ one or sometimes multiple modalities for real-time visualization of the catheter's current position. These modalities may include imaging techniques like fluoroscopy and ultrasound or tracking technologies that provide only the position and orientation of the catheter's tip, such as EM tracking, or Fiber Optic Shape Sensing (FOSS) [154]. Additional preoperative volumetric data, such as a patient's Computed Tomography Angiography (CTA) scan, may be available in certain instances. To effectively utilize preoperative and intraoperative data during endovascular procedures, the preoperative data must be transformed into the same coordinate space as the intraoperative data through a 3D – typically rigid – registration step.

8.1.1 Electromagnetic Tracking

As discussed in the earlier chapters, EM tracking is a tracking or localizing technology that enables users to determine the position and orientation of tracked sensors across five or six Degrees of Freedom (DoF). The advantage of EM tracking is that it does not require a direct line of sight, making it particularly well-suited for endovascular procedures. However, there is no inherent method to directly associate the tracked sensor's position with the patient's anatomy or a preoperative scan of it [54]. Despite the extensive research and widespread commercial adoption of EM tracking, it is crucial to acknowledge that EM tracking does not generate images. Instead, it identifies the position of the sensor within the EM field.

Consequently, clinicians may maintain reservations about integrating this technology in endovascular procedure guidance [54, 154]. This work's key challenge and focal point is registering the EM-tracked catheter tip with the patient and corresponding preoperative images. Implementing EM tracking in procedures requiring registration, particularly in soft anatomical regions like the abdomen or thorax, presents significant limitations. This is especially true for procedures involving minimally invasive vascular catheter insertions, where the complexity of registration significantly increases [4, 76, 218].

Various methods for registering preoperative patient data with the EM tracking space have been developed in the field of EM tracking, as demonstrated in the literature review. A prevalent technique involves using external structures like fiducials or markers affixed to the patient's skin while acquiring preoperative images. It is essential that these markers are securely attached to prevent movement, or they must allow reproducible reattachment from the time of preoperative imaging to the intervention itself. These markers are subsequently utilized to achieve registration between the preoperative and intraoperative coordinate systems, a method extensively acknowledged as a standard for EM tracking registration. Several studies documented the outcome of such marker-based registration methods [100, 115, 124, 207].

An alternative strategy involves employing internal anatomical features or landmarks for registration, identifiable through interventional imaging techniques [183]. Other research bodies have achieved registration by capturing an image of the EM field generator, noting its position in relation to anatomical structures for the purpose of registration [54]. Moreover, different registration approaches have been suggested that employ the paths traversed by the catheter as data for registration. Some bodies of work have focused on registering EM paths with the centerline of vessels [104, 135], while others have focused on registering EM paths with points along the vessel wall [91].

8.1.2 Bioelectric Sensing and Navigation

Bioelectric navigation represents a novel method for navigation in minimally invasive endovascular procedures, grounded in the concept of identifying local geometric features within the vasculature as the catheter tip passes through them [55, 189]. This technique employs a catheter equipped with electrodes along its shaft, generating a constant-amplitude AC current between a pair of these electrodes. The surrounding vasculature's shape influences the electric field generated by this current. Information about the vascular geometry near the catheter tip can be obtained by measuring the voltage between another pair of electrodes along the shaft and extracting the magnitude of the AC voltage at the stimulation frequency. Importantly, the magnitude of this voltage is inversely related to the cross-sectional area of the vessel at the corresponding location. Therefore, the cross-sectional lumen area of vessels can be estimated from voltage measurements taken while the vessel is flushed with a saline solution [85]. Moreover, vascular features that cause local changes in cross-sectional area, such as bifurcations, stenosis, aneurysms, or transitions from a larger vessel into smaller side branches, result in variations in the measured voltages. A sequence of voltage magnitudes recorded over time forms a signal that depicts the vascular geometry traversed by the catheter, with local extremes indicating vascular features.

Bioelectric Navigation suggests comparing the real-time signal recorded by the catheter with the expected reference signal derived from a preoperative segmented Computed Tomography Angiography (CTA) model of the patient's vasculature. By identifying the closest match, the catheter's position within the vascular tree can be determined [189]. Typically, this navigation method necessitates a preoperative model to generate expected reference signals.

While Bioelectric Navigation can ascertain the catheter's location within a specific vascular branch and its proximity to vascular features, it only indicates the catheter's position along the vessel's centerline without providing a 3D location or the orientation of the catheter tip. This limitation may restrict its use as an independent navigation technology. Nonetheless, combining it with EM tracking could address the limitations of both technologies, enhancing the automation of registration procedures and catheter tracking.

8.1.3 Electrophysiology-specific Registration

Electrophysiology (EP) ablation procedures are the benchmark for diagnosing and treating cardiovascular diseases linked to irregular heart rhythms, such as atrial fibrillation. In these procedures, EP catheters play a crucial role by generating an anatomical 3D surface map of the atria and their electrical activity and ablating the source regions responsible for the irregular activity through the application of radiofrequency energy. This is accomplished using electrodes positioned at the catheter tip [45]. In this domain, a known commercial mapping system is the CARTO® system (Irvine, California, USA), which employs EM tracking to determine the 3D position and orientation of the catheter, thereby facilitating the 3D surface reconstruction of heart anatomy including its chambers. Augmenting this with preoperative CT scans provides additional visualization and information, achieved by computing a registration between CT and EM spaces and integrating it into the CARTO® Merge module.

CARTO® introduces two approaches for this registration: feature-based and surface registration. The former approach relies on manually identified feature pairs between the CT data and the activation map. In contrast, the latter employs the reconstructed surface map from the CARTO® system to align it with the corresponding CT-derived surface [22]. Although surface registration can be automated, unlike feature-based registration, it necessitates a pre-registration anatomical map reconstruction, which in turn requires navigating the catheter within the heart, thereby postponing the availability of the registered CT data. Similar feature-based registration methods have been documented for other ablation systems like EnSite NavX (Abbott, Chicago, Illinois, United States) [162]. Moreover, the exploration of registration techniques in the context of EP procedures has been thorough, with reviews available that offer comprehensive insights for researchers and clinicians working in this field [99, 161].

8.2 Methodology

8.2.1 Overview of the Method

This work introduces a novel method for automatically registering the EM tracking space with preoperative volumetric data through Bioelectric sensing. During the preoperative planning phase, a series of distinct anatomical landmarks are labeled and marked along the centerline of the intended catheter pathway, including but not limited to bifurcations, stenosis, or aneurysms. These are landmarks that Bioelectric sensing is capable of recognizing automatically via template matching. The method requires identifying at least three feature points to initiate the feature-based registration process. Although a minimum of three vascular features is required for a successful registration, incorporating additional features may enhance the robustness of the registration, particularly in scenarios affected by outliers or similar factors that could impact the outcome of the registration process.

The Bioelectric sensing technique automatically recognizes the local geometrical vascular features the catheter encounters throughout the intraoperative catheterization process. The catheter, integrating EM-Bioelectric sensing, records the 3D location of each feature within the EM space, courtesy of the EM sensor affixed to the catheter. This leads to the formulation of coordinate pairs, with each pair containing the 3D EM coordinate of a detected feature alongside the corresponding coordinate of that feature as identified in the preoperative data.

The initial registration stage involves aligning these corresponding pairs of points through Singular Value Decomposition (SVD) to achieve a rigid transformation. This initial alignment is subsequently refined by employing an ICP path-based registration technique that matches the EM path with the vessel's centerline. This feature-based registration methodology presents a significant advantage by facilitating successful registration, even when the starting positions of the two point clouds are considerably distant. The ICP algorithm, on its own, may not converge if the initial distance between the point clouds is too far. In addition to centerline registration, an alternative method involves aligning the EM path with points along the vessel wall through ICP. This technique mirrors the catheter's trajectory along the vascular wall, offering another metric for evaluating the precision of the registration process.

EP catheters often come equipped with integrated EM tracking sensors and multiple electrodes along their length. This dual functionality enables the application of bioelectric navigation principles to these catheters. A significant benefit of the proposed approach is its ability to forego the need for manual labeling of anatomical features during the procedure or an anatomically reconstructed surface for registration purposes, thereby aligning seamlessly with EP procedures. The method innovatively leverages anatomical features automatically detected as the catheter navigates through the vasculature, avoiding any alterations to the interventional workflow. In the envisioned EM-guided process, the catheter identifies vascular landmarks essential for registration as it moves from the femoral arteries to the heart. Once the catheter arrives at the heart, the registration transformation is computed and applied to align the heart's anatomy with the EM tracking space. This registration, informed by preoperative CT scans, provides crucial clinical insights, facilitating enhanced navigation and the generation of activity maps.

8.2.2 System Setup

This study utilized a diagnostic EP catheter featuring ten circular electrodes near its tip (Boston Scientific EP XT, 110 cm long, 2 mm outer diameter, and 2-5-2 mm electrode spacing). For Bioelectric sensing, electrodes #2 and #9 functioned as the current-injecting electrodes, while electrodes #5 and #6 were designated as the voltage measurement electrodes (sensing electrodes; refer to Fig. 8.1). A sine wave voltage of 250 mV at 1 kHz was generated using the waveform generator of a Picoscope 2203 digital oscilloscope. This voltage was converted into an AC, constant amplitude current (100 μA peak-to-peak) through a bespoke circuit employing the Howland current source design. Subsequently, this current was administered via the current-injecting electrodes. The voltage across the sensing electrodes was recorded and digitized utilizing the same oscilloscope. Voltage readings and corresponding timestamps were logged via a Python script and then translated into the Fourier domain using a sliding window Fast Fourier Transform (FFT). The absolute magnitude at the stimulation frequency was derived from each FFT window and preserved for subsequent analysis. A six DoF EM Sensor (Aurora Flex Tube 1 mm) was affixed to the catheter, secured by heat shrink tubing, situated 2 cm away from the sensing electrodes. The arrangement of the EP catheter, the EM sensor, and their connection via shrink-tube is presented in Fig. 8.1. An Aurora Field Generator Tabletop 50-70 from Northern Digital Inc – NDI (Waterloo, Ontario, Canada) generated the EM tracking field. The EM tracking data, complete with timestamps, was captured along the trajectory using the ImFusion Suite (ImFusion GmbH, Munich, Germany). Data processing for registration purposes were conducted on a laptop equipped with Windows 11 Pro, 64bit, Intel Core i7-8565U CPU @ 1.80GHz, 16GB RAM, and Intel UHD Graphics 620.

8.2.3 Vascular Phantom

For this proof-of-concept study, a simplified vascular model obtained from an online public repository was utilized [189]. The STL model was adjusted by cropping and scaling up to accommodate the catheter and EM tracker and then 3D printed using clear polylactic acid (PLA) material. This resulted in a transparent, rigid phantom measuring 22 cm in length, featuring vessels with diameters ranging from 5 mm to 15 mm. The design of the

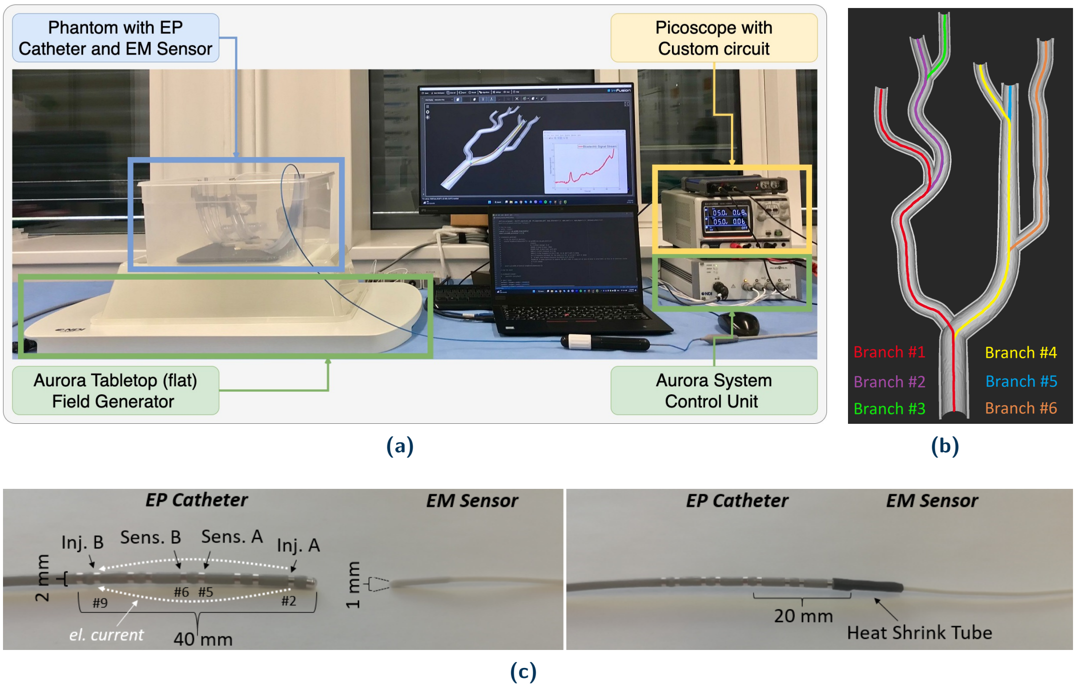

Fig. 8.1. System setup and components for feature-based catheter tracking and registration. (a) Complete experimental setup and its components, (b) Illustration of a phantom with navigated paths for data collection, and (c) EP catheter tip design showing detection and injection electrodes for bioelectric sensing, EM sensor tip size, and the coupling of the catheter and EM sensor with heat shrink tubing.
Note: Figures reused without changes © 2023 IEEE [156]. Used with permission.

phantom aims to mimic real vascular features, including curved branches of varying diameters, bifurcations, and stenosis, serving as a testbed for evaluating the proposed catheterization technique's precision and reliability. Silicone tubing was affixed to each end of the phantom to facilitate access and ensure it was watertight. Before the experiments, the phantom was filled with saline solution to simulate the conductivity of blood within vessels during an actual procedure. It was securely mounted inside a plastic container positioned directly atop the EM field generator. The entire assembly is presented in Fig. 8.1a, with a top-down view of the phantom's vascular layout shown in Fig. 8.1b and Fig. 8.2.

8.2.4 Data Processing

The automatic feature-based registration method introduced here involves both preoperative and intraoperative phases. This process is depicted in Fig. 8.3. An STL model of a vascular phantom, which mimics the vascular structure, served as the preoperative volumetric data. In real clinical scenarios, this would be replaced by a segmentation of the patient's vasculature derived from a CTA scan.

During the preoperative phase, the centerlines of six paths within the phantom were segmented using the SlicerVMTK toolkit in 3D Slicer, as illustrated in Fig. 8.1b. This toolkit employs a centerline extraction algorithm based on a Voronoi model, optimizing for the inverse of the maximum inscribed sphere radii along each centerline. The extracted centerlines were then

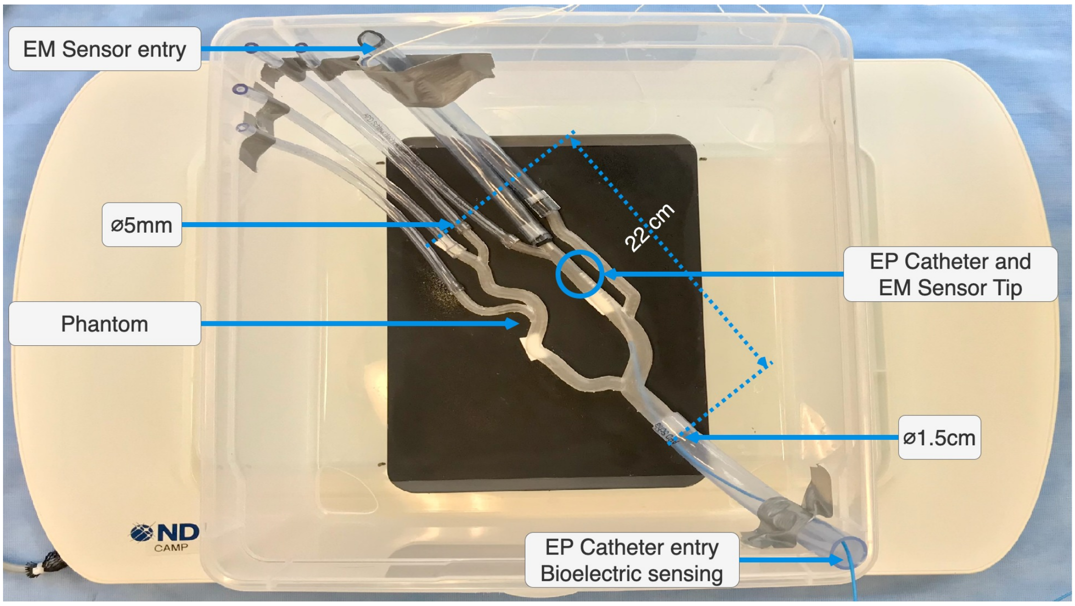

Fig. 8.2. Top-view of the phantom setup and its components for feature-based catheter tracking. The image highlights the EM sensor and an EP catheter outfitted with bioelectric sensing capabilities, the entry and exit points of the phantom, and the EM tracking field generator positioned underneath.
Note: Figure reused without changes © 2023 IEEE [156]. Used with permission.

visualized within the STL model using the ImFusion Suite. Three points corresponding to distinct vascular features, such as bifurcations, stenosis, or vascular turns, were manually identified and marked on each centerline. An example of such point annotation is presented in Fig. 8.3. These identified points are henceforth referred to as preoperative centerline points $x_{\text{preop,stl}}$, situated within the preoperative coordinate space $\mathbb{C}_{\text{preop,stl}}$. For adequate preoperative preparation, selecting at least three points for each centerline is essential, so that a unique plane can be defined that intersects all the three points.

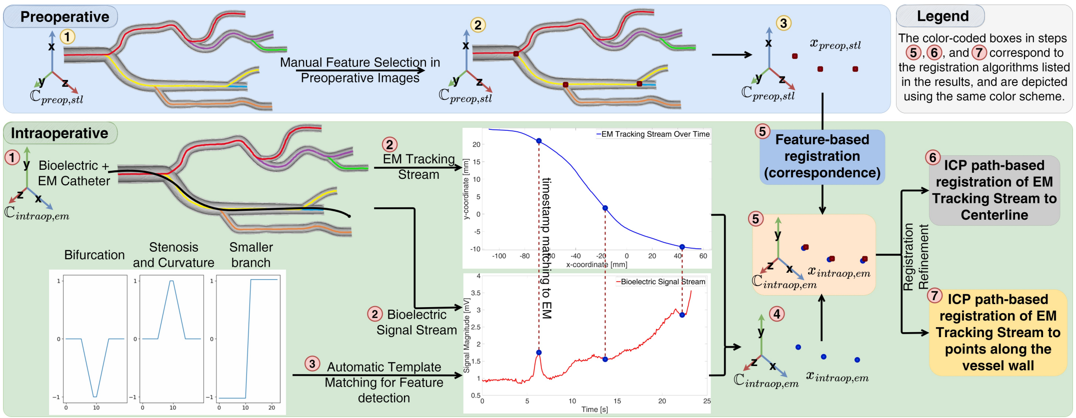

Fig. 8.3. Registration process overview for feature-based catheter tracking. Preoperative centerline points are labeled on the preoperative model in the coordinate space $\mathbb{C}_{\text{preop,stl}}$. During the procedure, corresponding local vascular features are identified through template matching within the Bioelectric signal. The positions of these features in the EM coordinate space $\mathbb{C}_{\text{intraop,em}}$ are determined intraoperatively using EM tracking data and the Bioelectric signal. A registration is then computed between these point sets.
Note: Figure reused without changes © 2023 IEEE [156]. Used with permission.

The initial step performed intraoperatively involves inserting the catheter into the phantom equipped with an attached EM tracker. As the catheter is withdrawn from the root of the vascular tree towards the narrower diameter outlets, streams of EM tracking data are captured. Following the completion of a path, both the Bioelectric sensing data and the EM tracking streams, along with their respective timestamps, are saved. The EM tracking data is then subjected to a Gaussian filter (with σ=50, applied in rotation and translation motions) to mitigate and smooth out any noise in the tracking signal. Similarly, the Bioelectric signal undergoes smoothing by applying a five–sample uniform filter.

The process then involves calculating the cumulative sum of the distances between successive EM coordinates, yielding, at each timestamp, the total distance the EM sensor has traversed since the start of the recording. This correlation between the distance covered and time is utilized with the timestamps from the Bioelectric signal to organize the Bioelectric measurements based on the distance traveled. This adjustment accounts for variations in the catheter's movement speed. While the Bioelectric signal's appearance might vary over time due to the speed at which the catheter crosses an anatomical feature, its profile relative to the distance traveled remains comparatively stable across different speeds. This stability is crucial for feature identification through template matching, eliminating the need to adjust for signal distortion caused by varying movement speeds.

Subsequently, its automatic counterpart within the Bioelectric stream was identified through template matching for each manually identified preoperative centerline feature $x_{\text{preop,stl}}$. This process leverages the preoperative annotations, precisely the manually marked feature locations in the STL model and the feature type (such as bifurcation, stenosis, high curvature, or entry into a branching vessel). The templates utilized for matching are illustrated in Fig. 8.3. Initially, the algorithm selects an anchor feature, typically the first feature annotated for each phantom branch, to serve as a reference point. Sliding windows are then extracted from the Bioelectric signal, normalized by their mean and standard deviation, and the algorithm searches for the location within the first few centimeters of the signal that exhibits the maximum correlation with the template. This process determines the timestamp at which the sensing electrodes encountered the specific feature. Utilizing this timestamp, the corresponding EM coordinate linked to the feature is identified. Given that the Bioelectric and EM streams are recorded at different sampling frequencies, the nearest timestamp in the EM stream is selected to match the Bioelectric timestamp. Additionally, the 2 cm distance between the EM sensor and the Bioelectric electrodes, a consequence of the sensor's integration into the catheter, is considered.

The distance from each vascular feature to the designated anchor feature along the centerline is computed following the manual annotations within the preoperative data. Subsequently, segments of the signal within a vicinity ($\pm$1.5 cm) of the anticipated feature location are extracted. This extraction is facilitated by accumulating the distances between successive EM coordinates until the aggregate matches the centerline distance noted in the preoperative data. Within these segments, template matching is applied to identify the points of highest correlation, which are assumed to be the locations of the features. The corresponding timestamps are then determined to locate the associated EM tracking points. The intraoperative EM locations corresponding to these points are marked as $x_{\text{intraop,em-offset}}$.

To accommodate the 2 cm offset between the EM sensor and the Bioelectric sensing electrodes, the procedure involves navigating the EM tracking data from the point $x_{\text{intraop,em-offset}}$, cumulatively adding the Euclidean distances between consecutive points until a total of 2 cm is reached. The EM location thus identified, adjusted for the offset, is then recognized as the position of the relevant vascular feature point $x_{\text{intraop,em}}$, situated within the intraoperative EM coordinate space $\mathbb{C}_{\text{intraop,em}}$. This approach ensures that the spatial discrepancy between the sensing modalities is effectively bridged, thereby accurately aligning the detected features within the intraoperative workflow.

These procedures result in the creation of two distinct point sets, $x_{\text{preop,stl}}$ within the preoperative coordinate space $\mathbb{C}_{\text{preop,stl}}$, and $x_{\text{intraop,em}}$ within the intraoperative EM coordinate space $\mathbb{C}_{\text{intraop,em}}$. For each point in the preoperative set, a corresponding point in the intraoperative set is established via the Bioelectric feature matching previously outlined. A point-based correspondence registration is carried out to align these two sets of points using SVD. This process aims to derive an automatic rigid transformation that minimizes the sum of squared distances between corresponding points in the two sets, thereby efficiently aligning them. This process results in a rigid transformation between the corresponding point sets, representing the initial approach to registration discussed in this work.

To enhance the precision of the initial registration between the EM path and the vessel's centerline, an ICP path-based registration is employed as a subsequent refinement step, drawing on methodologies described in previous works [134, 135, 150]. The ICP algorithm adjusts the entire EM path against the centerline, including the correspondence points previously determined. In this process, the selected correspondence points are treated equally with others in their respective point sets without any special weighting in the ICP algorithm. This stage constitutes the second approach to registration within this work.

The underlying assumption is that this refinement, which aligns all points of the EM path with those of the centerline through path-based registration, can correct inaccuracies originating from the feature detection in the Bioelectric signal. Additionally, an alternative refinement technique was explored to enhance the accuracy of the registration. This third approach differs by adjusting the initially registered EM path to align with points along the vessel wall rather than its centerline. This method matches the catheter's path more closely to the vessel's boundaries, offering another dimension of registration refinement as Lambert et al. [91].

The process of aligning two sets of points, x and y, through the ICP algorithm in this research is encapsulated in Eq. 8.1, where x denotes points along the EM path, and y signifies points along the centerline or vessel wall. The ICP algorithm seeks to find the transformation matrix $T = (R, t)$, comprising a rotation matrix $R_{3\times3}$ and a translation vector t. This transformation is determined by minimizing the distances between corresponding points in the two point sets, achieving an optimal alignment of the point clouds.

$$R, t = \arg\min_{R,t} \sum_{i=1}^{n} \sum_{j=1}^{m} ||Rx_i + t - y_j||^2 \tag{8.1}$$

In this context, R represents the 3×3 rotation matrix, and t is the 3×1 translation vector. These components are optimized to minimize the sum of squared distances between the transformed points in the form of $Rx_i + t$ and their corresponding counterparts in the y pointcloud. Here, x_i and y_j refer to specific points within the x and y pointcloud, and n and m denote the number of points in the x and y pointclouds, respectively. The notation $|| \cdot ||$ signifies the Euclidean norm. The iterative process of the ICP algorithm continues until it converges, progressively reducing the distance between the two sets of points by adjusting the rotation and translation parameters to achieve an optimal alignment.

8.3 Evaluation and Results

Two state-of-the-art metrics, Root Mean Square Error (RMSE) and Mean Minimum Error (MME), were utilized to evaluate the accuracy of the proposed registration methods in relation to the ground truth. The procedure involved conducting catheter pull-throughs across each of the six branches five times, ensuring a comprehensive dataset for analysis. The ground truth for registration was established through a marker-based approach, aligning multiple points on the phantom with their counterparts in the preoperative model, providing a reliable benchmark for comparison.

The recording and processing of signal streams were carefully carried out to facilitate an accurate and meaningful evaluation of the outcomes. Notably, all registration algorithms applied in this research demonstrated computational efficiency, with a runtime of less than one second per execution for each algorithm. The comprehensive process, including data loading, feature detection, timestamp matching, and the execution of registration, was efficiently completed in under one minute on average. This study undertakes the evaluation of three distinct registration approaches to determine their precision and effectiveness in aligning preoperative and intraoperative data sets:

1. **Automatic Feature-based Registration**: This approach involves the translation of EM feature-points and the EM path utilizing an automatic feature-based correspondence registration technique. It primarily focuses on aligning points identified as significant through Bioelectric sensing with their preoperative counterparts designated in the model.

2. **ICP Registration of the EM Path to the Vessel's Centerline**: Serving as a refinement to the initial results from the automatic feature-based registration, this method applies the ICP algorithm to align the entire EM path with the centerline of the vessel. It aims to improve the initial alignment by considering the complete trajectory of the EM path in relation to the central anatomical structure of the vessel.

3. **ICP Registration of the EM Path to Points Along the Vessel Wall**: This approach further refines the outcomes of the automatic feature-based registration by aligning the EM path with points located on the vessel wall, rather than its centerline. By focusing on the vessel's outer boundaries, this method seeks to enhance the accuracy of the registration process, potentially offering a more nuanced understanding of the catheter's position within the vascular network.

Fig. 8.5a and Fig. 8.5b display the outcomes from the first, second, and third registration approaches, marked by orange, grey, and yellow colors, respectively. In addition, Fig. 8.5a shows the RMSE values calculated exclusively on the three feature points (excluding all other EM points) following the automatic feature-based registration, indicated in blue. The visualization of all registration results for branch five is presented in Fig. 8.4, where the results are color-coded to reflect the distinct registration algorithms applied.

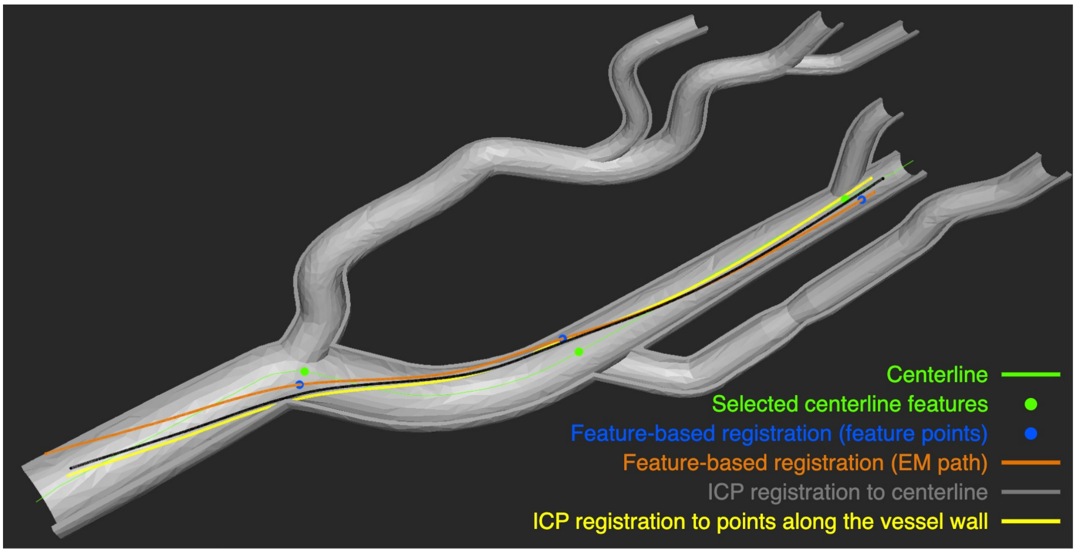

Fig. 8.4. Registration results for feature-based catheter tracking. Visualization of registration results for branch 5, with color-coding to indicate the respective registration algorithms used.
Note: Figures reused without changes © 2023 IEEE [156]. Used with permission.

8.3.1 RMSE from ground truth

For the initial evaluation metric, RMSE is determined between EM points transformed via the ground truth registration and EM points transformed by the three registration methods previously described (refer to Eq. 8.2). The evaluation outcomes are depicted in Fig. 8.5a.

$$\text{RMSE} = \sqrt{\frac{1}{N}\sum_{i=1}^{N} ||\hat{X}_i - X_i||^2} \tag{8.2}$$

In Eq. 8.2, $\hat{X}_i$ denotes a point along the EM path that the automatic feature-based registration algorithm has transformed. In contrast, X_i signifies a point along the EM path that the ground truth registration has transformed. The notation $||\cdot||$ represents the Euclidean norm.

8.3.2 MME from ground truth

As the second evaluation metric, the distance between each point transformed by the registration method and the nearest point in the ground truth registration is computed. The average of these distances constitutes the MME, which is detailed in Eq. 8.3. The findings based on this metric are illustrated in Fig. 8.5b.

$$\text{MME} = \frac{1}{N} \sum_{i=1}^{N} \min_{j} ||\hat{X}_i - X_j|| \tag{8.3}$$

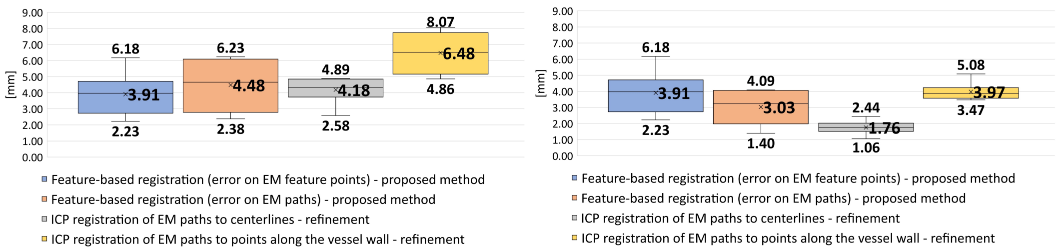

(a) (b)

Fig. 8.5. Registration results from feature-based catheter tracking. Results across all branches and attempts, measured in [mm]. Bars represent the standard deviation, whiskers indicate the minimum and maximum errors. The following color codes are used: blue represents our proposed registration method of feature points, orange represents our proposed registration method of the entire EM path, gray represents the ICP refinement, and yellow represents the registration of the EM path with the vessel wall. a) Indicate the RMSE registration results, and b) Indicate the MME registration results.
Note: Figures reused without changes © 2023 IEEE [156]. Used with permission.

8.4 Discussion

This research utilized two metrics for evaluation, RMSE, and MME, to gauge the effectiveness of the registration approaches. The findings reveal that the initial automatic feature-based registration method, focusing solely on the selected feature points, delivers promising outcomes with an RMSE and MME of 3.91 mm. When this registration method is extended to the entire EM path, the RMSE slightly increases to 4.48 mm, whereas the MME improves to 3.03 mm. According to standards set in prior research, specifically for aortic endovascular procedures, registration accuracy of less than 5 mm is considered clinically acceptable [135]. The results showcased in Fig. 8.5a and Fig. 8.5b demonstrate that refining the registration of the EM path to the vessel's centerline via the ICP method enhances the results, yielding an RMSE of 4.18 mm and reducing the MME to 1.76 mm.

Conversely, refining the registration to align the EM path with points along the vessel wall increases errors, with the RMSE and MME reaching 6.48 mm and 3.97 mm, respectively. These outcome variations can be attributed to the distinct methodologies of the two evaluation metrics. The RMSE method, due to its point-by-point sequential comparison, tends to generate higher error values. In contrast, by assessing EM points against their nearest ground truth counterparts in a non-sequential manner, the MME method offers a different perspective on registration accuracy.

Previous research has indicated that registering the EM path to centerlines yields outcomes that are on par with or surpass those of alternative registration methods [135]. Similarly, earlier findings have suggested that aligning the EM path with points along the vessel wall can also achieve satisfactory results [91]. However, this proof-of-concept study observes an increase in error for both evaluation metrics when the EM path is registered to points along the vessel wall compared to centerline registration.

The rationale behind the effectiveness of centerline registration lies in the assumption that the catheter navigates through the central axis of the vessel, thereby capping the potential error for any given data point at half the vessel's diameter. Conversely, registration to points along the vessel wall introduces the possibility of the maximal error reaching up to the full diameter of the vasculature, particularly when the actual catheter position diverges to the opposite side of the derived registration results.

Despite both approaches yielding registrations within the clinically acceptable error margin, the findings of this study underscore a preference for ICP registration to the centerline over registration to points along the vessel wall. This preference is attributed to the inherent limitations and potential for increased error associated with wall-based registration, highlighting centerline-based methods' relative accuracy and reliability.

Tab. 8.1 offers a detailed comparison between the registration outcomes of this research and the results reported in previous studies that explicitly document registration errors. This study's findings align with the benchmarks set by state-of-the-art research, with the added benefit of enhancing the degree of automation within the registration process. Specifically, the registration method involving the EM path to the vessel's centerline shows notable improvements over the results documented in studies like those by Luo [104] and Nypan et al. [135]. Compared with the study by Manstad-Hulaas et al. [115], which employ marker-based registration techniques, this study reveals slightly lower accuracy in phantom experiments but showcases better performance in in-vivo scenarios.

Furthermore, while the comparison with the study by Lambert et al. [91] indicates a marginal decrease in accuracy, the outcomes still fall within the clinically acceptable error range. It is important to note that while numerous studies have investigated registration methods, many focus on the cannulation success rate and the procedure duration without delving into precise error metrics. Consequently, the comparison within this study only includes those studies that provide explicit error measurements, ensuring a focused and relevant evaluation of registration accuracy.

Tab. 8.1. Comparison of registration accuracy of our feature-based approach with other studies.
Note: Table reused without changes © 2023 IEEE [156]. Used with permission.

Research study	Reported error [mm]
Ramadani et al. [156] (our)	3.03 | 1.76 | 3.97
Manstad-Hulaas et al. [115]	1.28 and 4.18 (marker-based reg.)
Nypan et al. [135]	3.75 (reg. to centerline)
Luo [104]	4.50 (reg. to centerline)
Lambert et al. [91]	1.30 (reg. vessel walls)

The template matching strategy outlined in this research presupposes that the catheter has already navigated a portion of the path, including the vascular features marked beforehand, and that the catheter's current branch is identified (to facilitate the selection of an appropriate template set). Should this information not be predetermined, a preliminary path classification could be executed utilizing the Bioelectric signal, mirroring the approach detailed in prior research [189]. At this stage, it is expected that a certain level of expert knowledge is requisite for the annotation of features during the preoperative phase. A prospective direction for further research is the automation of feature annotations alongside the generation of simulated Bioelectric signals at these feature points. Such advancements aim to reduce the reliance on annotated features and the necessity for feature templates, paving the way for a more automated and less labor-intensive registration process.

The outcomes from the phantom experiments highlight the prospective efficacy of the proposed registration method, showcasing its applicability in a controlled environment. Nonetheless, further experimentation is essential to thoroughly evaluate the system's capability to handle the complexities of more realistic vascular structures – characterized by increased curvatures, bifurcations, and additional anatomical variations. Conducting animal studies is a crucial next step to authenticate the system's applicability and performance in more complex anatomies, thereby providing a more accurate assessment and clinical relevance.

Currently, many existing solutions for initializing the registration process in such interventions require alterations to the standard procedural workflow, additional external imaging modalities, or the use of registration markers. In contrast, the method proposed in this study leverages technologies already integrated into EP procedures, necessitating only minor adjustments, such as including a signal generator for Bioelectric sensing. Importantly, this approach does not impose any modifications on the intraoperative workflow. Instead, it facilitates the initialization of the registration process following the catheter's navigation through a series of vascular features identified via Bioelectric sensing, offering a streamlined and minimally invasive solution to the challenge of accurate catheter registration.

8.5 Summary

This work introduced a novel automated process for registering EM tracking space with preoperative data, utilizing features identified through Bioelectric sensing. The method's effectiveness was evaluated through the deployment of two distinct evaluation metrics across various registration techniques, encompassing alignment to both the centerline and points along the vessel wall. This introduced approach successfully registered EM tracking space with preoperative data within a vascular phantom setting.

Future research might extend the evaluation of this approach to more complex and anatomically realistic vascular phantoms, particularly those that closely mimic the cardiovascular anatomy of the heart, which holds significant relevance for EP procedures. Additionally, exploring this method's applicability and performance in actual tissue settings remains a compelling direction for research.

The methodology proposed herein offers a directly applicable solution for EP procedures, capitalizing on the existing integration of EM tracking technology and catheters equipped with electrodes for Bioelectric sensing. By harnessing these technologies, the approach presents a promising and streamlined direction for enhancing the precision and efficiency of catheter navigation and registration in endovascular procedures.

9 Dynamic Time Warping: Catheter Registration for EM-guided Procedures

The following chapter of the dissertation elaborates upon another of our work contributions to the 26th International Conference on Medical Image Computing and Computer Assisted Intervention (MICCAI 2023), titled "WarpEM: Dynamic Time Warping for Accurate Catheter Registration in EM-guided Procedures" [155]. This part of the dissertation serves as a direct contribution to the *Registration* component of the catheter tracking pipeline, introduced in Chapter 6: Catheter Tracking Concepts and Methodologies.

Accurate catheter tracking plays a significant role in the success of minimally invasive endovascular procedures, with Electromagnetic (EM) tracking technology being a suitable technology to achieve this. Nevertheless, aligning preoperative images with the EM tracking system poses significant challenges. Current registration methods often necessitate manual interaction, which not only extends the duration of the procedures but also elevates the potential for errors and necessitates alterations in the procedural workflow.

Among the various approaches to catheter tracking registration, including marker-based and path-based techniques, each has limitations that could impact the tracking technology's precision and decrease the procedure's effectiveness. These challenges underscore the need for developing more streamlined and error-resistant registration methods that can enhance the accuracy of EM tracking without imposing additional steps on the procedural workflow.

This part of this dissertation presents a new automated approach to catheter registration for EM-guided endovascular procedures. Leveraging the potential of 3D signal temporal analysis, notably through the application of Dynamic Time Warping (DTW) algorithms, this method seeks to enhance the accuracy and reliability of registration beyond the capabilities of current techniques. DTW is adept at flexibly warping and aligning EM-tracked paths with the vessel's centerline, offering a significant advantage in achieving precise registration. This proposal aims to automatize the registration process, potentially transforming the efficiency and success rate of EM-guided endovascular procedures by mitigating the limitations associated with manual and less dynamic registration methods. This approach to catheter registration exhibits numerous benefits over existing state-of-the-art methods, including high registration accuracy, the elimination of the need for initial setup or initialization, and a significant enhancement in the level of automation. These advantages collectively represent a substantial advancement in the field of EM-guided minimally invasive endovascular procedures, potentially setting a new standard for efficiency and efficacy in catheter tracking and registration.

9.1 Introduction

Minimally invasive endovascular procedures are gaining popularity as a preferred treatment method, attributed to their minimally invasive characteristics and the reduced recovery time compared to traditional open surgery. Nowadays, minimally invasive endovascular procedures include a range of applications, including but not limited to targeting complex interventions in organs such as the kidneys, liver, brain, aorta, and heart. An indispensable facet of these procedures are the catheter tracking techniques, crucial in navigating the catheters precisely through the complex vascular system. This advanced navigation capability is fundamental in ensuring the success and safety of minimally invasive endovascular procedures [4].

EM tracking is a well-established technology for catheter tracking in minimally invasive endovascular procedures, yet registering preoperative images with the EM tracking system accurately is challenging [54, 154]. Current methods for this registration often involve manual steps, which can be time-consuming and may disrupt the usual procedural workflow. Achieving precise registration is crucial for effectively integrating EM tracking, preoperative images, and the patient into the same coordinate space during procedures.

9.2 Related Work

9.2.1 Electromagnetic Tracking

As already discussed, EM tracking is a very popular technology for tracking, which employs sensors integrated at the catheter's tip along with a field generator, facilitating the localization of the sensor's pose in 3D. Its ability to operate without requiring line-of-sight makes EM tracking especially interesting [218]. The sensors, available in various shapes and sizes, can be precisely tracked in terms of their position and orientation relative to the EM generated field. Consequently, EM tracking is often utilized alongside intraoperative or preoperative images to accurately navigate the procedure [54, 154].

9.2.2 Registration

Registration is essential in enabling intraoperative navigation for procedures utilizing tracking technologies like EM tracking. Various EM tracking registration methods have been developed, specifically emphasizing applications in endovascular procedures [99, 119]. Among these, a widely employed technique involves the use of external markers or fiducials, which are attached to the patient's body throughout the preoperative and intraoperative phases. This approach requires physicians to identify and match multiple marker points with their corresponding positions in preoperative images, establishing a series of point correspondences. These correspondences are then utilized to compute the transformation needed for registration. While marker-based registration has become a standard, it presents several challenges, including disruptions to the procedural workflow, the imperative of marker stability across phases, and vulnerability to anatomical variations [100, 115, 124, 207].

Alternative registration strategies have explored leveraging the paths of EM-tracked catheters and their registration to the vessel's centerline via Iterative Closest Point (ICP) [104, 135], or to specific points within the vasculature [91]. Such methods have been the subject of considerable research, yielding results that underscore their accuracy and dependability. Nonetheless, they also face limitations, including challenges in precisely tracing the catheter's path, the necessity for accurate initial positioning to achieve precise registration, and potential declines in accuracy due to data gaps or a sparse number of points.

9.3 Dynamic Time Warping

DTW is a widely used technique in signal processing for comparing and synchronizing two time-series sequences. DTW assesses the similarity between sequences by optimally aligning them through non-linear adjustments, accommodating variances in time and sequence sampling rates. This warping function matches equivalent features across sequences, facilitating precise alignment despite temporal discrepancies or absent data points. DTW's usability spans various fields, including biomedical signal processing and speech and gesture recognition [47, 126].

However, the potential of DTW as a registration tool in EM-tracked minimally invasive endovascular procedures has yet to be fully explored. While prior research has applied DTW alongside EM tracking, these instances have primarily focused on data analysis and evaluation, capitalizing on DTW's strength in handling intravariability rather than registration [182, 220]. This part of dissertation proposes a novel application of DTW for registering EM tracking systems with preoperative images. To our knowledge, this marks the first attempt at employing temporal analysis of 3D EM-tracked catheter paths for registration purposes, aiming to align two systems within a singular coordinate framework. By leveraging DTW, the method warps the 3D EM-tracked catheter path onto the centerline of the vasculature, establishing matching points between the two entities. These points are subsequently refined using the minimal cost output from DTW, culminating in a set of correspondences critical for registration.

9.4 Methodology

This contribution introduces a novel method for automatically registering EM tracking systems with preoperative images via DTW. The process encompasses a preoperative phase where targeted vasculature is segmented from imaging modalities such as Magnetic Resonance Imaging (MRI), Computed Tomography (CT), or Computed Tomography Angiography (CTA). Subsequently, the centerlines of these segmented images are extracted using the SlicerVMTK toolkit. During the intraoperative phase, a catheter, equipped with an EM sensor at its tip, navigates through a specified branch of the vascular tree, recording a 3D EM path. For the purposes of this proof-of-concept study, a catheter-shaped EM sensor is utilized. The DTW algorithm processes the captured EM path, aligning it with the centerline and establishing point correspondences between the EM path and the centerline. These correspondences then facilitate a closed-form solution using the Coherent Point Drift (CPD) algorithm, which accurately maps the EM path onto the centerline, effectively registering the two sets of coordinate spaces. An in-depth illustration of this method is provided in Fig. 9.2.

9.4.1 Electromagnetic Tracking

The EM tracking system employed for this proof-of-concept study is the Aurora system from Northern Digital Inc. – NDI (Waterloo, Ontario, Canada). This system consists of an integrated tracking module, a sensor interface unit, and a tabletop field generator, enabling EM sensor tracking within a 42×60×60 cm volume. The Aurora tracking system can capture data at frequencies up to 50 Hz. The specific EM sensor used for catheter simulation in this research is the Aurora six Degrees of Freedom (DoF) FlexTube, which has a diameter of 1 mm, showcasing its adaptability for various applications as a standalone navigational instrument or when integrated within catheters. For the purposes of this experiment, the EM sensor was utilized independently of a catheter and maneuvered within the phantom via its attached cable. Data was acquired using ImFusion Suite (ImFusion GmbH, Munich, Germany), executed on a laptop configured with Windows 11 Pro, powered by an Intel Core i7-8565U CPU, equipped with 16GB RAM and Intel UHD 620 Graphics. An illustrative overview of the experimental setup, highlighting the EM tracking system and the phantom model, is depicted in Fig. 9.1.

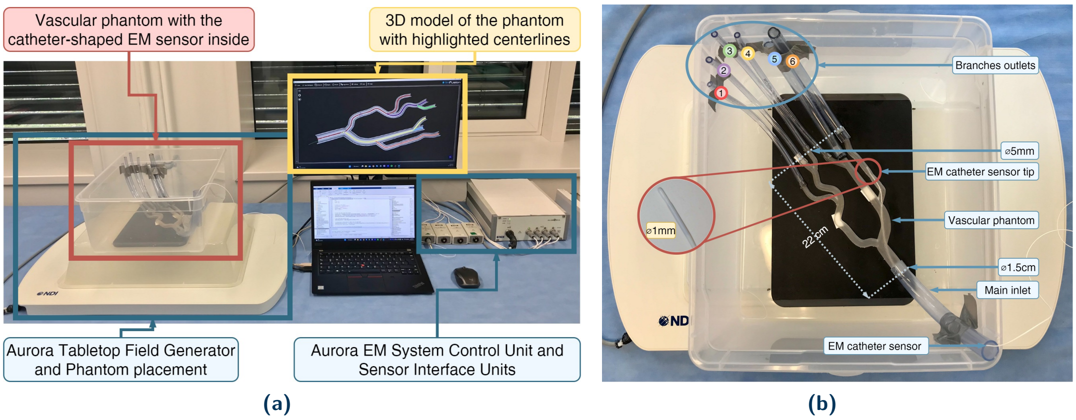

Fig. 9.1. Full system setup for the DTW catheter registration. (a) EM tracking system with the vascular phantom, catheter-shaped EM sensor, and visualization of the phantom model on the screen, and (b) Top view of the vascular phantom used in the experiments, showcasing labeled branches for straightforward identification, color-coordinated with the experimental results.
Note: Figure reused without changes © 2023 Springer Nature [155]. Reprinted with permission. License Number 5811040315432.

9.4.2 Phantom

For the acquisition of EM tracking data, an STL model from a previous work was employed [156, 189]. This model was adjusted to simplify its structure while retaining six primary branches that closely mimic natural vasculature. The model underwent resizing to make it compatible with catheterization practices, featuring vasculature diameters that range from 5 mm to 15 mm and a total length of 22 cm. To ensure that the catheter-shaped EM sensor could be observed externally, the phantom was printed using a rigid, transparent polylactic acid (PLA) material via 3D printing. For the experimental setup, the phantom was securely affixed within a box and placed atop the EM tracking field generator, facilitating the experimental procedures and recording EM tracking data. A visual depiction of the phantom and the catheter-shaped EM sensor used in this research is provided in Fig. 9.1b.

9.4.3 Dynamic Time Warping Registration

In the intraoperative phase of the procedure, two key preoperative elements are utilized: the segmented vascular model and the centerline points of its branches. These centerline points are denoted as $p_c^n \in \mathbb{P}^3_{\text{preop}}$, where n indicates the total number of points, and $\mathbb{P}^3_{\text{preop}}$ symbolizes the 3D preoperative coordinate space. The initial step involves navigating the EM catheter-shaped sensor through the vascular phantom, during which the EM-tracked catheter path is recorded. The EM path points are represented as $p_{em}^m \in \mathbb{P}^3_{em}$, with m marking the count of points and $\mathbb{P}^3_{em}$ standing for the 3D coordinate space of the EM tracking.

For DTW to be applicable to 3D signals, both signals must have an equal number of points. In order to reconcile any discrepancies in point counts between the signals, linear interpolation is employed to adjust the signal with fewer points to match the point count of the other signal. In this context, the centerline points are interpolated to equate to the number of EM path points $p_c^n \to p_c^m$, ensuring compatibility for DTW analysis.

Continuing the introduced method, the centerline and the EM-tracked catheter path signals undergo normalization in 3D space so that their coordinates fit between -1 and 1. This step aims to align the signals within a temporary shared coordinate space, facilitating a more straightforward comparison.

From this point, DTW tackles the 3D signals by dividing them into their component axes, specifically, the x, y, and z axes over time. It proceeds to align each point along the EM-tracked catheter path with its nearest equivalent point along the centerline. This iterative mechanism adjusts the signals by warping them until the cumulative Euclidean distances between matched points reach a minimal value. The outcome of this adjustment is a series of warp paths delineated by the DTW algorithm, which delineate the paired indices now aligned at minimal cost, represented as $c_{i,j}^u = (p_c^i, p_{em}^j)$. In this notation, c signifies the set of corresponding points between the two signals, u indicates the total count of such correspondences, and i and j mark the indices of the matched points within the centerline and EM-tracked catheter path, respectively. Thus, for each point identified along the EM-tracked catheter path, one or multiple corresponding points along the centerline are identified as matching pairs, and the reverse is also true.

For readers interested in diving deeper into the DTW algorithm and its application as discussed in this dissertation, further information and implementation details can be found in the foundational works of Paliwal et al. [140] and Sakoe and Chiba [171].

In order to achieve registration between the two signals, the DTW method capitalizes on the point correspondences established by the DTW algorithm. Three sets of correspondences, $c_{i,j}^3 = (p_c^i, p_{em}^j)$, are selected from three equally divided segments of the signals, ensuring a broad distribution across the signal length. This selection is based on the DTW algorithm's minimum cost return function, which aims to minimize the sum of Euclidean distances between corresponding points. Segmenting the signals into thirds and choosing correspondences from each segment ensures an even distribution of point matches, enhancing the reliability of the registration by avoiding over-reliance on any single vascular section.

These strategically chosen correspondence points are the basis for calculating the rigid transformation using the CPD algorithm [129]. The CPD algorithm, a closed-form solution, is designed to find a transformation $T = (R, t)$ that aligns the sets of correspondence points by reducing the distance between them. Within this transformation, R is the 3×3 rotation matrix, and t is the 3×1 translation vector.

Upon determining this transformation, it is then applied to the entire recorded EM-tracked catheter path, effectively registering the EM tracking system with the preoperative images within the same intraoperative 3D coordinate space, denoted as $p_c^m, p_{em}^m \in \mathbb{P}^3_{\text{intraop}}$. This step finalizes the registration of the two systems, enabling accurate navigation and positioning during the procedure based on preoperative planning.

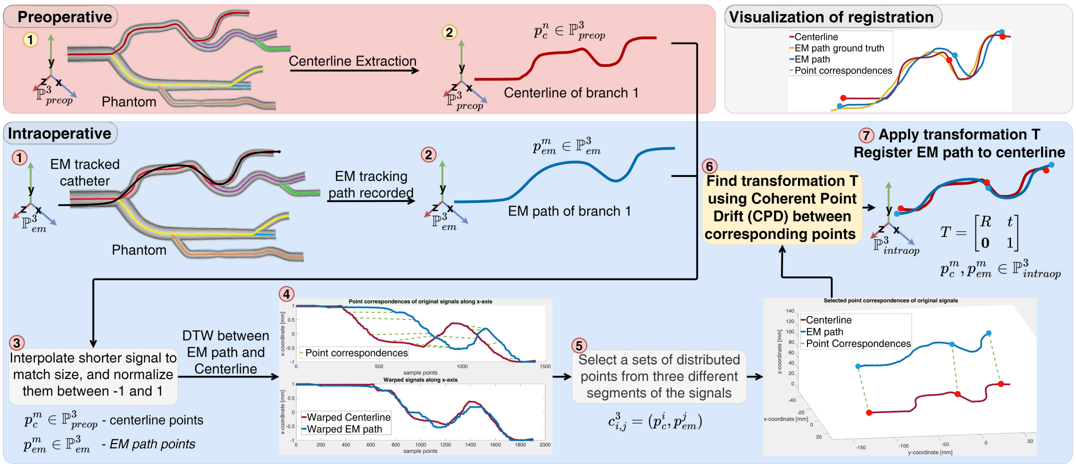

Fig. 9.2. Overview of the DTW registration method for EM-guided minimally invasive endovascular procedures. The image details the procedural aspects of registration over two phases of the procedure.
Note: Figure reused without changes © 2023 Springer Nature [155]. Reprinted with permission. License Number 5811040315432.

9.5 Evaluation

The introduced DTW method for registering EM-guided minimally invasive endovascular procedures is evaluated through the Mean Minimum Error (MME) registration criterion and benchmarked against state-of-the-art path-based ICP registration methods. In order to verify the registration accuracy of the DTW approach, experiments were performed by documenting EM-tracked pathways while navigating through each of the phantom's six branches a total of five times. During each iteration, the EM catheter-shaped sensor was manually navigated from the phantom's primary inlet to the outlets of each branch, maintaining an average velocity of 1–2 cm/s. The collected EM-tracked catheter paths were aligned with the phantom's centerline utilizing the DTW method introduced herein.

A marker-based registration method was employed to establish a ground truth in this work, serving as a gold standard within existing literature. Utilizing ten distinct and easily identifiable landmarks distributed throughout the phantom, the preoperative model was aligned with the EM tracking system, providing a basis for calculating the ground truth registration.

9.5.1 Mean Minimum Error Registration

The MME registration criterion serves as a measure to evaluate the precision of the introduced DTW method relative to the ground truth registration. This metric is determined by aggregating the Euclidean distances from each point along the DTW-registered EM-tracked catheter path to the nearest point on the ground truth EM-registered path. The formula used for calculating the MME registration is presented in Eq. 9.1, providing a quantifiable means to assess the DTW approach's accuracy against the established ground truth registration benchmark.

$$\text{MME} = \frac{1}{m}\sum_{i=1}^{m} \min_{j} ||p_{em}^{i} - p_{gt}^{j}|| \tag{9.1}$$

In the evaluation of the MME registration, p_{em}^{i} denotes a point on the EM-tracked catheter path that has been transformed by the DTW registration method introduced in this work. p_{gt}^{j} is the nearest point on the ground truth path relative to p_{em}^{i}. The variable m signifies the total points count across the DTW-registered and ground truth signals. The notation $||\cdot||$ represents the Euclidean norm. This framework is utilized to compute the MME, directly comparing the DTW method's precision relative to the ground truth. The findings derived from this evaluation metric are illustrated in Fig. 9.3, visually representing the accuracy achieved through the DTW registration approach.

9.6 Results and Discussion

Following the described experimental setup and evaluation criteria, this proof-of-concept study outcomes are presented in detail in Fig. 9.3. Across all branches and individual runs, the MME registered at 2.22 mm. This figure comfortably sits within the clinically acceptable error margin of less than 5 mm, aligning with standards reported in previous research [135, 156]. Notably, the DTW registration method showcased in this work exhibited a marginally better performance compared to the path-based ICP registration method, which recorded a MME registration of 2.86 mm. This comparison underscores the DTW method's efficacy in enhancing the accuracy of EM-guided minimally invasive endovascular procedures.

The results discussed in this work highlight the DTW registration method's capacity for achieving both accurate and reliable registration. This technique surpasses traditional path-based registration approaches utilizing ICP across all evaluated branches. It is observed that the variability in registration accuracy is more pronounced in predominantly straight vessels, where the automated selection of feature points for registration tends to follow a linear trajectory. This variation is particularly evident in the results from Branchs 4 and 5, where, despite correct translation matching, the orientation alignment between the signals is not as accurate, leading to a standard deviation that surpasses those achieved with ICP. Nevertheless, in branches with more vascular features, the standard deviation remains within an acceptable level.

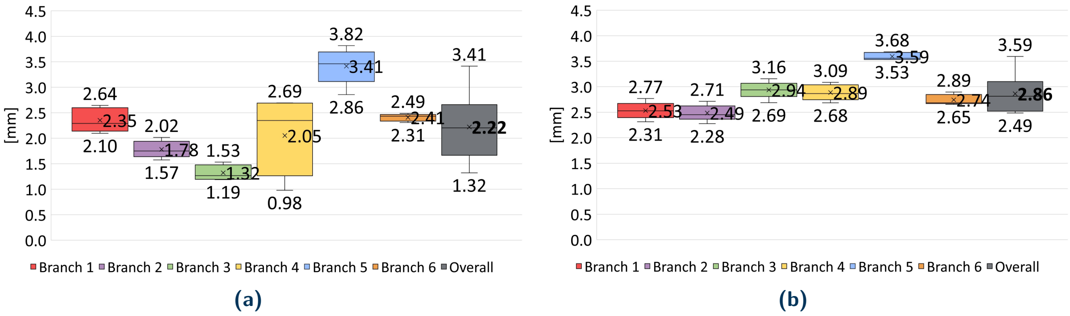

Fig. 9.3. Registration results from the DTW method for EM-guided endovascular procedures. MME registration results across all branches and attempts, measured in [mm]. Bars represent the standard deviation, whiskers indicate the minimum and maximum errors. The color-coded information in the graphs corresponds to the colored branches in the phantom. (a) Indicates the DTW registration of EM paths to centerlines, and (b) Indicates the ICP registration of EM paths to centerlines.
Note: Figure reused without changes © 2023 Springer Nature [155]. Reprinted with permission. License Number 5811040315432.

One of the key strengths of the introduced method is its ability to automate the registration process without necessitating alterations to the intraoperative workflow. Contrary to marker-based registration methods that demand manual interaction for point matching, the DTW approach seamlessly adapts the signals, identifies corresponding points, and executes the registration autonomously. Moreover, unlike other path-based registration methods that hinge on precise initialization to yield successful transformations, the DTW method exhibits independence from such initial conditions. In our analysis, the ICP method required preliminary positioning via the DTW method to ensure convergence, underscoring the DTW's superiority in bridging significant signal disparities where direct ICP application would fail without an accurate initialization.

Unlike other path-based registration techniques, the DTW registration method diverges from the necessity of aligning the entire EM path with the centerline. ICP-based approaches strive to minimize discrepancies across all points involved in the registration process. Consequently, any distortion within a signal segment could influence the overall alignment outcome. In contrast, DTW prechecks the registration by matching points between the signals in advance and utilizes algorithms designed to evaluate the confidence level of these matched correspondences. This preliminary step ensures that the selected set of points for registration is reliable and facilitative to a successful alignment, thereby offering a potentially more accurate registration outcome than methods that attempt to consider the entirety of the data sets indiscriminately.

Compared to previous works, the registration accuracy of the DTW method presented in this chapter is competitive with other advanced techniques within the research community. Marker-based approaches, as detailed in studies like the one by Manstad-Hulaas et al. [115], have demonstrated registration errors as low as 1.28 mm in phantom studies and up to 4.18 mm in in-vivo experiments. Similarly, studies utilizing path-based ICP registration methods have reported accuracy of 3.75 mm and 4.50 mm, as seen in the works of Luo [104] and Nypan et al. [135], respectively. Another approach leveraging ICP registration documented by Lambert et al. [91] has shown a mean registration accuracy of 1.30 mm. Although direct comparisons may be nuanced due to variations in the tracking data and experimental setups employed across these studies, they collectively underscore the capability of the DTW method to achieve a level of registration accuracy that aligns with the current state-of-the-art, affirming its potential within the scope of EM-guided minimally invasive endovascular procedures.

Future research directions for the DTW registration method presented here involve further validation through diverse phantom studies and potential in-vivo experiments, which could solidify its applicability in clinical environments. An additional aspect worthy of exploration is the influence of catheter dynamics on DTW signal matching. Variability in catheter movement, including alternating forward or backward trajectories, can substantially alter signal characteristics, potentially leading to inaccuracies in matching.

A promising strategy to address these challenges involves leveraging the 3D localization and motion capture capabilities inherent to EM tracking technology. This could facilitate the detection of catheter movement direction, enabling the backward warping of signals upon direction reversal to maintain consistency in signal representation. Moreover, the development and integration of sophisticated algorithms capable of more precisely simulating the dynamics of catheter motion hold the potential to enhance the overall accuracy of the registration process. Despite the advances, there remains a notable discrepancy between the modeled catheter movements and their actual trajectories as compared to the centerline, indicating a significant opportunity for improvement in achieving accurate registration outcomes.

9.7 Summary

In the field of minimally invasive endovascular procedures, precise catheter tracking is essential, and this chapter presented an innovative approach to catheter registration employing DTW. To the best of our knowledge, this marks the first exploration of utilizing temporal analysis of 3D EM for catheter registration. The evaluation conducted within a vascular phantom framework, using marker-based registration as a benchmark for ground truth, demonstrates that the DTW method achieves accurate and reliable registration results. Notably, it surpasses the performance of traditional path-based ICP registration techniques.

This method distinguishes itself from existing approaches by offering several key benefits. It achieves high registration accuracy and fully automates the registration process, thus maintaining the integrity of the procedural workflow without necessitating manual initialization. Although the research presented here serves as a proof-of-concept, it lays the groundwork for future experiments to further validate and refine its effectiveness in a clinical context.

In summary, the DTW registration method introduced in this dissertation holds promise for significantly improving the precision and dependability of catheter tracking within endovascular procedures, offering a substantial contribution to the field and paving the way for enhanced patient outcomes through more accurate navigational support.

Part IV

Conclusion and Future Outlook

Conclusion

10

This dissertation presented a detailed and comprehensive work that encapsulates the extent of knowledge acquired throughout my doctoral journey, specifically focusing on multimodal minimally invasive catheter tracking concepts and methodologies for endovascular procedures. It serves as an extensive overview that introduces the reader to some of the most challenging aspects of this field. Through an exhaustive review of state-of-the-art solutions, this dissertation highlighted the existing gaps in the current body of research and proposed detailed solutions to address these identified challenges. The dissertation concludes with a reflective discussion, synthesizing the findings and projects potential paths for future research, offering a comprehensive roadmap for succeeding research in this field.

10.1 Conclusions

To accurately comprehend the challenges associated with catheter-based endovascular procedures, it is crucial to first outline several core keywords and terminology that play a vital role in understanding the nuanced aspects of this field. As such, this dissertation begins by defining crucial catheter-related terminology such as visualization, detection, tracking, and navigation. This initial section also delves into a comprehensive discussion on the catheter navigation techniques, endovascular instruments, the registration methodologies, tracking systems, and their relation to imaging modalities. This preliminary discussion provided readers with a robust conceptual framework, enabling a deeper understanding of the fundamental components of navigating the complex field of catheter-based endovascular procedures.

The following section of this dissertation further explored the background and theoretical aspects of the field. It begins by familiarizing readers with the subject matter and explaining the necessity for developing various tracking technologies within the context of human anatomy. An overarching view of human anatomy is provided, emphasizing the cardiovascular system, the heart, and prevalent vascular and cardiac diseases that may be treated through catheter-based endovascular procedures. This progression from a general overview to specific medical conditions underscores the critical role of catheter-tracking technologies in diagnosing and treating these conditions.

Following this, this dissertation introduced an essential dimension of this doctoral journey – insights garnered from extensive catheterization laboratory (cath lab) visits across various hospitals in Munich, complemented by investigations into actual clinical practices. This chapter encapsulated a detailed narrative of a patient's journey from admission to release, with a particular focus on those undergoing diagnosis or treatment via catheter-based endovascular procedures. The documentation of these experiences offers a careful perspective on the procedural nuances, challenges, and considerations involved in patient care within this specialized medical domain, thus providing a real-world context to the theoretical and technical discussions preceding it.

The literature review forms a substantial portion of this dissertation, mainly as it draws inspiration from one of the main contributions to the field – a survey paper that carefully reviews and categorizes all existing catheter tracking concepts and methodologies [154]. Over 150 papers focused on catheter-tracking technologies were exhaustively analyzed, with selections for inclusion in this dissertation being made based on their direct relevance to tracking technology. This careful curation process has enabled a focused discussion on the reviewed tracking technologies, assessing their classification, precision, and user-friendliness. This comprehensive review highlighted the field's diversity and innovation and critically evaluated the methodologies' practical implications in clinical settings.

In the methodology and discussion part of this dissertation, considerable time and careful attention were dedicated to examining the state-of-the-art to identify research gaps and potential areas for contribution. This segment delves deeply into the contributions made, beginning with an overview of catheter tracking concepts and methodologies as previously described, encompassing a broad spectrum of tracking technologies. A detailed tracking pipeline is presented, covering the majority of contemporary catheter-based endovascular procedures and providing a framework for understanding the current landscape. Through an in-depth analysis of this pipeline, several potential paths for contributing to the advancement of the field have been described. These paths, which represent significant opportunities to enhance the state-of-the-art in catheter tracking, are explored in subsequent sections, highlighting the directions pursued during this doctoral journey.

The first paper introduced a novel hybrid approach that combined bioelectric navigation with electromagnetic tracking to facilitate feature-based registration. The second paper introduces, for the first time, the use of dynamic time warping algorithms in aligning 3D tracking signals for registration purposes. This approach marks a significant advancement in utilizing time series analysis techniques for improving registration accuracy and reliability of catheter tracking in 3D space. Together, these contributions address current challenges in catheter-based endovascular procedures and establish a foundation for ongoing research, pointing towards further exploration and development in achieving more accurate and seamless registration.

10.2 Clinical Translation and Outlook

From a clinical perspective, in addition to the technical difficulties associated with the tracking technologies under discussion, numerous challenges impede the integration of current research solutions into routine clinical practice. While most research works are centered on showcasing the technological advancements and the technical merits of their tracking solutions, there remains to be more discussion regarding the limitations and practical challenges of translating these innovations into the clinical environment. This gap highlights the need for a more holistic approach to developing catheter-based tracking solutions that emphasize technical superiority and critically address the feasibility, adaptability, and practical implications of deploying such solutions in a real-world healthcare setting.

The ease of integration is a crucial factor for the successful adoption of scientific solutions within clinical practice. From a research standpoint, it is critical that the development of these solutions proactively considers their usability and adaptability in clinical environments from the beginning. This entails examining existing clinical workflows carefully and pinpointing the modifications necessary for seamlessly integrating new solutions. We believe that minimizing disruptions to clinical workflows and ensuring user-friendliness in the design of tracking solutions are critical to their successful integration. While specific innovative solutions may necessitate significant changes to existing procedures, their advantages should decisively outweigh the challenges their integration poses. This includes the need for comprehensive training programs for physicians. For example, robotic technologies can enhance procedural precision beyond human capabilities but demand carefully curated training to facilitate their acceptance and integration into clinical routines. Thus, alongside technological advancements, there is a pressing need to develop sophisticated simulation and training frameworks to support the transition of these innovations into clinical practice.

Another critical factor influencing advancements in research, particularly the integration of solutions into clinical routines, is the presence of significant bureaucratic barriers associated with clinical trials. These hurdles, especially pronounced in the field of catheter-based solutions, necessitate a considerable commitment regarding documentation and time investment. Often, the duration required to navigate these bureaucratic processes exceeds the term of a doctoral candidate's studies. From our perspective, one pathway to facilitate the transition of more solutions into clinical practice involves closing the gap between physicians and researchers. Enhancing close collaborations and fostering the careful integration of solutions through streamlined clinical trials, careful evaluations, and targeted training programs can significantly alleviate the challenges posed by these bureaucratic obstacles. By facilitating a more collaborative and integrated approach, introducing innovative solutions into clinical settings can become more efficient and effective, ultimately benefiting patient care.

One of the significant challenges in catheter tracking is compensating for the movement of the target anatomy, a task compounded by the fact that catheters provide positional data in 3D, necessitating more intelligent solutions to verify their location within the vascular tree. This complexity is amplified when attempting to pinpoint the catheter's exact 3D location using preoperative Computed Tomography Angiography (CTA), adding another layer of difficulty to the clinical application of these tracking solutions. This challenge is particularly relevant for tracking technologies requiring additional equipment and calibration or registration procedures, such as electromagnetic tracking and shape sensing.

On the other hand, technologies like bioelectric navigation, which aim to localize the catheter within the vascular tree, demand the development and regulatory approval of new instruments, further delaying their adoption in clinical settings. Therefore, it is essential for the research community to carefully understand and model the clinical workflow, establishing short-term, mid-term, and long-term strategies for the incorporation of various tracking technologies into clinical practice. Additionally, there is an urgent need to educate the next generation of physicians in these advanced technologies to enhance the efficacy of routine procedures, ensuring they are equipped to leverage these innovations to improve patient outcomes effectively.

A significant benefit of the advanced technologies explored in this dissertation is their ability to reduce the variability in surgical outcomes traditionally influenced by the surgeon's experience and skill. Furthermore, these technologies present the opportunity to gather and analyze procedural data, thereby enriching the collective knowledge and expertise of physicians. The methodologies presented facilitate the seamless fusion of preoperative imaging data from sources such as CTA or Magnetic Resonance Angiography (MRA) with real-time intraoperative imaging. This harmonization is needed to move the development of intelligent surgical systems that could, in the near future, autonomously plan and execute patient-specific endovascular procedures. Such advancements signify a critical step forward in the evolution of personalized medicine, offering a tailored approach to surgical care that optimizes outcomes for individual patients.

10.3 Epilogue

Minimally invasive catheter-based endovascular procedures represent a crucial advancement in medical procedures, allowing physicians to access targeted anatomies efficiently while minimizing patient trauma. These procedures facilitate crucial in-situ measurements, localized treatments, and the deployment of sophisticated therapeutic instruments directly to the affected areas. The beginnings of robotic catheterization and the integration of machine learning are set to further revolutionize this field by enabling computer-assisted systems to interpret more complex semantic information, paving the path for semi-automatic to fully automatic manipulation of catheters. The incorporation of automated tracking solutions will be instrumental in achieving these advancements.

We believe that catheter-tracking technologies are expected to continue to evolve rapidly, building upon the significant progress made to date but accelerating in pace. Future systems are expected to combine the advantages of existing tracking technologies while being adapted to specific anatomies and the requirements of individual clinical procedures. We hope this dissertation will serve as a comprehensive resource for researchers, aiding them in familiarizing themselves with the state-of-the-art of this field and facilitating the integration of these technologies into their computer-assisted endovascular procedure systems. This dissertation aims not only to pave the course of current research but also to inspire future innovations in the field of minimally invasive catheter-based endovascular procedures.

Part V

Appendix

Publications

A

List of Publications

1. **Ardit Ramadani**†,∗, M. Bui∗, T. Wendler, H. Schunkert, P. Ewert, and N. Navab, "A Survey of Catheter Tracking Concepts and Methodologies," *Medical Image Analysis*, vol. 82, p. 102584, Nov. 2022, doi: 10.1016/j.media.2022.102584. (Impact Factor: 13.82).

2. **Ardit Ramadani**†,∗, H. Maier∗, F. Bourier, C. Meierhofer, P. Ewert, H. Schunkert, and N. Navab, "Feature-Based Electromagnetic Tracking Registration Using Bioelectric Sensing," *IEEE Robotics and Automation Letters*, vol. 8, no. 6, pp. 3286–3293, Jun. 2023, doi: 10.1109/LRA.2023.3262988. (Impact Factor: 5.2).

3. **Ardit Ramadani**†, P. Ewert, H. Schunkert, and N. Navab, "WarpEM: Dynamic Time Warping for Accurate Catheter Registration in EM-guided Procedures," in *Medical Image Computing and Computer Assisted Intervention – MICCAI 2023*, vol. 14226, pp. 802–811, Oct. 2023, doi: 10.1007/978-3-031-43990-2_75.

† – Corresponding Author
∗ – Equal Contribution

Bibliography

[1] M. Abayazid, M. Kemp, and S. Misra. “3D flexible needle steering in soft-tissue phantoms using Fiber Bragg Grating sensors”. In: *2013 IEEE International Conference on Robotics and Automation*. Karlsruhe, Germany: IEEE, May 2013, pp. 5843–5849. DOI: 10.1109/ICRA.2013.6631418 (cit. on pp. 70, 72).

[2] M. E. M. K. Abdelaziz, D. Kundrat, M. Pupillo, G. Dagnino, T. M. Y. Kwok, W. Chi, V. Groenhuis, F. J. Siepel, C. Riga, S. Stramigioli, and G. Yang. “Toward a Versatile Robotic Platform for Fluoroscopy and MRI-Guided Endovascular Interventions: A Pre-Clinical Study”. In: *2019 IEEE/RSJ International Conference on Intelligent Robots and Systems*. Nov. 2019, pp. 5411–5418. DOI: 10.1109/IROS40897.2019.8968237 (cit. on pp. 73, 74, 76).

[3] M. E. M. K. Abdelaziz, L. Tian, M. Hamady, G.-Z. Yang, and B. Temelkuran. “X-ray to MR: the progress of flexible instruments for endovascular navigation”. In: *Progress in Biomedical Engineering* 3.3 (July 2021), p. 032004. DOI: 10.1088/2516-1091/ac12d6 (cit. on pp. 4, 11, 64).

[4] N. Abi-Jaoudeh, J. Kruecker, S. Kadoury, H. Kobeiter, A. M. Venkatesan, E. Levy, and B. J. Wood. “Multimodality Image Fusion–Guided Procedures: Technique, Accuracy, and Applications”. In: *CardioVascular and Interventional Radiology* 35.5 (Oct. 2012), pp. 986–998. DOI: 10.1007/s00270-012-0446-5 (cit. on pp. 3, 108, 122).

[5] A. Agrawal, D. K. Hogarth, and S. Murgu. “Robotic bronchoscopy for pulmonary lesions: a review of existing technologies and clinical data”. In: *Journal of Thoracic Disease* 12.6 (June 2020), pp. 3279–3286. DOI: 10.21037/jtd.2020.03.35 (cit. on p. 77).

[6] O. Al-Ahmad, M. Ourak, J. V. Roosbroeck, J. Vlekken, and E. V. Poorten. “Improved FBG-Based Shape Sensing Methods for Vascular Catheterization Treatment”. In: *2020 IEEE Robotics and Automation Letters* 5.3 (July 2020), pp. 4687–4694. DOI: 10.1109/LRA.2020.3003291 (cit. on pp. 69, 70, 72).

[7] A. Aktas, A. A. Demircali, R. Secoli, B. Temelkuran, and F. Rodriguez y Baena. “Towards a Procedure-Optimised Steerable Catheter for Deep-Seated Neurosurgery”. In: *Biomedicines* 11.7 (July 2023), p. 2008. DOI: 10.3390/biomedicines11072008 (cit. on p. 98).

[8] M. Amanzadeh, S. M. Aminossadati, M. S. Kizil, and A. D. Rakić. “Recent developments in fibre optic shape sensing”. In: *Measurement* 128 (Nov. 2018), pp. 119–137. DOI: 10.1016/j.measurement.2018.06.034 (cit. on pp. 68–70).

[9] P. Ambrosini, D. Ruijters, W. J. Niessen, A. Moelker, and T. van Walsum. “Continuous roadmapping in liver TACE procedures using 2D—3D catheter-based registration”. In: *International Journal of Computer Assisted Radiology and Surgery* 10.9 (Sept. 2015), pp. 1357–1370. DOI: 10.1007/s11548-015-1218-x (cit. on pp. 55, 57).

[10] P. Ambrosini, D. Ruijters, W. J. Niessen, A. Moelker, and T. van Walsum. “Fully Automatic and Real-Time Catheter Segmentation in X-Ray Fluoroscopy”. In: *Medical Image Computing and Computer-Assisted Intervention 2017*. 2017, pp. 577–585. DOI: 10.1007/978-3-319-66185-8_65 (cit. on pp. 54, 57).

[11] P. Ambrosini, I. Smal, D. Ruijters, W. J. Niessen, A. Moelker, and T. van Walsum. "3D Catheter Tip Tracking in 2D X-Ray Image Sequences Using a Hidden Markov Model and 3D Rotational Angiography". In: *Augmented Environments for Computer-Assisted Interventions 2015*. 2015, pp. 38–49. DOI: 10.1007/978-3-319-24601-7_5 (cit. on pp. 55, 57).

[12] M. Analoui, J. D. Bronzino, and D. R. Peterson, eds. *Medical Imaging: Principles and Practices*. 1st edition. New York, United States of America: Taylor & Francis/CRC Press, 2013 (cit. on pp. 23–27).

[13] F. Attivissimo, A. M. L. Lanzolla, S. Carlone, P. Larizza, and G. Brunetti. "A novel electromagnetic tracking system for surgery navigation". In: *Computer Assisted Surgery* 23.1 (Jan. 2018), pp. 42–52. DOI: 10.1080/24699322.2018.1529199 (cit. on p. 65).

[14] X. Bao, S. Guo, N. Xiao, Y. Zhao, C. Zhang, C. Yang, and R. Shen. "Toward cooperation of catheter and guidewire for remote-controlled vascular interventional robot". In: *2017 IEEE International Conference on Mechatronics and Automation (ICMA)*. Aug. 2017, pp. 422–426. DOI: 10.1109/ICMA.2017.8015854 (cit. on pp. 73, 76).

[15] J. Bastian. "Vision and electroreception: Integration of sensory information in the optic tectum of the weakly electric fish *Apteronotus albifrons*". In: *Journal of comparative physiology* 147.3 (Sept. 1982), pp. 287–297. DOI: 10.1007/BF00609662 (cit. on p. 72).

[16] C. Baur, S. Albarqouni, S. Demirci, N. Navab, and P. Fallavollita. "CathNets: Detection and Single-View Depth Prediction of Catheter Electrodes". In: *Medical Imaging and Augmented Reality 2016*. 2016, pp. 38–49. DOI: 10.1007/978-3-319-43775-0_4 (cit. on pp. 53, 57).

[17] C. Baur, F. Milletari, V. Belagiannis, N. Navab, and P. Fallavollita. "Automatic 3D reconstruction of electrophysiology catheters from two-view monoplane C-arm image sequences". In: *International Journal of Computer Assisted Radiology and Surgery* 11.7 (July 2016), pp. 1319–1328. DOI: 10.1007/s11548-015-1325-8 (cit. on pp. 53, 56, 57).

[18] H. J. Bender, R. Männer, C. Poliwoda, S. Roth, and M. Walz. "Reconstruction of 3D Catheter Paths from 2D X-ray Projections". In: *Medical Image Computing and Computer-Assisted Intervention 1999*. 1999, pp. 981–989. DOI: 10.1007/10704282_107 (cit. on p. 55).

[19] J. M. Benyus. *Biomimicry: innovation inspired by nature*. Nachdr. New York, United States of America: Perennial, 2009 (cit. on p. 83).

[20] L. Biga, S. Bronson, S. Dawson, A. Harwell, R. Hopkins, J. Kaufmann, M. LeMaster, P. Matern, K. Morrison-Graham, K. Oja, D. Quick, and J. Runyeon. *Anatomy & Physiology*. Oregon, United States of America: Oregon State University, Sept. 2019 (cit. on pp. 33, 35, 36, 39, 101).

[21] M. Borot de Battisti, B. Denis de Senneville, M. Maenhout, J. J. W. Lagendijk, M. van Vulpen, G. Hautvast, D. Binnekamp, and M. A. Moerland. "Fiber Bragg gratings-based sensing for real-time needle tracking during MR-guided brachytherapy". In: *Medical Physics* 43.10 (Sept. 2016), pp. 5288–5297. DOI: 10.1118/1.4961743 (cit. on pp. 70, 72).

[22] F. Bourier, R. Fahrig, P. Wang, P. Santangeli, K. Kurzidim, N. Strobel, T. Moore, C. Hinkel, and A. Al-Ahmad. "Accuracy assessment of catheter guidance technology in electrophysiology procedures: a comparison of a new 3D-based fluoroscopy navigation system to current electroanatomic mapping systems". In: *Journal of Cardiovascular Electrophysiology* 25.1 (Jan. 2014), pp. 74–83. DOI: 10.1111/jce.12264 (cit. on p. 110).

[23] W. G. Bradley. "History of Medical Imaging". In: *Proceedings of the American Philosophical Society* 152.3 (2008). URL: https://www.jstor.org/stable/40541591, pp. 349–361 (cit. on p. 48).

[24] P. N. Brett, X. Du, M. Z. Assadi, F. Rodriguez y Baena, F. Liu, R. Hinchliffe, and M. Thompson. "Design and Experimental Demonstration of a Mechatronic Solution for Endovascular Catheters". In: *Mechatronics and Machine Vision in Practice 3*. 2018, pp. 247–252. DOI: 10.1007/978-3-319-76947-9_18 (cit. on pp. 74, 76).

[25] B. Breyer and I. Cikeš. "Ultrasonically marked catheter—a method for positive echographic catheter position identification". In: *Medical and Biological Engineering and Computing* 22.3 (May 1984), pp. 268–271. DOI: 10.1007/BF02442755 (cit. on pp. 49, 60, 61, 63).

[26] A. Brost, R. Liao, J. Hornegger, and N. Strobel. "3-D Respiratory Motion Compensation during EP Procedures by Image-Based 3-D Lasso Catheter Model Generation and Tracking". In: *Medical Image Computing and Computer-Assisted Intervention 2009*. 2009, pp. 394–401. DOI: 10.1007/978-3-642-04268-3_49 (cit. on p. 55).

[27] A. Brost, A. Wimmer, R. Liao, J. Hornegger, and N. Strobel. "Catheter Tracking: Filter-Based vs. Learning-Based". In: *Pattern Recognition 2010*. 2010, pp. 293–302. DOI: 10.1007/978-3-642-15986-2_30 (cit. on pp. 55, 57).

[28] M. Bui, F. Bourier, C. Baur, F. Milletari, N. Navab, and S. Demirci. "Robust navigation support in lowest dose image setting". In: *International Journal of Computer Assisted Radiology and Surgery* 14.2 (Feb. 2019), pp. 291–300. DOI: 10.1007/s11548-018-1874-8 (cit. on p. 53).

[29] H. Busse, R. Trampel, W. Gründer, M. Moche, and T. Kahn. "Method for automatic localization of MR-visible markers using morphological image processing and conventional pulse sequences: Feasibility for image-guided procedures". In: *Journal of Magnetic Resonance Imaging* 26.4 (2007), pp. 1087–1096. DOI: https://doi.org/10.1002/jmri.21129 (cit. on p. 63).

[30] A. E. Campbell-Washburn, M. A. Tavallaei, M. Pop, E. K. Grant, H. Chubb, K. Rhode, and G. A. Wright. "Real-time MRI guidance of cardiac interventions". In: *Journal of Magnetic Resonance Imaging* 46.4 (2017), pp. 935–950. DOI: https://doi.org/10.1002/jmri.25749 (cit. on p. 59).

[31] F. Carpi and C. Pappone. "Stereotaxis Niobe magnetic navigation system for endocardial catheter ablation and gastrointestinal capsule endoscopy". In: *Expert Review of Medical Devices* 6.5 (Sept. 2009), pp. 487–498. DOI: 10.1586/erd.09.32 (cit. on pp. 68, 69).

[32] P. Chang, A. Rolls, H. D. Praetere, E. V. Poorten, C. V. Riga, C. D. Bicknell, and D. Stoyanov. "Robust Catheter and Guidewire Tracking Using B-Spline Tube Model and Pixel-Wise Posteriors". In: *2016 IEEE Robotics and Automation Letters* 1.1 (Jan. 2016), pp. 303–308. DOI: 10.1109/LRA.2016.2517821 (cit. on pp. 53, 57).

[33] C. Chautems, A. Tonazzini, D. Floreano, and B. J. Nelson. "A variable stiffness catheter controlled with an external magnetic field". In: *2017 IEEE/RSJ International Conference on Intelligent Robots and Systems*. Sept. 2017, pp. 181–186. DOI: 10.1109/IROS.2017.8202155 (cit. on p. 69).

[34] C. Chen, C. Qin, H. Qiu, G. Tarroni, J. Duan, W. Bai, and D. Rueckert. "Deep Learning for Cardiac Image Segmentation: A Review". In: *Frontiers in Cardiovascular Medicine* 7 (2020). DOI: 10.3389/fcvm.2020.00025 (cit. on pp. 54, 79).

[35] F. Chen, J. Liu, and H. Liao. "3D Catheter Shape Determination for Endovascular Navigation Using a Two-Step Particle Filter and Ultrasound Scanning". In: *2017 IEEE Transactions on Medical Imaging* 36.3 (Mar. 2017), pp. 685–695. DOI: 10.1109/TMI.2016.2635673 (cit. on pp. 57–59).

[36] F. Chen, J. Liu, X. Zhang, D. Zhang, and H. Liao. "Improved 3D Catheter Shape Estimation Using Ultrasound Imaging for Endovascular Navigation: A Further Study". In: *IEEE Journal of Biomedical and Health Informatics* 24.12 (Dec. 2020), pp. 3616–3629. DOI: 10.1109/JBHI.2020.3026105 (cit. on pp. 57, 59).

[37] A. Cheng, Y. Kim, Y. Itsarachaiyot, H. K. Zhang, C. R. Weiss, R. H. Taylor, and E. M. Boctor. "Photoacoustic-based catheter tracking: simulation, phantom, and in vivo studies". In: *Journal of Medical Imaging* 5.2 (Mar. 2018), p. 021223. DOI: 10.1117/1.JMI.5.2.021223 (cit. on pp. 61, 63).

[38] S. Çimen, A. Gooya, M. Grass, and A. F. Frangi. "Reconstruction of coronary arteries from X-ray angiography: A review". In: *Medical Image Analysis* 32 (2016), pp. 46–68. DOI: 10.1016/j.media.2016.02.007 (cit. on p. 56).

[39] W. Clements, M. Scicchitano, J. Koukounaras, T. Joseph, and G. Goh. “Use of the Magellan Robotic System for Conventional Transarterial Chemoembolization (cTACE): A 6-Patient Case Series Showing Safety and Technical Success”. In: *Journal of Clinical Interventional Radiology (ISVIR)* 3.2 (July 2019), pp. 142–146. DOI: 10.1055/s-0039-1694093 (cit. on pp. 75, 76).

[40] S. Condino, V. Ferrari, C. Freschi, A. Alberti, R. Berchiolli, F. Mosca, and M. Ferrari. “Electromagnetic navigation platform for endovascular surgery: how to develop sensorized catheters and guidewires: Electromagnetic navigation platform for endovascular surgery”. In: *The International Journal of Medical Robotics and Computer Assisted Surgery* 8.3 (Sept. 2012), pp. 300–310. DOI: 10.1002/rcs.1417 (cit. on pp. 64, 69).

[41] A. Crummy, C. Strother, J. Sackett, D. Ergun, C. Shaw, R. Kruger, C. Mistretta, W. Turnipseed, R. Lieberman, P. Myerowitz, and F. Ruzicka. “Computerized fluoroscopy: digital subtraction for intravenous angiocardiography and arteriography”. In: *American Journal of Roentgenology* 135.6 (Dec. 1980), pp. 1131–1140. DOI: 10.2214/ajr.135.6.1131 (cit. on p. 49).

[42] G. Dagnino, J. Liu, M. E. M. K. Abdelaziz, W. Chi, C. Riga, and G. Yang. “Haptic Feedback and Dynamic Active Constraints for Robot-Assisted Endovascular Catheterization”. In: *2018 IEEE/RSJ International Conference on Intelligent Robots and Systems*. Oct. 2018, pp. 1770–1775. DOI: 10.1109/IROS.2018.8593628 (cit. on pp. 74, 76).

[43] A. Denasi, F. Khan, K. J. Boskma, M. Kaya, C. Hennersperger, R. Göbl, M. Tirindelli, N. Navab, and S. Misra. “An Observer-Based Fusion Method Using Multicore Optical Shape Sensors and Ultrasound Images for Magnetically-Actuated Catheters”. In: *2018 IEEE International Conference on Robotics and Automation*. Brisbane: IEEE, May 2018, pp. 50–57. DOI: 10.1109/ICRA.2018.8462695 (cit. on pp. 76, 78, 80).

[44] T. Doby. “Cerebral Angiography and Egas Moniz”. In: *American Journal of Roentgenology* 159.2 (Aug. 1992), p. 364. DOI: 10.2214/ajr.159.2.1632357 (cit. on p. 48).

[45] J. Dong, H. Calkins, S. B. Solomon, S. Lai, D. Dalal, A. Lardo, E. Brem, A. Preiss, R. D. Berger, H. Halperin, and T. Dickfeld. “Integrated Electroanatomic Mapping With Three-Dimensional Computed Tomographic Images for Real-Time Guided Ablations”. In: *Circulation* 113.2 (Jan. 2006), pp. 186–194. DOI: 10.1161/circulationaha.105.565200 (cit. on p. 109).

[46] J. Edelmann, A. J. Petruska, and B. J. Nelson. “Magnetic control of continuum devices”. In: *The International Journal of Robotics Research* 36.1 (Jan. 2017), pp. 68–85. DOI: 10.1177/0278364916683443 (cit. on pp. 67, 69).

[47] A. Efrat, Q. Fan, and S. Venkatasubramanian. “Curve Matching, Time Warping, and Light Fields: New Algorithms for Computing Similarity between Curves”. In: *Journal of Mathematical Imaging and Vision* 27.3 (Apr. 2007), pp. 203–216. DOI: 10.1007/s10851-006-0647-0 (cit. on p. 123).

[48] S. Elayaperumal, J. C. Plata, A. B. Holbrook, Y.-L. Park, K. B. Pauly, B. L. Daniel, and M. R. Cutkosky. “Autonomous Real-Time Interventional Scan Plane Control With a 3-D Shape-Sensing Needle”. In: *2014 IEEE Transactions on Medical Imaging* 33.11 (Nov. 2014), pp. 2128–2139. DOI: 10.1109/TMI.2014.2332354 (cit. on pp. 70, 72).

[49] A. Eldirdiri, F. Courivaud, R. Palomar, P. K. Hol, and O. J. Elle. “Catheter tip tracking for MR-guided interventions using discrete Kalman filter and mean shift localization”. In: *International Journal of Computer Assisted Radiology and Surgery* 9.2 (Mar. 2014), pp. 313–322. DOI: 10.1007/s11548-013-0933-4 (cit. on p. 59).

[50] E. Eulig, J. Maier, M. Knaup, N. R. Bennett, K. Hörndler, A. S. Wang, and M. Kachelrieß. “Deep learning-based reconstruction of interventional tools and devices from four X-ray projections for tomographic interventional guidance”. In: *Medical Physics* 48.10 (Oct. 2021), pp. 5837–5850. DOI: 10.1002/mp.15160 (cit. on p. 56).

[51] A. Favaro, L. Cerri, S. Galvan, F. R. Y. Baena, and E. D. Momi. "Automatic Optimized 3D Path Planner for Steerable Catheters with Heuristic Search and Uncertainty Tolerance". In: *2018 IEEE International Conference on Robotics and Automation*. May 2018, pp. 9–16. DOI: 10.1109/ICRA.2018.8461262 (cit. on pp. 74, 76).

[52] E. J. Finnesgard, J. P. Simons, H. Marecki, I. Ofori, T. Kölbel, G. W. H. Schurink, J. A. van Herwaarden, and A. Schanzer. "Fiber Optic RealShape technology in endovascular surgery". In: *Seminars in Vascular Surgery* 34.4 (Dec. 2021), pp. 241–246. DOI: 10.1053/j.semvascsurg.2021.10.001 (cit. on p. 72).

[53] W. Forssmann. "Die Sondierung des Rechten Herzens". In: *Klinische Wochenschrift* 8.45 (Nov. 1929), pp. 2085–2087. DOI: 10.1007/BF01875120 (cit. on pp. 48, 49).

[54] A. M. Franz, T. Haidegger, W. Birkfellner, K. Cleary, T. M. Peters, and L. Maier-Hein. "Electromagnetic Tracking in Medicine – A Review of Technology, Validation, and Applications". In: *2014 IEEE Transactions on Medical Imaging* 33.8 (Aug. 2014), pp. 1702–1725. DOI: 10.1109/TMI.2014.2321777 (cit. on pp. 3, 4, 19, 64, 108, 122).

[55] B. Fuerst, E. E. Sutton, R. Ghotbi, N. J. Cowan, and N. Navab. "Bioelectric Navigation: A New Paradigm for Intravascular Device Guidance". In: *Medical Image Computing and Computer-Assisted Intervention 2016*. 2016, pp. 474–481. DOI: 10.1007/978-3-319-46720-7_55 (cit. on pp. 72, 109).

[56] G. Gao, G. Penney, N. Gogin, P. Cathier, A. Arujuna, M. Wright, D. Caulfield, A. Rinaldi, R. Razavi, and K. Rhode. "Rapid Image Registration of Three-Dimensional Transesophageal Echocardiography and X-ray Fluoroscopy for the Guidance of Cardiac Interventions". In: *2010 Information Processing in Computer-Assisted Interventions*. 2010, pp. 124–134. DOI: 10.1007/978-3-642-13711-2_12 (cit. on p. 58).

[57] I. Gergel, J. Hering, R. Tetzlaff, H.-P. Meinzer, and I. Wegner. "An electromagnetic navigation system for transbronchial interventions with a novel approach to respiratory motion compensation". In: *Medical Physics* 38.12 (Nov. 2011), pp. 6742–6753. DOI: 10.1118/1.3662871 (cit. on pp. 65, 69).

[58] V. Gilard, N. Magne, E. Gerardin, S. Curey, V. Pelletier, P. Hannequin, and S. Derrey. "Comparison of electromagnetic neuronavigation system and free-hand method for ventricular catheter placement in internal shunt". In: *Clinical Neurology and Neurosurgery* 158 (July 2017), pp. 93–97. DOI: 10.1016/j.clineuro.2017.05.007 (cit. on pp. 67, 69).

[59] T. R. Gildea, P. J. Mazzone, D. Karnak, M. Meziane, and A. C. Mehta. "Electromagnetic Navigation Diagnostic Bronchoscopy: A Prospective Study". In: *American Journal of Respiratory and Critical Care Medicine* 174.9 (Nov. 2006), pp. 982–989. DOI: 10.1164/rccm.200603-344OC (cit. on pp. 66, 69).

[60] R. Göbl, N. Navab, and C. Hennersperger. "SUPRA: open-source software-defined ultrasound processing for real-time applications: A 2D and 3D pipeline from beamforming to B-mode". In: *International Journal of Computer Assisted Radiology and Surgery* 13.6 (June 2018), pp. 759–767. DOI: 10.1007/s11548-018-1750-6 (cit. on p. 99).

[61] M. S. Grady, M. A. Howard, R. G. Dacey, W. Blume, M. Lawson, P. Werp, and R. C. Ritter. "Experimental study of the magnetic stereotaxis system for catheter manipulation within the brain". In: *Journal of Neurosurgery* 93.2 (Aug. 2000), pp. 282–288. DOI: 10.3171/jns.2000.93.2.0282 (cit. on p. 69).

[62] X. Guo, H. J. Kang, R. Etienne-Cummings, and E. M. Boctor. "Active ultrasound pattern injection system (AUSPIS) for interventional tool guidance". In: *PLoS ONE* 9.10 (2014). DOI: 10.1371/journal.pone.0104262 (cit. on pp. 60, 63).

[63] X. T. Ha, M. Ourak, O. Al-Ahmad, D. Wu, G. Borghesan, A. Menciassi, and E. Vander Poorten. "Robust Catheter Tracking by Fusing Electromagnetic Tracking, Fiber Bragg Grating and Sparse Fluoroscopic Images". In: *IEEE Sensors Journal* 21.20 (Oct. 2021), pp. 23422–23434. DOI: 10.1109/JSEN.2021.3107036 (cit. on pp. 76, 78).

[64] J. B. Harley and D. Woodward, eds. *Cartography in Prehistoric, Ancient, and Medieval Europe and the Mediterranean*. Vol. 1. The History of Cartography. Chicago, United States of America: The University of Chicago Press, 2020 (cit. on p. 84).

[65] H. Hautmann, A. Schneider, T. Pinkau, F. Peltz, and H. Feussner. "Electromagnetic Catheter Navigation During Bronchoscopy: Validation of a Novel Method by Conventional Fluoroscopy". In: *Chest* 128.1 (July 2005), pp. 382–387. DOI: 10.1378/chest.128.1.382 (cit. on pp. 65, 69).

[66] H. Heibel, B. Glocker, M. Groher, M. Pfister, and N. Navab. "Interventional Tool Tracking Using Discrete Optimization". In: *2013 IEEE Transactions on Medical Imaging* 32.3 (Mar. 2013), pp. 544–555. DOI: 10.1109/TMI.2012.2228879 (cit. on pp. 53, 57).

[67] W. R. Hendee. "Cross sectional medical imaging: a history." In: *RadioGraphics* 9.6 (Nov. 1989), pp. 1155–1180. DOI: 10.1148/radiographics.9.6.2685939 (cit. on pp. 23, 48, 49).

[68] K. Henken, D. Van Gerwen, J. Dankelman, and J. Van Den Dobbelsteen. "Accuracy of needle position measurements using fiber Bragg gratings". In: *Minimally Invasive Therapy & Allied Technologies* 21.6 (Nov. 2012), pp. 408–414. DOI: 10.3109/13645706.2012.666251 (cit. on pp. 70, 72).

[69] E. J. Hermann, H.-H. Capelle, C. A. Tschan, and J. K. Krauss. "Electromagnetic-guided neuronavigation for safe placement of intraventricular catheters in pediatric neurosurgery: Clinical article". In: *Journal of Neurosurgery: Pediatrics* 10.4 (Oct. 2012), pp. 327–333. DOI: 10.3171/2012.7.PEDS11369 (cit. on pp. 67, 69).

[70] H. W. Herr. "'Crushing the stone': a brief history of lithotripsy, the first minimally invasive surgery". In: *British Journal of Urology International – BJUI* 102.4 (2008), pp. 432–435. DOI: 10.1111/j.1464-410X.2008.07639.x (cit. on p. 47).

[71] D. L. G. Hill, P. G. Batchelor, M. Holden, and D. J. Hawkes. "Medical image registration". In: *Physics in Medicine and Biology* 46.3 (Feb. 2001), R1–R45. DOI: 10.1088/0031-9155/46/3/201 (cit. on pp. 18, 98).

[72] C. M. Hillenbrand, D. R. Elgort, E. Y. Wong, A. Reykowski, F. K. Wacker, J. S. Lewin, and J. L. Duerk. "Active device tracking and high-resolution intravascular MRI using a novel catheter-based, opposed-solenoid phased array coil". In: *Magnetic Resonance in Medicine* 51.4 (2004), pp. 668–675. DOI: 10.1002/mrm.20050 (cit. on p. 63).

[73] M. Hoffmann, A. Brost, C. Jakob, F. Bourier, M. Koch, K. Kurzidim, J. Hornegger, and N. Strobel. "Semi-automatic Catheter Reconstruction from Two Views". In: *Medical Image Computing and Computer-Assisted Intervention 2012*. 2012, pp. 584–591. DOI: 10.1007/978-3-642-33418-4_72 (cit. on pp. 56, 57).

[74] X. Hu, A. Chen, Y. Luo, C. Zhang, and E. Zhang. "Steerable catheters for minimally invasive surgery: a review and future directions". In: *Computer Assisted Surgery* 23.1 (Jan. 2018), pp. 21–41. DOI: 10.1080/24699322.2018.1526972 (cit. on pp. 4, 73).

[75] S. J. Hutchison and K. C. Holmes. *Principles of Vascular and Intravascular Ultrasound*. Principles of Cardiovascular Imaging. Pennsylvania, United States of America: Elsevier/Saunders, 2012 (cit. on pp. 17, 24).

[76] S. Jäckle, T. Eixmann, F. Matysiak, M. M. Sieren, M. Horn, H. Schulz-Hildebrandt, G. Hüttmann, and T. Pätz. "3D Stent Graft Guidance based on Tracking Systems for Endovascular Aneurysm Repair". In: *Current Directions in Biomedical Engineering* 7.1 (Aug. 2021), pp. 17–20. DOI: 10.1515/cdbme-2021-1004 (cit. on p. 108).

[77] S. Jäckle, T. Eixmann, H. Schulz-Hildebrandt, G. Hüttmann, and T. Pätz. “Fiber optical shape sensing of flexible instruments for endovascular navigation”. In: *International Journal of Computer Assisted Radiology and Surgery* 14.12 (Dec. 2019), pp. 2137–2145. DOI: 10.1007/s11548-019-02059-0 (cit. on pp. 71, 72).

[78] S. Jäckle, V. García-Vázquez, T. Eixmann, F. Matysiak, F. von Haxthausen, M. M. Sieren, H. Schulz-Hildebrandt, G. Hüttmann, F. Ernst, M. Kleemann, and T. Pätz. “Three-dimensional guidance including shape sensing of a stentgraft system for endovascular aneurysm repair”. In: *International Journal of Computer Assisted Radiology and Surgery* 15.6 (June 2020), pp. 1033–1042. DOI: 10.1007/s11548-020-02167-2 (cit. on pp. 77, 78, 80).

[79] S. Jäckle, V. García-Vázquez, F. von Haxthausen, T. Eixmann, M. M. Sieren, H. Schulz-Hildebrandt, G. Hüttmann, F. Ernst, M. Kleemann, and T. Pätz. “3D catheter guidance including shape sensing for endovascular navigation”. In: *Medical Imaging 2020: Image-Guided Procedures, Robotic Interventions, and Modeling*. Vol. 11315. Mar. 2020, p. 1131504. DOI: 10.1117/12.2548094 (cit. on pp. 77, 78).

[80] H. A. Jaeger, P. Nardelli, C. O’shea, J. Tugwell, K. A. Khan, T. Power, M. O’shea, M. P. Kennedy, and P. Cantillon-Murphy. “Automated Catheter Navigation With Electromagnetic Image Guidance”. In: *2017 IEEE Transactions on Biomedical Engineering* 64.8 (Aug. 2017), pp. 1972–1979. DOI: 10.1109/TBME.2016.2623383 (cit. on pp. 65, 69).

[81] H. A. Jaeger and P. Cantillon-Murphy. “Electromagnetic Tracking Using Modular, Tiled Field Generators”. In: *IEEE Transactions on Instrumentation and Measurement* 68.12 (Dec. 2019), pp. 4845–4852. DOI: 10.1109/TIM.2019.2900884 (cit. on p. 65).

[82] H. A. Jaeger, F. Trauzettel, P. Nardelli, F. Daverieux, E. F. Hofstad, H. O. Leira, M. P. Kennedy, T. Langø, and P. Cantillon-Murphy. “Peripheral tumour targeting using open-source virtual bronchoscopy with electromagnetic tracking: a multi-user pre-clinical study”. In: *Minimally Invasive Therapy & Allied Technologies* 28.6 (Nov. 2019), pp. 363–372. DOI: 10.1080/13645706.2018.1544911 (cit. on p. 69).

[83] C. Ji, Z.-G. Hou, and X.-L. Xie. “An image-based guidewire navigation method for robot-assisted intravascular interventions”. In: *2011 Annual International Conference of the IEEE Engineering in Medicine and Biology Society*. Aug. 2011, pp. 6680–6685. DOI: 10.1109/IEMBS.2011.6091647 (cit. on pp. 77, 78).

[84] Z. Jing, H. Mao, and W. Dai, eds. *Endovascular Surgery and Devices*. Springer Singapore, 2018. DOI: 10.1007/978-981-10-8270-2 (cit. on pp. 16, 17).

[85] G. S. Kassab, E. R. Lontis, and H. Gregersen. “Measurement of Coronary Lumen Area Using an Impedance Catheter: Finite Element Model and in Vitro Validation”. In: *Annals of Biomedical Engineering* 32.12 (Dec. 2004), pp. 1642–1653. DOI: 10.1007/s10439-004-7817-2 (cit. on p. 109).

[86] M. Kellermeier, J. Herbolzheimer, S. Kreppner, M. Lotter, V. Strnad, and C. Bert. “Electromagnetic tracking technology for improved treatment quality assurance in interstitial brachytherapy”. In: *Journal of Applied Clinical Medical Physics* 18.1 (Jan. 2017), pp. 211–222. DOI: 10.1002/acm2.12021 (cit. on p. 90).

[87] S. B. Kesner and R. D. Howe. “Position Control of Motion Compensation Cardiac Catheters”. In: *IEEE Transactions on Robotics* 27.6 (Dec. 2011), pp. 1045–1055. DOI: 10.1109/TRO.2011.2160467 (cit. on p. 14).

[88] F. Khan, A. Denasi, D. Barrera, J. Madrigal, S. Sales, and S. Misra. “Multi-Core Optical Fibers With Bragg Gratings as Shape Sensor for Flexible Medical Instruments”. In: *2019 IEEE Sensors Journal*. 14. July 2019, pp. 5878–5884. DOI: 10.1109/JSEN.2019.2905010 (cit. on pp. 69, 71, 72).

[89] G. K. Korir, B. O. Ochieng, J. S. Wambani, I. K. Korir, and C. Y. Jowi. "Radiation exposure in interventional procedures". In: *Radiation Protection Dosimetry* 152.4 (Dec. 2012), pp. 339–344. DOI: 10.1093/rpd/ncs072 (cit. on pp. 3, 4).

[90] M. E. Ladd and H. H. Quick. "Reduction of resonant RF heating in intravascular catheters using coaxial chokes". In: *Magnetic Resonance in Medicine* 43.4 (Apr. 2000), pp. 615–619. DOI: 10.1002/(SICI)1522-2594(200004)43:4<615::AID-MRM19>3.0.CO;2-B (cit. on p. 63).

[91] A. de Lambert, S. Esneault, A. Lucas, P. Haigron, P. Cinquin, and J. L. Magne. "Electromagnetic Tracking for Registration and Navigation in Endovascular Aneurysm Repair: A Phantom Study". In: *European Journal of Vascular and Endovascular Surgery* 43.6 (June 2012), pp. 684–689. DOI: 10.1016/j.ejvs.2012.03.007 (cit. on pp. 19, 66, 69, 108, 115, 118, 119, 123, 128).

[92] F. Langsch, S. Virga, J. Esteban, R. Göbl, and N. Navab. "Robotic Ultrasound for Catheter Navigation in Endovascular Procedures". In: *2019 IEEE/RSJ International Conference on Intelligent Robots and Systems*. Nov. 2019, pp. 5404–5410. DOI: 10.1109/IROS40897.2019.8967652 (cit. on pp. 24, 57–59).

[93] P. Legeza, K. Sconzert, J.-M. Sungur, T. M. Loh, G. Britz, and A. Lumsden. "Preclinical study testing feasibility and technical requirements for successful telerobotic long distance peripheral vascular intervention". In: *The International Journal of Medical Robotics and Computer Assisted Surgery* 2021 (July 2021), e2249. DOI: 10.1002/rcs.2249 (cit. on pp. 75, 76).

[94] D. Lesage, E. D. Angelini, I. Bloch, and G. Funka-Lea. "A review of 3D vessel lumen segmentation techniques: Models, features and extraction schemes". In: *Medical Image Analysis* 13.6 (Dec. 2009), pp. 819–845. DOI: 10.1016/j.media.2009.07.011 (cit. on p. 54).

[95] S. Lessard, C. Lau, R. Chav, G. Soulez, D. Roy, and J. A. de Guise. "Guidewire tracking during endovascular neurosurgery". In: *Medical Engineering & Physics* 32.8 (Oct. 2010), pp. 813–821. DOI: 10.1016/j.medengphy.2010.05.006 (cit. on p. 54).

[96] M. Li, T. Bien, and G. Rose. "FPGA based electromagnetic tracking system for fast catheter navigation". In: *International Journal of Scientific and Engineering Research* 4.9 (Sept. 2013), pp. 2566–2570. DOI: 10.14299/ijser.2013.09.001 (cit. on pp. 66, 69).

[97] R. Q. Li, G. Bian, X. Zhou, X. Xie, Z. Ni, and Z. Hou. "A Two-Stage Framework for Real-Time Guidewire Endpoint Localization". In: *Medical Image Computing and Computer Assisted Intervention 2019*. 2019, pp. 357–365. DOI: 10.1007/978-3-030-32254-0_40 (cit. on p. 54).

[98] T. Li, A. K. Sahu, A. Talwalkar, and V. Smith. "Federated Learning: Challenges, Methods, and Future Directions". In: *IEEE Signal Processing Magazine* 37.3 (May 2020), pp. 50–60. DOI: 10.1109/MSP.2020.2975749 (cit. on p. 79).

[99] R. Liao, L. Zhang, Y. Sun, S. Miao, and C. Chefd'Hotel. "A Review of Recent Advances in Registration Techniques Applied to Minimally Invasive Therapy". In: *IEEE Transactions on Multimedia* 15.5 (Aug. 2013), pp. 983–1000. DOI: 10.1109/TMM.2013.2244869 (cit. on pp. 4, 54, 110, 122).

[100] Q. Lin, R. Yang, Z. Dai, H. Chen, and K. Cai. "Automatic registration method using EM sensors in the IoT operating room". In: *EURASIP Journal on Wireless Communications and Networking* 2020.1 (Dec. 2020), p. 136. DOI: 10.1186/s13638-020-01754-w (cit. on pp. 108, 122).

[101] N. Lo, J. A. Gutierrez, and R. V. Swaminathan. "Robotic-Assisted Percutaneous Coronary Intervention". In: *Current Treatment Options in Cardiovascular Medicine* 20.2 (Feb. 2018), p. 14. DOI: 10.1007/s11936-018-0608-0 (cit. on p. 75).

[102] E. Lugez, H. Sadjadi, C. P. Joshi, S. G. Akl, and G. Fichtinger. "Improved electromagnetic tracking for catheter path reconstruction with application in high-dose-rate brachytherapy". In: *International Journal of Computer Assisted Radiology and Surgery* 12.4 (Apr. 2017), pp. 681–689. DOI: 10.1007/s11548-017-1534-4 (cit. on pp. 66, 69).

[103] K. T. Lund, G. A. Tangen, and F. Manstad-Hulaas. “Electromagnetic navigation versus fluoroscopy in aortic endovascular procedures: a phantom study”. In: *International Journal of Computer Assisted Radiology and Surgery* 12.1 (Jan. 2017), pp. 51–57. DOI: 10.1007/s11548-016-1466-4 (cit. on pp. 66, 69).

[104] X. Luo. “A bronchoscopic navigation system using bronchoscope center calibration for accurate registration of electromagnetic tracker and CT volume without markers: A bronchoscopic navigation system”. In: *Medical Physics* 41.6 (May 2014), p. 061913. DOI: 10.1118/1.4876381 (cit. on pp. 19, 108, 119, 123, 128).

[105] H. Ma, I. Smal, J. Daemen, and T. v. Walsum. “Dynamic coronary roadmapping via catheter tip tracking in X-ray fluoroscopy with deep learning based Bayesian filtering”. In: *Medical Image Analysis* 61 (Apr. 2020), p. 101634. DOI: 10.1016/j.media.2020.101634 (cit. on pp. 55, 57).

[106] Q. Ma, J. D. Davis, A. Cheng, Y. Kim, G. S. Chirikjian, and E. M. Boctor. “A new robotic ultrasound system for tracking a catheter with an active piezoelectric element”. In: *2016 IEEE/RSJ International Conference on Intelligent Robots and Systems*. Oct. 2016, pp. 2321–2328. DOI: 10.1109/IROS.2016.7759362 (cit. on pp. 61, 63).

[107] Y. Ma, N. Gogin, P. Cathier, R. J. Housden, G. Gijsbers, M. Cooklin, M. O’Neill, J. Gill, C. A. Rinaldi, R. Razavi, and K. S. Rhode. “Real-time x-ray fluoroscopy-based catheter detection and tracking for cardiac electrophysiology interventions”. In: *Medical Physics* 40.7 (2013), p. 071902. DOI: 10.1118/1.4808114 (cit. on pp. 53, 57).

[108] Y. Ma, R. James Housden, A. Fazili, A. V. Arujuna, and K. S. Rhode. “Real-time registration of 3D echo to x-ray fluoroscopy based on cascading classifiers and image registration”. In: *Physics in Medicine & Biology* 66.5 (Mar. 2021), p. 055019. DOI: 10.1088/1361-6560/abe420 (cit. on p. 58).

[109] Y. Ma, A. P. King, N. Gogin, C. A. Rinaldi, J. Gill, R. Razavi, and K. S. Rhode. “Real-Time Respiratory Motion Correction for Cardiac Electrophysiology Procedures Using Image-Based Coronary Sinus Catheter Tracking”. In: *Medical Image Computing and Computer-Assisted Intervention 2010*. 2010, pp. 391–399. DOI: 10.1007/978-3-642-15705-9_48 (cit. on pp. 53, 55, 57).

[110] P. Magnusson, E. Johansson, S. Månsson, J. S. Petersson, C.-M. Chai, G. Hansson, O. Axelsson, and K. Golman. “Passive catheter tracking during interventional MRI using hyperpolarized ^{13}C”. In: *Magnetic Resonance in Medicine*. Vol. 57. 6. 2007, pp. 1140–1147. DOI: 10.1002/mrm.21239 (cit. on p. 63).

[111] L. Maier-Hein, A. M. Franz, W. Birkfellner, J. Hummel, I. Gergel, I. Wegner, and H. P. Meinzer. “Standardized assessment of new electromagnetic field generators in an interventional radiology setting: Assessment of EM field generators”. In: *Medical Physics* 39.6Part1 (May 2012), pp. 3424–3434. DOI: 10.1118/1.4712222 (cit. on p. 65).

[112] J. Maintz and M. A. Viergever. “A survey of medical image registration”. In: *Medical Image Analysis*. Vol. 2. 1. 1998, pp. 1–36. DOI: 10.1016/S1361-8415(01)80026-8 (cit. on p. 13).

[113] K. K. Mandal, F. Parent, S. Martel, R. Kashyap, and S. Kadoury. “Calibration of a needle tracking device with fiber Bragg grating sensors”. In: *Medical Imaging 2015: Image-Guided Procedures, Robotic Interventions, and Modeling*. Vol. 9415. Mar. 2015, p. 94150X. DOI: 10.1117/12.2081198 (cit. on pp. 70, 72).

[114] F. Manstad-Hulaas, G. A. Tangen, T. Dahl, T. A. N. Hernes, and P. Aadahl. “Three-Dimensional Electromagnetic Navigation vs. Fluoroscopy for Endovascular Aneurysm Repair: A Prospective Feasibility Study in Patients”. In: *Journal of Endovascular Therapy* 19.1 (Feb. 2012), pp. 70–78. DOI: 10.1583/11-3557.1 (cit. on pp. 66, 69).

[115] F. Manstad-Hulaas, G. A. Tangen, L. G. Gruionu, P. Aadahl, and T. A. N. Hernes. “Three-Dimensional Endovascular Navigation With Electromagnetic Tracking: Ex Vivo and In Vivo Accuracy”. In: *Journal of Endovascular Therapy* 18.2 (Apr. 2011), pp. 230–240. DOI: 10.1583/10-3301.1 (cit. on pp. 18, 108, 119, 122, 128).

[116] E. N. Marieb and K. Hoehn. *Human Anatomy & Physiology*. 11th edition. Global edition. Harlow, United Kingdom: Pearson Education Limited, 2019 (cit. on pp. 28, 33–37, 39, 40, 101).

[117] P. Markelj, D. Tomaževič, B. Likar, and F. Pernuš. "A review of 3D/2D registration methods for image-guided interventions". In: *Medical Image Analysis* 16.3 (Apr. 2012), pp. 642–661. DOI: 10.1016/j.media.2010.03.005 (cit. on p. 54).

[118] E. Matheson and F. Rodriguez y Baena. "Biologically Inspired Surgical Needle Steering: Technology and Application of the Programmable Bevel-Tip Needle". In: *Biomimetics* 5.4 (Dec. 2020), p. 68. DOI: 10.3390/biomimetics5040068 (cit. on pp. 73, 74, 76, 95, 96, 98).

[119] S. Matl, R. Brosig, M. Baust, N. Navab, and S. Demirci. "Vascular image registration techniques: A living review". In: *Medical Image Analysis* 35 (Jan. 2017), pp. 1–17. DOI: 10.1016/j.media.2016.05.005 (cit. on pp. 18, 122).

[120] S. A. Meyer and P. D. Wolf. "Application of sonomicrometry and multidimensional scaling to cardiac catheter tracking". In: *1997 IEEE Transactions on Biomedical Engineering* 44.11 (Nov. 1997), pp. 1061–1067. DOI: 10.1109/10.641333 (cit. on pp. 61, 63).

[121] C. Miller. *Human Anatomy and Physiology*. Human Biology. British Columbia, Canada: Thompson Rivers University, Sept. 2020 (cit. on pp. 33, 36–39, 101).

[122] F. Milletari, V. Belagiannis, N. Navab, and P. Fallavollita. "Fully Automatic Catheter Localization in C-Arm Images Using $l1$-Sparse Coding". In: *Medical Image Computing and Computer-Assisted Intervention 2014*. 2014, pp. 570–577. DOI: 10.1007/978-3-319-10470-6_71 (cit. on pp. 53, 57).

[123] F. Milletari, N. Navab, and P. Fallavollita. "Automatic Detection of Multiple and Overlapping EP Catheters in Fluoroscopic Sequences". In: *Medical Image Computing and Computer-Assisted Intervention 2013*. Berlin, Heidelberg: Springer, 2013, pp. 371–379. DOI: 10.1007/978-3-642-40760-4_47 (cit. on pp. 53, 57).

[124] B. J. Mittmann, A. Seitel, G. Echner, W. Johnen, R. Gnirs, L. Maier-Hein, and A. M. Franz. "Reattachable fiducial skin marker for automatic multimodality registration". In: *International Journal of Computer Assisted Radiology and Surgery* 17.11 (Nov. 2022), pp. 2141–2150. DOI: 10.1007/s11548-022-02639-7 (cit. on pp. 18, 108, 122).

[125] R. K. Mukherjee, H. Chubb, S. Roujol, R. Razavi, and M. D. O'Neill. "Advances in Real-Time MRI-Guided Electrophysiology". In: *Current Cardiovascular Imaging Reports* 12.2 (Feb. 2019), p. 6. DOI: 10.1007/s12410-019-9481-9 (cit. on p. 59).

[126] M. Müller. "Dynamic Time Warping". In: *Information Retrieval for Music and Motion*. Berlin, Heidelberg: Springer, 2007, pp. 69–84. DOI: 10.1007/978-3-540-74048-3_4 (cit. on p. 123).

[127] J. Mung, S. Han, and J. T. Yen. "Design and in vitro evaluation of a real-time catheter localization system using time of flight measurements from seven 3.5 MHz single element ultrasound transducers towards abdominal aortic aneurysm procedures". In: *Ultrasonics* 51.6 (2011), pp. 768–775. DOI: 10.1016/j.ultras.2011.03.005 (cit. on pp. 61–63).

[128] J. C. Mung, S. G. Huang, J. M. Moos, J. T. Yen, and F. A. Weaver. "Stereotactic endovascular aortic navigation with a novel ultrasonic-based three-dimensional localization system". In: *Journal of Vascular Surgery* 57.6 (2013), pp. 1637–1644. DOI: 10.1016/j.jvs.2012.09.078 (cit. on pp. 61, 63).

[129] A. Myronenko and X. Song. "Point Set Registration: Coherent Point Drift". In: *IEEE Transactions on Pattern Analysis and Machine Intelligence* 32.12 (Dec. 2010), pp. 2262–2275. DOI: 10.1109/TPAMI.2010.46 (cit. on p. 126).

[130] C. Nafis, V. Jensen, L. Beauregard, and P. Anderson. "Method for estimating dynamic EM tracking accuracy of surgical navigation tools". In: *Medical Imaging 2006: Visualization, Image-Guided Procedures, and Display*. Vol. 6141. 2006, pp. 152–167. DOI: 10.1117/12.653448 (cit. on p. 65).

[131] M. Nagel, M. Hoheisel, R. Petzold, W. A. Kalender, and U. H. W. Krause. "Needle and catheter navigation using electromagnetic tracking for computer-assisted C-arm CT interventions". In: *Medical Imaging 2007: Visualization and Image-Guided Procedures*. Vol. 6509. Mar. 2007, 65090J. DOI: 10.1117/12.709435 (cit. on pp. 66, 69).

[132] O. Nassar, D. Mager, and J. G. Korvink. "A Novel Sensor Design and Fabrication for Wireless Interventional MRI Through Induction Coupling". In: *2019 IEEE Sensors Journal*. Oct. 2019, pp. 1–4. DOI: 10.1109/SENSORS43011.2019.8956525 (cit. on p. 63).

[133] A. Nguyen, D. Kundrat, G. Dagnino, W. Chi, M. E. M. K. Abdelaziz, Y. Guo, Y. Ma, T. M. Y. Kwok, C. Riga, and G.-Z. Yang. "End-to-End Real-time Catheter Segmentation with Optical Flow-Guided Warping during Endovascular Intervention". In: *2020 IEEE International Conference on Robotics and Automation*. May 2020, pp. 9967–9973. DOI: 10.1109/ICRA40945.2020.9197307 (cit. on p. 54).

[134] E. Nypan, G. A. Tangen, R. Brekken, and F. Manstad-Hulaas. "A Steerable and Electromagnetically Tracked Catheter: Navigation Performance Compared With Image Fusion in a Swine Model". In: *Journal of Endovascular Therapy* (Sept. 2022), p. 152660282211234. DOI: 10.1177/15266028221123434 (cit. on p. 115).

[135] E. Nypan, G. A. Tangen, F. Manstad-Hulaas, and R. Brekken. "Vessel-based rigid registration for endovascular therapy of the abdominal aorta". In: *Minimally Invasive Therapy & Allied Technologies* 28.2 (Mar. 2019), pp. 127–133. DOI: 10.1080/13645706.2019.1575240 (cit. on pp. 19, 66, 69, 108, 115, 118, 119, 123, 127, 128).

[136] C. de Nys, E. S. Liang, M. Prior, M. Woodruff, J. Novak, A. Murphy, Z. Li, C. Winter, and M. Allenby. *Royal Brisbane_TOFMRA_Intracranial Aneurysm_Database*. OpenNeuro, 2024. DOI: 10.18112/openneuro.ds005096.v1.0.0 (cit. on p. 28).

[137] K. O'Donoghue. "Electromagnetic tracking and steering for catheter navigation". PhD thesis. Ireland: University College Cork, Oct. 2014 (cit. on p. 64).

[138] A. d. Oliveira, J. Rauschenberg, D. Beyersdorff, W. Semmler, and M. Bock. "Automatic passive tracking of an endorectal prostate biopsy device using phase-only cross-correlation". In: *Magnetic Resonance in Medicine* 59.5 (2008), pp. 1043–1050. DOI: 10.1002/mrm.21430 (cit. on p. 59).

[139] F. P. Oliveira and J. M. R. Tavares. "Medical image registration: a review". In: *Computer Methods in Biomechanics and Biomedical Engineering* 17.2 (2014), pp. 73–93. DOI: 10.1080/10255842.2012.670855 (cit. on p. 18).

[140] K. Paliwal, A. Agarwal, and S. Sinha. "A modification over Sakoe and Chiba's dynamic time warping algorithm for isolated word recognition". In: *Signal Processing* 4.4 (July 1982), pp. 329–333. DOI: 10.1016/0165-1684(82)90009-3 (cit. on p. 125).

[141] L. Pancaldi, P. Dirix, A. Fanelli, A. M. Lima, N. Stergiopulos, P. J. Mosimann, D. Ghezzi, and M. S. Sakar. "Flow driven robotic navigation of microengineered endovascular probes". In: *Nature Communications* 11.1 (Dec. 2020), p. 6356. DOI: 10.1038/s41467-020-20195-z (cit. on pp. 68, 69).

[142] F. Parent, M. Gérard, F. Monet, S. Loranger, G. Soulez, R. Kashyap, and S. Kadoury. "Intra-Arterial Image Guidance With Optical Frequency Domain Reflectometry Shape Sensing". In: *2019 IEEE Transactions on Medical Imaging* 38.2 (Feb. 2019), pp. 482–492. DOI: 10.1109/TMI.2018.2866494 (cit. on pp. 69, 72).

[143] F. Parent, S. Loranger, K. K. Mandal, V. L. Iezzi, J. Lapointe, J.-S. Boisvert, M. D. Baiad, S. Kadoury, and R. Kashyap. "Enhancement of accuracy in shape sensing of surgical needles using optical frequency domain reflectometry in optical fibers". In: *Biomedical Optics Express* 8.4 (Apr. 2017), pp. 2210–2221. DOI: 10.1364/BOE.8.002210 (cit. on pp. 69, 72).

[144] O. Pauly, H. Heibel, and N. Navab. "A Machine Learning Approach for Deformable Guide-Wire Tracking in Fluoroscopic Sequences". In: *Medical Image Computing and Computer-Assisted Intervention 2010*. 2010, pp. 343–350. DOI: 10.1007/978-3-642-15711-0_43 (cit. on pp. 53, 57).

[145] T. Penzkofer, H. S. Na, P. Isfort, C. Wilkmann, S. Osterhues, A. Besting, C. Hänisch, S. Bisplinghoff, J. Jansing, S. von Werder, J. Gooding, M. de la Fuente, A. H. Mahnken, C. Disselhorst-Klug, T. Schmitz-Rode, C. Kuhl, and P. Bruners. “Electromagnetically Navigated In Situ Fenestration of Aortic Stent Grafts: Pilot Animal Study of a Novel Fenestrated EVAR Approach”. In: *CardioVascular and Interventional Radiology* 41.1 (Jan. 2018), pp. 170–176. DOI: 10.1007/s00270-017-1769-z (cit. on pp. 66, 69).

[146] T. Petković, R. Homan, and S. Lončarić. “Real-time 3D position reconstruction of guidewire for monoplane X-ray”. In: *Computerized Medical Imaging and Graphics* 38.3 (Apr. 2014), pp. 211–223. DOI: 10.1016/j.compmedimag.2013.12.006 (cit. on p. 56).

[147] R. Piazza, S. Condino, A. Alberti, R. N. Berchiolli, G. Coppi, M. Gesi, V. Ferrari, and M. Ferrari. “Design of a sensorized guiding catheter for in situ laser fenestration of endovascular stent”. In: *Computer Assisted Surgery* 22.1 (Jan. 2017), pp. 27–38. DOI: 10.1080/24699322.2017.1358403 (cit. on pp. 64, 69).

[148] M. Pinzi, S. Galvan, T. Watts, R. Secoli, and F. Rodriguez y Baena. “Path Replanning for Orientation-constrained Needle Steering”. In: *IEEE Transactions on Biomedical Engineering* 2021 (Feb. 2021), pp. 1–1. DOI: 10.1109/TBME.2021.3060470 (cit. on pp. 74, 76).

[149] G. Pocock and C. D. Richards. *Human Physiology: The Basis of Medicine*. 3rd edition. Oxford, United Kingdom: Oxford University Press, 2006 (cit. on pp. 28, 33–41, 101).

[150] F. Pomerleau, F. Colas, R. Siegwart, and S. Magnenat. “Comparing ICP variants on real-world data sets: Open-source library and experimental protocol”. In: *Autonomous Robots* 34.3 (Apr. 2013), pp. 133–148. DOI: 10.1007/s10514-013-9327-2 (cit. on p. 115).

[151] J. Prince and J. Links. *Medical Imaging: Signals and Systems*. New Jersey, United States of America: Pearson Education, 2014 (cit. on pp. 23–27, 84, 86, 95, 98).

[152] H. Rafii-Tari, C. J. Payne, and G.-Z. Yang. “Current and Emerging Robot-Assisted Endovascular Catheterization Technologies: A Review”. In: *Annals of Biomedical Engineering* 42.4 (Apr. 2014), pp. 697–715. DOI: 10.1007/s10439-013-0946-8 (cit. on pp. 13, 73, 79).

[153] K. Ralovich. “Image-based Treatment Outcome Prediction and Intervention Guidance for Cardiovascular Diseases”. PhD thesis. Germany: Technical University of Munich, 2018 (cit. on p. 48).

[154] A. Ramadani, M. Bui, T. Wendler, H. Schunkert, P. Ewert, and N. Navab. “A survey of catheter tracking concepts and methodologies”. In: *Medical Image Analysis* 82 (Nov. 2022), p. 102584. DOI: 10.1016/j.media.2022.102584 (cit. on pp. 3, 4, 11–13, 19, 47, 50, 57–59, 61, 63, 64, 69, 70, 72, 76, 78, 84, 85, 88, 89, 108, 122, 134).

[155] A. Ramadani, P. Ewert, H. Schunkert, and N. Navab. “WarpEM: Dynamic Time Warping for Accurate Catheter Registration in EM-Guided Procedures”. In: *Medical Image Computing and Computer Assisted Intervention – MICCAI 2023*. 2023, pp. 802–811. DOI: 10.1007/978-3-031-43990-2_75 (cit. on pp. 121, 124, 126, 128).

[156] A. Ramadani, H. Maier, F. Bourier, C. Meierhofer, P. Ewert, H. Schunkert, and N. Navab. “Feature-Based Electromagnetic Tracking Registration Using Bioelectric Sensing”. In: *IEEE Robotics and Automation Letters* 8.6 (June 2023), pp. 3286–3293. DOI: 10.1109/LRA.2023.3262988 (cit. on pp. 19, 107, 112, 113, 117–119, 124, 127).

[157] M. Rea, D. McRobbie, H. Elhawary, Z. T. H. Tse, M. Lamperth, and I. Young. “Sub-pixel localisation of passive micro-coil fiducial markers in interventional MRI”. In: *Magnetic Resonance Materials in Physics, Biology and Medicine* 22.2 (Apr. 2009), pp. 71–76. DOI: 10.1007/s10334-008-0143-1 (cit. on p. 59).

[158] A. Reichert, S. Reiss, A. J. Krafft, and M. Bock. “Passive needle guide tracking with radial acquisition and phase-only cross-correlation”. In: *Magnetic Resonance in Medicine* 85.2 (2021), pp. 1039–1046. DOI: 10.1002/mrm.28448 (cit. on p. 59).

[159] T. Reichl, J. Gardiazabal, and N. Navab. “Electromagnetic Servoing – A New Tracking Paradigm”. In: *2013 IEEE Transactions on Medical Imaging* 32.8 (Aug. 2013), pp. 1526–1535. DOI: 10.1109/TMI.2013.2259636 (cit. on pp. 76, 78).

[160] J. Reisenauer, M. J. Simoff, M. A. Pritchett, D. E. Ost, A. Majid, C. Keyes, R. F. Casal, M. S. Parikh, J. Diaz-Mendoza, S. Fernandez-Bussy, and E. E. Folch. “Ion: Technology and Techniques for Shape-sensing Robotic-assisted Bronchoscopy”. In: *The Annals of Thoracic Surgery* 113.1 (Jan. 2022), pp. 308–315. DOI: 10.1016/j.athoracsur.2021.06.086 (cit. on p. 78).

[161] K. Rhode and M. Sermesant. “Modeling and Registration for Electrophysiology Procedures Based on Three-Dimensional Imaging”. In: *Current Cardiovascular Imaging Reports* 4.2 (Apr. 2011), pp. 116–126. DOI: 10.1007/s12410-011-9067-7 (cit. on p. 110).

[162] L. Richmond, K. Rajappan, E. Voth, V. Rangavajhala, M. J. Earley, G. Thomas, S. Harris, S. C. Sporton, and R. J. Schilling. “Validation of computed tomography image integration into the EnSite NavX mapping system to perform catheter ablation of atrial fibrillation”. In: *Journal of cardiovascular electrophysiology* 19.8 (2008), pp. 821–827. DOI: 10.1111/j.1540-8167.2008.01127.x (cit. on p. 110).

[163] R. J. Roesthuis, S. Janssen, and S. Misra. “On using an array of fiber Bragg grating sensors for closed-loop control of flexible minimally invasive surgical instruments”. In: *2013 IEEE/RSJ International Conference on Intelligent Robots and Systems*. Nov. 2013, pp. 2545–2551. DOI: 10.1109/IROS.2013.6696715 (cit. on pp. 70, 72).

[164] R. J. Roesthuis, M. Kemp, J. J. van den Dobbelsteen, and S. Misra. “Three-Dimensional Needle Shape Reconstruction Using an Array of Fiber Bragg Grating Sensors”. In: *2014 IEEE/ASME Transactions on Mechatronics* 19.4 (Aug. 2014), pp. 1115–1126. DOI: 10.1109/TMECH.2013.2269836 (cit. on pp. 70, 72).

[165] R. J. Roesthuis and S. Misra. “Steering of Multisegment Continuum Manipulators Using Rigid-Link Modeling and FBG-Based Shape Sensing”. In: *2016 IEEE Transactions on Robotics* 32.2 (Apr. 2016), pp. 372–382. DOI: 10.1109/TRO.2016.2527047 (cit. on pp. 70, 72).

[166] X. Roothaer. “Multi-scale study of the mechanical behaviour of bearing and bone-bearing bones: towards personalization of FE human models”. PhD thesis. Université Polytechnique Hauts-de-France, Nov. 2019 (cit. on p. 29).

[167] D. Rueckert and J. A. Schnabel. “Medical Image Registration”. In: *Biomedical Image Processing*. 2011, pp. 131–154. DOI: 10.1007/978-3-642-15816-2_5 (cit. on pp. 18, 86, 98).

[168] S. C. Ryu and P. E. Dupont. “FBG-based shape sensing tubes for continuum robots”. In: *2014 IEEE International Conference on Robotics and Automation*. May 2014, pp. 3531–3537. DOI: 10.1109/ICRA.2014.6907368 (cit. on pp. 70, 72).

[169] S. K. Sahu, C. Sozer, B. Rosa, I. Tamadon, P. Renaud, and A. Menciassi. “Shape Reconstruction Processes for Interventional Application Devices: State of the Art, Progress, and Future Directions”. In: *Frontiers in Robotics and AI* 8 (2021). DOI: 10.3389/frobt.2021.758411 (cit. on p. 70).

[170] C. E. Saikus and R. J. Lederman. “Interventional Cardiovascular Magnetic Resonance Imaging: A New Opportunity for Image-Guided Interventions”. In: *Journal of the American College of Cardiology – JACC: Cardiovascular Imaging* 2.11 (Nov. 2009), pp. 1321–1331. DOI: 10.1016/j.jcmg.2009.09.002 (cit. on p. 63).

[171] H. Sakoe and S. Chiba. “Dynamic programming algorithm optimization for spoken word recognition”. In: *IEEE Transactions on Acoustics, Speech, and Signal Processing* 26.1 (Feb. 1978), pp. 43–49. DOI: 10.1109/TASSP.1978.1163055 (cit. on p. 125).

[172] A. Schwein, B. Kramer, P. Chinnadurai, S. Walker, M. O’Malley, A. Lumsden, and J. Bismuth. “Flexible robotics with electromagnetic tracking improves safety and efficiency during in vitro endovascular navigation”. In: *Journal of Vascular Surgery* 65.2 (Feb. 2017), pp. 530–537. DOI: 10.1016/j.jvs.2016.01.045 (cit. on pp. 77, 78).

[173] A. Schwein, B. Kramer, P. Chinnadurai, N. Virmani, S. Walker, M. O'Malley, A. B. Lumsden, and J. Bismuth. "Electromagnetic tracking of flexible robotic catheters enables "assisted navigation" and brings automation to endovascular navigation in an in vitro study". In: *Journal of Vascular Surgery* 67.4 (Apr. 2018), pp. 1274–1281. DOI: 10.1016/j.jvs.2017.01.072 (cit. on pp. 77, 78).

[174] R. Secoli, E. Matheson, M. Pinzi, S. Galvan, A. Donder, T. Watts, M. Riva, D. D. Zani, L. Bello, and F. Rodriguez y Baena. "Modular robotic platform for precision neurosurgery with a bio-inspired needle: System overview and first in-vivo deployment". In: *PLOS ONE* 17.10 (Oct. 2022), e0275686. DOI: 10.1371/journal.pone.0275686 (cit. on p. 98).

[175] S. Sefati, R. Hegeman, F. Alambeigi, I. Iordachita, and M. Armand. "FBG-Based Position Estimation of Highly Deformable Continuum Manipulators: Model-Dependent vs. Data-Driven Approaches". In: *2019 IEEE International Symposium on Medical Robotics*. Apr. 2019, pp. 1–6. DOI: 10.1109/ISMR.2019.8710179 (cit. on pp. 70, 72).

[176] D. J. Shah, R. K. Sachs, and D. J. Wilson. "Radiation-induced cancer: a modern view". In: *The British Journal of Radiology* 85.1020 (Dec. 2012), e1166–e1173. DOI: 10.1259/bjr/25026140 (cit. on pp. 3, 4).

[177] Z. Shaikh, M. Eilenberg, and T. Cohen. "The Amigo™ Remote Catheter System: From Concept to Bedside". In: *The Journal of Innovations in Cardiac Rhythm Management* 8.8 (Aug. 2017), pp. 2795–2802. DOI: 10.19102/icrm.2017.080806 (cit. on pp. 75, 76).

[178] G. Shao and Y.-X. Guo. "An Optimal Design for Passive Magnetic Localization System Based on SNR Evaluation". In: *IEEE Transactions on Instrumentation and Measurement* 69.7 (July 2020), pp. 4324–4333. DOI: 10.1109/TIM.2019.2947173 (cit. on p. 69).

[179] C. Shi, S. Giannarou, S. L. Lee, and G. Z. Yang. "Simultaneous catheter and environment modeling for Trans-catheter Aortic Valve Implantation". In: *2014 IEEE/RSJ International Conference on Intelligent Robots and Systems*. Sept. 2014, pp. 2024–2029. DOI: 10.1109/IROS.2014.6942832 (cit. on pp. 76, 78).

[180] C. Shi, X. Luo, P. Qi, T. Li, S. Song, Z. Najdovski, T. Fukuda, and H. Ren. "Shape Sensing Techniques for Continuum Robots in Minimally Invasive Surgery: A Survey". In: *2017 IEEE Transactions on Biomedical Engineering* 64.8 (Aug. 2017), pp. 1665–1678. DOI: 10.1109/TBME.2016.2622361 (cit. on p. 69).

[181] C. Shi, C. Tercero, X. Wu, S. Ikeda, K. Komori, K. Yamamoto, F. Arai, and T. Fukuda. "Real-time *in vitro* intravascular reconstruction and navigation for endovascular aortic stent grafting: Real-time intravascular reconstruction for aortic stent grafting". In: *The International Journal of Medical Robotics and Computer Assisted Surgery* 12.4 (Dec. 2016), pp. 648–657. DOI: 10.1002/rcs.1736 (cit. on pp. 67, 69).

[182] T. Sielhorst, T. Blum, and N. Navab. "Synchronizing 3D movements for quantitative comparison and simultaneous visualization of actions". In: *Fourth IEEE and ACM International Symposium on Mixed and Augmented Reality (ISMAR05)*. Oct. 2005, pp. 38–47. DOI: 10.1109/ISMAR.2005.57 (cit. on p. 123).

[183] Y. Song, J. Totz, S. Thompson, S. Johnsen, D. Barratt, C. Schneider, K. Gurusamy, B. Davidson, S. Ourselin, D. Hawkes, and M. J. Clarkson. "Locally rigid, vessel-based registration for laparoscopic liver surgery". en. In: *International Journal of Computer Assisted Radiology and Surgery* 10.12 (Dec. 2015), pp. 1951–1961. DOI: 10.1007/s11548-015-1236-8 (cit. on p. 108).

[184] J. Sra, G. Narayan, D. Krum, A. Malloy, R. Cooley, A. Bhatia, A. Dhala, Z. Blanck, V. Nangia, and M. Akhtar. "Computed Tomography-Fluoroscopy Image Integration-Guided Catheter Ablation of Atrial Fibrillation". In: *Journal of Cardiovascular Electrophysiology* 18.4 (2007), pp. 409–414. DOI: 10.1111/j.1540-8167.2006.00734.x (cit. on p. 51).

[185] J. Stoll, P. Novotny, R. Howe, and P. Dupont. "Real-time 3D ultrasound-based servoing of a surgical instrument". In: *Proceedings of the 2006 IEEE International Conference on Robotics and Automation*. May 2006, pp. 613–618. DOI: 10.1109/ROBOT.2006.1641778 (cit. on pp. 62, 63).

[186] J. Stoll, H. Ren, and P. E. Dupont. "Passive Markers for Tracking Surgical Instruments in Real-Time 3-D Ultrasound Imaging". In: *2012 IEEE Transactions on Medical Imaging* 31.3 (Mar. 2012), pp. 563–575. DOI: 10.1109/TMI.2011.2173586 (cit. on pp. 62, 63).

[187] J. Stoll and P. Dupont. "Passive Markers for Ultrasound Tracking of Surgical Instruments". In: *Medical Image Computing and Computer-Assisted Intervention 2005*. 2005, pp. 41–48. DOI: 10.1007/11566489_6 (cit. on pp. 62, 63).

[188] V. Subramanian, H. Wang, J. T. Wu, K. C. L. Wong, A. Sharma, and T. Syeda-Mahmood. "Automated Detection and Type Classification of Central Venous Catheters in Chest X-Rays". In: *Medical Image Computing and Computer Assisted Intervention 2019*. 2019, pp. 522–530. DOI: 10.1007/978-3-030-32226-7_58 (cit. on p. 54).

[189] E. E. Sutton, B. Fuerst, R. Ghotbi, N. J. Cowan, and N. Navab. "Biologically Inspired Catheter for Endovascular Sensing and Navigation". In: *Scientific Reports* 10.1 (Mar. 2020), p. 5643. DOI: 10.1038/s41598-020-62360-w (cit. on pp. 72, 73, 109, 111, 120, 124).

[190] M. C. Svendsen, D. Birrer, B. Jansen, S. D. Teague, B. Combs, G. J. Schears, and G. S. Kassab. "Accurate nonfluoroscopic guidance and tip location of peripherally inserted central catheters using a conductance guidewire system". In: *Journal of Vascular Surgery: Venous and Lymphatic Disorders* 1.2 (Apr. 2013), 202–208.e1. DOI: 10.1016/j.jvsv.2012.10.065 (cit. on pp. 72, 73).

[191] R. Szeliski. *Computer Vision: Algorithms and Applications*. 2nd edition. Texts in computer science. Cham: Springer, 2022 (cit. on pp. 19–22).

[192] N. Tajbakhsh, L. Jeyaseelan, Q. Li, J. N. Chiang, Z. Wu, and X. Ding. "Embracing imperfect datasets: A review of deep learning solutions for medical image segmentation". In: *Medical Image Analysis* 63 (July 2020), p. 101693. DOI: 10.1016/j.media.2020.101693 (cit. on p. 79).

[193] G. Thörmer, N. Garnov, M. Moche, J. Haase, T. Kahn, and H. Busse. "Simultaneous 3D localization of multiple MR-visible markers in fully reconstructed MR images: proof-of-concept for subsecond position tracking". In: *Magnetic Resonance Imaging* 30 (Apr. 2012), pp. 371–381. DOI: 10.1016/j.mri.2011.10.006 (cit. on p. 59).

[194] P. Tinguely, M. Schwalbe, T. Fuss, D. P. Guensch, A. Kohler, I. Baumgartner, S. Weber, and D. Candinas. "Multi-Operational Selective Computer-Assisted Targeting of hepatocellular carcinoma – Evaluation of a novel approach for navigated tumor ablation". In: *PLoS ONE* 13.5 (May 2018). DOI: 10.1371/journal.pone.0197914 (cit. on pp. 66, 69).

[195] M. Torabinia, A. Caprio, S.-J. Jang, T. Ma, H. Tran, L. Mekki, I. Chen, M. Sabuncu, S. C. Wong, and B. Mosadegh. "Deep learning-driven catheter tracking from bi-plane X-ray fluoroscopy of 3D printed heart phantoms". In: *Mini-invasive Surgery* 5.32 (June 2021). DOI: 10.20517/2574-1225.2021.63 (cit. on p. 4).

[196] P. Turski, M. Stieghorst, C. Strother, A. Crummy, R. Lieberman, and C. Mistretta. "Digital subtraction angiography "road map"". In: *American Journal of Roentgenology* 139.6 (Dec. 1982), pp. 1233–1234. DOI: 10.2214/ajr.139.6.1233 (cit. on p. 49).

[197] A. Vandini, B. Glocker, M. Hamady, and G.-Z. Yang. "Robust guidewire tracking under large deformations combining segment-like features (SEGlets)". In: *Medical Image Analysis* 38 (May 2017), pp. 150–164. DOI: 10.1016/j.media.2017.02.001 (cit. on pp. 54, 57).

[198] M. A. Viergever, J. A. Maintz, S. Klein, K. Murphy, M. Staring, and J. P. Pluim. "A survey of medical image registration – under review". In: *Medical Image Analysis* 33 (Oct. 2016), pp. 140–144. DOI: 10.1016/j.media.2016.06.030 (cit. on p. 4).

[199] A. Vlontzos and K. Mikolajczyk. "Deep segmentation and registration in X-ray angiography video". In: *2018 British Machine Vision Conference* (2018). URL: http://bmvc2018.org/contents/papers/0994.pdf (cit. on p. 54).

[200] M. Wagner, S. Schafer, C. Strother, and C. Mistretta. "4D interventional device reconstruction from biplane fluoroscopy". In: *Medical Physics* 43.3 (Mar. 2016), pp. 1324–1334. DOI: 10.1118/1.4941950 (cit. on p. 53).

[201] M. G. Wagner, C. R. Hatt, D. A. P. Dunkerley, L. E. Bodart, A. N. Raval, and M. A. Speidel. "A dynamic model-based approach to motion and deformation tracking of prosthetic valves from biplane x-ray images". In: *Medical Physics* 45.6 (June 2018), pp. 2583–2594. DOI: 10.1002/mp.12913 (cit. on p. 56).

[202] P. Wang, T. Chen, Y. Zhu, W. Zhang, S. K. Zhou, and D. Comaniciu. "Robust guidewire tracking in fluoroscopy". In: *2009 IEEE Conference on Computer Vision and Pattern Recognition*. June 2009, pp. 691–698. DOI: 10.1109/CVPR.2009.5206692 (cit. on pp. 53, 57).

[203] C. Watson and T. K. Morimoto. "Permanent Magnet-Based Localization for Growing Robots in Medical Applications". In: *IEEE Robotics and Automation Letters* 5.2 (Apr. 2020), pp. 2666–2673. DOI: 10.1109/LRA.2020.2972890 (cit. on p. 69).

[204] R. v. d. Weide, K. J. Zuiderveld, C. J. G. Bakker, C. Bos, H. F. M. Smits, T. Hoogenboom, J. J. van Vaals, and M. A. Viergever. "An image processing environment for guiding vascular MR interventions". In: *Medical Image Computing and Computer-Assisted Intervention 1998*. 1998, pp. 317–324. DOI: 10.1007/BFb0056215 (cit. on p. 63).

[205] R. v. d. Weide, C. J. G. Bakker, and M. A. Viergever. "Localization of intravascular devices with paramagnetic markers in MR images". In: *2001 IEEE Transactions on Medical Imaging* 20.10 (Oct. 2001), pp. 1061–1071. DOI: 10.1109/42.959303 (cit. on p. 63).

[206] J. B. West. "The beginnings of cardiac catheterization and the resulting impact on pulmonary medicine". In: *American Journal of Physiology-Lung Cellular and Molecular Physiology* 313.4 (Aug. 2017), pp. L651–L658. DOI: 10.1152/ajplung.00133.2017 (cit. on p. 48).

[207] B. J. Wood, H. Zhang, A. Durrani, N. Glossop, S. Ranjan, D. Lindisch, E. Levy, F. Banovac, J. Borgert, S. Krueger, J. Kruecker, A. Viswanathan, and K. Cleary. "Navigation with Electromagnetic Tracking for Interventional Radiology Procedures: A Feasibility Study". In: *Journal of Vascular and Interventional Radiology* 16.4 (Apr. 2005), pp. 493–505. DOI: 10.1097/01.RVI.0000148827.62296.B4 (cit. on pp. 108, 122).

[208] W. Wu, T. Chen, P. Wang, S. K. Zhou, D. Comaniciu, A. Barbu, and N. Strobel. "Learning-based hypothesis fusion for robust catheter tracking in 2D X-ray fluoroscopy". In: *2011 IEEE Conference on Computer Vision and Pattern Recognition*. June 2011, pp. 1097–1104. DOI: 10.1109/CVPR.2011.5995553 (cit. on pp. 53, 57).

[209] X. Wu, J. Housden, Y. Ma, B. Razavi, K. Rhode, and D. Rueckert. "Fast Catheter Segmentation From Echocardiographic Sequences Based on Segmentation From Corresponding X-Ray Fluoroscopy for Cardiac Catheterization Interventions". In: *2015 IEEE Transactions on Medical Imaging* 34.4 (Apr. 2015), pp. 861–876. DOI: 10.1109/TMI.2014.2360988 (cit. on pp. 53, 54, 57, 59).

[210] X. Wu, J. Housden, N. Varma, Y. Ma, D. Rueckert, and K. Rhode. "Catheter tracking in 3D echocardiographic sequences based on tracking in 2D X-ray sequences for cardiac catheterization interventions". In: *2013 IEEE International Symposium on Biomedical Imaging*. Apr. 2013, pp. 25–28. DOI: 10.1109/ISBI.2013.6556403 (cit. on p. 59).

[211] W. Xia, S. J. West, M. C. Finlay, J. M. Mari, S. Ourselin, A. L. David, and A. E. Desjardins. "Looking beyond the imaging plane: 3D needle tracking with a linear array ultrasound probe". In: *Scientific Reports* 7.1 (2017), pp. 1–9. DOI: 10.1038/s41598-017-03886-4 (cit. on pp. 61–63).

[212] H. Yang, C. Shan, A. F. Kolen, and P. H. N. d. With. "Efficient Medical Instrument Detection in 3D Volumetric Ultrasound Data". In: *2021 IEEE Transactions on Biomedical Engineering* 68.3 (Mar. 2021), pp. 1034–1043. DOI: 10.1109/TBME.2020.2999729 (cit. on pp. 58, 59).

[213] H. Yang, C. Shan, A. F. Kolen, and P. H. N. de With. "Catheter localization in 3D ultrasound using voxel-of-interest-based ConvNets for cardiac intervention". In: *International Journal of Computer Assisted Radiology and Surgery* 14.6 (June 2019), pp. 1069–1077. DOI: 10.1007/s11548-019-01960-y (cit. on p. 58).

[214] H. Yang, C. Shan, A. F. Kolen, and P. H. N. de With. "Deep Q-Network-Driven Catheter Segmentation in 3D US by Hybrid Constrained Semi-supervised Learning and Dual-UNet". In: *Medical Image Computing and Computer Assisted Intervention 2020*. 2020, pp. 646–655. DOI: 10.1007/978-3-030-59710-8_63 (cit. on p. 58).

[215] H. Yang, C. Shan, T. Tan, A. F. Kolen, and P. H. N. de With. "Transferring from ex-vivo to in-vivo: Instrument Localization in 3D Cardiac Ultrasound Using Pyramid-UNet with Hybrid Loss". In: *Medical Image Computing and Computer Assisted Intervention 2019*. 2019, pp. 263–271. DOI: 10.1007/978-3-030-32254-0_30 (cit. on p. 58).

[216] Z. Yaniv, E. Wilson, D. Lindisch, and K. Cleary. "Electromagnetic tracking in the clinical environment". In: *Medical Physics* 36.3 (2009), pp. 876–892. DOI: 10.1118/1.3075829 (cit. on pp. 64, 65).

[217] X. Yi, J. Qian, L. Shen, Y. Zhang, and Z. Zhang. "An Innovative 3D Colonoscope Shape Sensing Sensor Based on FBG Sensor Array". In: *2007 IEEE International Conference on Information Acquisition*. July 2007, pp. 227–232. DOI: 10.1109/ICIA.2007.4295731 (cit. on pp. 71, 72).

[218] H. Zhang, F. Banovac, R. Lin, N. Glossop, B. J. Wood, D. Lindisch, E. Levy, and K. Cleary. "Electromagnetic tracking for abdominal interventions in computer aided surgery". In: *Computer Aided Surgery* 11.3 (Jan. 2006), pp. 127–136. DOI: 10.3109/10929080600751399 (cit. on pp. 108, 122).

[219] K. Zhang, A. J. Krafft, R. Umathum, F. Maier, W. Semmler, and M. Bock. "Real-time MR navigation and localization of an intravascular catheter with ferromagnetic components". In: *Magnetic Resonance Materials in Physics, Biology and Medicine* 23.3 (June 2010), pp. 153–163. DOI: 10.1007/s10334-010-0214-y (cit. on p. 63).

[220] Z. Zhang, Z. Liu, and R. Singapogu. "Extracting Subtask-specific Metrics Toward Objective Assessment of Needle Insertion Skill for Hemodialysis Cannulation". In: *Journal of Medical Robotics Research* 04.03n04 (Sept. 2019), p. 1942006. DOI: 10.1142/S2424905X19420066 (cit. on p. 123).

[221] J. Zhou, E. Sebastian, V. Mangona, and D. Yan. "Real-time catheter tracking for high-dose-rate prostate brachytherapy using an electromagnetic 3D-guidance device: A preliminary performance study". In: *Medical Physics* 40.2 (2013), p. 021716. DOI: 10.1118/1.4788641 (cit. on pp. 66, 69).

[222] Y. J. Zhou, X. L. Xie, X. H. Zhou, S. Q. Liu, G. B. Bian, and Z. G. Hou. "A Real-Time Multifunctional Framework for Guidewire Morphological and Positional Analysis in Interventional X-Ray Fluoroscopy". In: *IEEE Transactions on Cognitive and Developmental Systems* 13.3 (Sept. 2021), pp. 657–667. DOI: 10.1109/TCDS.2020.3023952 (cit. on p. 54).

[223] M. Zweng, P. Fallavollita, S. Demirci, M. Kowarschik, N. Navab, and D. Mateus. "Automatic Guide-Wire Detection for Neurointerventions Using Low-Rank Sparse Matrix Decomposition and Denoising". In: *Augmented Environments for Computer-Assisted Interventions*. 2015, pp. 114–123. DOI: 10.1007/978-3-319-24601-7_12 (cit. on p. 54).

List of Figures

List of Tables